UNIVERSITÉ DE NEUCHÂTEL

" INSTITUTE OF BIOLOGY - DEPARTMENT OF CELLULAR AND MOLECULAR BIOLOGY"

Rue Emile - Argand 11, 2009 Neuchâtel

LOCALIZATION AND INTERACTION OF AtRMR RECEPTORS IN THE PLANT SECRETORY PATHWAY

PhD thesis presented by Occhialini Alessandro

Prof. Jean-Marc Neuhaus (University of Neuchâtel), director

Dr. Guillaume Gouzerh (University of Neuchâtel), expert

Prof. Niko Geldner (University of Lausanne), expert

Université de Neuchâtel

FACULTE DES SCIENCES
Secrétariat-Décanat de la faculté
Rue Emile-Argand 11
CH-2000 Neuchâtel

IMPRIMATUR POUR LA THESE

Localization and interaction of AtRMR receptors in the plant secretory pathway

Alessandro OCCHIALINI

UNIVERSITE DE NEUCHATEL

FACULTE DES SCIENCES

La Faculté des sciences de l'Université de Neuchâtel,
sur le rapport des membres du jury

MM. Jean-Marc Neuhaus (directeur de thèse, Université de Neuchâtel),
Niko Geldner (Université de Lausanne)
et Guillaume Gouzerh (Université de Neuchâtel)

autorise l'impression de la présente thèse.

Neuchâtel, le 7 juin 2011

Le doyen :
P. Kropf

Téléphone : +41 32 718 21 00 E-mail : secretariat.sciences@unine.ch www.unine.ch/sciences

Acknowledgements

Firstly I want to thank my supervisor Prof. Jean-Marc Neuhaus for giving me the opportunity to follow this PhD project.

I thank so much Dr. Guillaume Gouzerh, Dr. Egidio Stigliano, Dr. Didier Schaffer, Sanaa Ayachi, Sophie Marc-Martin and all the members of the Laboratory of Molecular and Cell Biology for their support and the nice discussions we had during my PhD.

I thank Prof. David Robinson, Dr. Giselbert Hinz, Dr. Stefan Hillmer, Dr. Corrado Viotti and Stephanie Gold for having received me in their laboratory and for giving me the opportunity to perform Immunogold experiments.

I thank Prof. Niko Geldner for the nice suggestions and the interesting discussion we had during my defence.

I thank Prof. Liwen Jiang for providing me the construct pBI GFP-BP80.

I thank Dr. Gian-Pietro Di Sansebastiano for providing me the cDNA coding for the fusion protein Venus-SYP61.

I thank Prof. Valerian V. Dolja for providing me the cDNA coding for the viral protein p6.

I thank Dr. Christophe Ritzenthaler for providing me the construct coding for the silencing inhibitor p19.

Index

Abbreviations

ABA: Abscisic Acid
ADP: Adenosine Diphosphate
AP: Adaptin Protein
ARF: ADP Ribosylation Factor
ATP: Adenosine Triphosphate
ATF6: Activating Transcription Factor 6
ATPase: Adenosine Triphosphate Hydrolase
BiFC: Bimolecular Fluorescence Complementation
Bip: Binding Immunoglobulin Protein
BFA: Brefeldine A
BP-80: Binding Protein of 80 kDa
BRET: Bioluminescence Resonance Energy Transfer
BRI1: Brassinosteroid-insensitive 1
CCV: Clathrin-Coated Vesicle
CFP: Cyan Fluorescent Protein
COPI: Coat Protein I
COPII: Coat Protein II
CtVSD: C-terminal Vacuolar Sorting Determinant
DCL1: Dicer-like1
DIP: Dark-Induced Protein
DNA: Deoxyribonucleic Acid
DV: Dense Vesicle
EGF: Epidermal Growth Factor
EGFR: Epidermal Growth Factor Receptor
ER: Endoplasmic Reticulum
ERAD: Endoplasmic Reticulum Associated Degradation
ERD2: Endoplasmic Reticulum Retention Defective 2
ERES: Endoplasmic Reticulum Exporting Site
ERIS: Endoplasmic Reticulum Importing Site
ESCRT: Endosomal Sorting Complex Required For Transport
FRAP: Fluorescence Recovery After Photobleaching
FRET: Forster Resonance Energy Transfer
GAP: GTPase Activating Protein
GDP: Guanosine Diphosphate
GEF: GTP Exchange Factor
GFP: Green Fluorescent Protein
GRAIL: Gene Related to T-cell Anergy in Lymphocytes
GREUL1: Goliath Related E3 Ubiquitin Ligase 1
GTP: Guanosine Triphosphate
GTPase: Guanosine Triphosphate Hydrolase
Hsp: Heat Shock Protein
HYL1: Hyponastic Leaves 1
IEM: Immuno-electron Microscopy
IRE1: Inositol-requiring Enzyme 1
KO: Knock-out
LV: Lytic Vacuole
MbYTH: Membrane Yeast Two Hybrid System
MS: Mass Spectrometry
MVB: Multivesicular Body
NLS: Nuclear Localization Signal
NSF: N-ethylmaleimide Sensitive Fusion Protein
PA domain: Protein Associated Domain

PAC: Precursor Accumulating Vesicle

PEPK: Protein Kinase RNA-like Endoplasmic Reticulum Kinase

PDI: Protein Disulfide Isomerase

PM: Plasma Membrane

PSM: Prostate-specific Membrane Antigen Protein

PSV: Protein Storage Vacuole

psVSD: Protein Structure Dependent Vacuolar Sorting Determinant

PVC: Prevacuolar Compartment

Rab: Ras-related in Brain

Ras: RAt Sarcoma

RING: Really Interesting New Gene

RFP: Red Fluorescent Protein

RMR: Receptor-like Membrane Ring-H2

RNF13: RING Finger Protein 13

SAV: Senescence Associated Vacuole

SE: Serrate

SNAP: Soluble NSF Attachment protein

RNA: Ribonucleic Acid

SNARE: Soluble N-ethylmaleimide-sensitive Protein Attachment Protein Receptor

SNX: Sorting Nexins

SP: Signal Peptide

SRP: Signal Recognition Particle

SYP: Synaptophysin

ssVSD: Sequence-specific Vacuolar Sorting Determinant

TGN: Trans-Golgi Network

TIP: Tonoplast Intrinsic Protein

UBP: Ubiquitin Protease

UPR: Unfolded Protein Response

VAMP: Vesicle Associated Membrane Protein

VCL1: VACUOLELESS1

VIP1: Vire2-Interacting Protein 1

Vps: Vacuolar Protein Sorting

VSD: Vacuolar Sorting Determinant

VSR: Vacuolar Sorting Receptor

VSV-G: Vesicular Stomatitis Virus Glycoprotein

YFP: Yellow Fluorescent Protein

ZIP: Leucine Zipper

Abstract

In the last few years, it was demonstrated that many vacuolar proteins are sorted to their final destination by cargo receptors. Therefore in this study I focused on RMR proteins (Receptor Membrane Ring-H2), a new family of putative receptors, composed of six genes in *Arabidopsis thaliana* (AtRMR), probably involved in protein transport to vacuoles (Jiang *et al.*,, 2000; Park *et al.*, 2005; Park *et al.*, 2007; Hinz *et al.*, 2007). These receptors were identified by their homology to the PA domain (Protease Associated Domain) present in the Vacuolar Sorting Receptors (VSR) that are well known to bind and sort vacuolar proteins (Paris *et al.*, 2002).

Much less is known about these proteins than about VSRs. In the present study I focused on the localization of the different members present in plant cells. Moreover I studied the possible dimerization (homo end/or hetero) between the different types of AtRMR receptors.

For the localization, I have generated different plant expression vectors carrying different fluorescent protein reporters fused to AtRMRs to use in a confocal microscope experiment. The localization was performed in *Arabidopsis thaliana* transgenic plants and *Nicotiana benthamiana* leaves transformed by agro-infiltration. In these experiments AtRMR1 and AtRMR2 showed different subcellular localizations. AtRMR1 localizes in TGN while AtRMR2 localizes in the membrane of ER. This different localization is due by the presence of a putative localization signal present in the sequence linker of AtRMR1. In fact this sequence, when is placed on AtRMR2, is able to relocate the protein in the TGN.

To test the possible AtRMR-AtRMR dimerization I developed Bimolecular Fluorescence Complementation (BiFC) reporters. Using this technique I demonstrated that AtRMR1 can make homodimers and can interact with AtRMR2 making heterodimers. Moreover homo- and heterodimers showed the same localization in the TGN. This result demonstrated that AtRMR2 can exit from the ER as a heterodimer thanks to the presence of the localization signal in the sequence linker of AtRMR1. Moreover using AtRMR deletion mutants I demonstrated that the transmembrane domain and the sequence linker are probably the domains involved in protein-protein interaction.

Introduction of plant secretory pathways

1. General view of plant secretory pathways

The vacuole is an organelle of plant cells that plays a central role in many plant processes. It can function as a reservoir for ions, secondary metabolites, storage proteins, carbohydrates and other compounds, depending on tissue type. It is also involved in many essential functions of plant growth, development and response to biotic and abiotic stress. This wide range of physical and metabolic functions gives the vacuole an essential position in plant life (Marty *et al.,* 1999). For instance a KO mutant of the *A.thaliana* VCL1 gene is characterized by serious defects in vacuolar formation resulting in aberrant morphogenesis and embryonic lethality. This confirms that the vacuole occupies a central role in plant life (Rojo *et al.,* 2001).

To assume this wide range of functions, plant cells can have vacuoles with different functions. In our laboratory, we are focusing our interest on the two types of vacuoles present in vegetative tissues: the protein storage vacuole (PSV) and the lytic vacuole (LV) (Paris *et al.,* 1996; Di Sansebastiano *et al.,* 1998; Di Sansebastiano *et al.,* 2001). More precisely we are interested in the sorting processes and mechanisms that specifically lead the secretory proteins to these two compartments.

Vacuolar proteins reach the different types of vacuoles through the secretory pathway which includes the ER, the Golgi apparatus, the endosomes/prevacuoles and the transport by vesicles (figure I) (Vitale *et al.,* 1999). In the last few years, it has been demonstrated that many vacuolar proteins are sorted to their final destination by cargo receptors. These receptors are transmembrane proteins that are able to bind a specific element present in vacuolar protein precursors, a vacuolar sorting determinant (VSD). In this way the vacuolar proteins can be packed within vesicles and therefore transported to their final destination (Kirsch *et al.,* 1994; Paris *et al.,* 1997; Miller *et al.,* 1999).

In plant cells two different types of membrane receptors that could be involved in protein sorting to vacuole were found: The VSR family (Vacuolar Sorting Receptor) (Paris *et al.,* 1997), encoded by seven genes in *Arabidopsis thaliana* (from AtVSR1 to AtVSR7) and the RMR family (Receptor Membrane Ring-H2) (Cao *et al.,* 2000) encoded by six genes in *A.thaliana* (from AtRMR1 to AtRMR6). Originally this second family has been identified by their homology to the PA domain (Protease-Associated Domain) also present in the luminal part of AtVSR proteins. This domain plays a central role in a vacuolar receptor because it is the domain involved in the binding with

vacuolar proteins (Cao *et al.*, 2000) (figure II).

It is well know that the VSR family is involved in vacuolar sorting to LV through the binding of a sequence-specific sorting determinant (ssVSD) present in certain vacuolar proteins (Kirsch *et al.*, 1994, 1996; Ahmed *et al.*, 2000). On the contrary, the RMR family was proposed to be implicated in the traffic to PSV of proteins with C-terminal sorting determinants (ctVSD). However the role assumed by this second family needs to be elucidated. Therefore in the last few years the research in our laboratory has been focused on this second type of putative vacuolar receptors.

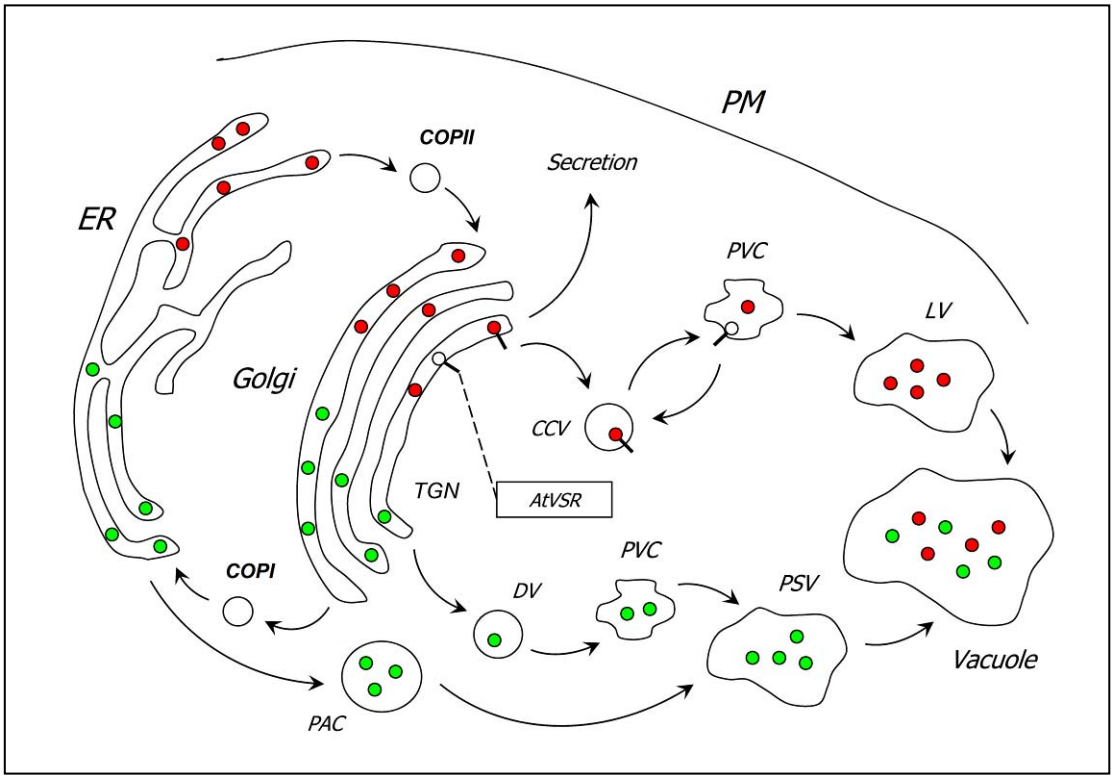

Figure I: Protein sorting to vacuoles. Vacuolar proteins with a sequence specific vacuolar sorting determinant (ssVSD) (in red) and with C-terminal vacuolar sorting determinant (ctVSD) (in green) reach respectively the lytic vacuole (LV) and protein storage vacuole (PSV) through the secretory pathway: ER (endoplasmic reticulum), Golgi (Golgi apparatus), TGN (trans-Golgi network), PVC (prevacuolar compartment) and vacuoles (LV and/or PSV). COPII and COPI are the vesicles involved in anterograde and retrograde traffic between ER and Golgi. At the TGN the proteins with an ssVSD (in red) are packaged in clathrin-coated vesicles (CCV) by binding with a vacuolar receptor (AtVSR family) and then transported to LV via a PVC. The low pH in the lumen of PSV is involved in the dissociation between receptors and protein cargos. Instead, most storage proteins in seeds (in green) with a ctVSD are transported to PSV by condensation which results in dense vesicles (DV) formation. At the level of TGN the budding DV reach the PSV passing by the PSV which is called multivesicular bodies (MVB) in storage tissues. Moreover, it was described a direct route from ER to PSV involved in the traffic of certain storage proteins having a ctVSD. This route involves a particular kind of vesicles named PAC (precursor accumulating vesicles).LV and PSV can coexist in the same cell or fuse forming a big vacuole depending on different cell types and cellular conditions.

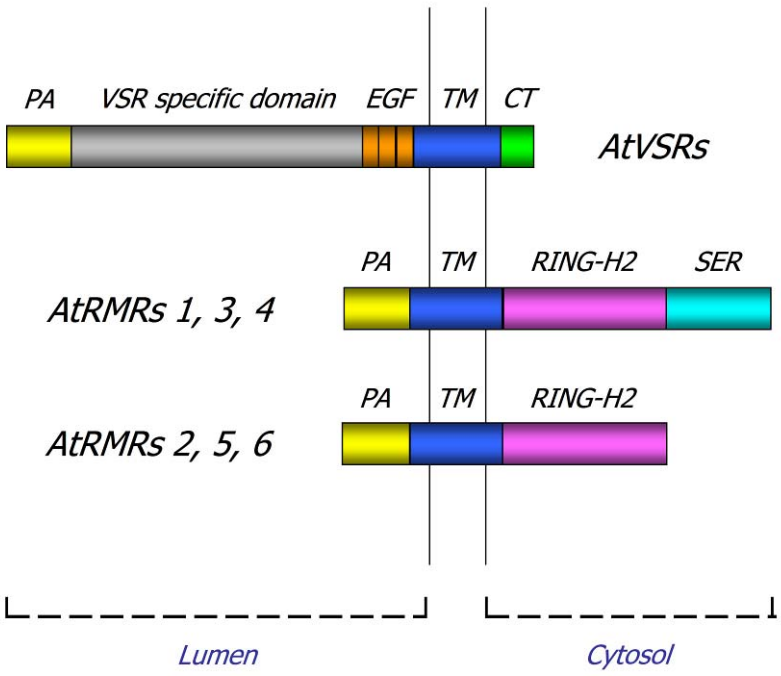

Figure II: Vacuolar receptors in plant cells. In plant cells there are two different types of vacuolar receptors, the VSR family consisting of seven genes in *Arabidopsis thaliana* (from AtVSR1 to AtVSR7) and the RMR family (Receptor Membrane Ring-H2) consisting of six genes in *A. thaliana* (from AtRMR1 to AtRMR6). The most part of the N-terminal luminal part of AtRMR proteins is constituted by a PA domain (yellow). This family is subdivided in two groups: AtRMR 1, 3, and 4 with a predicted Ser-Rich domain (in cyan) in the cytosolic part of the proteins; and AtRMR 2, 5, 6 without a predicted Ser-Rich domain. Moreover in the cytosolic part of both groups, there is a predicted Ring-H2 domain (in violet).
In the N-terminal luminal part of AtVSR proteins there present: a Protease-Associated domain (PA) (in yellow), a VSR-Specific domain (in grey) and three Cys-Rich EGF Repeats (in orange) (Epidermal Growth Factor). The cytosolic part of AtVSR proteins is restricted to a short Tail Domain (in green).
Both families of vacuolar receptors are membrane proteins with a single transmembrane domain (in blue).

2. The endomembrane system

It is composed of different organelles which subdivide the cell in different structural and functional compartments. The endomembrane system assumes very important roles in production, maturation, storage and turnover of macromolecules.

In plant cells this system includes: the nuclear envelope; the endoplasmic reticulum (ER); the Golgi apparatus; the endosomes/prevacuoles; the vacuoles; and the plasma membrane. These compartments constitute functional units which can be physically connected or separated. Two compartments physically separated communicate with each other through highly regulated vesicular transport. In contrast the membranes of mitochondria and chloroplasts do not belong to the endomembrane system.

2.1. Vesicle trafficking

The plant cells are subdivided in different compartments and organelles which communicate with each other by vesicular trafficking. Therefore, a highly regulated process, involving different kinds of vesicles, mediates protein sorting between the different compartments constituting the secretory pathway. Vesicles are small bilayer membrane structures involved in transport of cellular material travelling from a donor to an acceptor organelle. The specificity of the traffic is due to the action of several factors which are involved in vesicle formation, recognition of target organelle and membrane fusion (Bassham *et al.*, 2008; Sanderfoot *et al.*, 1999; Jürgens *et al.*, 2004).

2.1.1. Vesicle formation

The vesicle formation is not a passive event but needs a specific driving force provided by several factors (figure III). It is based on a series of highly regulated events which start with cargo selection and recognition on the luminal side of the donor organelle. It is not well known how soluble protein cargos are selected on the membrane, but in some cases it has been demonstrated that specific protein receptors are involved. A process of signaling is involved in the site recognition of vesicle formation on the cytosolic side of the membrane. After that, coat factors lead to membrane distortion and dissociation with the consequent formation of vesicle.

A specific coat protein GTPase (G-protein) play a main role in this process giving the driving force and coordinating the coating process. In plant cell there are several G-proteins which differ in their specificity for certain donor compartments. For instance ARFs are a wide family of G-proteins necessary for COPI vesicles and CCV formation with 21 members in *A.thaliana*, while the SAR1 family presents different homologues in *A.thaliana* and is mainly involved in COPII vesicle

formation (Bassham *et al.*, 2008; Sanderfoot *et al.*, 1999; Jürgens *et al.*, 2004). Normally the G-protein exists in an inactive cytosolic GDP-binding form. When a membrane vesicle has to be formed, a specific GTP exchange factor (GEF) recruits the G-protein to the vesicle formation site. The recruitment induces the activation of the G-protein by replacing the GDP with GTP and the membrane association. The coat formation implies the recruitment of several factors such as coat proteins and effector proteins with specific enzymatic activities. Among these effectors, Rab GTPases play a fundamental role in target recognition and membrane fusion in association with tethering and docking factors such as SNAREs. Coat assembly and membrane distortion lead to the formation of free vesicles by scission from the donor membrane. Several factors play an important role in membrane scission: the different proteins of the coat; the particular lipid composition at the vesicle formation site; and other protein machinery, such as dynamin, which could play a role in this process. After vesicle formation, the coat is disassembled to allow fusion with the target membrane. The driving force for coat disassembly is provided by a GTPase activating protein (GAP) which helps the G-protein to hydrolyse GTP. The coat then depolymerizes and consequently the G-protein is released in its inactive GDP form. The uncoated vesicle is thus ready to reach the target compartment with the specific action of Rabs and of tethering proteins and then to fuse with it (Bassham *et al.*, 2008; Sanderfoot *et al.*, 1999; Jürgens *et al.*, 2004).

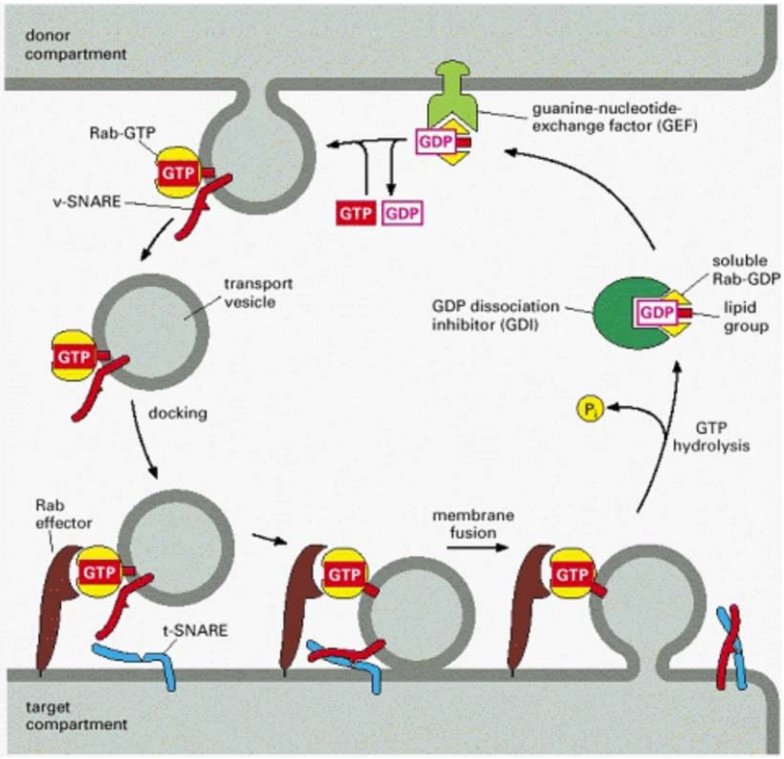

Figure III: Vesicle trafficking between donor and target compartments (The Molecular Biology of The Cell, Alberts *et al.*, 2002). A specific Rab protein is recognized by a GEF factor (guanidine-nucleotide exchange factor) localized in the membrane of donor compartment. GEF is able to associate with a soluble inactive Rab binding a GDP. The GEF activates the Rab inducing the exchanging of the GDP with GTP. The Rab-GTP binds to the membrane by a covalently attached lipid group. This process lead to the formation of a transport vesicle carrying specific v-SNAREs. The combined action of Rab and Rab effectors help the docking of the vesicle to the target membrane. The recognition between the specific v-SNARE (on the vesicle) and t-SNAREs (on target membrane) determines the vesicle fusion with the target compartment. Finally the Rab protein is released in the cytosol upon hydrolysis of the GTP. The inactive GDP-binding Rab is then recognized by GDP dissociation inhibitor (GDI) which prevents the dissociation of GDP. The cytosolic Rab protein is now able for another cycle of vesicle formation.

2.1.2. Vesicle fusion

The uncoated vesicles are free in the cytosol and can reach and fuse specifically to their target compartment by the action of certain factors which reside on the vesicle membrane (figure IV) (Sanderfoot *et al.,* 1999). The principal factors involved in this process are: Rab GTPases (Ras-related in Brain), SNAREs (Soluble N-ethylmaleimide-sensitive Protein Attachment Protein Receptor), proteins of Sec1p family, NSF (N-ethylmaleimide Sensitive Fusion Protein) and α-SNAP (Soluble NSF Attachment protein).

The SNAREs are important effector proteins involved in recognition and fusion between uncoated vesicles and their target membrane. They are anchored, *via* a C-terminal hydrophobic domain or a lipid tail in the membrane of transport vesicles and of target compartments. Based on their localization, the SNAREs have been classified in two groups: v-SNAREs, which have been found in vesicles originating from the donor compartment, and t-SNAREs which are localized in the membrane of the target compartment. Therefore, the traffic specificity is due to the recognition of a particular v-SNARE in the vesicle and of t-SNAREs in the target compartment. The t-SNAREs are more permanent resident proteins of an organelle than the v-SNAREs which traffic between two compartments. For this reason the t-SNARE are often used as protein markers for organelle identification and characterization. A new classification of SNARE based on structural features was proposed. They are divided in the R-SNAREs and Q-SNAREs which differ in the main aminoacid involved in formation of the core SNARE complex. In R-SNAREs the main aminoacid is an arginine (R), while in Q-SNARE it is a glutamine (Q). For the fusion process, a four helix bundle must form, including one R-SNARE and three Q-SNAREs. Therefore the Q-SNAREs are subdivided in Qa-, Qb and Qc-SNAREs (Bassham *et al.,* 2008; Sanderfoot *et al.,* 1999; Jürgens *et al.,* 2004).

Several general factors are needed to regulate the SNARE functions, such as NSF (N-ethylmaleimide sensitive factor) and α-SNAP (soluble NSF attachment protein). The NSF is a homohexameric AAA ATPase which dissociates the v/t-SNARE complex after membrane fusion. α-SNAP plays an important role in the recruitment of NSF to the SNARE complex (Malhotra *et al.,* 1988; Sato *et al.,* 1997; Eakle *et al.,* 1988).

Two other families of protein effectors play an important role in the regulation of the SNARE complexes: the Sec1p family and the Rab family.

Rabs are a family of small GTPases. They are involved in many steps of vesicular trafficking such as recruitment of docking factors and molecular motor proteins. They are small lipid anchor proteins which are associated to the membrane by a prenyl group attached on a C-terminal Cys–motif of the protein. Rabs work in a cycle of association and dissociation from membranes. In GDP-

bound form they are inactive and soluble in the cytosol where they have been found in association with a RabGDI (GDP disassociation inhibitor). When the GDP is substituted with a GTP by the intervention of a compartment-specific Rab-GEF (Rab guanine exchange factor), the Rab is activated and attached to the particular membrane (Bassham *et al.,* 2008; Sanderfoot *et al.,* 1999; Jürgens *et al.,* 2004).

The Rab family is divided in eight types which are further subdivided in different groups. In *A.thaliana,* 57 different Rabs were identified, probably involved in many different vesicular trafficking events. Therefore Rabs have been used as protein markers for the characterization of different compartments (Bassham *et al.,* 2008).

The second group of protein effectors involved in the regulation of the SNARE complex is the Sec1p family which is composed of 6 members in *A.thaliana* (Sanderfoot *et al.,* 2007). It was demonstrated that the members of this family are able to interact with Qa-SNARE (syntaxins) in order to allow the formation of SNARE complex. This interaction leads to a conformational change of the SNARE from a closed structure to an open structure, which allows the formation of the SNARE complex (Hanson *et al.,* 2000; Dulubova *et al.,* 1999).

2.1.3. Mechanism of vesicle fusion

The mechanism by which a vesicle fuses specifically with the target membrane involves both vesicle factors and factors on the target membrane (figure IV). Therefore the vesicles present activated v-SNARE and Rab-GTP, while the membrane of the target organelle contains a t-SNARE complex associated with Sec1p which maintains the t-SNARE in an inactive form. When the vesicle and target make contact, the Rab-GTP displaces the Sec1p exposing the t-SNARE which is now in active form. Consequently the t-SNARE is able to interact with the v-SNARE present on the membrane surface of vesicles (docking). This interaction probably involves the N-terminal cytosolic coiled-coil domains of both t- and v-SNARE which are able to associate following a “zippering-up” process (Chen *et al.,* 1999; Melia *et al.,* 2002). This association provides sufficient energy for membrane fusion.

Then the factor α-SNAP specifically binds to the v-/t-SNARE recruiting the NSF factor on this complex. Subsequently NSF catalyzes the disassembly of v-/t-SNARE complex upon hydrolysis of ATP, releasing v- and t-SNARE. Finally, the v-SNARE is recycled back to the donor compartment, while the t-SNARE is available for another cycle of vesicle fusion (Hay *et al.,* 1997; Rothman *et al.,* 1997; Weber *et al.,* 1998).

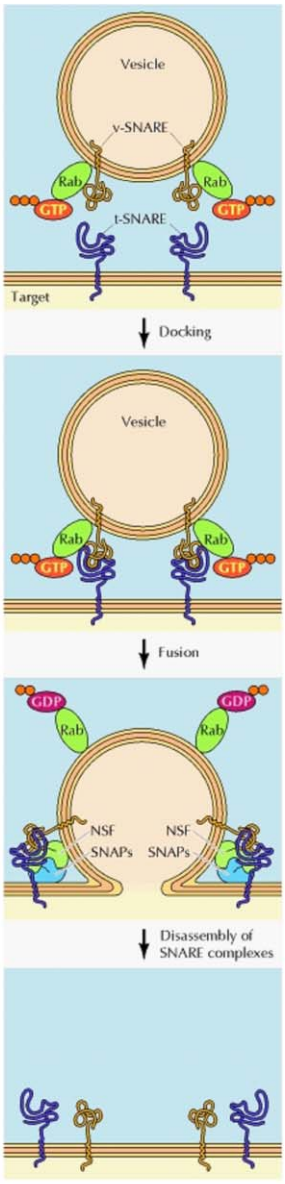

Figure IV: Mechanism of vesicle fusion (The Cell a Molecular Approch, Cooper *et al.*, 2009). The mechanism of vesicle docking and fusion is mediated by several vesicle and target membrane factors. A transport vesicle exposes on the surface specific v-SNARE and GTP-bound Rab, while the target membrane exposes specific t-SNAREs. In the next step the recognition between v- and t-SNAREs mediates the vesicle docking. Rab proteins play a fundamental role in the regulation of this process. The association between v- and t-SNAREs determines the vesicle fusion with the target organelle. Finally the two associated factors α-SNAP and NSF dissociate the SNARE complex upon hydrolysis of ATP.

3. Endoplasmic Reticulum

The endoplasmic reticulum (ER) represents the first compartment of plant secretory system (Vitale *et al.,* 1999). The membrane of ER includes the nuclear envelope and ramifies into the cytoplasm forming a wide network of thin tubules and cisternae in the cortical and inner parts of the cell (Bassham *et al.,* 2008). This compartment is highly mobile and subjected to constant remodeling with a few fixed points such as the plasmodesmata (Hepler *et al.,* 1990).

This compartment is the most versatile organelle of eukaryotic cells and an important site for many biochemical and metabolic roles. The ER maintains contact with the others organelles, likely contributing to their several functions (Bassham *et al.,* 2008).

Soluble secretory proteins are synthesized with an N-terminal signal peptide (SP) which allows them to enter the ER lumen. The SP is a small sequence of 20 - 30 aminoacids composed of three distinct domains: an N-terminal region including 1 - 5 positively charged aminoacids; a central hydrophobic region of 7 – 15 residues; and a polar domain composed of 3 – 7 aminoacids (Von Heijne *et al.,* 1990). During protein translation, a newly synthesized protein which exposes a signal peptide is recognized by a signal recognition particle (SRP). After binding to the nascent protein and the ribosome, SRP allows the complex to attach to the surface of the ER and the nascent polypeptide can enter the ER cotranslationally through a protein pore, the translocon (Hamman *et al.,* 1998). The translocation is a passive process which does not require additional energy. In fact the push provided by the synthesizing ribosome is enough for the nascent polypeptide translocation (Vitale *et al.,* 1999).

The emerging signal peptide is then proteolytically removed in the ER lumen and the newly synthesized protein starts to fold correctly (Vitale *et al.,* 1993). At the end of protein translation, soluble proteins leave the pore and enter into the lumen, while membrane proteins are cotranslationally anchored into the lipid bilayer by one or several hydrophobic transmembrane domains (Vitale *et al.,* 1999).

The endoplasmic reticulum is the compartment involved in folding and assembly of newly synthesized proteins destined to the secretory system. In fact many molecular chaperones involved in these processes have been identified, including chaperonins, the heat shock proteins 70 (Hsp 70), 100 (Hsp 100) and the small HSPs (Boston *et al.,* 1996). The most studied ER chaperone of eukaryotic cells is Bip which belongs to the Hsp 70 family. This family is composed of chaperones of approximately 70 kDa which are expressed upon heat shock and can be involved in plant defence (Boston *et al.,* 1996). Bip is an ATPase involved in the catalysis of protein folding and assembly. It shows high *in vitro* affinity for hydrophobic heptapeptides which are exposed on the surface of unfolded or newly synthesized proteins (Hartl *et al.,* 1996).

Protein disulfide isomerases (PDI) which catalyze the formation and rearrangement of disulfide bonds are also present in the lumen of ER and play an important role in protein folding and maturation (Vitale *et al.*, 1999).

The endoplasmic reticulum is also an important site of protein modification. In this compartment many secretory proteins are N-glycosylated on specific asparagines (Asn) present in the consensus sequence Asn – X (any amino-acid except Pro) – Ser/Thr. N-glycosylation is catalyzed by the multisubunit enzyme oligosaccharyl transferase which is associated in the luminal side of every translocon pore. The modification usually occurs cotranslationally during protein synthesis (Vitale *et al.*, 1999), but a post-translational glycosylation can also occur (Vitale *et al.*, 1993). The main role of glycosylation in plant cells is to assure correct protein folding and to give the protein a good solubility.

The endoplasmic reticulum represents also an important storage compartment in seeds. In fact it has been demonstrated that cereal storage proteins accumulate in the ER lumen forming electron-dense structure named protein bodies (Herman *et al.*, 1999). These aggregates of storage proteins can be permanently stored in the ER or alternatively, directly transferred to protein storage vacuole by a specific pathway. The ability to store proteins in the lumen of ER is a peculiarity of plants, while in animals protein aggregation in the ER is always associated with a pathological state (Vitale *et al.*, 2004). Protein aggregation in not sufficient to generate proteins bodies, but the formation of these structures requires the presence of specific factors and specific properties of the storage proteins themselves (Vitale *et al.*, 2004).

The process involved in protein body formation has been widely studied in maize. This plant possesses different kinds of zeins which are all important in protein body formation. It was demonstrated that both homotypic and heterotypic interactions between the different zeins are important for formation and stability of these structures (Kim *et al.*, 2002). The mechanism leading to the retention of storage proteins in the ER and subsequent formation of proteins bodies is still unclear. It is possible that the lack of an export signal and the intervention of molecular chaperones such as BiP are involved in accumulation of storage proteins in the ER. Alternatively, a direct interaction between the storage proteins and the membrane bilayer could be involved (Kogan *et al.*, 2004).

The region involved in ER retention of γ-zein has been identified as a pro-rich tandem repeat domain, a linker region and a C-terminal Cys-rich domain. This region is probably involved in the binding of Bip which has been found in protein bodies (Geli *et al.*, 1994). Bip can be released from these structures by adding ATP as expected for a chaperone. Therefore it could drive the formation of protein bodies by mediating the retention of storage proteins. Zein protein bodies can also be

solubilized by adding reducing agents, demonstrating the importance of disulfide bonds in protein body formation (Mainieri *et al.,* 2004).

The endoplasmic reticulum is also the principal site of lipid biosynthesis and of oil body formation, which is a very important process in seed development. The ER can exchange material with other organelles, such as plastids, mitochondria and the peroxisomes. Specific ER domains are thought to be involved but the mechanism is still unclear (Bassham *et al.,* 2008).

3.1. Quality control in the endoplasmic reticulum

The ER is also an important check point of correct protein folding and assembly, which can be affected by physical and chemical stresses. This process in which many molecular chaperones play an important role in monitoring the proper folding of proteins is called ER quality control (Hurtley *et al.,* 1989). Thereby a misfolded protein is recognized by the ER quality control and then degraded in a process called ER-associated degradation (ERAD).

In a first step, the misfolded proteins are recognized by molecular chaperones such as Bip and consequently retained in the lumen of ER. The chaperones attempt to refold the proteins to their native structure. The association between defective secretory proteins and Bip is much longer than with newly synthesized correct proteins. A protein that stays associated with Bip for a long time constitutes an ERAD substrate (Vitale *et al.,* 2008). The irreversibly mis-folded proteins are transferred in the cytosol for degradation by the proteasome system. On the contrary, the correctly refolded proteins recover a normal cell function (Hiller *et al.,* 1996). The ER quality control plays several important roles in the cell: to increase the efficiency of protein folding and assembly; to prevent the delivery to target organelles of defective proteins which could interfere with the normal cell functions; to maintain the protein homeostasis, recycling amino-acids (Vitale *et al.,* 1999).

The glycosylation process plays an important role in protein folding, giving the protein more solubility. Inhibition of N-glycosylation by the antibiotics tunicamycin causes many proteins to misfold and many molecular chaperons are then induced (Denecke *et al.,* 1995; Pedrazzini *et al.,* 1996). Two ER-resident lectins (calnexin and calreticulin) are also involved in protein quality control (figure V). These proteins recognize the monoglucosylated glycans of misfolded glyco-proteins and allow their correct refolding and deglucosylation. On the contrary correctly folded glycoproteins are not recognized by this system (Helenius *et al.,* 1997).

The ER quality control is closely related to the unfolded protein response (UPR) which is involved in the protection against severe ER stress (Vitale *et al.,* 2008). Several chemical and physical stress such as treatment with reducing agents or high temperature cause mis-folding of proteins which tend to accumulate in the lumen of ER. Consequently the accumulation of mis-folded proteins lead

to the activation of several genes involved in response to these ER stresses. The UPR mechanism has been well studied in yeast and mammalian cells and is being characterized in plant cells (Vitale *et al.,* 2004).

In mammal cells most Bip molecules are normally associated with three ER transmembrane receptors: PEPK, IRE1 and ATF6 (Rutkowski *et al.,* 2004) (figure VI and VII). Upon different ER stresses the molecular chaperones are requested in the lumen and consequently Bip dissociates from the receptors. PERK and IRE1 are then free to homo-dimerize activating a signal cascade which results in the activation of specific UPR genes, While ATF6 in dissociated form does not make dimers, but can be exported from the ER to the Golgi. In this compartment ATF6 is proteolytically cleaved releasing the N-terminal domain which is translocated to the nucleus where it is involved in activation of several UPR genes (Malhotra *et al.,* 2007).

In plant cells, there are two different candidate activators of UPR: the ER stress-inducer leucine-zipper AtZIP60 (Iwata *et al.,* 2005); and the membrane-associated transcription factor AtZIP28 (Liu *et al.,* 2007). Both proteins are able to activate UPR genes but their specific roles remain to be established (Vitale *et al.,* 2008).

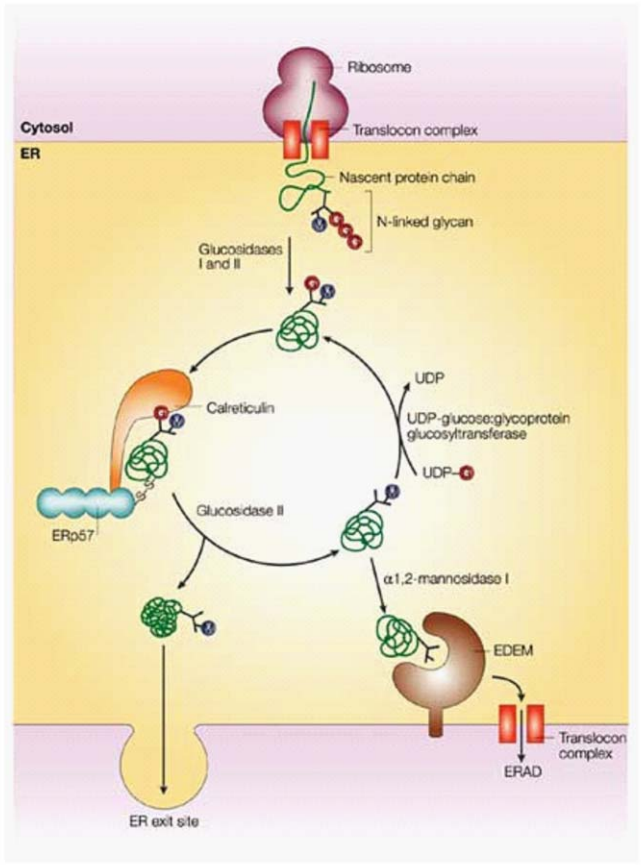

Figure V: The calnexin/calreticulin cycle (Ellgaard *et al.*, 2003). A nascent protein chain is glycosylated in the lumen of ER (the glucose is indicated in red and the mannose in blue). The glucosidases I and II modify the glycan by removing of two glucoses. This reaction creates a monoglucosylated protein which constitutes a specific substrate for calnexin and calreticulin. These two proteins can interact with ERp57 which is a specific disulphide oxidoreductase to form disulphide-bonds with the substrate glycoproteins. Then a specific glucosidase II catalyzes the removal of the last glucose and the resulting folded glycoprotein can be export from ER. In contrast misfolded glycoproteins are the substrates for a UDP-glucose glycoprotein glucosyltransferase which catalyzes the addiction of a glucose. Therefore the mis-folded glycoprotein is now the substrate for a new calnexin/calreticulin cycle. When the glycoprotein is permanently mis-folded, a specific α1,2-mannosidase is able to remove the mannose group. This allows the glycoprotein recognition by EDEM (ER degradation enhancing 1,2-mannosidase like protein) which probably targets the substrate for degradation (ERAD).

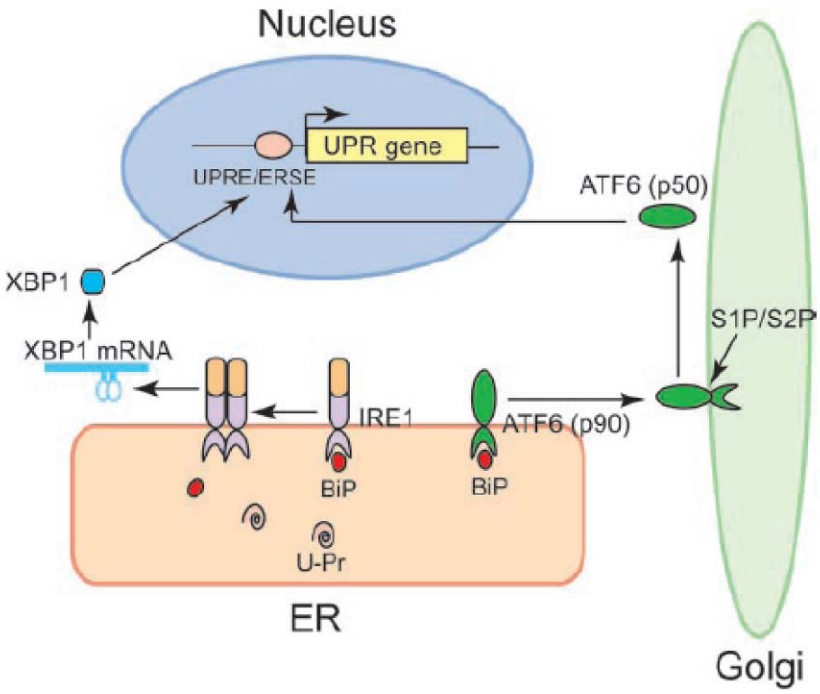

Figure VI: Unfolded protein response mediated by IRE1 and ATF6 (Zhang *et al.*, 2004). The molecular chaperon Bip is released from IRE1 after accumulation of unfolded proteins in the lumen of ER. Consequently, IRE1 can dimerize activating a cascade signal which results in the activation of many UPR genes. This process is mediated by the activation of the transcription factor XBP1. Contrary, ATF6 in monomeric form cannot dimerize, but it can be re-localized in the Golgi apparatus. Then the cytosolic domain of ATF6 can be released in the cytosol upon proteolytic cleavage. Finally, this domain can reach the nucleus activating specific UPR genes.

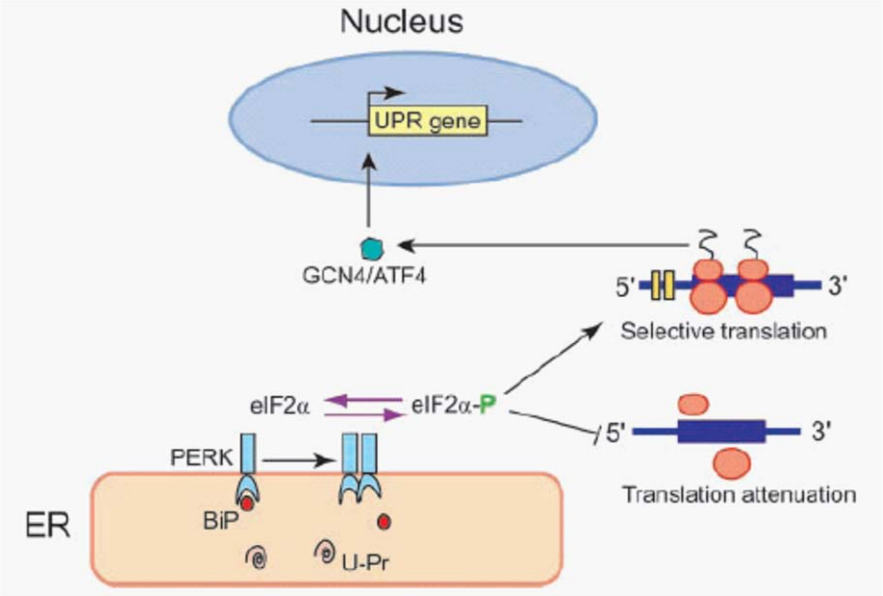

Figure VII: Unfolded protein response mediated by PERK (Zhang *et al.*, 2004). The molecular chaperon Bip can be release from PERK after accumulation of unfolded proteins in the lumen of ER. PERK can then dimerize activating a cascade signal which results in the activation of many UPR genes. This process initiates after phosphorylation of eIFα which activates GCN4/ATF4 transcription factor.

3.2. Traffic between endoplasmic reticulum and Golgi

The ER and Golgi communicate with each other through a highly regulated traffic involving two different kinds of morphologically and biochemically different vesicles. The COPII vesicles are involved in anterograde traffic from ER to Golgi, while the COPI vesicles are implicated in retrograde traffic from Golgi to ER and in internal traffic between Golgi cisternae (figure VIII). The anterograde traffic starts at specific ER domains called ERES (ER exporting site). The presence of ERIS (ER importing site) involved in ER import of COPI vesicles has not been demonstrated. Compared to animal cells, the transport between ER and Golgi in plant cells does not require intermediate compartment and seems to occur directly by vesicular trafficking (Bassham *et al.*, 2008).

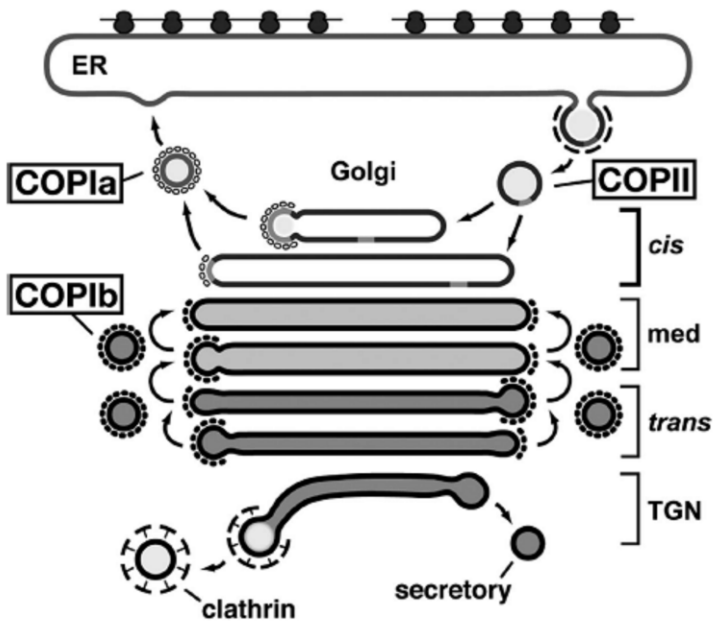

Figure VIII: Traffic between ER and Golgi [Donohoe *et al.*, 2007]. Two different classes of vesicles are involved in the traffic between ER and Golgi (cis, med and trans-Golgi). The COPII vesicles are implicated in anterograde traffic from ER to Golgi. Instead the COPI vesicles are implicated in retrograde traffic from Golgi to ER. It is possible to distinguish two different types of COPI vesicles: COPIa vesicles which bud from cis-Golgi; And COPIb vesicles which bud from medial (med) and trans-Golgi.
At the trans-Golgi network (TGN), two different kinds of vesicles are represented: clathrin-coated vesicles (CCV) and secretory vesicles.

3.2.1. COPII vesicles

The COPII vesicles mediate the anterograde traffic from endoplasmic reticulum to Golgi apparatus in eukaryotic cells. These vesicles have been well characterized in mammalian cells and in yeast, whereas in plant cells they have not been isolated (Hanton *et al.,* 2005). Nevertheless, homologues of many components which constitute the COPII coat have been identified in the *A.thaliana* genome (Movafeghi *et al.,* 1999). Some of these plant components can complement *Saccharomyces cerevisiae* mutants, demonstrating the similarity between the two systems (d'Enfert *et al.,* 1992).

Two models were proposed for the export of soluble proteins by COPII vesicles: the first model involves a passive diffusion of soluble proteins into COPII vesicles; while according to the second model soluble proteins are packaged into COPII vesicles by binding with a specific trans-membrane receptor. Supporting this second model, it was demonstrated that some membrane proteins such as ERGIC53, Em24p and Erv29p are involved in the binding and export of some soluble proteins (Vitale *et al.,* 1999; Barlowe *et al.,* 2003).

The process of COPII vesicle formation requires a specific GTPase which activates the coat assembly, resulting in the budding of vesicles (figure IX). In yeast and mammalian cells, a GTPase named Sar1p is involved in this process. In *A.thaliana* three different homologues of Sar1p have been identified (Movafeghi *et al.,* 1999) and one of these at least is able to complement *S.cerevisiae* (d'Enfert *et al.,* 1992).

COPII coat formation starts with the activation of Sar1p by a guanine nucleotide exchange factor (GEF) named Sec12p. This trans-membrane protein recruits Sar1p at the membrane of ER, activates it by exchange of GDP for GTP. Once activated, Sar1p can recruit all coat proteins (Hanton *et al.,* 2005). The COPII coat is constituted of two sequentially recruited complexes: the Sec23/24p heterodimers which interact with Sar1p and constitute the first layer; and the Sec 13/31p complex which completes the COPII coat (Movafeghi *et al.,* 1999). The coat formation causes membrane curvature and budding of COPII vesicle (Huang *et al.,* 2001). The GTPase-activating protein (GAP) Sec23p is involved in the stimulation of GTP hydrolysis by interaction with Sar1p (Yoshihisa *et al.,* 1993). The dissociation of Sar1p from the membrane causes the disassembly of the coat allowing fusion with the membrane of cis-Golgi. The proteins of the COPII coat are recycled back to endoplasmic reticulum for another cycle of vesicle formation (Hanton *et al.,* 2005).

Interfering with COPII traffic has a marked effect on the protein sorting. For instance, a single point mutation in the aminoacid sequence of Sar1p prevents vesicles budding in mammals, yeast and plants with drastic consequences for endomembrane traffic (Takeuchi *et al.,* 1998).

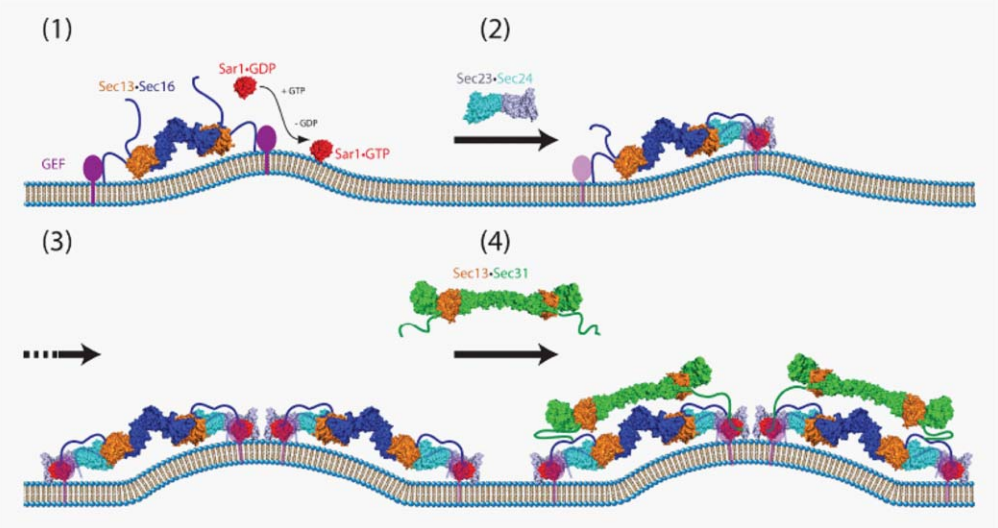

Figure IX: Mechanism of COPII vesicle formation (Whittle *et al.*, 2010). A specific GTPase named Sar1 is involved in the activation of COPII coat assembly. This process starts with the activation of Sar1 by a GEF factor. GEF catalyzes the substitution of a GDP by GTP which results in the activation of Sar1. GEF is a trans-membrane protein which is stably associated with Sec13/Sec16 in a complex. Then the process of COPII coat assembly starts with the recruitment of two complexes: the Sec23/24 heterodimers which constitute the inner part of the coat; and the Sec 13/31 complex which completes the COPII coat. The assembly of coat and the hydrolysis of GTP lead to the membrane curvature and budding of the new COPII vesicle.

3.2.2. Endoplasmic reticulum export site (ERES)

The anterograde traffic from ER to Golgi take place from a specific domain of ER named ERES where the different factors needed for COPII vesicle formation are assembled (Hawes *et al.,* 2008). It is probable that additional proteins are implicated in the formation of membrane scaffold structures which establish the identity of ERES. For instance the two proteins p125 and Sec16 are implicated in the establishment of ERES in mammalian and yeast cells (Espenshade *et al.,* 1995; Shimoi *et al.,* 2005) but no homologues have been identified in plants.

In plant cell, the COPII vesicles have not been isolated and there is not sufficient proof of their existence. The possibility of a direct and transitory connection between ER and Golgi has been debated and many results obtained by electron-microscopy support this hypothesis (Robinson *et al.,* 2007). In fact most evidence which supports normal traffic by COPII vesicles came from *in vitro* studies, but the *in vivo* situation could be very different. Therefore there is no reason to prefer the classical COPII traffic rather than a direct ER/Golgi connection.

The recruitment of cargo proteins at ERES is poorly understood in plant cells. The process is probably similar to mammal cells where the protein cargos are recruited to ERES, incorporated in COPII vesicles and then transported to Golgi (Aridor *et al.,* 2001). Conversely, it is also possible that the cargo recruits COPII factors at ERES and is then transported to Golgi apparatus. Some studies performed in epidermal cell of tobacco leaves have demonstrated an increase of Sec24 recruitment at ERES upon over-expression with a Golgi membrane marker (Hanton *et al.,* 2005). It is therefore likely that the cargo induces the recruitment of COPII factors at ERES. Other studies have also shown a probable increase in ERES site number upon cargo over-expression (Hanton *et al.,* 2007).

3.2.3. ER export signal

Studies performed in mammal cells have demonstrated the presence of specific signals on cargo proteins involved in the COPII assembly and recognition. These signals are specific aminoacid sequences present in the cytosolic part of trans-membrane cargo proteins involved in the interaction with some components of COPII coats (Aridor *et al.,* 1998). Moreover it has been demonstrated that the length of trans-membrane domain influences the localization of single-spanning membrane proteins in the plant endomembrane system (Brandizzi *et al.,* 2002). Probably the length is not sufficient by itself to determine the localization, but other factors could play a role in this process. In fact the ER exporting signals could facilitate protein export by recruiting the COPII coat, overriding the transmembrane length (Hanton *et al.,* 2005).

Different types of signals have been identified in mammalian and yeast cells. In plant cells this mechanism has not been well studied yet, but the signals could be very similar considering the high homology between COPII proteins in mammalian and plant cells (Hanton *et al.,* 2005).

The di-acidic motif (DxE/ExE) was initially characterized in vesicular stomatitis virus glycoprotein VSV-G which is a type I membrane protein of the virus envelope. The DxE motif in the cytosolic C-terminal tail was demonstrated to be involved in export from ER (Nishimura *et al.,* 1997). This motif has been found in several secretory proteins, including the Kir2.1 potassium channel and the yeast membrane proteins Sys1p and Gap1p (kappeler *et al.,* 1997; Malkus *et al.,* 2002). Recently, the presence of di-acidic motif was also demonstrated in plants. The potassium channel KAT1 has two putative DxE sequences, one of which was shown to be involved in ER export (Homann *et al.,* 2006, personal communication).

The second ER export signal to be described was the di-aromatic or di-hydrophobic motif which is constituted by a pair of bulky hydrophobic residues. The type I trans-membrane protein ERGIC53 possesses two aromatic residues in the cytosolic tail involved in protein trafficking between ER and Golgi (Kappeler *et al.,* 1997). The Phe in position -2 (F509) was shown to be implicated in COPII binding, whereas the Glu (Q501) is probably involved in the optimal exposition of F509 (Nufer *et al.,* 2003). Furthermore, the yeast ERGIC53 homolog also presents two hydrophobic residues (LL) involved in ER export. These two aminoacids accelerate the traffic from ER to the Golgi when placed on a reporter protein (Nufer *et al.,* 2002). Another group of proteins which contain a di-aromatic/di-hydrophobic motif is the p24 family. This family is composed of several members of putative cargo receptors which have been found in mammals, yeast and plants. All members contain a conserved Phe (-7 position) and another bulky hydrophobic aminoacid (in most cases a second Phe at -8 position). These two aminoacids were demonstrated to be involved in binding Sec23/Sec24p, the first layer of the COPII coat (Dominguez *et al.,* 1998). Moreover some members contain a di-lysine motif in -3, -4 positions which was demonstrated to interact with COPI coatomers (Letourneur *et al.,* 1994). Plant p24 proteins still have to be shown to bind COPI and COPII coats, respectively to be involved in retrograde and anterograde traffic between ER and Golgi (Belden *et al.,* 2001).

The third ER export signal is based on the presence of basic aminoacids such as arginine and lysine. For instance some Golgi glycosyltransferases possess at their trans- membrane border a di-basic cytosolic motif (RKxRK) which is involved in the interaction with COPII components (Dominguez *et al.,* 1998).

3.2.4. ER retention signals

The aminoacidic sequence H/KDEL is responsible for the retention of soluble proteins in the lumen of ER.

The mechanism was firstly elucidated by fusing the KDEL signal to the lysosomal enzyme cathepsin D which normally localizes in post-Golgi compartments (Pelham *et al.,* 1988). The signal leads to protein retention in the ER and the protein never got the typical modifications by Golgi enzymes. A membrane receptor is involved in binding KDEL, leading to the retrieval of proteins which escape from the ER. The receptor binds the ER proteins at cis-Golgi and sends them back to the ER by retrograde transport. The discovery of the receptor (ERD2) confirmed this mechanism (Lewis *et al.,* 1992). ER-resident proteins such as Bip have never been found in anterograde vesicles suggesting that ER retention is very efficient. Therefore, ERD2 is involved in the retrograde transport of proteins which accidentally escaped by passive diffusion. The receptor does not posses a classical di-lysine motif involved in COPI interaction and the mechanism which leads to retrograde traffic remains to be elucidated (Vitale *et al.,* 1999). However it has been demonstrated that ERD2 receptor is able to self oligomerizes and to interact with the GAP protein ARF1 which is a very important factor involved in COPI formation (Aoe *et al.,* 1997).

3.2.5. COPI vesicles

The COPI vesicles mediate the retrograde traffic from cis-Golgi apparatus to endoplasmic reticulum in eukaryotic cells. Contrary to COPII vesicles, the COPI have also been well characterized in plant cell (Pimpl *et al.,* 2000). This pathway is very important to recycle proteins and lipids back to the ER in order to maintain the equilibrium between the two compartments (Hanton *et al.,* 2005). Moreover in plant cells, it is possible to distinguish two different types of COPI vesicles, the COPIa and COPIb vesicles. The COPIa vesicles bud from cis-Golgi and probably are involved in the retrograde traffic between this compartment and the ER, while the COPIb vesicles form on medial and trans-Golgi and occupy the space around this compartment. Base on this different localization, it is likely that COPIb vesicles are involved in the traffic between the Golgi cisternae (Donohoe *et al.,* 2007).

The COPI formation is induced by the exchange of GDP for GTP on ARF1p factor (figure X). This process start when the ARF1p factor interacts with the Golgi transmembrane protein p23 (Gommel *et al.,* 2001). Then the GDP is exchanged for GTP by a GEF protein, leading to a conformational change of ARF1p which allows its association with the membrane (Helms *et al.,* 1992). This protein associates with the membrane bilayer by insertion of its N-terminal sequence (Antonny *et al.,* 1997). After ARF1p activation, it recruits the COPI coatomer from the cytosol causing

membrane curvature end vesicle budding (Rothman *et al.,* 1996). The COPI coatomer is preassembled in the cytosol and consists of seven subunits: α-, β-, β'-, γ-, δ-, ε-, ζ-COP (Waters *et al.,* 1991). Finally the hydrolysis of GTP by ARF1p causes its dissociation from the membrane and uncoating of the vesicle (Hanton *et al.,* 2005). This process is regulated by an ARF-GAP protein. Plants have many ARF-GAPs, e.g. 15 for *A.thaliana* (Vernoud *et al.,* 2003).

ARF1 activation is specifically inhibited by a lactone antibiotic called Brefeldine A. Inactivation of ARF1 affects the COPI coat formation blocking the retrograde transport from cis-Golgi to ER. This process results in protein accumulation in the lumen of ER. Based on this effect, Brefeldine A is widely used to study protein transport by blocking the ER/Golgi transport (Helms *et al.*, 1992).

The COPI pathway is very important to maintain the equilibrium between retrograde and anterograde traffic. Indeed experiments have demonstrated that the specific disruption of COPI mediated transport by a mutant form of ARF1p results also in an inhibition of COPII anterograde pathway (Pimpl *et al.,* 2003).

The presence of specialized ER domains (ERES) where the formation of COPII vesicles takes place is well documented (Hawes *et al.,* 2008). On the contrary, the existence of ERIS (endoplasmic reticulum import site), i.e. ER sites involved in COPI fusion, remains to be demonstrated (Foresti *et al.,* 2008).

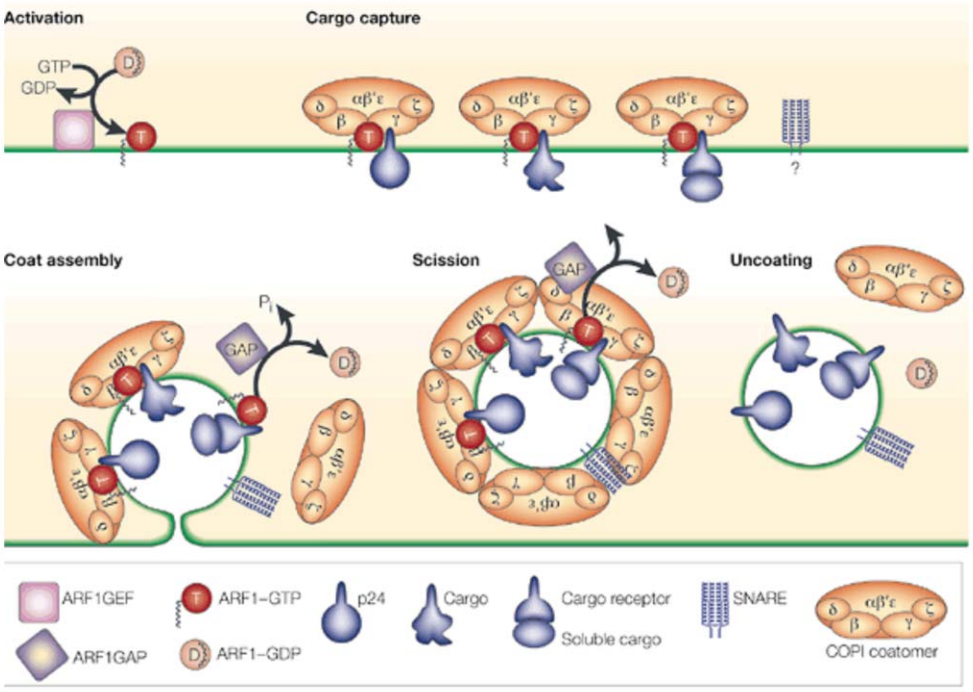

Figure X: Mechanism of COPI vesicle formation (Kirchhausen *et al.*, 2000). The activation of COPI formation is induced by the exchange of GDP for GTP on ARF1 factor. This substitution is catalyzed by a specific GEF factor. The active form ARF1-GTP is now inserted in the membrane activating the COPI assembly. In the first step ARF1-GTP associates with a membrane cargo. After that ARF1-GTP recruits the pre-assembled COPI coatomer (α-, β-, β'-, γ-, δ-, ε-, ζ) with the consequent membrane curvature and vesicle budding. Finally, the hydrolysis of GTP present on ARF1 induces the dissociation of COPI coat resulting in the formation of uncoated vesicles. The hydrolysis of GTP is regulated by a specific GAP protein.

3.2.6. Mechanism of traffic between ER and Golgi apparatus

The anterograde traffic from ER to the Golgi occurs between specific domains of endoplasmic reticulum named ER export site (ERES) and cis-Golgi. In plant cells, the Golgi stacks have been found everywhere in the cytosol and they move very fast along actin filaments. The ER is also a very dynamic and motile compartment constantly assembling and dismantling its interconnections (Boevink *et al.,* 1999). Based on this high motility in plant cells, three different mechanisms of traffic between ER and Golgi have been proposed (figure XI).

The first model, the vacuum-cleaner model, is based on the observation that Golgi stacks move along the ER. During this movement they take protein cargos from ER which is able to export proteins from its entire surface (Boevink *et al.,* 1998).

In the second model, the stop-and-go model, the Golgi bodies move on the ER surface and stop at specific ERES. Therefore, the Golgi apparatus moves from ERES to ERES collecting receptors taking the cargos in charge (Nebenfuhr *et al.,* 1999). This model suggests the presence of specific signals in ERES which cause the detachment of Golgi from microfilaments and a temporary association between the two compartments and transfer of cargos (Hanton *et al.,* 2005).

The last model, the mobile ERES model, is based on the *in vivo* observation that ERES are also moving along the ER and are strictly associated with Golgi bodies (daSilva *et al.,* 2004). Therefore Golgi bodies and ERES move together with a continuous transport of cargos between the two organelles. The nature of contact between ER and Golgi and how the two organelles can move together remain to be established (Hanton *et al.,* 2005).

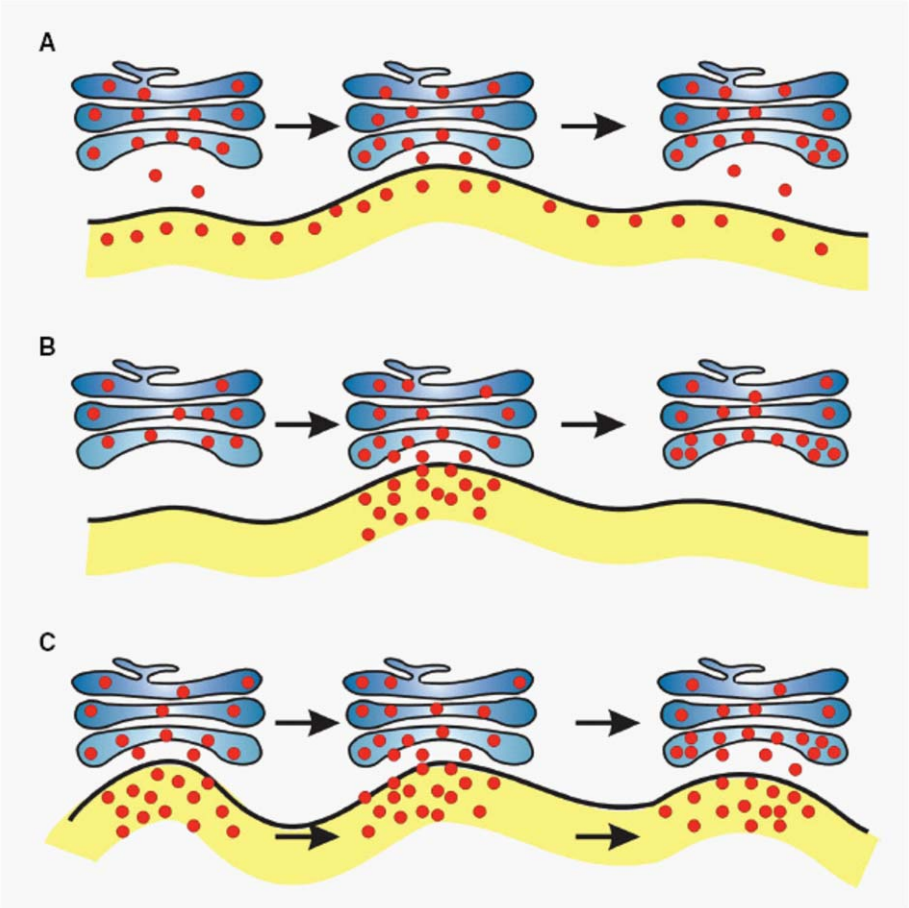

Figure XI: Putative models for protein transport between ER and Golgi apparatus (Hanton *et al.*, 2005). Three different models were proposed to describe the traffic between ER export site (ERES) and Golgi. The vacuum cleaner model, based on the fact that Golgi bodies move along the ER which is able to export cargos from all its surface (A); The stop-and-go model, in which Golgi bodies move along the ER and stop at fixed points where ERES take place (B); And the mobile ERES model, where ERES and Golgi bodies move together (C).

4. The Golgi apparatus

The Golgi apparatus is a central compartment in the secretory system composed of stacked cisternae. In a single stack there are from four to eight cisternae organized in three different regions with different functions: cis-Golgi, medial-Golgi and trans-Golgi. The cis-Golgi constitutes the entrance of the apparatus and the trans-Golgi represents the face where the vesicles leave to reach their final destination (Matheson *et al.*, 2006; Hawes *et al.,* 2008).

The Golgi plays a central role in the plant secretory system, constituting an important traffic point between different organelles, such as endoplasmic reticulum, vacuoles and plasma membrane. It is also a major site of glycan synthesis. It has even been proposed that the Golgi could be implicated in protein traffic with non-secretory organelles like peroxisomes and chloroplasts (Matheson *et al.*, 2006; Hawes *et al.,* 2008).

In plant cells the Golgi stacks are more or less distributed in all the cytoplasm. They are really motile and they can be found subdivided in two different groups: closely associated and isolated from endoplasmic reticulum (Hawes *et al.,* 2008).

There are two different theories for the formation of the Golgi apparatus. The first proposes *de novo* formation from endoplasmic reticulum while the second proposes its formation by division from an existing stack (Shorter *et al.,* 2002). Recent studies in *Chlamydomonas noctigama* (Hummel *et al.,* 2007) and in BY-2 cell (Langhans *et al.,* 2007) suggest that both mechanisms can coexist in the same cell. The experiments were based on complete destruction of the Golgi apparatus by Brefeldine A (BFA) treatment and subsequent washout of the drug. During recovering, they observed a *de novo* formation of Golgi from endoplasmic reticulum. This process was observed to start from small vesicular clusters which fused to form mini-Golgi stacks. A mini-Golgi stack measured about 200 nm and was constituted of at least five cisternae with early cis- to trans-polarity. In both organisms, it was demonstrated that COPII vesicles did participate in early phases of Golgi biogenesis. In contrast, it is likely that COPI vesicles are implicated in membrane fusion, forming initial Golgi cisternae. After regeneration, the cisternae doubled in size and then divided from cis- to trans-Golgi, forming two new Golgi stacks (Hummel *et al.*, 2007; Langhans *et al.*, 2007). In mammals, it was demonstrated that the two matrix proteins, GM130 and p115, could play an important role in Golgi biogenesis (Puri *et al.*, 2004). Many homologues of mammalian matrix proteins have been characterized in plants, suggesting a conservation of the process in the two kingdoms (Latijnhouwers *et al.,* 2005; Latijnhouwers *et al.*, 2007).

The Golgi apparatus of plant cell has many biosynthetic functions and plays an important role in post-translational modification of many secretory proteins. It is responsible of modification and assembly of oligosaccharides present in glycoprotein and proteoglycan. The proteins are N-

glycosylated in the lumen of endoplasmic reticulum by addition of a high-mannose 14-sugar oligosaccharide. In the next step the oligosaccharide is modified by the removal of three terminal glucosyl residues and then transported to the Golgi apparatus. In this compartment several glycosidases and glycosyltransferases are involved in processing and modification of oligosaccharide side chains (Zhang *et al.,* 1992). This compartment is also involved in the biosynthesis of many polysaccharide such as hemicellulose and acidic pectic polysaccharides which are very important components of the cell wall matrix (Bolwell *et al.,* 1988).

The Golgi stacks are organized as a series of cisternae specialized in biosynthetic functions and post-translational modifications of many secretory proteins. Proteins enter the cis-Golgi move then through the medial cisternae and reach the trans-Golgi where the modification process is completed. Each cisterna contains specific modification enzymes to form a multistage processing unit, where the modification occurs in spatially separated successive steps. The enzymes involved in early modification steps are present in cis-Golgi, whereas the enzymes involved in later modification steps are concentrated in medial and trans-Golgi. The functional difference between cis- medial- and trans-Golgi was demonstrated by localizing the glycan modifying enzymes in different cisternae of the stack. This localization was performed by fractionation on sucrose gradient and by immuno-electron microscopy using antibodies against different modification enzymes (Glick *et al.,* 2000).

4.1. Transport through the Golgi apparatus

The mechanism by which the proteins and others compounds move within the Golgi cisternae is not yet clear. Therefore several models have been postulated to describe the protein traffic through the Golgi cisternae (figure XII).

The first, “old model” or vesicular transport model, is based on the presence of transport vesicles involved in the transport of proteins cargos through the Golgi apparatus (Rothman *et al.,* 1994; Rothman *et al.,* 1996). According to this model the Golgi is a static structure of cisternae which contain modification enzymes involved in protein maturation. Therefore each cisterna, from cis- to trans-Golgi, is a stable compartment containing specific enzymes which work one after the other during Golgi transport of protein cargos. In this model, protein-transporting vesicles form on one cisterna and fuse to the next providing anterograde traffic. In this way the molecules can be transported through the Golgi and modified by specific enzymes (Donaldson *et al.,* 2009). Therefore it is likely that vesicles characterized by different coat adaptor proteins are involved in the traffic between cis-Golgi and ER and through the Golgi cisternae. Initial *in vitro* transport

assays and the abundant presence of vesicles in proximity of Golgi stack lead the scientific community to support this first hypothesis.

An alternative “new model” or cisternal maturation model was proposed (Glick *et al.*, 1998). This model considers the Golgi apparatus as a dynamic structure in which the cisternae undergo a maturation process from cis to trans-Golgi. Accordingly, new cisternae are formed by fusion of ER-to-Golgi transport intermediates and of retrograde vesicles which originated on trans- or medial-Golgi. Consequently news cisternae are formed at cis-Golgi and then progressively mature to form medial and trans-Golgi cisternae. Therefore in the Golgi stack, an older cisterna is replaced by the following younger cisterna. Based on this model, the contents of cisternae, such as the modification enzymes, continuously move forward from cis- to trans-Golgi during the maturation process. To restore the proper localization of these enzymes, a continuous flow of budding COPI-coated vesicles takes them back to earlier Golgi cisternae. Functional evidence from live-cell imaging of yeast Golgi where cisternae are not stacked but distant from each other suggest that the traffic through the Golgi follow this second model (Losev *et al.*, 2006; Matsuura-Tokita *et al.*, 2006; Donaldson *et al.*, 2009). The maturation of cisternae was demonstrated by visualizing the replacement of an early marker with a late marker during the maturation of single cisterna from cis- to trans-Golgi.

Recently, a modified cisternal maturation model was proposed. This model is based on a cisternal maturation process in which tubular connections can form between the Golgi cisternae. These connections could be involved in an alternative and rapid transport of protein cargos through the Golgi. This theory is supported on the observation that certain cargos are able to move very fast through the cisternae (Donaldson *et al.*, 2009).

Patterson *et al* performed a study of cargo transport dynamics in living cells, developing a new model of transport through the Golgi apparatus (Patterson *et al.*, 2008). The cisternal maturation model is based on cargo entering in the lumen of Golgi apparatus, while vesicles take the modification enzymes back in the cisternae where the cargos are located. After entering of the cargos in the lumen of the Golgi and the consequent trafficking of modifications enzymes, a lag time is predicted before cargo can leave the Golgi. On the contrary Patterson *et al* demonstrated that cargos exit from the Golgi has an exponential kinetics, with no lag time upon entering the Golgi (Patterson *et al.*, 2008). Based on these experiments they developed a new “rapid-partitioning model”, respecting this kinetic of cargo. Cargos are transported from endoplasmic reticulum to the cis-Golgi, and then are distributed into specific cisternae sub-domains containing the modification enzymes. When cargos enter the Golgi, they can move in a bidirectional manner from cis to trans and from trans to cis-Golgi by specific vesicular traffic. After modification in these specific

domains, the cargos are concentrated in different regions in the same cisternae which are specialized for the exit from the Golgi. Therefore each cisterna is separated in two spatially and functionally different regions. Moreover in this model protein cargos can be exported from the Golgi to plasma membrane from all cisternae and not only from trans-Golgi (Patterson *et al.*, 2008; Donaldson *et al.*, 2009).

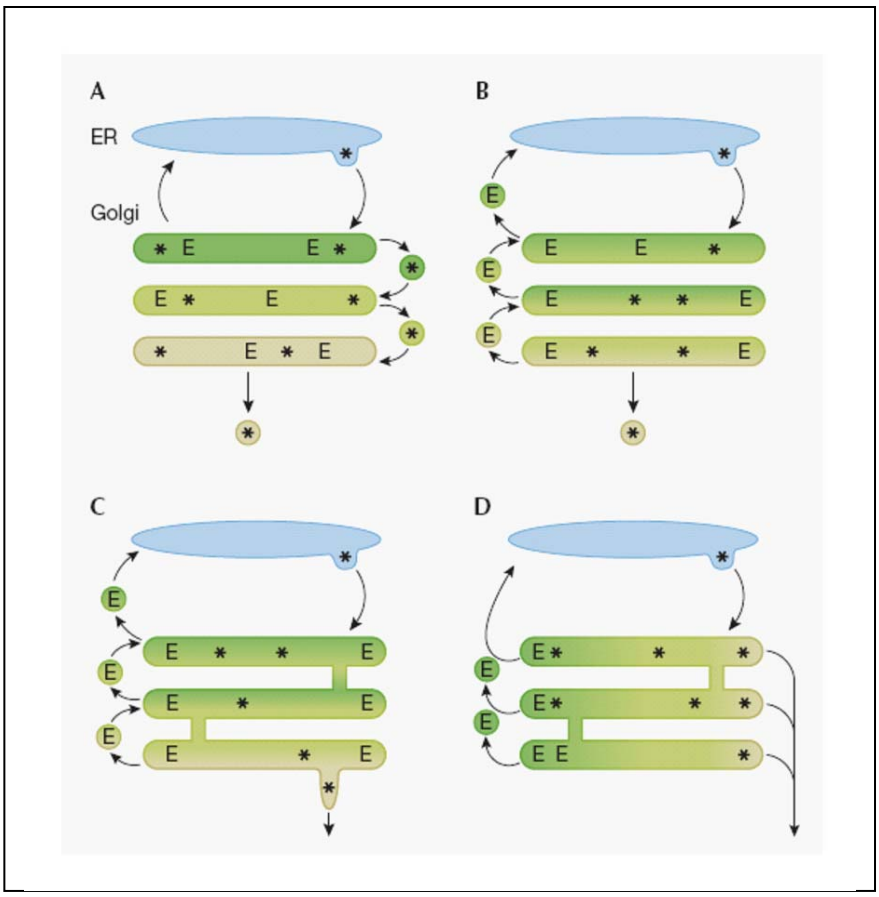

Figure XII: Putative models for protein transport through the Golgi apparatus (Donaldson *et al.*, 2009). Four different models were proposed to describe the traffic through the Golgi apparatus. The "old model" or vesicular transport model; the Golgi cisternae are considered static structures containing modification enzymes and protein cargos move along Golgi stack by vesicular transport (A). The "new model" or cisternal maturation model; the protein cargos remain in the cisternae which progress from cis- to trans-Golgi during a maturation process, at the same time the modification enzymes move back by retrograde vesicular transport to reconstitute the previous cisternae (B). The modified cisternal maturation model is a cisternal maturation model in which tubular connections are involved in a fast transport of certain cargos between the cisternae (C). The rapid-partitioning model; each Golgi cisternae is subdivided in two different domains, one containing modification enzymes and one containing cargos ready to be exported (D).
ER, endoplasmic reticulum. Golgi, Golgi apparatus. E, modification enzyme. Asterisk, protein cargo.

5. The endosomal system and the pre-vacuoles in plants

Endosomes are parts of the secretory pathway which mediates protein traffic to vacuoles. In fact endosomes are important branching points for newly synthesized proteins derived from ER and for proteins coming from the outside (Lam *et al.*, 2007).

In animal cells the endosomal system is divided in early and late endosomes which are morphologically and functionally distinct domains. Early endosomes are then subclassified in sorting and recycling endosomes. Sorting endosomes represent an important center for protein sorting while recycling endosomes especially assume a role in protein recycling. In animal cells the TGN is physically and functionally distinct from endosomes (Raposo *et al.*, 2007).

In plant cells the endosomes and pre-vacuoles mainly include the trans Golgi network (TGN) and the multivesicular bodies (MVB) which have been molecularly characterized with different protein markers such as Rabs and SNAREs (Samaj *et al.*, 2005) (figure XIII). The MVB has been characterized structurally as a compartment containing internal small vesicle structures giving to the organelle a multivesiculated structure. So far, it has also been demonstrated that the MVB represents the prevacuolar compartment (PVC) in seeds and vegetative tissues (Tse *et al.*, 2004; Otegui *et al.*, 2006; Wang *et al.*, 2007). The plant TGN is physically and functionally distinct from the trans-Golgi. In fact the TGN appears to be a completely different organelle, often clearly separated from Golgi bodies (Uemura *et al.*, 2004). In tobacco epidermal cells a fluorescent marker for TGN does not co-localize with a Golgi marker (Foresti *et al.*, 2008). As in animal cells, upon BFA treatment, the TGN aggregates with endosomes to form a TGN-endosomal hybrid compartment, while the Golgi apparatus fuses with ER to form another hybrid organelle. This further supports the notion that TGN and Golgi are functionally and spatially separated (Samaj *et al.*, 2004). Therefore the TGN is part of the endocytic network and consequently the name TGN is not coherent with the proposed function, but on the contrary the correct term would be post-Golgi network (Uemura *et al.*, 2004).

In last few years several experiments investigated the plant endosomal/pre-vacuolar system. The styryl dye FM4-64 as a fluorescent tracer has allowed the visualization of all these compartments. This molecule is internalized into the cell by an active endocytosis process allowing the visualization of internal organelles. After internalization and depending on the incubation time, a succession of different compartments can be visualized (Samaj *et al.*, 2005). In these experiments, the TGN was labeled in an early phase whereas the PVC was labeled later (Dettmer *et al.*, 2006). Based on analogy with animal cells, it has been proposed that plants TGN and PVC correspond respectively to the animal early and late endosomes (Foresti *et al.*, 2008). However after 15 minutes of incubation with FM4-64, 60% of labeled compartments did not co-localized with TGN but with

an earlier compartment which remains to be characterized (Lam *et al.*, 2007). Based on analogy with animal cell, it could represent an endosome involved in recycling of endocitosed proteins. In fact in animal cells the GTPase rab11 localized in recycling endosome which is considered distinct from both TGN and early endosome. The recycling endosome is the earliest endocytic compartment involved in the recycling of cargos back to plasma membrane (Van Ljzendoorn *et al.*, 2006). In contrast the rab11 homologue in plant cells localizes in the TGN, suggesting that this compartment could be the recycling endosome in plants (Foresti *et al.*, 2008)

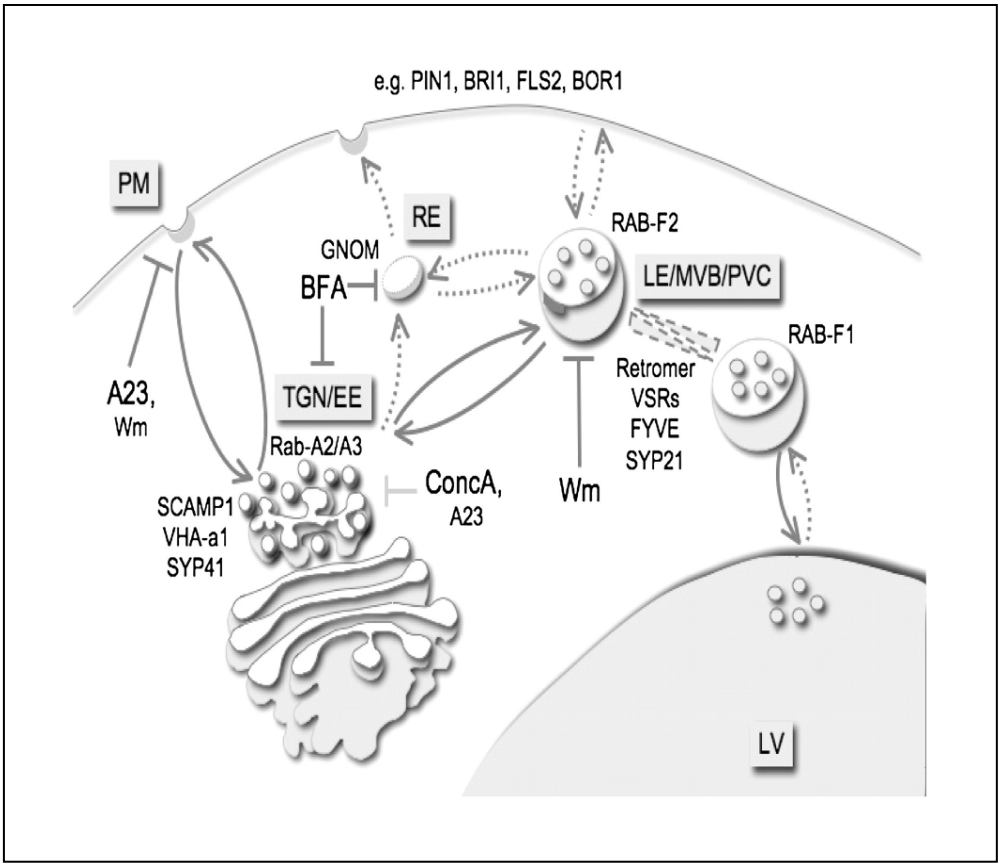

Figure XIII: The endosomal system of plant cell (Robinson *et al.*, 2008). The name of compartments which constitute this system are indicated in boxes: PM (plasma membrane); RE (recycling endosome); TGN/EE (trans-Golgi network/early endosome); LE/MVB/PVC (late endosome/multivesicular body/prevacuolar compartment); LV (lytic vacuole). Different protein markers for different compartments are indicated next to each compartment. The targets of the inhibitors BFA, ConcA, tyrphostin-A23 (A23) and wortmannin (Wm) are indicated in the picture. Arrows indicate trafficking pathways between the compartments: full arrows indicate already described trafficking pathways; whereas dashed arrows indicate hypothetical pathways.

5.1. Endocytosis process

The endocytic machinery involved in the internalization of protein cargos to endosomes/prevacuoles is well conserved in plants. In plant as in animals and yeast, the protein cargos are internalized by first binding with a specific receptor localized in the plasma membrane. The receptor/cargo complexes are then packaged into CCV and delivered to endosomes. In plant cells, CCVs are about 70-90 nm compared to about 120 nm in animal cells. This smaller size facilitates the uptake into cells with a high turgor pressure. Several factors involved in CCV formation in animal, such as AP180 and two adaptins have also been found in plants (Meckel *et al.,* 2004; Barth *et al.,* 2004). Others cargo proteins are internalized into cells at specific plasma membrane micro-domains enriched in sterols, the lipid rafts. In plant cells this second endocytic route is not well characterized but has been proposed to be involved in constitutive endocytosis cycling of some membrane transport proteins (Samaj *et al.,* 2005; Murphy *et al.,* 2005; Borner *et al.,* 2005).

The internalization of some cargo proteins is mediated by specific membrane receptors. The cargo/receptor complex is packaged into vesicles and then delivered to early endosomes which have been identified as TGN in plants. Receptor-dependent endocytosis has been demonstrated for several transmembrane proteins such as the brassinosteroid receptor (BRI1) and the LRR kinase BAK1 (Russinova *et al.,* 2004). Mono-ubiquitination represents an endocytic signal for many membrane receptors and in some cases plays also a role in traffic into internal vesicles of MVB (Mukhopadhyay *et al.,* 2007). From the TGN, the cargo proteins can be transported to MVBs which have been identified as late endosomes. In this compartment four complexes named ESCRT-0, -I, -II and III (endosomal sorting complexes required for transport) collaborate to form the internal vesicles (Bassereau *et al.,* 2010) (figure XIV). In an early step ESCRT-0 is involved in the clustering of ubiquitylated cargos. ESCR-I and ESCR-II then form membrane invaginations next to the clusters. These two complexes are localized inside the bud neck. At this point ubiquitylated cargos can move from the clusters to the bud membrane. Finally ESCRT-III localizes at the neck of the bud and causes to vesicle scission.

ESCRT complexes are well characterized in animal and yeast and are likely to have a conserved role in all eukaryotic cells including plants (Bassham *et al.,* 2008).

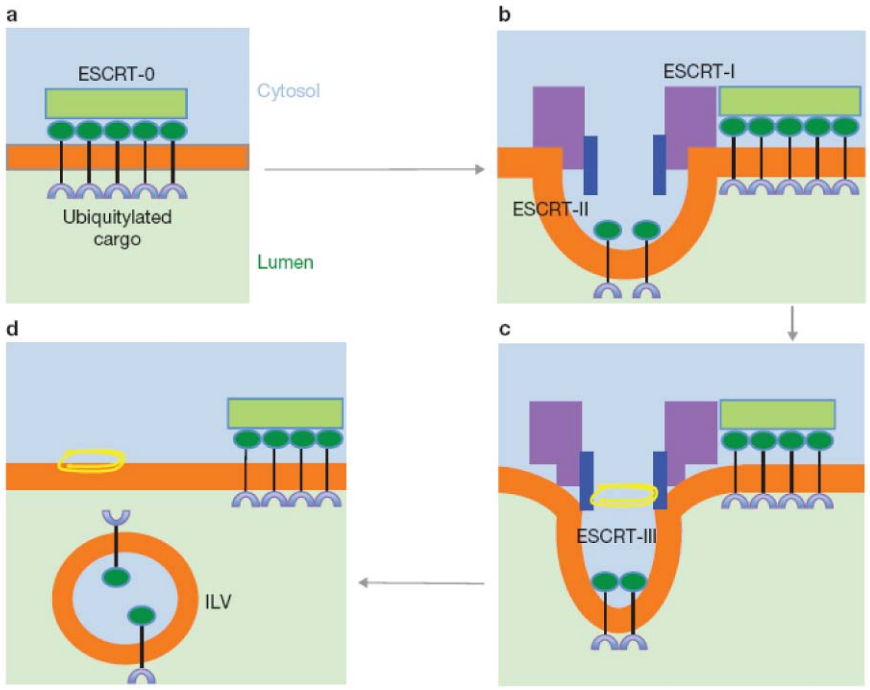

Figure XIV: Intralumenal vesicle formation by ESCRT complexes (Bassereau *et al.*, 2010). (a) ESCRT-0 is involved in the clustering of ubiquitylated cargoes. (b) ESCRT-I and ESCRT-II localize in the bud neck and lead to the membrane invaginations. (c) ESCRT-III localized in the bud neck. (d) Finally ERCRT-III is involved in the vesicle scission leading to the formation of an intralumenal vesicle.

5.2. Traffic at the exit of trans Golgi network

The trans-Golgi network assumes a very important role in the traffic to several post-Golgi compartments such as endosomes/pre-vacuoles, lytic (LV) and protein storage (PSV) vacuoles and plasma membrane (Jürgens *et al.,* 2004). Most vacuolar proteins have specific vacuolar sorting determinants which are involved in the traffic to vacuoles, while proteins lacking these signals are destined to plasma membrane (Hwang *et al.,* 2008). It is generally assumed that vacuolar proteins reach the LV and PSV through separate sorting mechanisms (Robinson *et al.,* 2005). In fact it was demonstrated that the two vacuolar pathways depend on two different SNARE proteins, supporting this model (Sanmartin *et al.,* 2007).

Soluble vacuolar proteins are sorted to lytic vacuoles by binding to a vacuolar sorting receptor (VSR) which is able to recognize specifically the vacuolar sorting determinant present in the aminoacid sequence of the proteins. The first VSR called BP80 was isolated from pea membrane fractions enriched in clathrin (Kirsch *et al.,* 1994; Kirsch *et al.,* 1996). In *A.thaliana* there are seven homologues of BP80 (Hadlington *et al.,* 2000).

The usual model proposed that vacuolar proteins are recognized by VSRs in the lumen of TGN and then transported to prevacuolar compartment (PVC) by clathrin coated vesicles (CCVs). In this organelle, the cargo-receptor complex is dissociated and the receptor is recycled back to TGN for another cycle of transport. The vacuolar cargos in PVC are then transported to lytic vacuole by an unknown mechanism (Hwang *et al.,* 2008).

In animal cells the vacuolar receptor is recycled back from the PVC to TGN by a multi-subunit complex named retromer (Bonifacino *et al.,* 2008) (figure XV). The retromer is a heteropentameric complex highly conserved in several organisms such as yeast, mouse and human. In yeast this complex is constituted of 5 Vps proteins (vacuolar protein sorting-associated): Vps35p, Vps26p, Vps29p, Vps17p and Vps5p. Whereas in mammals it constitute of: a sorting nexin dimer which is composed of an undefined combination of sorting nexins (SNX1, SNX2, SNX5 and SNX6); and a trimer involved in cargo recognition which is composed of Vps26, Vps29 and Vps35 (Bonifacino *et al.,* 2008).

Recently it has been suggested that the transport of vacuolar proteins to LV could be initiated in the ER. In fact, the inhibition of retromer function leads to the inhibition of AtVSR and cargos export from the ER. Moreover, the expression of an AtVSR mutant localized in the ER–leads to the retention of vacuolar proteins in ER lumen. All these results suggest that the ER, and not TGN, is the initial compartment where the interaction receptor/cargo occurs. Therefore it is possible that the retromer machinery mediate the recycling of the receptor from TGN back to ER (Niemes *et al.,* 2010).

Storage proteins are transported to protein storage vacuoles by a different mechanism which is based on protein aggregation. These proteins aggregate from cis-Golgi and continue through Golgi cisternae until the TGN where these structures are packaged in a specific kind of dense vesicles (DVs) (Hillmer *et al.,* 2001; Hinz *et al.,* 2007). The proteins are then transported to multivesicular bodies (MVB) and then to PSV. So far it has been demonstrated that the PVC and MVB are the same compartment in plans vegetative tissues and seeds (Otegui *et al.,* 2006). No vacuolar receptors seem to be involved in the mechanism of DV formation which could be regulated only by protein aggregation. In *A.thaliana*, it has been proposed that a family of putative vacuolar receptors named AtRMRs (receptor-like membrane RingH2) could be involved in this process by providing a nucleation point for storage protein aggregation (Jiang *et al.,* 2000; Park *et al.,* 2005). However, some results suggest that AtVSR1 could also be involved in sorting of storage proteins in seeds. Indeed, in the *A.thaliana atvsr1* mutant, a partial secretion of storage proteins in to the apoplastic space was observed, demonstrating a role of AtVSR in this sorting mechanism (Shimada *et al.,* 2003; Craddock *et al.,* 2008). According to this result, a portion of AtVSR has also been localized in DV (Otegui *et al.,* 2006), suggesting a possible overlap between the two sorting mechanisms.

The mechanism involved in vacuolar sorting of membrane proteins is not well known. However it is possible that these proteins follow the same pathways described before or alternatively, they reach the final compartment by distinct pathways (Hwang *et al.,* 2008). In fact, the existence of an alternative Golgi-independent pathway, involved in sorting of some tonoplast membrane proteins such as α-TIP, has been demonstrated (Jiang *et al.,* 1998).

From the trans-Golgi or TGN, the secretory proteins without any vacuolar sorting determinant are addressed to the plasma membrane or to the apoplastic space (Jürgens *et al.,* 2004). How this active process works and the number of different routes involved in the process are still to be determined. In fact no ultra-structural results have been provided to describe this process (Foresti *et al.,* 2008).

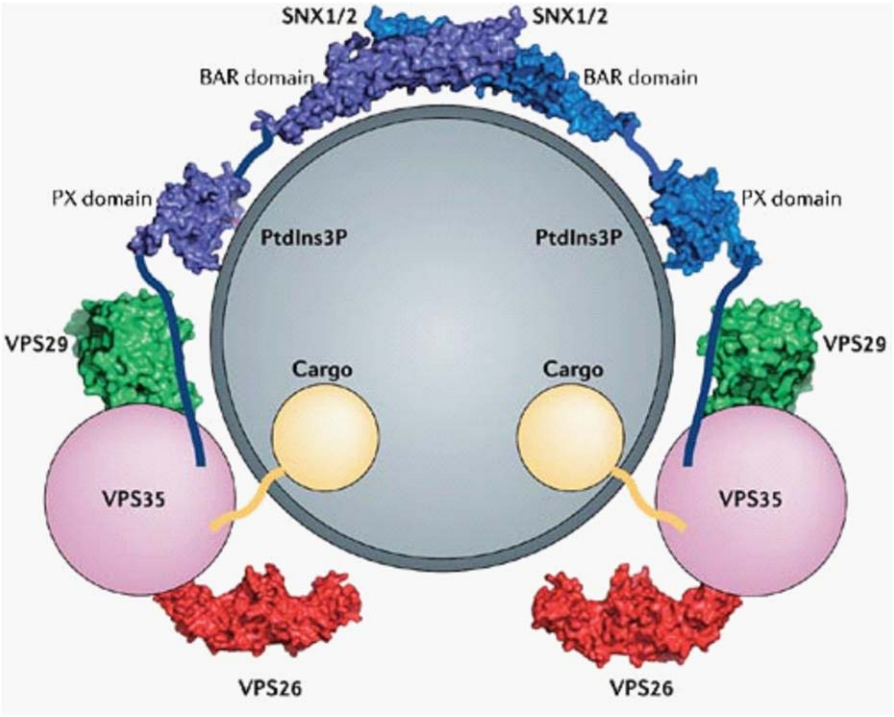

Figure XV: Representation of retromer complex (Bonifacino *et al.,* 2006). In mammals the retromer complex is constituted of: a sorting nexin dimer (SNX1/2); and a cargo recognition trimer (Vps26, Vps29 and Vps35). SNXs are members of a subfamily of sorting nexins containing a PX (Phox-homology) and BAR (Bin, amphiphysin, Rvs) domains. The PX domain is involved in the binding to phosphoinositides such as phosphatidylinositol-3-phosphate (PtdIns3P). Whereas the BAR domain is involved in the sorting nexin dimer formation and attachment to the membrane.

5.2.1. Clathrin coated vesicles (CCVs)

The clathrin-coated vesicles (CCVs) are the first kind of coated vesicles described in eukaryotes. The CCV mainly localize in PM and TGN/endosomes and are involved in traffic of protein cargo between these organelles (Kirchausen *et al.,* 2000).

The clathrin coat is formed by the assembly of single units of clathrin which interact with each others to form a particular cage surrounding the vesicles. A single unit of clathrin is composed of three heavy and three light chains associated to form a three-legged shape structure named a triskelion (Fotin *et al.,* 2004). The clathrin coat is the outer rigid layer structure of the CCV which also requires an internal layer formed by others factors, adaptor proteins such as adaptins (AP), small G-proteins from the ARF family, and/or phosphoinositides (Bassham *et al.,* 2008) (figure XVI).

The AP-family factors are involved in protein cargo selection and sometimes form coated vesicles without the participation of clathrin. In eukaryotes up to four different kinds of AP complexes, which are probably involved in different traffic pathways, have been found (AP1, AP2, AP3 and AP4). Each type of AP complex is constituted of: two large subunits, where the first is α, γ, δ, or ε and the other is β1-β4; one medium subunit (μ1-μ4); and one small subunit (σ1-σ4) (Boehm *et al.,* 2001; Dacks *et al.,* 2008).

The role of the AP complex is to recognize specific aminoacid motifs present on membrane cargo proteins such as tyrosine and leucine motifs. The Tyr motif is Yxxϕ, where Y means tyrosine, x a generic aminoacid and ϕ a bulky hydrophobic aminoacid. Different variants have been characterized differing in the xx, different surrounding aminoacids and different phosphorylation. These tyrosine motif variants can probably be recognized with different specificity by different AP complexes. The second consensus sequence is a di-leucine motif which consists of two bulky hydrophobic residues such as LL or LV. Also, in this case, different AP complexes have different specificity for di-leucine motifs in particular aminoacidic contexts (Rodionov *et al.,* 1998; Honing *et al.,* 1998; Rapoport *et al.,* 1998).

The AP1 complex (γ, β1, μ1 and σ1) has been proposed to be involved in CCV formation at the TGN and endosomes. Moreover, AP1 is the complex involved in the interaction with the tyrosine motif present on VSRs (Sanderfoot *et al.,* 1998). The AP2 complex (α, β2, μ2 and σ2) is involved in CCV formation implicated in endocytosis traffic from PM (Hirst *et al.,* 1998). The AP3 complex (δ, β3, μ3 and σ3) is probably involved in formation of vesicles without clathrin from TGN/endosomes. It has been propose that AP3 is involved in traffic of cargo proteins directly from TGN/endosomes to lysosome/vacuoles bypassing the PVC (Stepp *et al.,* 1997). Finally, the role of AP4 complex (ε, β4, μ4 and σ4) is not well known. It was postulated to be involved in vesicle (with of without

clathrin) formation on TGN. In animal cells this complex is probably involved in a particular kind of traffic between Golgi apparatus and endosome system (Dell'Angelica *et al.*, 1999; Hirst *et al.*, 1999).

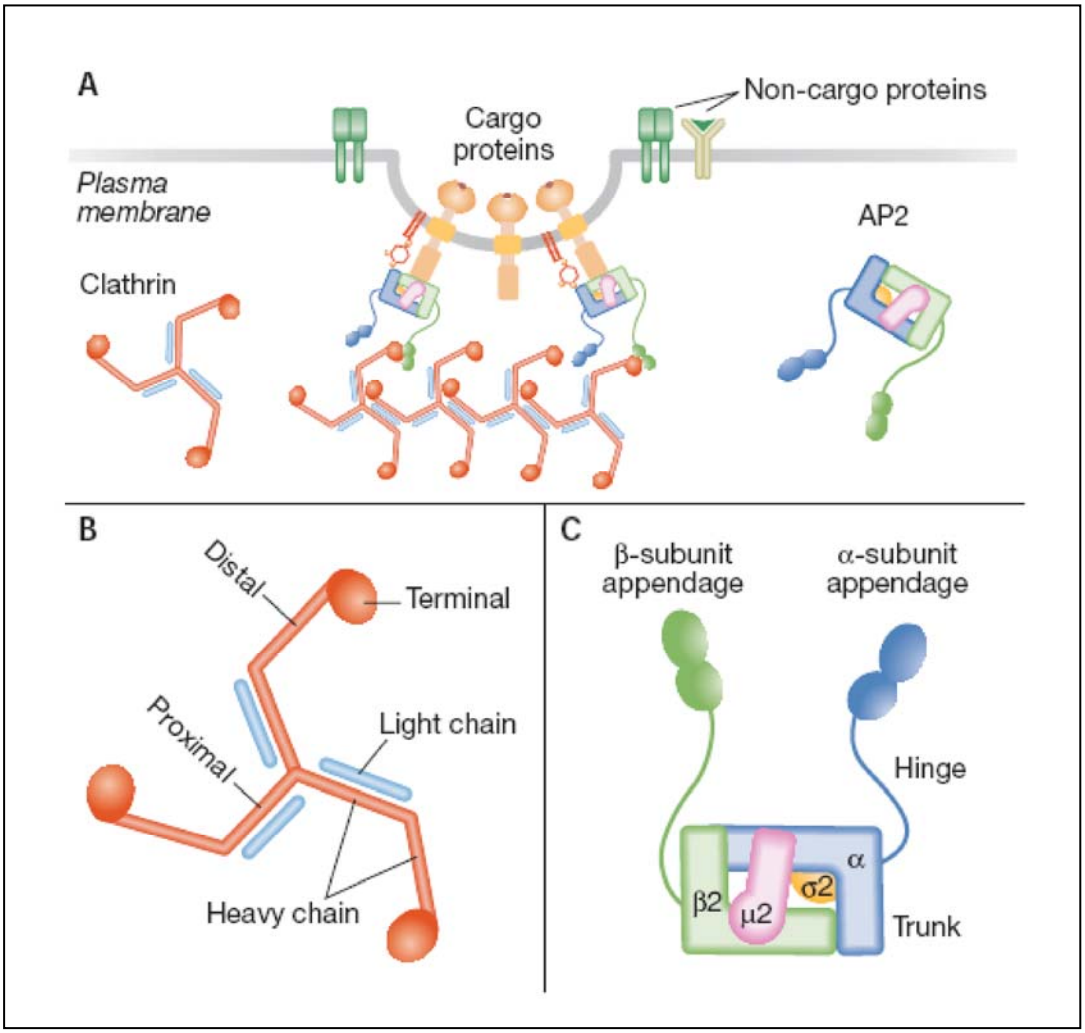

Figure XVI: Clathrin coated vesicles (CCVs) (Puertollano *et al.*, 2004). (A) Clathrin coated vesicles (CCVs) are composed of three different layers. The inner layer is constituted of cargo-binding membrane receptors. The medial layer shows the presence of several factors, such as adaptor proteins (AP) and coat-GTPase from the ARF family. AP proteins play an important role in cargo selection and interaction with the clathrin coat. Finally, the CCVs are surrounded by an external layer which is constituted of clathrin. (B) Schematic representation of clathrin which is composed of three heavy and three light chains associated forming a three-legged shape structure (triskelion). (C) Representation of the AP2 complex which is constituted by the association of several subunits (indicated in the picture). This protein is involved in CCV formation implicated in endocytosis traffic from PM.

5.3. Vacuolar sorting determinats

In several vacuolar proteins specific sequences involved in their sorting to vacuoles have been found by mutation and deletion analysis. Indeed without these VSDs the vacuolar proteins are secreted. In contrast when these sequences are added to a secreted protein, it is now sorted to a vacuole. This demonstrates vacuolar sorting is a dominant process and secretion is the default pathway (Matsuoka *et al.,* 1999).

Many vacuolar sorting signals have been first found by comparing predicted protein sequences and mature proteins. The sequences involved in vacuolar sorting are often present in N-terminal, C-terminal or internal propeptides which are removed during maturation after vacuolar sorting (Matsuoka *et al.,* 1999).

In plant cells three different kind of vacuolar sorting determinants (figure XVII) have been characterized: sequence-specific vacuolar sorting determinant (ssVSD); C-terminal vacuolar sorting determinant (ctVSD); and protein structure-dependent vacuolar sorting determinant (psVSD) (Hwang *et al.,* 2008). The sequence-specific vacuolar sorting determinant (ssVSD) is involved in protein traffic to LV by binding with the vacuolar receptor BP80 (Holwerda *et al.,* 1992; Koide *et al.,* 1999). This signal is based on a NPIR motif which can be present at N-terminal, C-terminal or internal part of many vacuolar cargo. The ssVSD has been amply studied in many vacuolar proteins such as the Cys protease Aleurain from barley (*Hordeum vulgare*) and the storage protein sporamin from sweet potato (*Ipomoea batatas*). Deletion analysis has shown that the NPIR sequence is critical for vacuolar sorting, and it has been demonstrated that the isoleucine in third position is essential for binding with vacuolar receptor. This isoleucine can be replaced only with a leucine without any effect on vacuolar sorting. Therefore, a strict conservation of NPIR sequence it is not essential to have an efficient vacuolar sorting, except for the I/L core (Kirsch *et al.,* 1996; Matsuoka *et al.,* 1999).

The second group of vacuolar sorting determinant is represented by C-terminal vacuolar sorting determinants (ctVSD) or C-terminal propeptides which are characterized by very low sequence specificity. In fact, among these signal no consensus motif has been identified, leading to the notion that the three-dimensional structure of the peptide is probably involved in the traffic (Nielsen *et al.,* 1996). These propeptides are present in aminoacid sequence of many proteins destined to PSV such as chitinase A, β-glucanase and concavalin A (Hwang *et al.,* 2008). For instance, the C-terminal propeptide of chitinase A is composed of seven aminoacids necessary and sufficient for protein sorting to PSV. It has been demonstrated that single point mutations of any of these aminoacids do not have a drastic effect on protein sorting. This demonstrates that no critical aminoacids are present and the entire motif is important for an efficient traffic to vacuole (Neuhaus *et al.,* 1994). On the

contrary, the protein sorting to vacuole is inhibited by putting one glycine residue or an N-glycosylation site just at the end of these propeptides (Matsuoka *et al.,* 1999). Maybe these groups prevent the accessibility of propeptide for binding with a putative vacuolar receptor.

The third class of vacuolar sorting is protein structure-dependent vacuolar sorting determinant (psVSD). In fact, it is well known that certain vacuolar storage proteins are sorted to vacuole by their biochemical properties. The psVSD can be subdivided in two types: the first type is constituted of a particular three-dimensional structure present in native proteins such as particular internal domains observed in legumin (Saalbach *et al.,* 1991). While, the second is based on protein aggregation which is linked to specific biochemical proprieties of some storage proteins (Vitale *et al.,* 1992). The precursor proteins are always more hydrophobic compared to the mature proteins and consequently they tent to form aggregates (Hinz *et al.,* 1997).

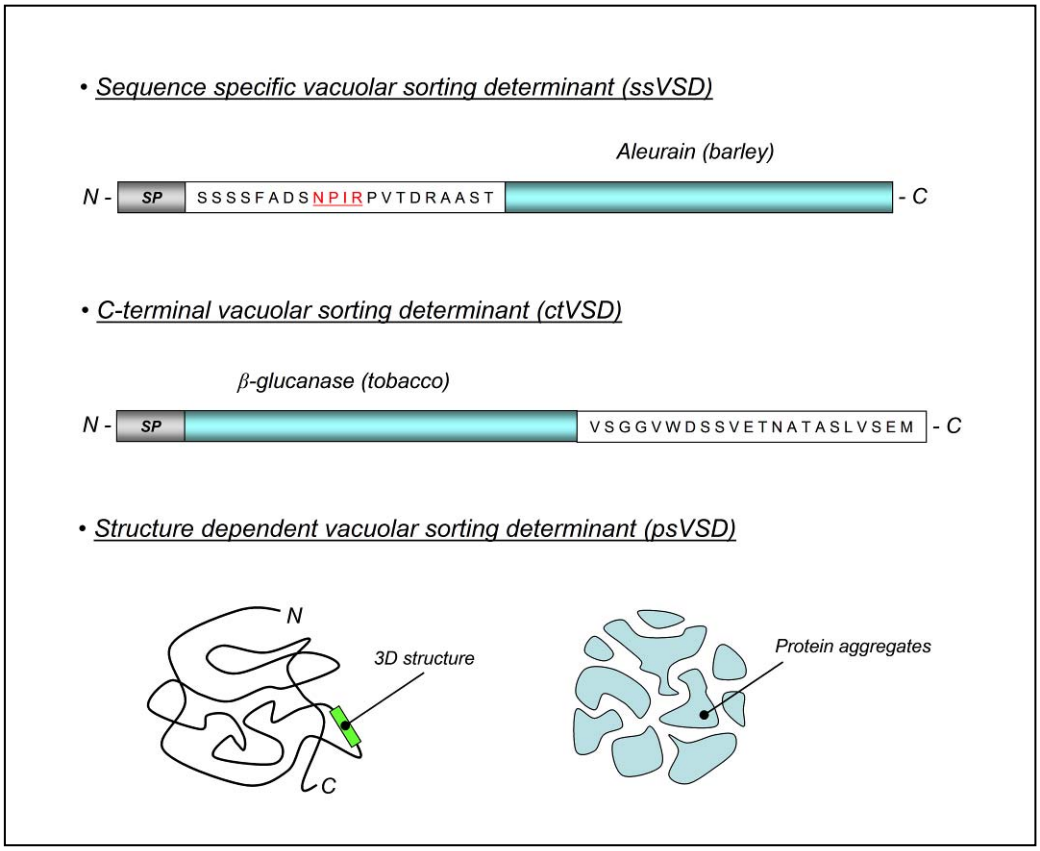

Figure XVII: Vacuolar sorting determinants. Schematic representation of three different vacuolar sorting determinants: the sequence specific vacuolar sorting determinant (ssVSD) of barley Aleurain; the C-terminal vacuolar sorting determinant (ctVSD) of tobacco chitinase; and structure dependent vacuolar sorting determinant (psVSD). The psVSD can be subdivided in two types: particular three-dimensional structures present in native protein; and protein aggregation which could determine vacuolar localization.

5.4. Vacuolar sorting receptors (VSR)

The vacuolar receptor BP80 was originally identified as an 80 kDa protein present in CCV-enriched membrane fractions from pea (Kirsch *et al.,* 1994; Kirsch *et al.,* 1996). This receptor is involved in protein sorting to LV by binding specifically the NPIR motif (ssVSDs) present in some vacuolar proteins such as sporamin and aleurain. In *A.thaliana* there are seven homologues of BP80, AtVSR family which is constituted of seven membrane receptors (Ahmed *et al.,* 2000). VSRs are type I transmembrane proteins which show sequence homology with a domain of the animal epidermal growth factor receptor (figure II). They are not related to sorting receptors at TGN such as MPRs in animal or Vps10 in yeast (Dintzis *et al.,* 1994; Horning *et al.,* 1997; Seaman *et al.,* 1997). AtVSRs are constituted of: a N-terminal luminal protease-associated domain (PA) which is involved in binding the ssVSD of vacuolar cargo; a VSR-specific domain of approximately 320 aminoacids; three Cys-Rich EGF (Epidermal Growth Factor) repeats of approximately 45 amino acids, each of which is predicted to coordinate calcium ions; a transmembrane domain composed of 23 aminoacids; and a C-terminal cytosolic tail composed of approximately 35-50 aminoacids (Hwang *et al.,* 2008).

Several lines of evidences support the involvement of AtVSRs in protein sorting to LV. Firstly, it was demonstrated that the PA domain of AtVSR is able to bind several ssVSDs such as the determinant present in barley aleurain and sporamin (Ahmed *et al.,* 2000). Secondly, in the C-terminal cytosolic tail of AtVSRs a tyrosine motif involved in traffic was discovered. This motif is involved in the interaction with μ-A, an homolog of animal μ-adaptin, which is a component of adaptor protein type 1 complex (AP-1) involved in the packaging into CCV (Happel *et al.,* 2004). Thirdly, the transmembrane domain and the C-terminal cytosolic tail are sufficient for protein localization (Sanderfoot *et al.,* 1998), indicating that the elements involved in protein localization reside in these portions. Fourthly Song *et al*. (Song *et al.,* 2006) demonstrated an interaction between AtVSR1 and the *A.thaliana* protein EpsinR1, a homolog of animal adaptor EpsinR/clint involved in CCV-mediated traffic to lysosome (Kalthoff *et al.,* 2002). They also demonstrated that EpsinR1 interacts with clathrin, actin filaments and AP-1 (Song *et al.,* 2006) indicating a direct role in receptor packaging into CCV. Fifthly it was demonstrated that the C-terminal cytosolic tail of AtVSR interact with VPS35 which is a component involved in receptor recycling in the PVC (Oliviusson *et al.,* 2006). Sixthly AtVSRs were mainly localized in PVC and for a small part in TGN (Miao *et al.,* 2006). This localization is in accordance with the assumption that the receptor cycles between these two compartments.

5.5. Another putative vacuolar receptor family: the RMRs

In contrast the vacuolar receptors involved in protein traffic to PSV are less characterized. It has been proposed that the RMR family (receptor-like membrane RingH2) could mediate this sorting route (Jiang *et al.*, 2000; Park *et al.*, 2005; Park *et al.*, 2007; Hinz *et al.*, 2007). RMR receptors were originally found by homology to the PA domain present in VSR receptors and could also be involved in binding vacuolar proteins. Therefore, it has been proposed that these transmembrane proteins could be the receptors for proteins carrying C-terminal vacuolar sorting determinant (ctVSD) destined to PSV. Supporting this notion, an *in vitro* interaction between RMR and vacuolar proteins with a ctVSD such as barley lectin, bean phaseolin and tobacco chitinase has been demonstrated (Jiang *et al.*, 2003; Park *et al.*, 2007). However, whether RMR really are the receptors for protein sorting to PSV is still unclear.

The RMR family is composed of six members in *A.thaliana* which is subdivided in two different subfamily based on the domain composition (figure II). All RMR receptors are type I transmembrane proteins composed of: a luminal N-terminal PA domain, involved in cargo recognition; a transmembrane domain of 23 amino-acids; and C-terminal cytosolic Ring-H2 domain. In this particular Ring finger domain two histidines and six cysteines are involved in the coordination of two zinc atoms (Cao *et al.*, 2000). In many other proteins, this domain has been shown to be involved in protein-protein interaction and dimerization (Katoh *et al.*, 2005). The first subfamily, AtRMR1, 3, and 4 has in addition a cytosolic Ser-Rich domain which is not present in the second subfamily, comprising AtRMR2, 5 and 6 (Jang *et al.*, 2000). In this domain, several serines are predicted to be phosphorylation sites and are probably involved in protein regulation.

One study in *A.thaliana* protoplasts demonstrated that the majority of AtRMR2 localizes in the prevacuolar compartment (PVC) accordingly with its proposed role in vacuolar sorting. In fact AtRMR2 co-localizes with dark-induced tonoplast intrinsic protein (DIP), a tonoplast water channel often used as a marker for the vacuolar compartments (Park *et al.*, 2005). AtRMR1 has been mainly localized in the late Golgi apparatus, DV and PSV in *A.thaliana* embryos using immunogold electron microscopy (Hinz *et al.*, 2007). This localization of AtRMR1 is also compatible with a role in protein sorting to PSV.

6. Plant vacuoles

Vacuoles are highly dynamic compartments of plant cells which are surrounded by a particular membrane called tonoplast. Most plant cells posses a large central vacuole, which in some cases can occupy more than the 80% total cell volume. This organelle is considered the final compartment of the plant secretory system for secretory proteins presenting a vacuolar sorting signal in their sequences. Plant cell vacuoles can vary in size, function and content based on the different tissues and cell type (figure XVIII). It is also possible that the same plant cell contains one or several kinds of vacuoles coexisting in a particular stage of development (Marty *et al.,* 1999).

Different experimental approaches have allowed the characterization and the functional definition of several kinds of vacuoles. Among the different role of vacuoles, some physical and chemical functions are fundamental for cell viability. These roles include mechanical support by turgor maintenance, which is also involved in cell growth. Moreover the vacuoles participate in homeostasis and degradation, sequestration of many plant compounds such as ions, pigments, secondary metabolites, enzymes involved in defence. In some reserve tissues, the vacuole also assumes an important role in storage protein accumulation (Marty *et al.,* 1999; Frigerio *et al.,* 2008). The vacuole is also implicated in autophagy, an auto-digestion of cell material involved in turnover of several cellular compounds and in defence against pathogens. In this process, new membranes originating from ER incorporate cellular material, leading to the formation of small vacuole which then fuses with the central vacuole. For instance, autophagy plays an important role in the sequestration of some cytoplasmic portions, senescent organelles and pathogens which are then degraded in central vacuole by hydrolytic enzymes (Liu *et al.,* 2005). Finally, the vacuole is also involved in programmed cell death which is an active process involved in the selective elimination of certain cells upon chemical and physical stresses. For instance after pathogen attack, the infected cell respond by eliminating the pathogen through autophagy. Then, if the cell is not able to recover a normal physiological function, it activates a specific program of cell death which leads to mobilization of hydrolytic enzymes in the cytosol by permeabilization of the tonoplast (Gietl *et al.,* 2001; Greenwood *et al.,* 2005).

Vacuoles are considered as very dynamic structures able to change their internal pH according to different physiological conditions. Moreover, they can fuse to form a unique large central compartment or convert between the several kinds of vacuoles of plant cells (Bethke *et al.,* 1999; He *et al.,* 2007).

Vacuoles can be subdivided in two different types: an acidic vacuole, named lytic vacuole (LV), containing hydrolytic enzymes involved in digestion and turnover of several compounds, which is similar to animal lysosome; and a vacuole involved in accumulation of storage proteins called

protein storage vacuoles (PSV) (Marty *et al.*, 1999; Frigerio *et al.*, 2008). These two compartments can be distinguished by their different pH which is visualized using probes sensitive to acidic environments (Swanson *et al.*, 1998). The tonoplast of such vacuoles is also characterized by different composition in membrane proteins and they can therefore be distinguished by using different membrane marker such as tonoplast intrinsic proteins (TIPs). Based on the TIP isoforms localization analysis, it seems that α-TIP is the marker for seed PSV, γ-TIP for lytic vacuole (Jauh *et al.*, 1999) and δ-TIP for PSV present in vegetative tissues (Jauh *et al.*, 1998). Moreover, the two vacuoles can also be differentiated by using different soluble markers such as vacuolar proteins with an ssVSD for LV and vacuolar proteins with ctVSD for PSV (Di Sansebastiano *et al.*, 1998).

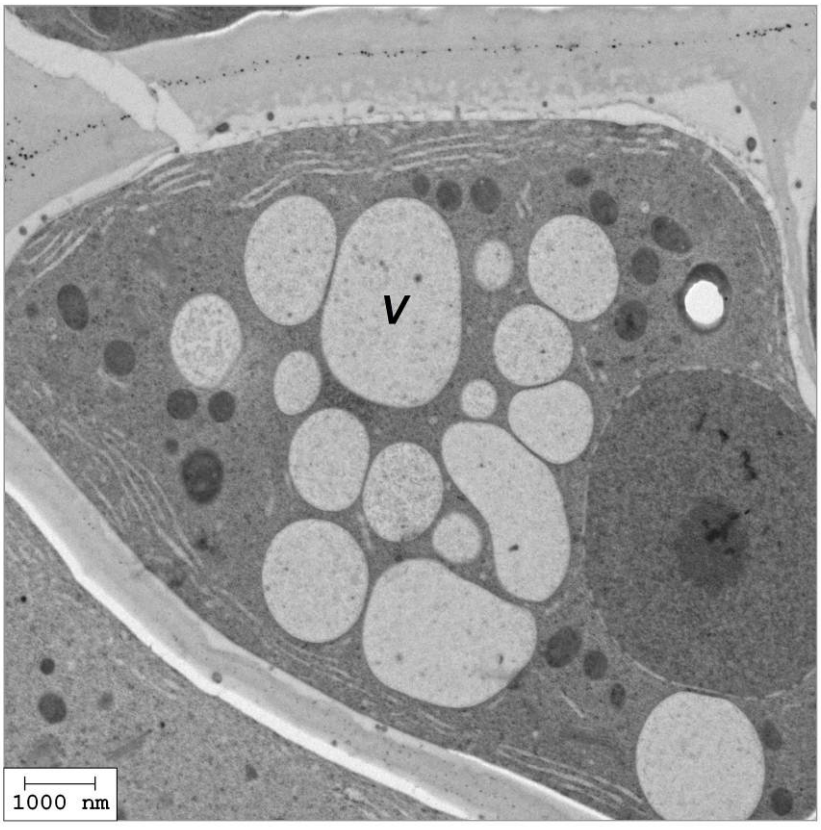

Figure XVIII: The plant vacuole. Overview of a root cell from wild type *A.thaliana* showing the high complexity of vacuolar structures. The many visible vacuolar structures probably constitute a single compartment. In root cells the vacuole can assume a typically branching form.
The vacuolar compartment is labelled (V). Bars = 100 nm.

6.1. Different vacuoles in plant cells

Based on the assumption that the vacuole is a highly dynamic organelle with a lot of function, it was postulated that different kind of vacuoles can coexist in the same cell. In fact, the presence of distinct vacuoles was demonstrated using fluorescent reporter fused to different VSDs and TIPs (Di Sansebastiano *et al.,* 1998; Jauh *et al.,* 1998; Jauh *et al.,* 1999). But in the last few years this idea has been modified based on new experimental evidences. Therefore recent experimental evidences suggested that the presence of several vacuoles in the same cell is rather an exception, present only at some particular stage of development, than a generality (Frigerio *et al.,* 2008).

6.1.1. Evidences supporting the presence of multiple vacuoles

There are only few evidences about the existence of multiple vacuoles in mature cells. For instance, in *Mesembryanthemum crystallinum* under some stresses such as salt stress, the mesophyll cells present two different vacuoles, an acidic vacuole and a neutral vacuole (Epimashko *et al.,* 2004). Also, in protoplasts from barley aleurone cells treated with ABA or gibberellic acid, a second kind of vacuole is generated. These vacuoles contain α-TIP but are physically separated from PSV and do not contain storage proteins in their lumen (Swanson *et al.,* 1998). During cell senescence in *A.thaliana* and soybean mesophyll and guard cells, small acidic vacuoles appear. These compartments are named senescence-associated vacuoles (SAV) and are characterized by the presence of senescence-specific cysteine protease SAG12 (Otegui *et al.,* 2005). Finally, during pea cotyledon development, two different types of vacuoles can coexist. During this stage, the PSV arise like a tubules which surround and subsequently incorporate a pre-existing LV through an autophagy process (Hoh *et al.,* 1995; Klauer *et al.,* 1997).

6.1.2. Data against the multiple vacuole theory

Several experiment performed using membrane and vacuolar soluble markers have provided data in disagreement with the multiple vacuole theory.

6.1.2.1. Tonoplast intrinsic proteins (TIPs)

In some studies performed in barley and pea root tips the presence of multiple vacuoles in the same cell was visualized. In the cell near the meristem they described two different vacuoles using different fluorescent markers: a PSV characterized by the presence of α-TIP and the storage protein barley lectin; and a second vacuole characterized by the presence of γ-TIP and aleurain which can be considered a LV (Paris *et al.,* 1996). On the contrary, a subsequent immunogold microscopy study using different antibodies against TIPs has not confirmed these first results. In root tips they

visualized the presence of only one vacuole containing storage proteins and characterized by the presence of both α-TIP and γ-TIP on the membrane (Olbrich *et al.*, 2007). This result is in agreement with a second study performed in root tips which prove that among the vacuoles present in meristem cells only 1% were LV, with only γ-TIP on the membrane (Jauh *et al.*, 1999).

The TIPs were also used to characterize *A.thaliana* vacuoles which contain 10 TIP isoforms: 3 γ-TIP; 3 δ-TIP; 1 α-TIP; 1 β-TIP; 1 ε-TIP; 1 ζ-TIP (Johanson *et al.*, 2001). Based on expression analysis, the ε-TIP and δ-TIP seem to be preferentially expressed in root, but they present a second peak of expression in floral organs. Moreover, γ-TIP3 and ζ-TIP are expressed in flowers, whereas α-TIP and β-TIP are expressed during seed maturation, and δ-TIP1, δ-TIP2, γ-TIP1 and γ-TIP2 are expressed during early stage of seed development (Frigerio *et al.*, 2008).

A recent study performed in *A.thaliana* stably expressing different TIP-FP fusions (α-, γ and δ-TIP) only one kind of vacuole was visualized. Moreover, in the developing embryos the three markers localized on the membrane of PSV demonstrating that probably only PSV is present at this stage. They also studied the temporal expression and the tissue specificity of the TIP markers by putting the genes under the control of endogenous promoters and terminators. These results showed that the expression of γ-TIP is limited to vegetative tissue except for root tips, while α-TIP is specifically expressed during seed maturation. Also, the third marker δ-TIP as well as γ-TIP, is limited to vegetative tissue except for root tips but in a later stage (Hunter *et al.*, 2007).

6.1.2.2. Vacuolar soluble markers

The first studies performed in tobacco protoplast and *A.thaliana* transgenic plants have demonstrated that the two fluorescent markers, Alu-GFP (containing a ssVSS) and GFP-Chi (containing a ctVSS), mainly localized in two different vacuoles: Aleu-GFP mainly localized in central acidic vacuole (LV), while GFP-Chi mainly localized in non-acidic dots separated from LV, which could be PSV (Di Sansebastiano *et al.*, 1998; Fluckiger *et al.*, 2003). Shortly after these studies were published, it was shown that, in acidic compartment, GFP is degraded by a cysteine protease in a light dependent process (Tamura *et al.*, 2003). Thus, this could have led to underestimation of acidic vacuole when using GFP markers. The problem of GFP degradation in acidic compartment was solved by using monomeric red fluorescent protein (mRFP) which is stable in this environment (Samalova *et al.*, 2006). In another study, transgenic *A.thaliana* plants expressing RFP fusion with either ssVSD (from proricin) or ctVSD (from phaseolin) have been generated. This study demonstrated that both markers localized in the same vacuole in seed, leaves and roots (Hunter *et al.*, 2007). This result was also confirmed by replacing RFP with GFP and putting the transgenic plants in the dark. Indeed in the dark the membrane pumps involved in

acidification does not work and consequently the cysteine proteases involved in GFP degradation are inactivated (Tamura *et al.,* 2003).

All these results support the notion that the two vacuolar sorting signals lead vacuolar proteins to the same vacuole probably through different mechanism.

6.2. Biogenesis of the vacuoles

During embryogenesis the two main kind of vacuole, LV and PSV appear sequentially.

The LV is the first vacuole to appear after fertilization. It is not well known how it is formed *de novo* from small pre-existing vacuoles during development. Nevertheless, it was demonstrated that the LV can be formed *de novo* in evacuolated protoplast, supporting the existence of a normal biogenesis process during plant life (Zouhar *et al.,* 2009).

So far it has been found that the *A.thaliana VCL1* gene, a component of C-VPS complex, is probably involved in LV formation during embryogenesis. Whether VCL1 regulates this process is not yet known, but it was supposed to regulate SYP21 and SYP22 which are involved in the fusion between PVC and tonoplast (Rojo *et al.,* 2003). According to this notion, the inactivation of *VCL1* gene in a KO mutant blocks the formation of LV during embryogenesis. In *vcl1* plant they also observed an accumulation of autophagosomes and thus supposed that the C-VPS complex could be involved in formation of LV from autophagosomes. This is supported by the fact that the homologue of the C-VPS complex in yeast and mammals is involved in autophagosome fusion with the vacuole (Zouhar *et al.,* 2009). In meristematic cells LV does not probably originate *de novo* from autophagosomes but from pre-existing small vacuoles which then expand following a process that could involve autophagy (Inoue *et al.,* 2006). Also in evacuolated protoplasts, the formation of LV was visualized as a process which occurs in parallel with autophagy of cytosolic material (Yano *et al.,* 2007).

It is likely that the PSV appears *de novo* after generation of LV during embryogenesis. Probably this vacuole arises like a tubular structure that grows and then incorporates a pre-existing LV. This is compatible with similar observations in tomato and tobacco seed describing PSV like a big organelle containing small compartment called globoids surrounded by a membrane. It was demonstrated that these globoids have lytic characteristic and they could correspond to a pre-existing LVs incorporated in PSV (Frigerio *et al.,* 2008; Jiang *et al.,* 2001).

Several studies performed in *A.thaliana* KO mutants have identified several genes which can be implicated in PSV formation. None of these KO mutants lacks a PSV, but some present evident alterations in vacuole morphology (Zouhar *et al.,* 2009). For instance the double mutant *vamp727/syp22* present partial secretion of storage protein and fragmented PSV in seeds. A possible

explanation could be that VAMP727 and SYP22 are involved in SNARE complex formation which plays a role in the fusion between PVC and PSV (Ebine *et al.*, 2008). This may explain the partial secretion of storage proteins and the fragmented morphology of PSV. Mutations of two proteins probably involved in plant retromer complex formation, also leads to a fragmented morphology of PSV (Shimada *et al.,* 2006; Yamazaki *et al.,* 2008). The retromer complex probably has several roles in traffic which may explain this altered vacuole morphology.

6.3. Direct traffic from ER to vacuoles

In plant cells, there is evidence suggesting the existence of a direct traffic from ER to vacuoles.

For integral membrane proteins the presence of at least two pathways was proposed; one being sensitive to brefeldin A (BFA), while the other is not (Gomez *et al.,* 1993; Jiang *et al.,* 1998).

Moreover, a direct route from ER to vacuoles bypassing the Golgi was demonstrated for certain vacuolar storage proteins. Electron-microscopy experiments using maturing pumpkin cotyledons showed that the storage protein proglobulin is sorted from ER to PSV *via* precursor accumulating (PAC) vesicles (Hara-Nishimura *et al.,* 1998). These vesicles are large structures about 200 – 400 nm containing unglycosylated precursors of storage proteins. After vesicle fusion with the vacuole, the precursors of vacuolar proteins are released in the vacuolar lumen where they undergo a maturation process. The existence of PACs is also supported by experiments on pumpkin cotyledons treated with monensin (Hayashi *et al.,* 1988). Monensin is an antibiotic from *Streptomyces cinnamonensis* which specifically inhibits protein traffic at the Golgi exit and consequently inhibits the vacuolar transport through the Golgi. However this drug does not inhibit the transport of proglobulin to PSV, supporting the hypothesis that this vacuolar protein follows a direct pathway from ER to PSV, bypassing the Golgi.

Finally, the PAC vesicles are incorporated in the lumen of PSV, following two possible models supported by different experimental evidences. It was postulated that the fusion between PACs and PSV could occur by autophagy or by direct membrane fusion. In maturing seeds of pea and in seedlings of mung bean, the autophagic incorporation of PACs in the lumen of PSV was observed, supporting this first theory (Robinson *et al.,* 1995; Van der Wilden *et al.,* 1980). Instead, supporting the theory of membrane direct fusion between PACs and PSV, two different small GTP binding proteins probably involved in fusion were found on the surface of PACs (Shimada *et al.,* 1994).

Experimental aims

It has been proposed that the RMR family could mediate vacuolar sorting of vacuolar storage proteins. According to this hypothesis, AtRMR1 and AtRMR2 were localized in post-Golgi compartments in the sorting route of PSV. But only few works support this localization and the results are a bit controversial. Therefore in the first part of this PhD project I focalized my attention on the localization of AtRMR1 and AtRMR2 which are the most expressed in leaves. This study was performed in *N.benthamiana* leaves transiently transformed with different AtRMRs fused to fluorescent reporters. Then I have generated stably transformed *A.thaliana* plants using the same constructs. Finally I have generated AtRMR deletion/replacement mutants of different domains in order to characterize putative localization signals.

In the second part of this PhD project I focalized my attention on AtRMR-AtRMR dimerization. To test this hypothesis I performed co-transformation experiment using different AtRMR fusion proteins to different fluorescent reporters. Moreover using deletion/replacement mutants I investigated about the AtRMR domains involved in protein-protein interaction. Finally these results were supported using a Bimolecular Fluorescent complementation technique which allowed investigating direct protein-protein interaction.

Results of localization

1. AtRMR localization

A few years ago a study by immunofluorescence localized most AtRMR2 in the prevacuolar compartment in *A.thaliana* protoplasts. AtRMR2 co-localized with the dark-induced tonoplast intrinsic protein (DIP), a tonoplast water channel often used as a marker for the vacuolar compartment (Park *et al.*, 2005). In contrast AtRMR1 was mainly localized in dense vesicles (DV) with a minor proportion in protein storage vacuoles and in the Golgi apparatus, using immunogold electron microscopy in *A.thaliana* embryos (Hinz *et al.,* 2007).

The proposed localization of these two members of the AtRMR family supports their involvement in vacuolar sorting of different vacuolar proteins to PSV. Contrary preliminary results were obtained in our laboratory. We studied knock out mutant (KO) of AtRMRs 1, 3 and 4 to find hints about the role of AtRMRs in the sorting of vacuolar proteins. However these studies remained preliminary, due to problems with the mutants. A different localization would allow us to formulate new hypotheses about the role of these proteins.

Firstly, I studied the subcellular localization of the receptors by confocal microscopy. This technique allows the visualization of the receptors in living cells when linked to a specific fluorescent protein reporter that we can visualize. For this purpose I generated different expression vectors for experiments in transiently or stably transformed plant cells. In these vectors I fused the coding sequence of different fluorescent proteins (YFP, CFP and eGFP) to either ends of AtRMRs under the control of the 35S promoter and terminator in pGREEN plant expression vector (Hellens *et al.*, 2000). The N- and C- terminal fusion proteins were tested in transient expression assays in *Nicotiana benthamiana* leaves using the agro-infiltration technique or in protoplasts. The same constructs were also used to generate stably transformed *A.thaliana* plants in order to localize the proteins in their plant of origin.

Moreover the same transgenic plants were used in immuno-electron microscopy (IEM) experiments using anti-GFP antibodies, which allowed us to confirm the localization obtained by confocal microscopy.

1.1. AtRMR2 localization in *N. benthamiana* leaves

For this purpose I generated two expression vectors carrying full length AtRMR2 fused to YFP at either C- or N-terminus. The fusion proteins were expressed under the control of the 35S promoter and terminator present in the plant expression vector pGREEN (Hellens *et al.,* 2000).

These constructs were first tested by transient expression in *N. benthamiana* leaves transformed by agro-infiltration. In both cases the pattern of the fluorescent signal was a network structure typical of ER localization (figures 1 and 2). In addition, the signal was also localized at the nuclear envelope supporting the ER localization. This localization was also observed in *A.thaliana* leaf protoplasts transformed with the same constructs (figure 3). Moreover, I co-transformed two different constructs encoding AtRMR2 fused at either ends with different fluorescent reporters (YFP at the C-terminus or mCHERRY at the N-terminus) in order to test if the position of the fluorescent reporter interferes with the localization of the protein. The two signals perfectly co-localized demonstrating that the presence of fluorescent reporter at either terminus has no effect on the localization (figure 4). The free extremities of the native protein are thus not needed for proper localization.

To finally support the ER localization of AtRMR2, I co-expressed the fusion protein AtRMR2-YFP with the ER marker p6-CFP (Peremyslov *et al.,* 2004). The two fusion proteins perfectly co-localized supporting the previous results (figures 5 and 6). Moreover by co-expressing AtRMR2-YFP with the Golgi marker GONST1-RFP (Baldwin *et al.,* 2001), it was possible to visualize a frequent close association between the two compartments (figure 7). Indeed in plant cells the Golgi population was shown to be divided in two different populations, one of which is associated with ER while the other is free in the cytosol (Hawes *et al.,* 2008).

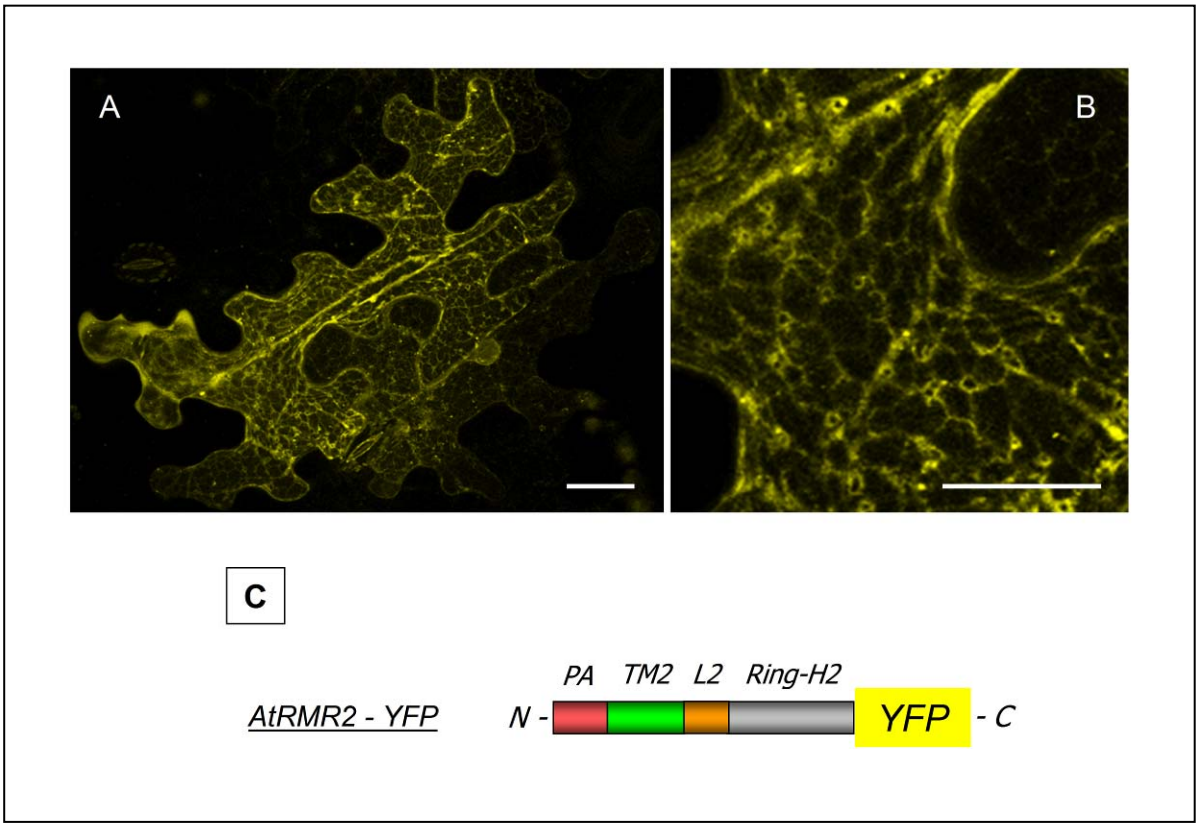

Figure 1: AtRMR2 localization in *N. benthamiana* leaves. Stack of confocal images (A whole cell, B higher magnification) of epidermal cells expressing the fusion protein AtRMR2-YFP. (C) Schematic representation of the fusion protein AtRMR2-YFP: full length AtRMR2 [PA (PA domain, rose); TM2 (transmembrane, green); L2 (sequence linker, orange); Ring-H2 domain (gray)] fused at its C-terminus with YFP. (A) Bar = 40 μm; (B) bar = 20 μm.

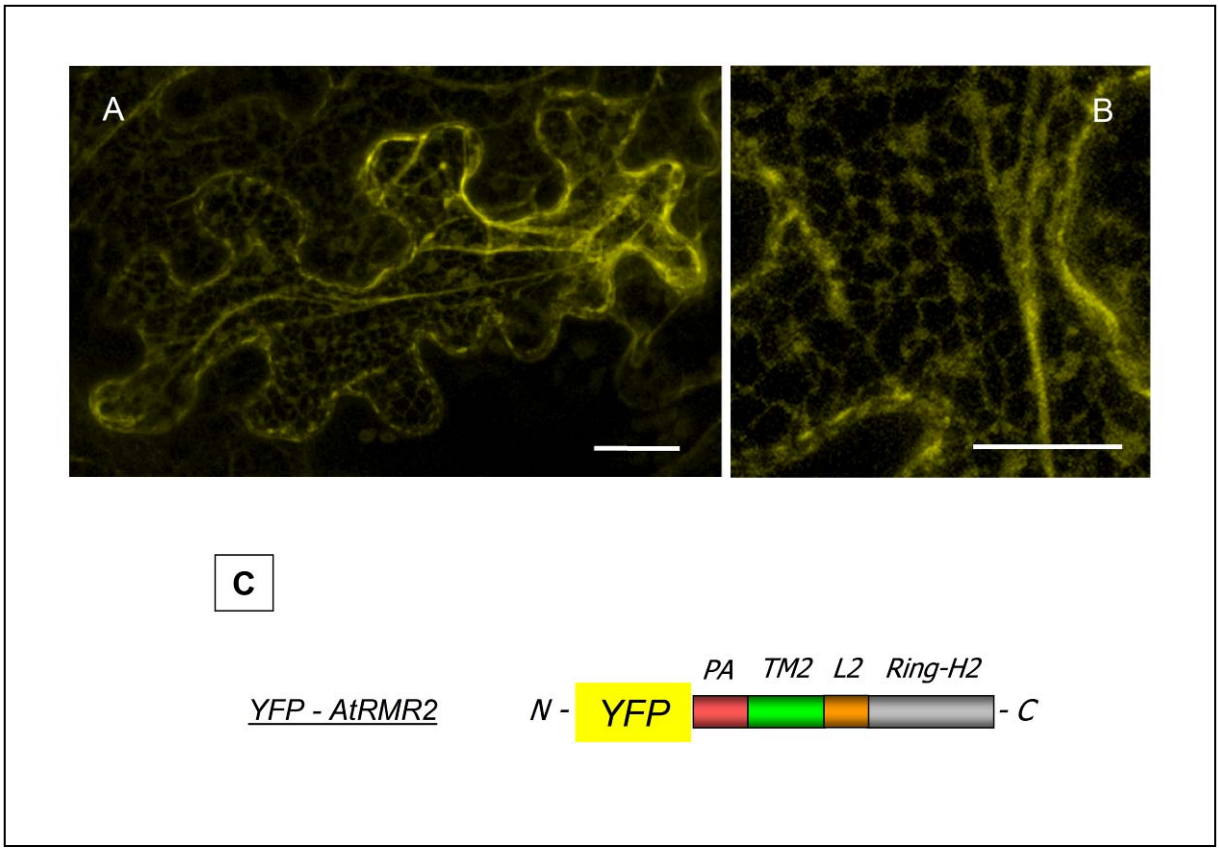

Figure 2: AtRMR2 localization in *N. benthamiana* leaves. Stack of confocal images (A whole cell, B higher magnification) of epidermal cells expressing the fusion protein YFP-AtRMR2. (C) Schematic representation of the fusion protein YFP-AtRMR2: full length AtRMR2 [PA (PA domain, rose); TM2 (transmembrane, green); L2 (sequence linker, orange); Ring-H2 domain (gray)] fused at its N-terminus with YFP. (A) Bar = 20 μm; (B) bar = 20 μm.

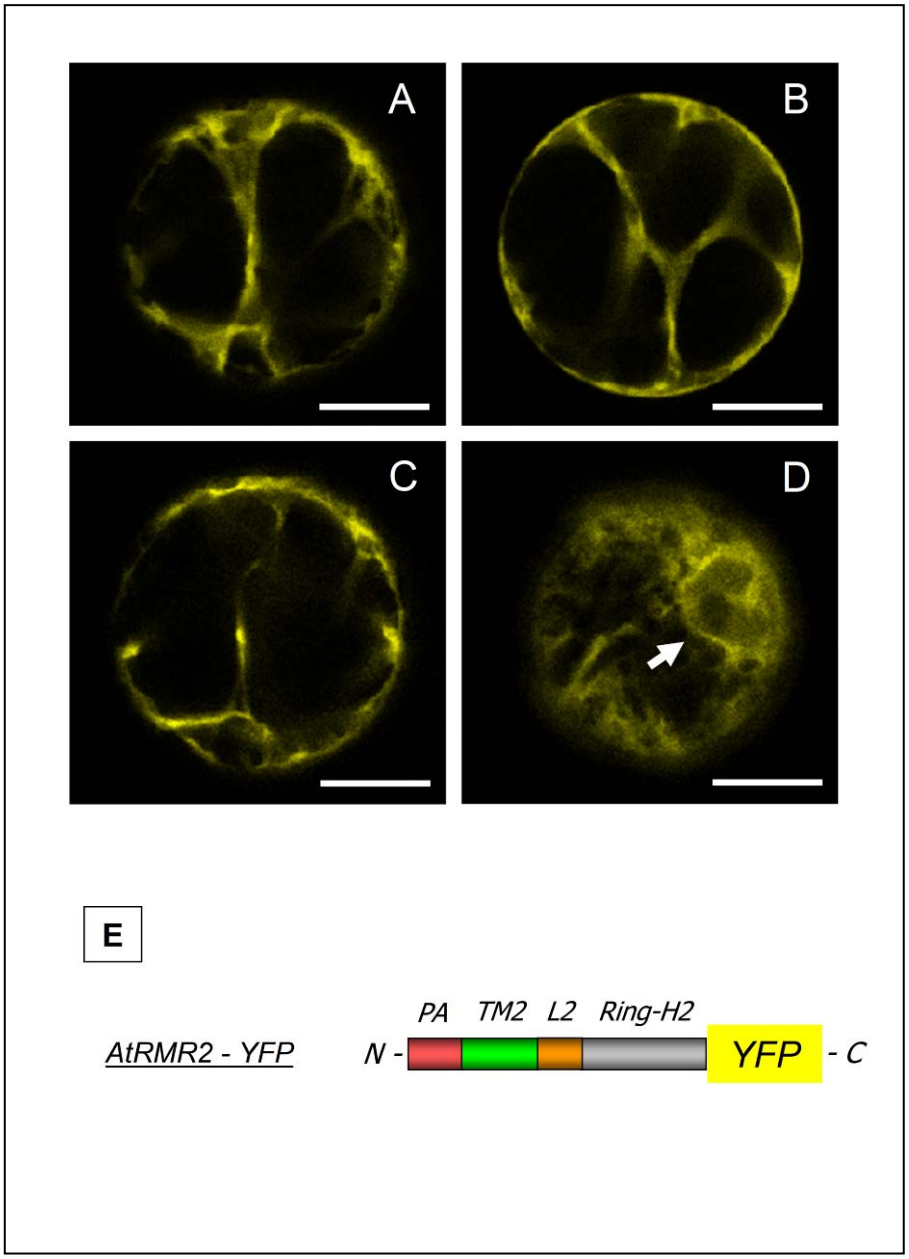

Figure 3: AtRMR2 localization in *A.thaliana* protoplasts. (A-D) Confocal images of a protoplast expressing the fusion protein AtRMR2-YFP. The images represent four sections of the same protoplast (from A, inner part of the cell to D, cell periphery). The arrow indicates the nuclear envelope (D). Scale bar: 10 µm.
(E) Schematic representation of the AtRMR2-YFP fusion protein: full length AtRMR2 [PA (PA domain, rose); TM2 (transmembrane, green); L2 (sequence linker, orange); Ring-H2 domain (gray)] fused at its C-terminus with YFP.

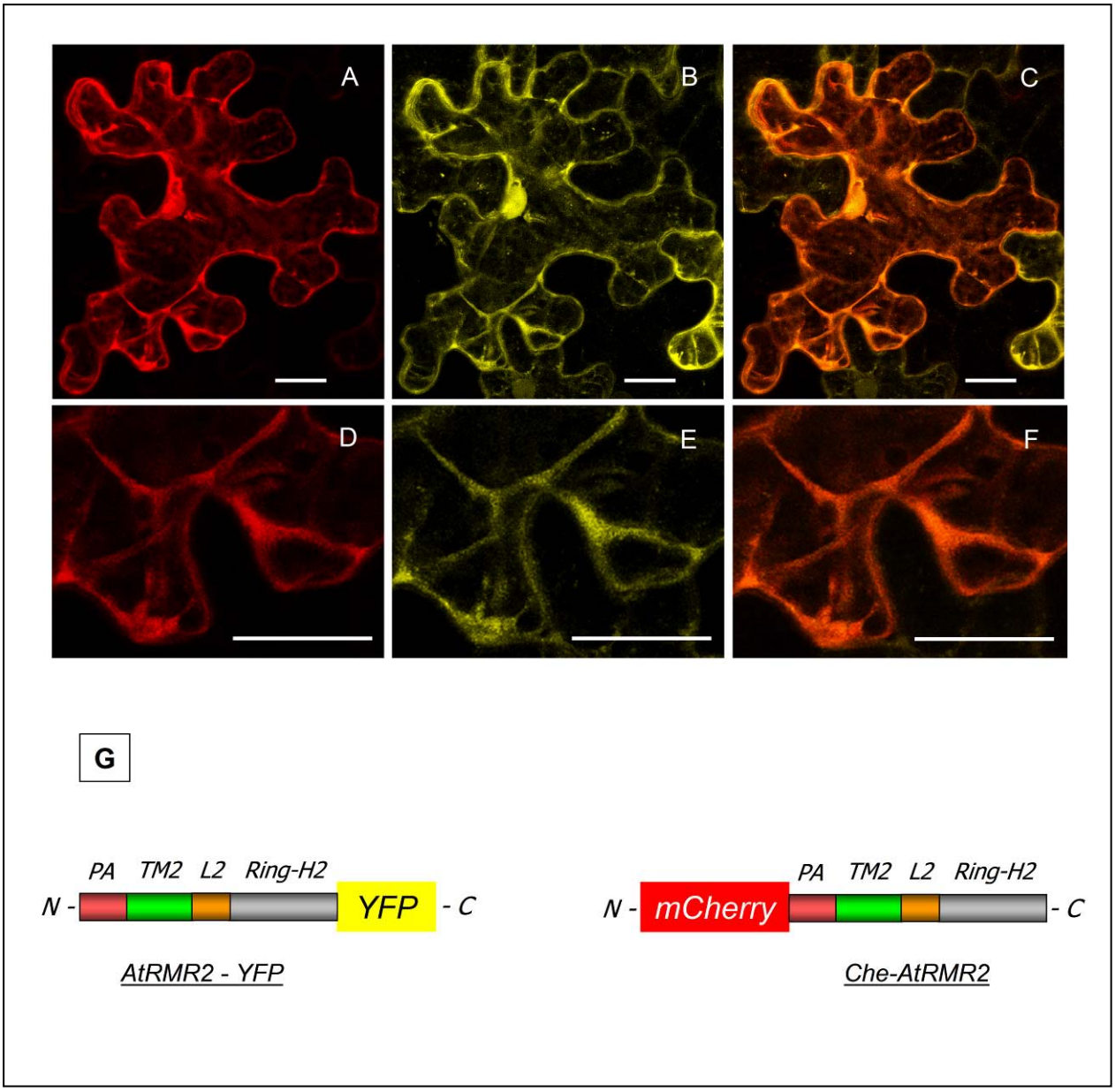

Figure 4: Confocal images of co-expression of Che-AtRMR2 and AtRMR2-YFP in *N. benthamiana* leaves. (A) mCHERRY signal; (B) YFP signal; (C) merged image of the two fluorescent signals. (D-F) higher magnification of a part of images A-C. A-F bar = 25 µm. (G) schematic representation of the fusion proteins Che-AtRMR2 and AtRMR2-YFP: full length AtRMR2 receptor (PA domain, rose; transmembrane, green; linker, orange; Ring-H2 domain, gray) fused at the at the C-terminus with YFP or at the N-terminus with mCHERRY.

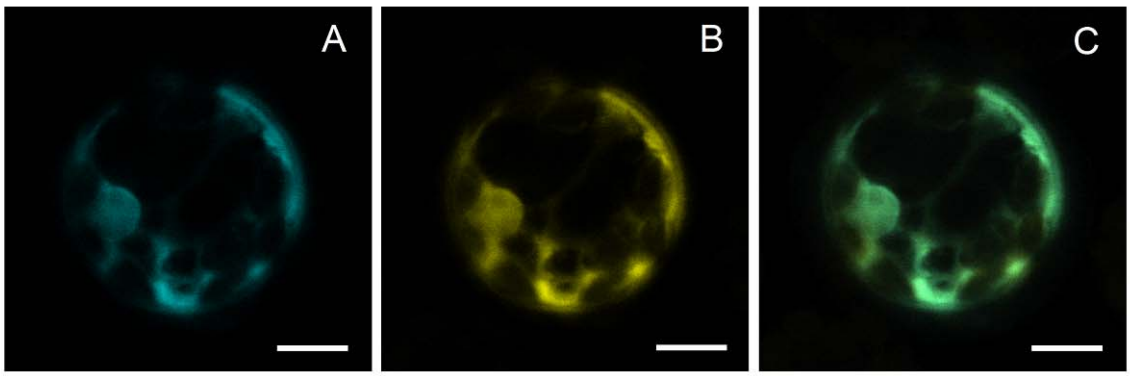

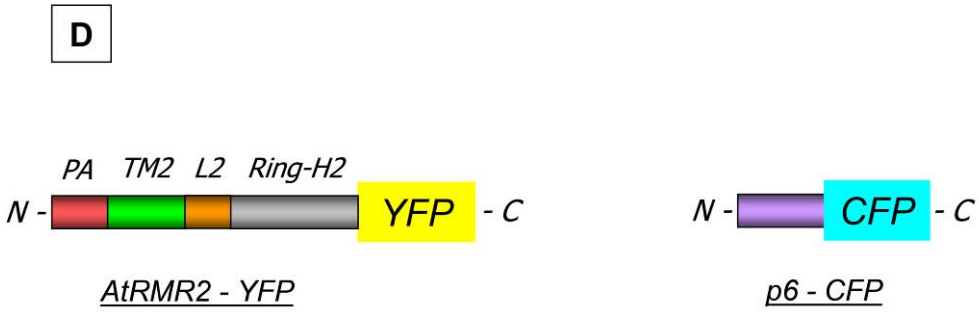

Figure 5: Confocal images of co-expression of p6-CFP and AtRMR2-YFP in *A.thaliana* leaf protoplasts. (A) CFP signal; (B) YFP signal; (C) merged image of the two fluorescent signals. A-C bar = 10 µm.
(D) schematic representation of the two fusion proteins. AtRMR2-YFP: full length AtRMR2 receptor (PA domain, rose; transmembrane, green; linker, orange; Ring-H2 domain, gray) fused at the at the C-terminus with YFP. p6-CFP: full length p6 protein (violet) (Peremyslov *et al.*, 2004) fused at the C-terminus with CFP.

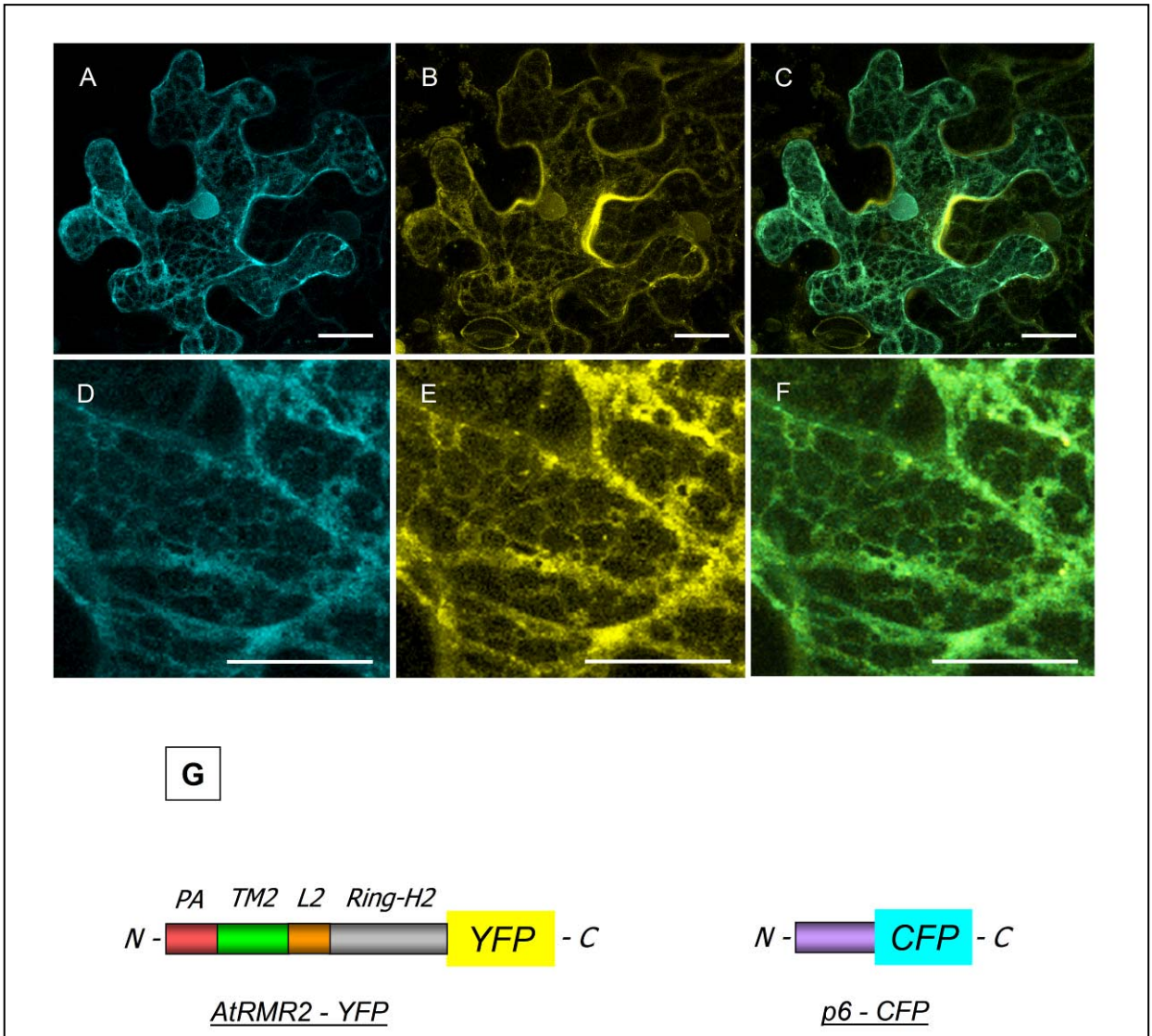

Figure 6: Confocal images of co-expression of p6-CFP and AtRMR2-YFP in *N. benthamiana* leaves. (A) CFP signal; (B) YFP signal; (C) merged image of the two fluorescent signals. (D-F) higher magnification of a part of images A-C. A-C bar = 20 µm; D-F bar = 15 µm.
(G) schematic representation of the two fusion proteins. AtRMR2-YFP: full length AtRMR2 receptor (PA domain, rose; transmembrane, green; linker, orange; Ring-H2 domain, grey) fused at the C-terminus with YFP. p6-CFP: full length p6 protein (violet) (Peremyslov *et al.*, 2004) fused at the C-terminus with CFP.

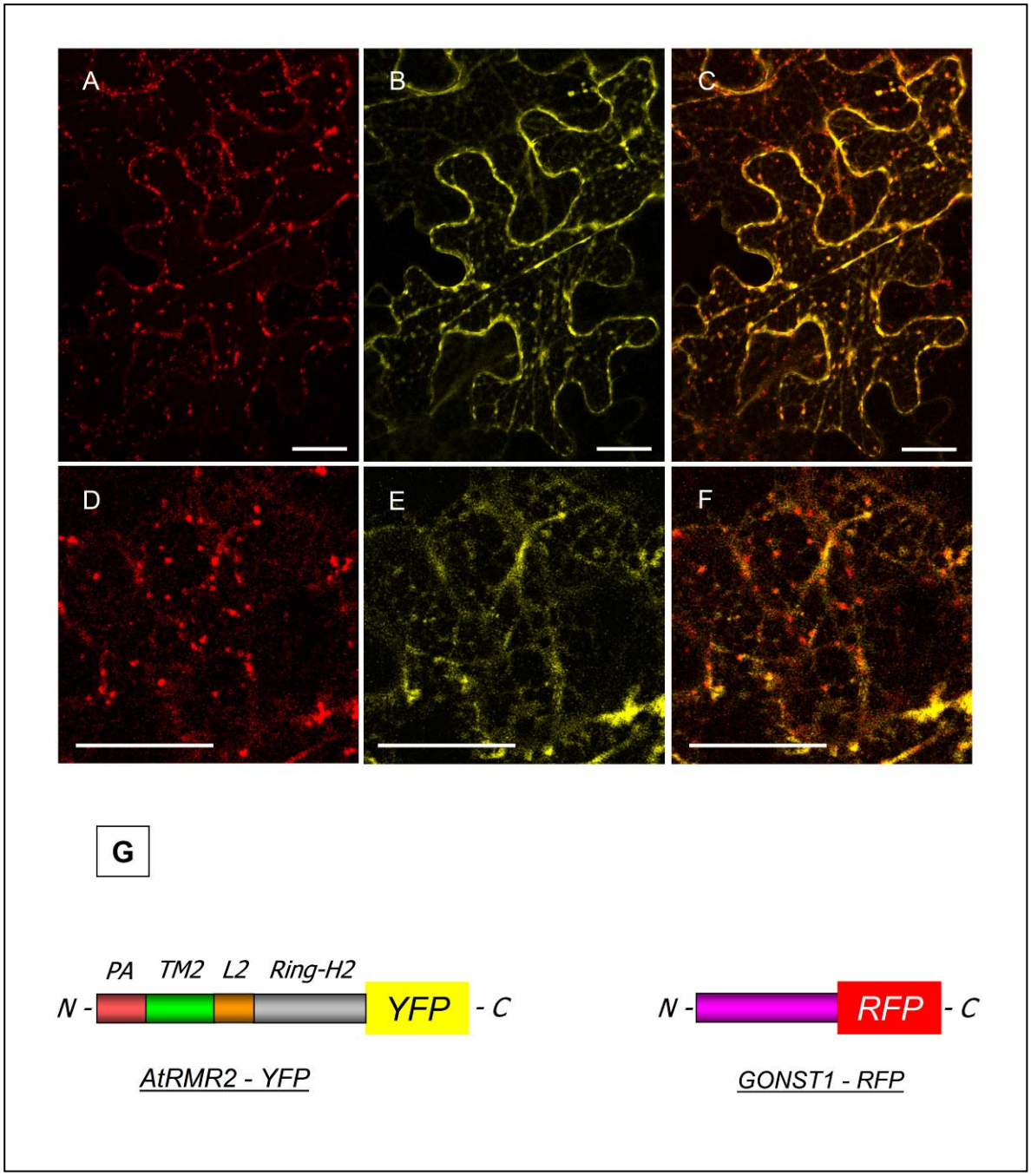

Figure 7: Confocal images of co-expression of GONST1-RFP and AtRMR2-YFP in *N. benthamiana* leaves. (A) RFP signal; (B) YFP signal; (C) merged image of the two fluorescent signals. (D-F) higher magnification of a part of images A-C. A-C bar = 25 µm; D-F bar = 20 µm.
(G) schematic representation of the two fusion proteins. AtRMR2-YFP: full length AtRMR2 receptor (PA domain, rose; transmembrane, green; linker, orange; Ring-H2 domain, grey) fused at the C-terminus with YFP. GONST1-RFP: full length GONST1 (lilac) (Baldwin *et al.*, 2001) fused at the C-terminus with RFP.

1.2. AtRMR2 localization in transgenic *Arabidopsis thaliana* plants

In order to check whether AtRMR2 also localizes in the ER in its plant of origin, I generated *A.thaliana* stably transformed with AtRMR2-YFP. To generate these plants I used a pGREEN plant expression vector (Hellens *et al.,* 2000) with the 35S promoter and terminator sequences which guarantee constitutive protein expression in most tissues.

After molecular characterization, small transgenic plants of four leaves were observed with a confocal microscope. Several plant organs and tissues were characterized, observing a faint YFP signal in all analysed samples (figures 8, 9 and 10). Theoretically the 35S promoter is active in all cells and tissues, but the signal was detected only in the epidermis in all observed samples. A possible explanation could be a silencing of the transgene or 35S promoter (Daxinger *et al.,* 2007) in certain tissues as a form of plant defence against overexpression of viral proteins. Moreover, the fusion protein could undergo a process of post-translational regulation by degradation which would prevent YFP signal observation in certain tissues.

In leaf epidermal cells, the low expression level of the construct prevents the clear localization of AtRMR2-YFP in the membrane of ER (figure 8). Moreover, epidermal cells have a large central vacuole which occupies most part of the cell volume preventing a good observation of ultrastructural structures. In contrast, in guard cells it was possible to localize the fluorescent signal around the nucleus in association with a faint ER network throughout the cytosol (figure 9). In these cells the signal was higher, probably because they are smaller than epidermal cells and consequently the signal is more concentrated. The same result was obtained in root epidermal cells where the nuclear envelope was easier to recognize thanks to the smaller dimension of the vacuole which allows clearer observation of ultrastructural structures (figure 10).

These results obtained in transgenic *A.thaliana* plant support the previous experiments in *N.benthamiana* leaves which had shown the ER localization of AtRMR2-YFP. In particular the observation of different cells in different tissues of transgenic plant has shown a clear fluorescent signal of the nuclear envelope which is typical for ER localization.

Finally, these transgenic plants do not present any morphological alteration and consequently they grow normally like wild type plants. Thus neither the presence of the AtRMR2-YFP transgene nor its site of integration interfered with normal plant growth.

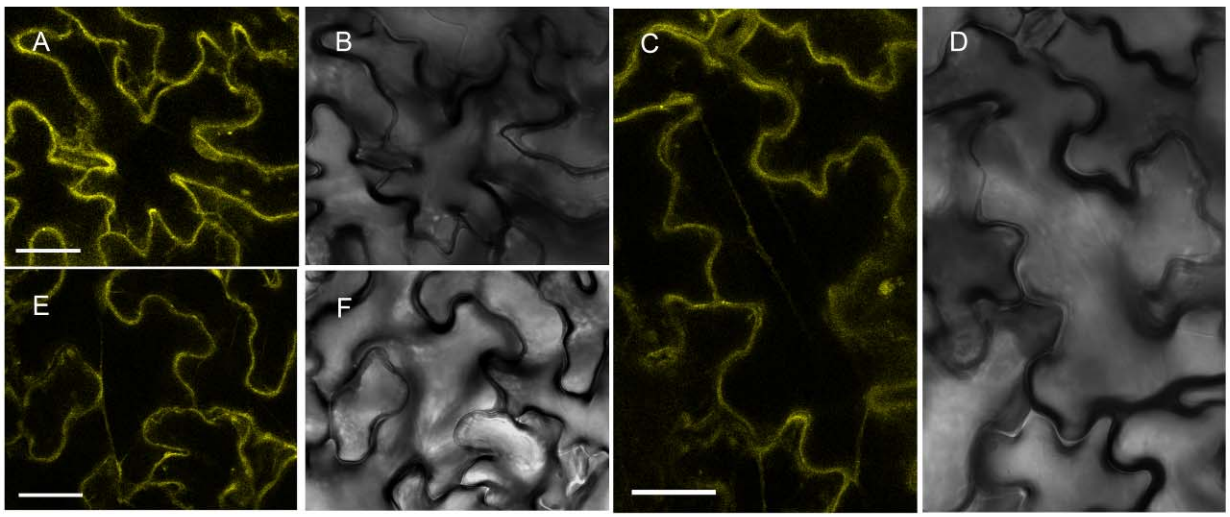

Figure 8: Leaf epidermal cells expressing AtRMR2-YFP. Confocal images of three epidermal cells (A and B; C and D; E and F) from *A.thaliana* stably transformed with AtRMR2-YFP. (A, C and E) YFP fluorescent signal; (B, D and F) bright field of the same cells. Scale bar = 20 μm.

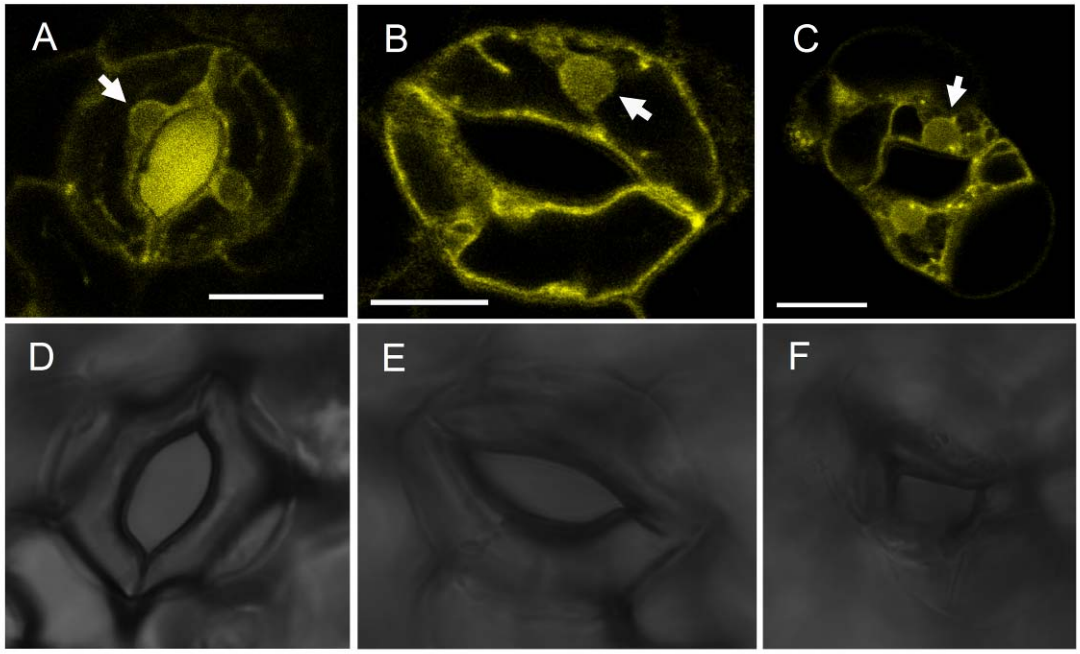

Figure 9: Guard cells expressing AtRMR2-YFP. Confocal images of three stomata (A and D; B and E; C and F) from *A.thaliana* stably transformed with AtRMR2-YFP. The six cells (A, C and E) show specific YFP fluorescence in an ER pattern; the arrows indicate the nuclei. (B, D and F) bright field of respective cells. Scale bar = 10 μm.

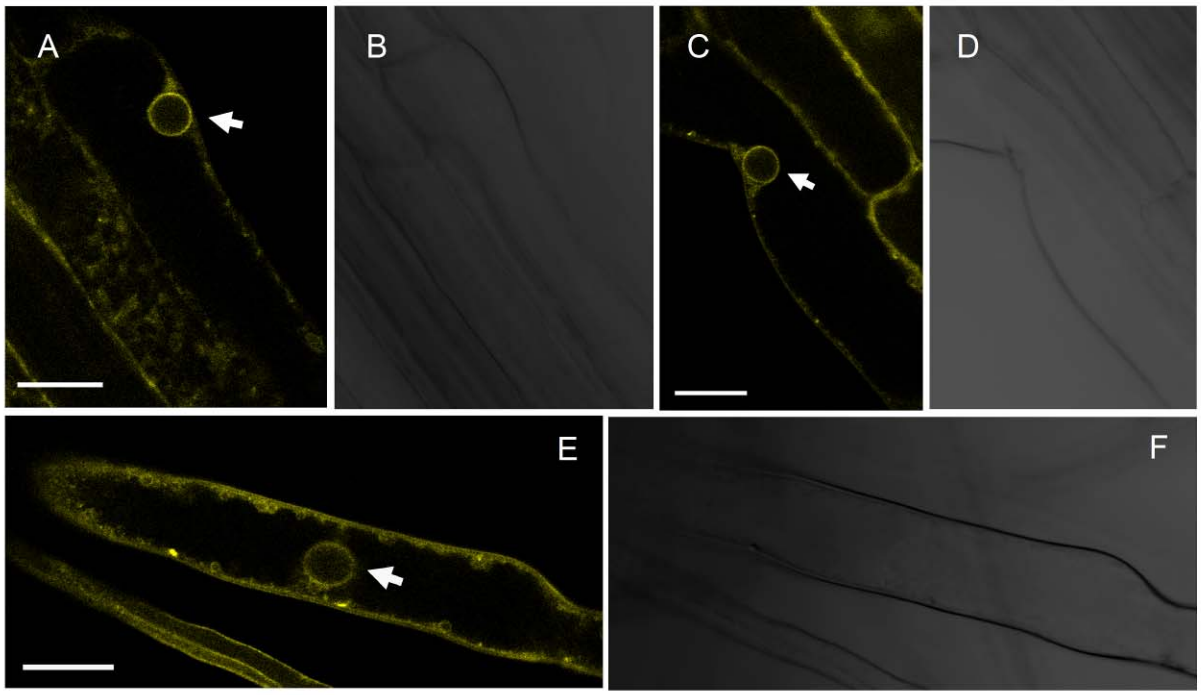

Figure 10: Root epidermal cells expressing AtRMR2-YFP. Confocal images of root cells (A and B; C and D; E and F) from *A.thaliana* stably transformed with AtRMR2-YFP. The three cells (A, C and E) show specific YFP fluorescent signal in an ER pattern; the white arrows indicate the nuclei. (B, D and F) bright field of respective cells. Bar = 20 μm.

1.3. Immuno-gold localization of AtRMR2-YFP in stably transformed *A. thaliana* plants

The previous results obtained by transient expression and transgenic plants support the ER localization of AtRMR2-YFP. The low fluorescence signal detected in transgenic plants prevented however a clear ER localization of fusion proteins. In order to confirm the pattern at higher resolution and to better define the ultrastructural localization, I performed immuno-gold electron-microscopy experiments on these transgenic plants.

These experiments were performed on young roots collected from seedlings. All the samples were prepared by high-pressure freezing followed by freeze-substitution of the samples. The cryofixation at high pressure guarantees a very fast and simultaneous fixation of biological materials. Moreover the low-temperature dehydration of the sample and the concomitant slow water substitution with fixative agents allow the best preservation of cellular structures for the following immuno-gold labelling.

The labelling was performed using a primary anti-GFP antibody and a secondary antibody conjugated with 10 nm gold particles. In root cells most gold particles localized in the ER with a very low unspecific labelling of cytosol and plastids (figure 11). The ER structure is not easy to recognize and necessitates high preservation of cellular structures. This compartment can be recognized as a small filament surrounded by ribosomes localized in both cortical and inner parts of the cells. Moreover the ER also constitutes the nuclear envelope which represents a clear proof of ER localization.

The detection of some unspecific signal in the cytosol could be due to the presence of some free YFP. Indeed fusion proteins are often unstable resulting in the splitting between the investigated protein and the fluorescent reporter. Consequently it is possible to find unspecific YFP signal in the cytosol and inside the nucleus. Cytosolic GFP is known to accumulate in the nucleus. Moreover, it is also possible to find some unspecific signal in plastids. The high protein concentration in these organelles can cause unspecific binding of antibodies.

Root cells from *A.thaliana* stable transformed with AtRMR2-YFP present particular plasma membrane structures which have never been described in plants (figure 12). These curved membrane invaginations grow into the cytosol partly surrounding internal material. They stop before closing the circle and forming a circular compartment independent from the plasma membrane. In some cases it was possible to observe internal structures forming sub-compartments within this circular compartment. These structures were also observed in wild type *A.thaliana*, but more frequently in transgenic plants. Therefore it is possible that the structures could be linked to

AtRMR2 over-expression. However, AtRMR2 seems not to be directly involved in the process because no AtRMR2 labelling was observed in either membrane or internal part of the structures. It is more probable that AtRMR2 is indirectly involved in the process by interfering with other factors.

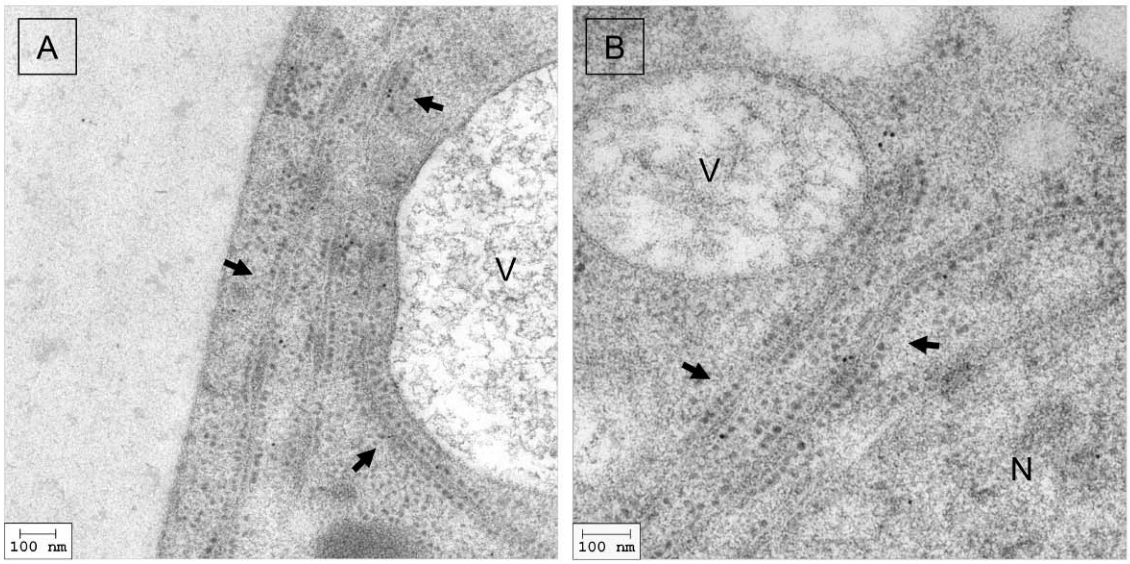

Figure 11: Immuno-gold electron microscopy of root cells of AtRMR2-YFP expressing *A. thaliana* plants. The two images (A and B) show specific YFP labelling of ER structures (black arrows). Vacuolar compartments (V) and the nucleus (N) are indicated. Bars = 100 nm in both images (A and B).

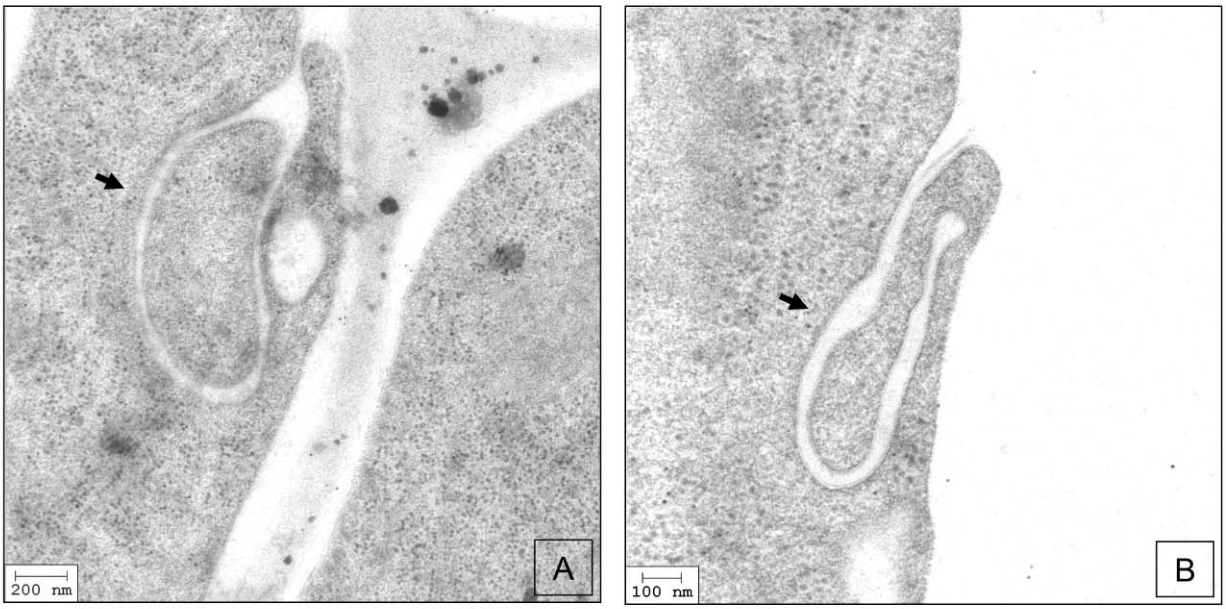

Figure 12: Unknown structures of the plasma membrane. Overview of two root cells from *A.thaliana* stably transformed with AtRMR2-YFP. The two images (A and B) show invaginations of the plasma membrane (black arrows). Bars = 200 nm images A and bar = 100 nm image B.

1.4. AtRMR1 localization in *Nicotiana benthamiana* leaves

For the localization of AtRMR1 I generated two pGREEN-based expression vectors (Hellens *et al.*, 2000) encoding full length AtRMR1 fused to YFP. This reporter was fused to either the C-terminus or the N-terminus. In these constructs the expression of fusion proteins is under the control of the 35S promoter and terminator.

The two constructs were tested in *N.benthamiana* leaves transformed by agro-infiltration. In both cases the fusion proteins localized in punctate structures demonstrating that the presence of the fluorescent reporter does not interfere with the localization of the proteins (figure 13 and 14). Consequently it is likely that free N- and C-termini are not required for the localization of AtRMR1. The same localization as in *N.benthamiana* leaves was obtained in *A.thaliana* leaf protoplasts transformed with the same constructs (figure 15).

In order to identify the compartments visualized as these punctate structures, I expressed AtRMR1 with a number of protein markers specific for different plant organelles. AtRMR1 did not co-localize with the viral protein p6 (Peremyslov *et al.*, 2004) (figure 16) nor with GONST1 (Baldwin *et al.*, 2001) (figure 17), markers respectively for ER and Golgi apparatus. In contrast AtRMR1 perfectly co-localized with the *trans*-Golgi network (TGN) marker SYP61 (Uemura *et al.*, 2004) (figure 18) and partially co-localized with the BP80 reporter (Miao *et al.*, 2006) (figure 19) which is a marker for PVC. According to these co-expression results AtRMR1 localizes at the level of the TGN. This is consistent with the partial co-localization with the BP80-based reporter which recycles between PVC and TGN. Indeed most of this marker was found in PVC but a small proportion was present in the TGN (Miao *et al.*, 2006). That AtRMR1 does not co-localize with GONST1 fits with the model that Golgi apparatus and TGN are two spatially separate organelles (Uemura *et al.*, 2004; Foresti *et al.*, 2008).

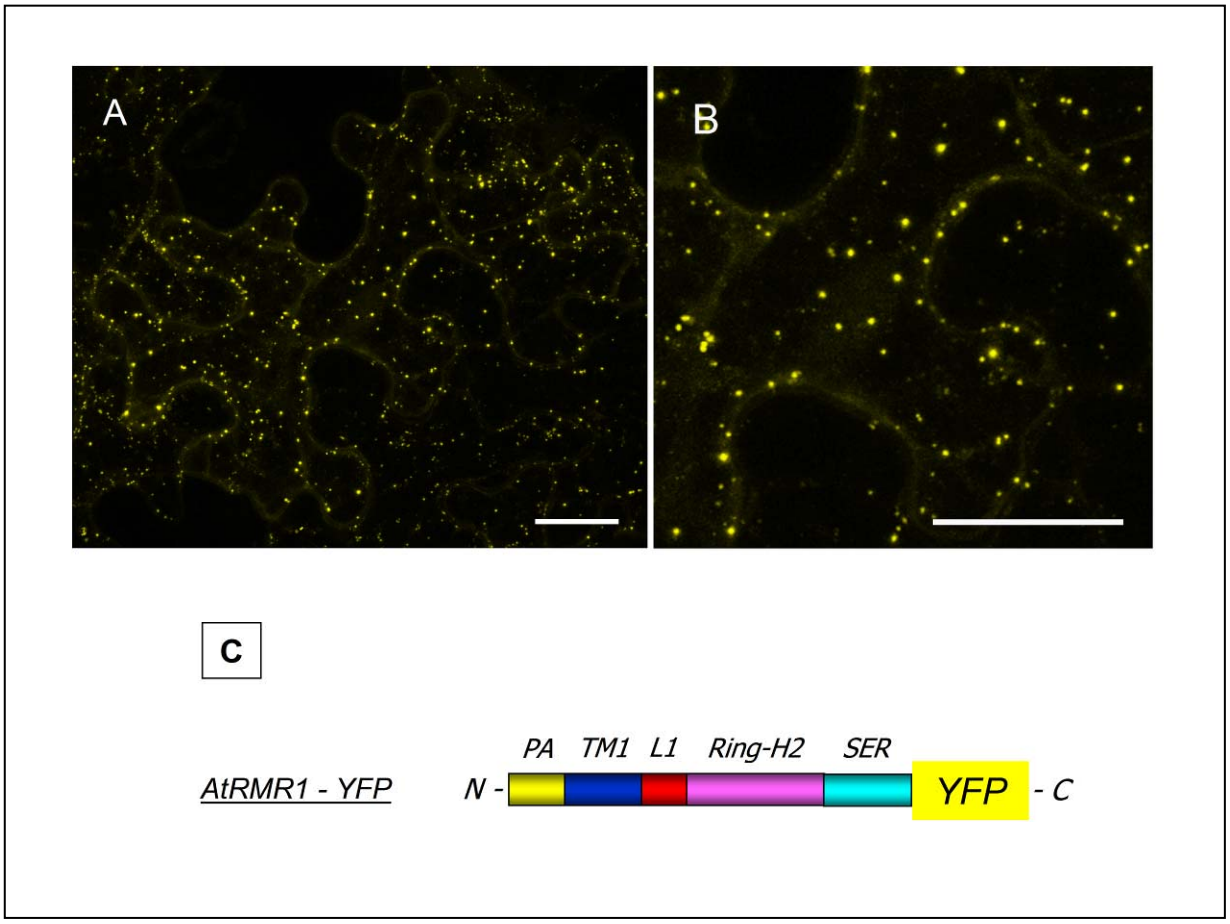

Figure 13: AtRMR1 localization in *N. benthamiana* leaves. Stack of confocal images (A whole cell, B higher magnification) of epidermal cells expressing the fusion protein AtRMR1-YFP. (C) Schematic representation of the fusion protein AtRMR1-YFP: full length AtRMR1 [PA (PA domain, yellow); TM1 (transmembrane, blue); L1 (sequence linker, red); Ring-H2 domain (violet); SER (Serine-Rich domain, cyan)] fused at its C-terminus with YFP. (A) Bar = 30 µm; (B) bar = 35 µm.

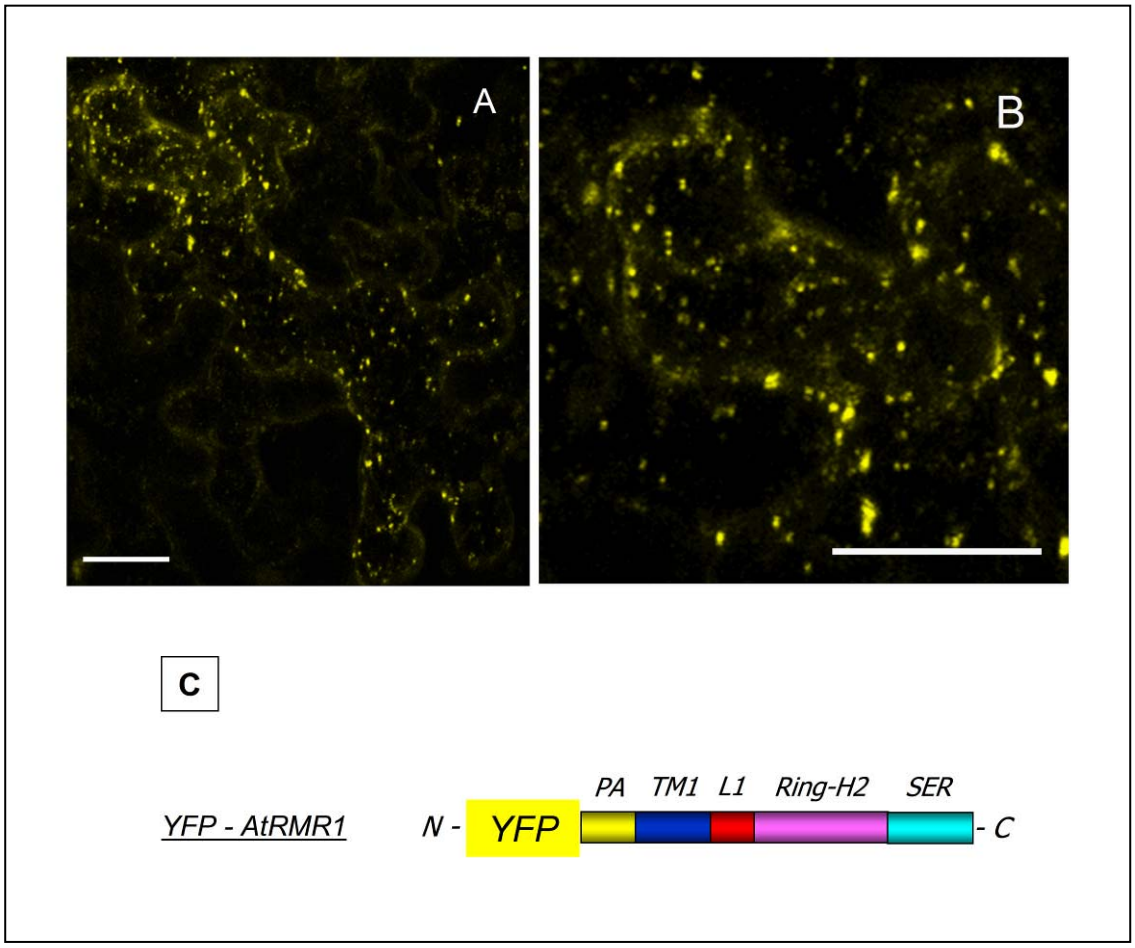

Figure 14: AtRMR1 localization in *N. benthamiana* leaves. Stack of confocal images (A whole cell, B higher magnification) of epidermal cells expressing the fusion protein YFP-AtRMR1. (C) Schematic representation of the fusion protein YFP-AtRMR1: full length AtRMR1 [PA (PA domain); TM1 (transmembrane); L1 (sequence linker); Ring-H2 domain; SER (Serine-Rich domain)] fused at its N-terminus with YFP. (A) Bar = 25 μm; (B) bar = 25 μm.

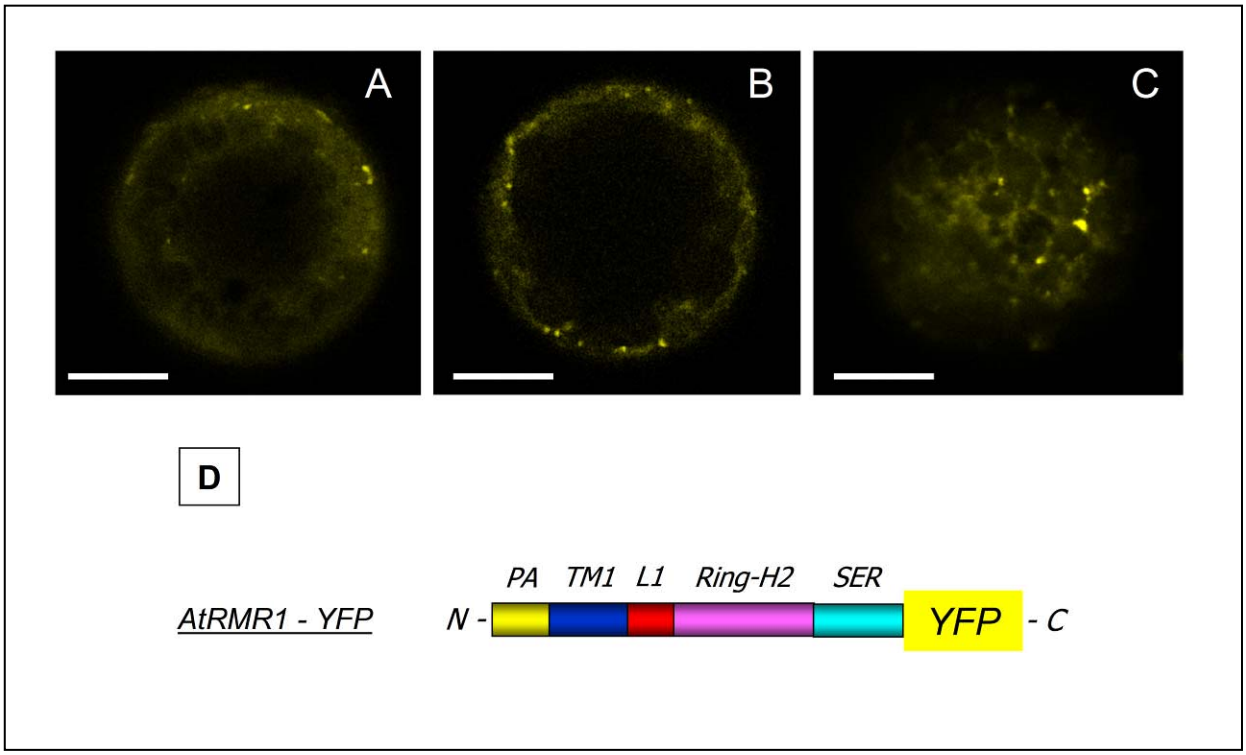

Figure 15: AtRMR1 localization in *A.thaliana* protoplasts. (A-C) Confocal images of a protoplast expressing the fusion protein AtRMR1-YFP. The images represent four sections of the same protoplast (from A, inner part of the cell to C, cell periphery). Scale bar: 10 µm. (D) Schematic representation of the AtRMR1-YFP fusion protein: full length AtRMR1 [PA (PA domain); TM1 (transmembrane); L1 (sequence linker); Ring-H2 domain; SER (Serine-Rich domain)] fused at its C-terminus with YFP.

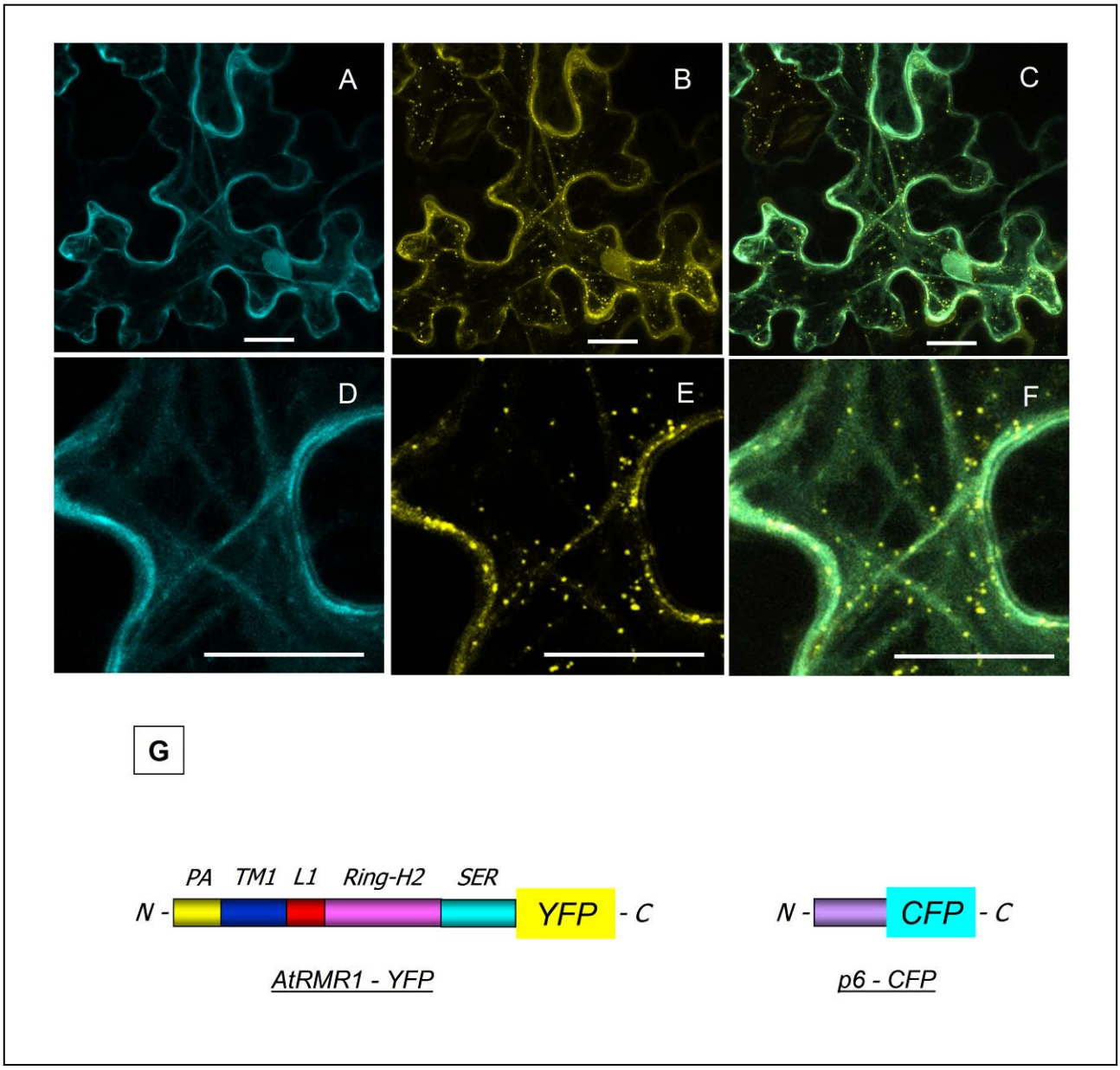

Figure 16: Co-expression of AtRMR1-YFP and the ER marker p6-CFP in *N. benthamiana* leaves. Confocal images of (A) CFP fluorescence signal; (B) YFP fluorescence signal; (C) merged image of the two fluorescence signals. D-F enlarged portion of the images A-C. (A-F) Scale bar = 20 µm

(G) Schematic representation of the two fusion proteins. AtRMR1-YFP: the full length AtRMR1 (PA domain, yellow; transmembrane, blue; linker, red; Ring-H2 domain, lilac; Serine-Rich domain, cyan) was fused at its C-terminus with YFP. p6-CFP: The full length p6 protein (violet) (Peremyslov *et al.*, 2004) was fused at its C-terminus with CFP.

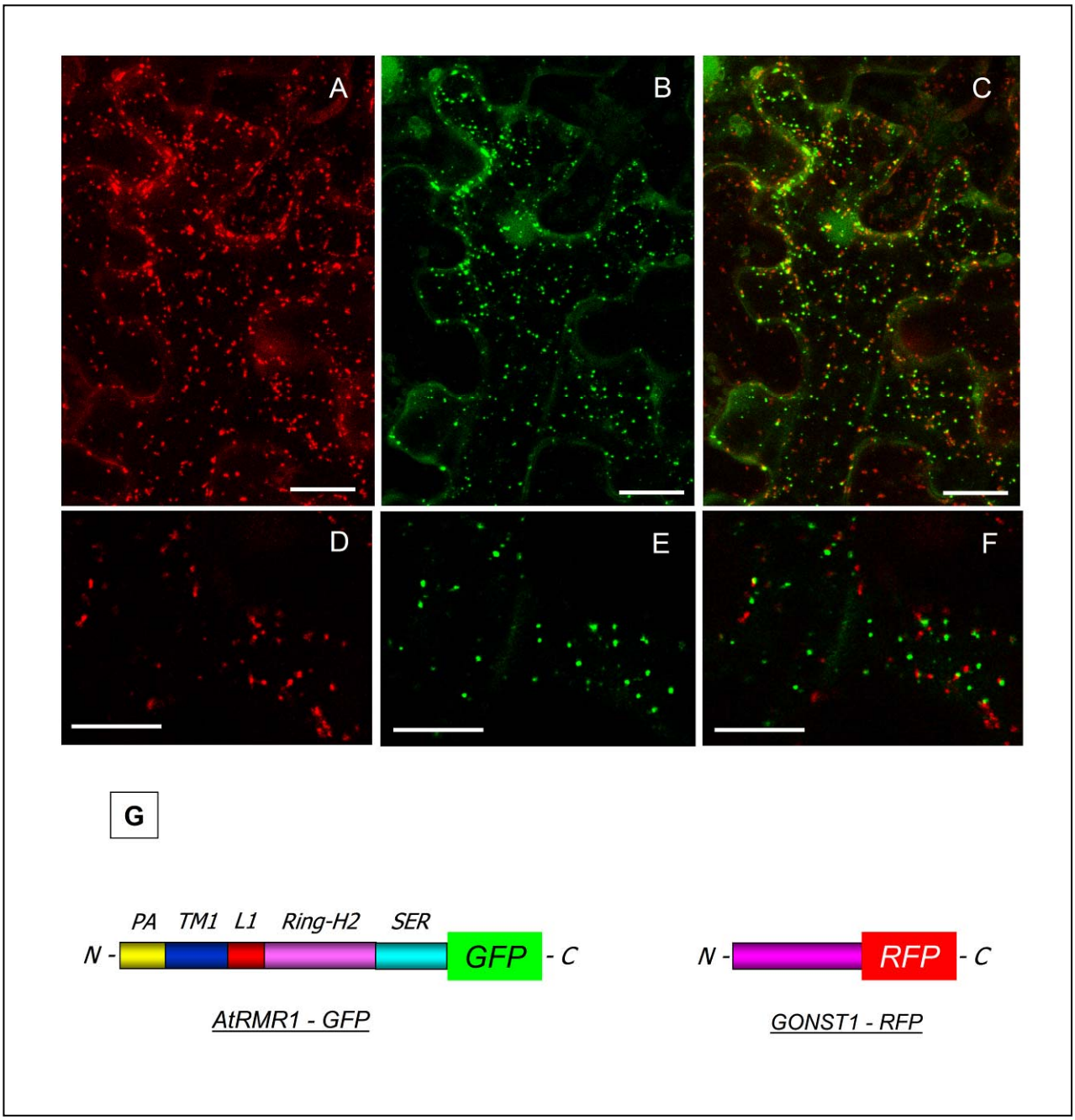

Figure 17: co-expression of AtRMR1-YFP and the Golgi marker GONST1-RFP in *N. benthamiana* leaves. Confocal images of (A) RFP fluorescence signal; (B) GFP fluorescence signal; (C) merged image of the two fluorescence signals. D-F enlarged portion of the images A-C. A-C bar = 20 µm; D-F bar = 15 µm.
(G) schematic representation of the two fusion proteins: AtRMR1-YFP: full length AtRMR1 (PA domain, yellow; transmembrane, blue; linker, red; Ring-H2 domain, lilac; Serine-Rich domain, cyan) fused at its C-terminus with GFP. GONST1-RFP: full length GONST1 (lilac) protein fused at its C-terminus with RFP.

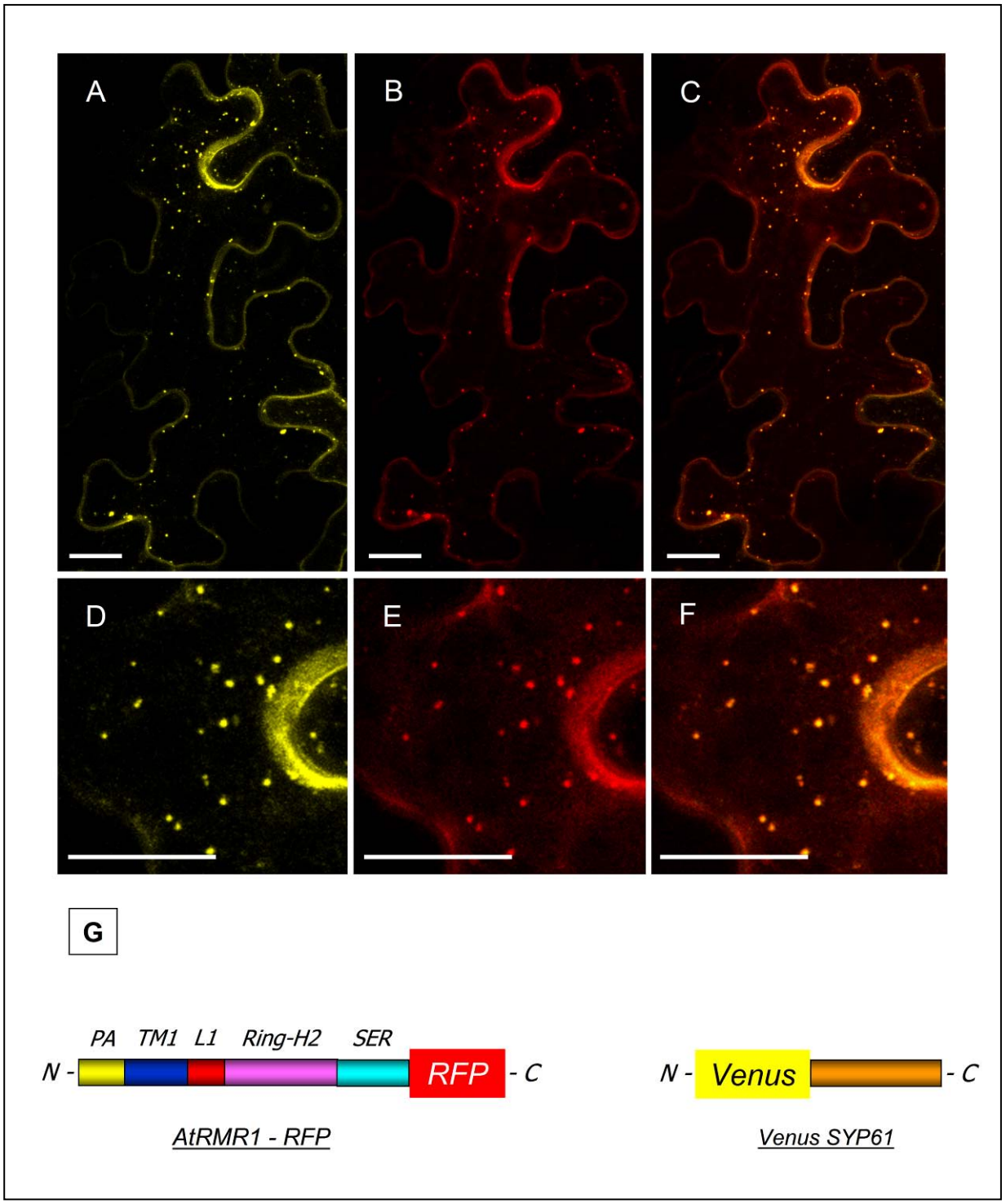

Figure 18: co-expression of AtRMR1-RFP and the TGN marker Venus-SYP61 in *N. benthamiana* leaves. Confocal images of (A) Venus fluorescence signal; (B) RFP fluorescence signal; (C) merged image of the two fluorescence signals. D-F enlarged portion of the images A-C. A-F bar = 20 µm.
(G) schematic representation of the two fusion proteins. AtRMR1-RFP: full length AtRMR1 (PA domain, yellow; transmembrane, blue; linker, red; Ring-H2 domain, lilac; Serine-Rich domain, cyan) fused at its C-terminus with RFP. Venus-SYP61: the full length SYP61 protein (orange) fused at its N-terminus with Venus fluorescent reporter (Uemura *et al.*, 2004).

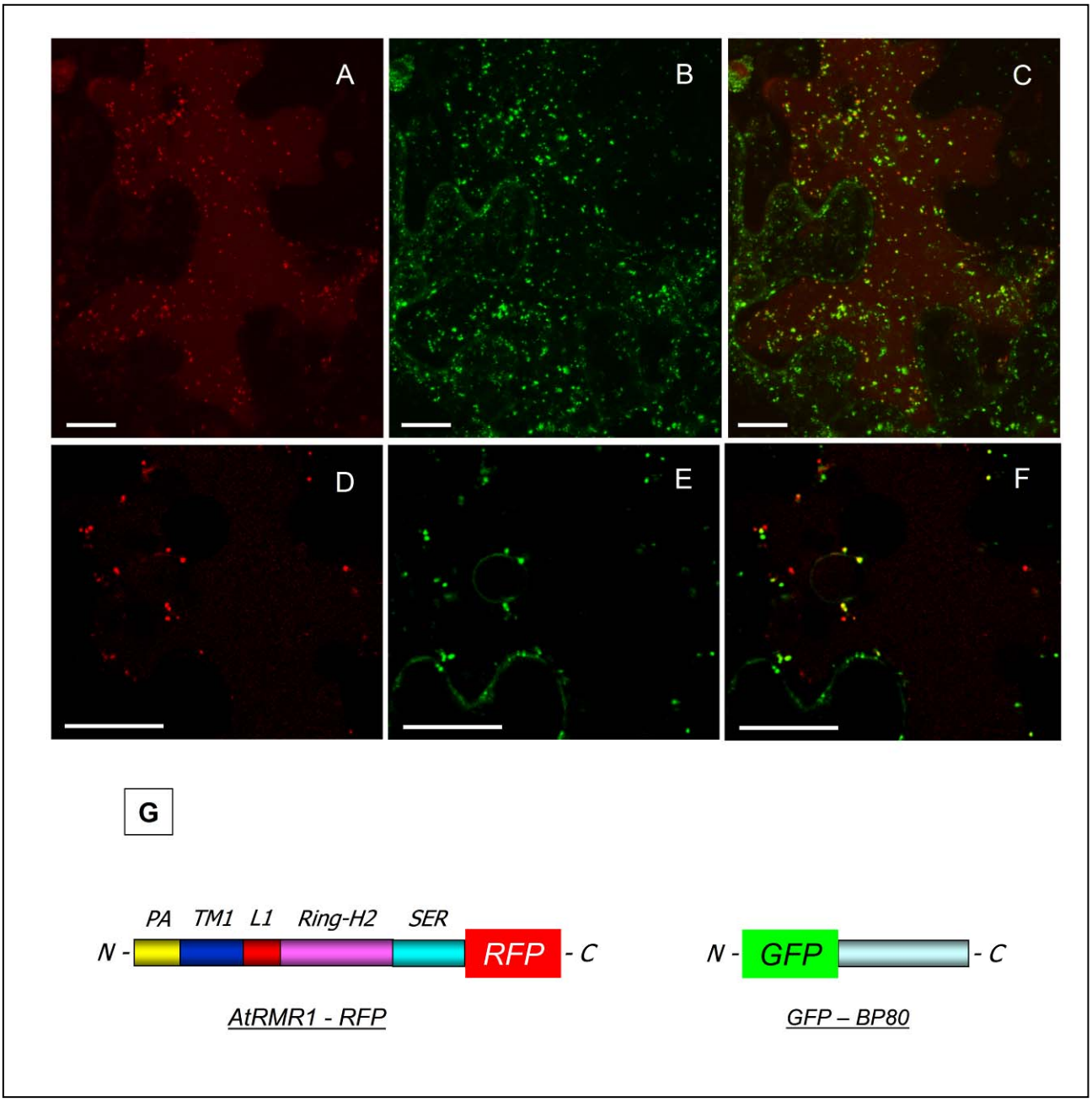

Figure 19: co-expression of AtRMR1-RFP and the PVC marker GFP-BP80 in *N. benthamiana* leaves. Confocal images of (A) RFP fluorescence signal; (B) GFP fluorescence signal; (C) merged image of the two fluorescence signals. D-F enlarged portion of the images A-C. A-F bar = 20 µm.
(G) schematic representation of the two fusion proteins. AtRMR1-RFP: full length AtRMR1 (PA domain, yellow; transmembrane, blue; linker, red; Ring-H2 domain, lilac; Serine-Rich domain, cyan) fused at its C-terminus with RFP. GFP-BP80: the transmembrane and the small cytosolic tail of BP80 receptor (gray) fused at its N-terminus with GFP (Miao *et al.*, 2006).

1.5. AtRMR1 localization in *Arabidopsis thaliana* transgenic plant

In order to confirm the results obtained in *N.benthamiana*, I generated *A.thaliana* stably transformed with AtRMR1-YFP. These transgenic plants were generated using a pGREEN expression vector carrying the full length AtRMR1 ORF fused at its C-terminal end with YFP. This coding sequence was cloned between the 35S promoter and terminator for constitutive expression in plant cells.

Several independent lines were regenerated and were examined in the confocal microscope without any positive result. Indeed neither the transcript nor consequently the fusion protein is detectable in any of the regenerated lines. Probably the overexpressed transgene undergoes a process of silencing which prevents the observation of the fusion protein. This result is in accordance with the fact that a sufficient expression of AtRMR1-YFP was only obtained in *N.benthamiana* by using the silencing inhibitor p19 (Voinnet *et al.*, 2002).

The mentioned transgenic plants grew normally and did not show any morphological alteration.

2. Characterization of AtRMR domains

Based on the previous results AtRMR1 and 2 show different localization in both transiently transformed *A.thaliana* protoplasts and agro-infiltrated *N.benthamiana*. Indeed the first localized in the TGN while the second localized in the ER membrane. These two type I transmembrane proteins have a predicted single transmembrane domain of 23 residues without obvious differences in aminoacid composition and a sequence identity of about 40%. So far the length of transmembrane-spanning sequences was demonstrated to influence the subcellular localization of transmembrane proteins, presumably depending on the membrane thickness (Brandizzi *et al.*, 2002; Sharpe *et al.*, 2010). Indeed, the membrane thickness increases from the ER to the plasma membrane due to differences in lipid composition. The thickness depends on acyl chain length in phospholipids and on the presence of sterols or sphingolipids (Brown *et al.*, 1998; Lewis *et al.*, 1983). Consequently membrane proteins with a longer transmembrane domain localize preferentially in post-Golgi compartments which present higher concentrations of sterols and sphingolipids. In contrast, membrane proteins with a shorter transmembrane domain tend to localize in early secretory compartments such as ER and Golgi. Moreover, the amino acid composition of the transmembrane domain could influence the protein localization. Indeed, transmembrane spanning domains enriched in particular aminoacids have a higher probability to localize in certain compartments (Sharpe *et al.*, 2010). For instance it has been suggested that phenylalanine residues could be involved in Golgi localization in mammalian cells (Munro *et al.*, 1995).

According to these notions, the localization of AtRMR1 is compatible with the length of its

transmembrane domain. Indeed, it has been demonstrated that membrane proteins with a single membrane spanning domain of 23 residues have high probability to localize in post Golgi compartments (Brandizzi *et al.,* 2002). In contrast, the transmembrane domain length of AtRMR2 is not consistent with an ER localization which is more likely for proteins with a shorter transmembrane domain (Brandizzi *et al.*, 2002). Therefore the transmembrane length of AtRMR1 and 2 seems to be not sufficient for protein localization, but it is more likely that the different localization could be due to particular amino acid sequences present in these proteins or to the influence of others proteins interacting with AtRMRs and determining their localization.

In order to define the role in localization of the domains present in AtRMR1 and 2, I generated different deletion mutants and tested their localization. Moreover I analyzed the transmembrane domain and the following small cytosolic sequence for the presence of aminoacids critical for protein localization. The role of these sequences was also determined by reciprocal replacement of sequences from AtRMR1 and 2 and observation of the effects on localization. In figure 20, an aminoacid alignment between AtRMR1 and AtRMR2 and the domain composition of the two receptors is represented.

Figure 20: Aminoacid sequence alignment of AtRMR1 and 2. The present picture represents an aminoacid alignment between AtRMR1 and AtRMR2 full length receptors. The alignment also includes the exact limits of the domain used for the generation of all deletion/replacement mutants. The different domains forming AtRMR1 and 2 are indicated in the picture: signal peptide (cyan); PA domain (red); transmembrane domain (green); sequence linker (lilac); Ring-H2 domain (orange); Serine-Rich domain (violet).

2.1. Localization of AtRMR2 deletion mutants in *N. benthamiana* leaves

For this purpose I generated two deletion mutants. The first mutant is ΔRingAtRMR2-YFP that includes AtRMR2 lacking the Ring-H2 domain and the short tail fused at its C-terminus with YFP. The other mutant is YFP-ΔPAAtRMR2 that includes AtRMR2 lacking the PA domain fused at its N-terminus with YFP. These two fusion proteins are expressed under the control of the 35S promoter and terminator in pGREEN (Hellens *et al.*, 2000). The localization of the mentioned fusion proteins was assessed in *N.benthamiana* leaves transformed by agro-infiltration.

The fluorescence pattern of the two mutants resembled the typical localization in the ER membrane (figure 21 and 22): in both cases the signal was mostly localized in networks which occupy the cortical and inner part of the cell. Moreover the signal localized in the nuclear envelope, around the nucleus.

A comparison of *N.benthamiana* epidermal cells expressing AtRMR2 full length fused to YFP at the either end (AtRMR2-YFP and YFP-AtRMR2) or the two deletion mutants, YFP-ΔPAAtRMR2 and ΔRingAtRMR2-YFP is represented in figure 23. The ER pattern of the full length proteins is indistinguishable from the pattern of the two deletion mutants, demonstrating that neither PA domain nor Ring-H2 domain are involved in protein localization.

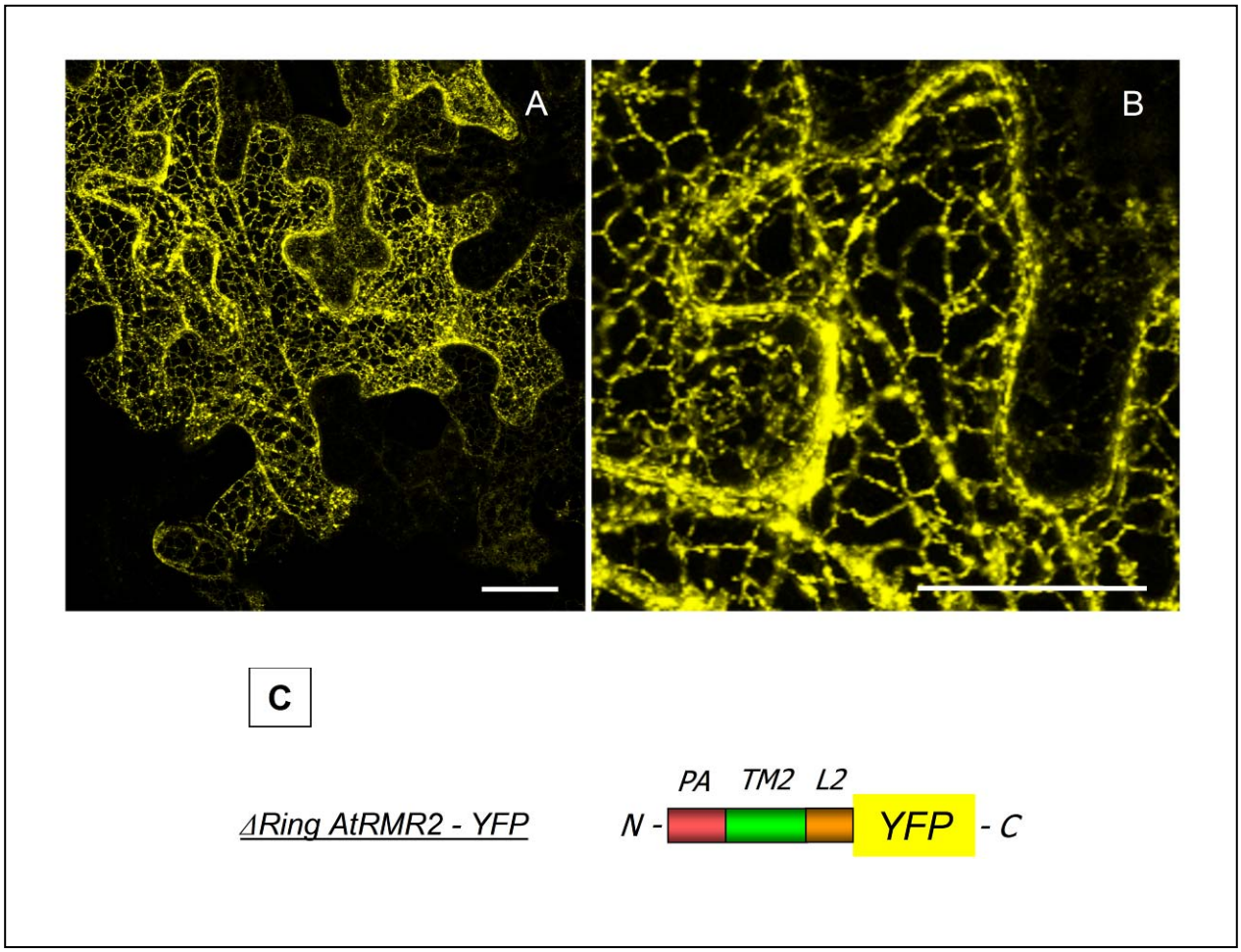

Figure 21: ΔRingAtRMR2 localization in *N. benthamiana* leaves. Stack of confocal images (A whole cell, B higher magnification) of epidermal cells expressing the fusion protein ΔRingAtRMR2-YFP. (C) Schematic representation of the fusion protein ΔRingAtRMR2-YFP: ΔRingAtRMR2 mutant [PA (PA domain, rose); TM2 (transmembrane, green); L2 (sequence linker, orange)] fused at its C-terminus with YFP. (A) Bar = 25 μm; (B) bar = 20 μm.

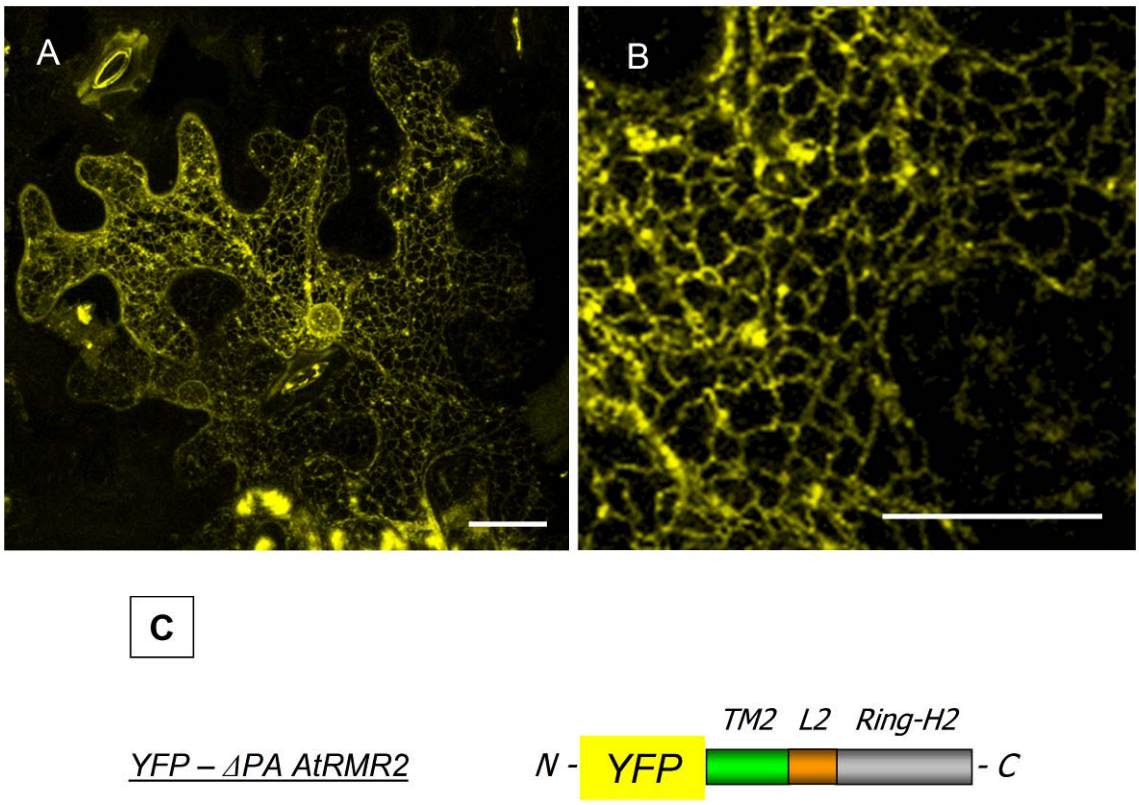

Figure 22: ΔPAAtRMR2 localization in *N. benthamiana* leaves. Stack of confocal images (A whole cell, B higher magnification) of epidermal cells expressing the fusion protein YFP-ΔPAAtRMR2. (C) Schematic representation of the fusion protein YFP-ΔPAAtRMR2: ΔPAAtRMR2 mutant [TM2 (transmembrane, green); L2 (sequence linker, orange); Ring-H2 domain (gray)] fused at its N-terminus with YFP. (A) Bar = 25 μm; (B) bar = 20 μm.

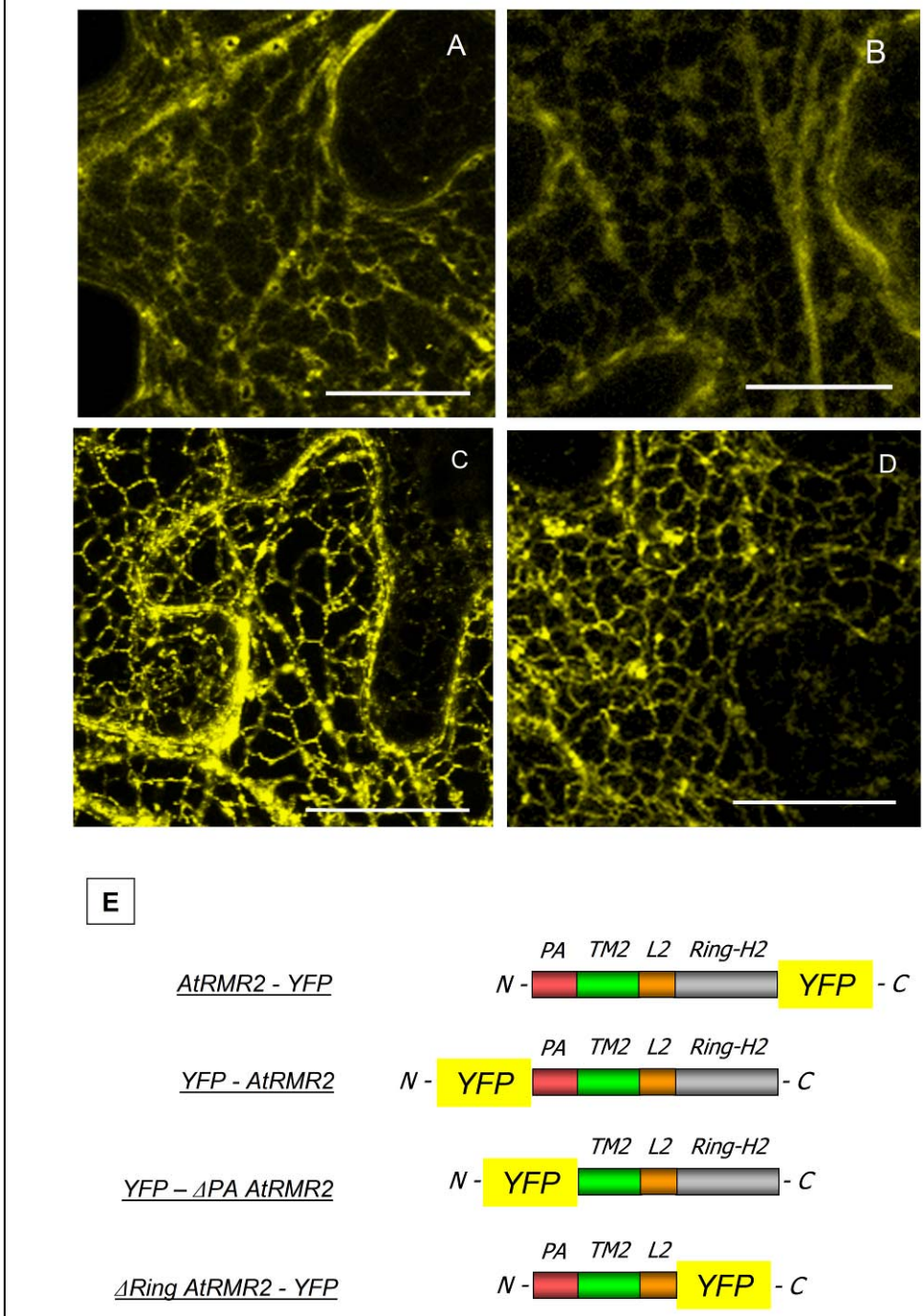

Figure 23: Comparison of different AtRMR2 fusion proteins. Stack of confocal images of epidermal cells expressing the following fusion proteins: (A) AtRMR2-YFP; (B) YFP-AtRMR2; (C) ΔRingAtRMR2-YFP; (D) YFP-ΔPAAtRMR2. (E) Below the pictures it is shown a schematic representation of all these fusion proteins: PA (PA domain, rose); TM2 (transmembrane domain, green); L2 (sequence linker, orange); Ring-H2 domain (gray). (A-D) bar = 20 μm.

2.2. Localization of AtRMR1 deletion mutants in *N. benthamiana* leaves

For AtRMR1 I also generated deletion mutants of different domains in order to assess their role in protein localization. I produced four different constructs which encode the following fusion proteins: the first mutant is ΔSAtRMR1-YFP, i.e. AtRMR1 lacking the Serine-Rich domain fused at its C-terminus with YFP (figure 24). The second mutant is ΔSRAtRMR1-YFP, i.e. AtRMR1 lacking both the Serine-Rich domain and the Ring-H2 domain, fused at its C-terminus with YFP (figure 25). The third mutant is YFP-ΔPAtRMR1, i.e. AtRMR1 lacking the PA domain, fused at its N-terminus with YFP (figure 26). The last mutant is YFP-ΔPSAtRMR1, i.e. AtRMR1 lacking both the PA domain and the Serine-Rich domain, fused at its N-terminus with YFP (figure 27). All these fusion proteins are expressed under the control of the 35S promoter of a pGREEN vector in *N.benthamiana* leaves transformed by agro-infiltration.

A comparison of *N.benthamiana* epidermal cells expressing full length AtRMR1 fused to YFP at either end (AtRMR1-YFP and YFP-AtRMR1) and the four deletion mutants revealed that the deletion mutants localize in punctate structures similar to the full length AtRMR1 (figure 28). The only exception was the ΔSRAtRMR1-YFP mutant which also localized in a structure similar to the nucleolus (figure 25). This mislocalization could due to the presence of a cryptic nucleolar localization signal which is exposed in this mutant lacking both Ring-H2 and Serine-Rich domains. Alternatively, this could be an effect of protein overproduction which leads to partially mis-localization of the mutant in the cytosol, with artefactual accumulation in the nucleolus. Indeed the expression level of ΔSRAtRMR1-YFP was very high compared to the others (data not shown).

The only information obtained from these pictures is that all deletion mutants localized in similar punctate structures. In order to determine if all fusion proteins localized in the same compartment as the full length AtRMR1 constructs, colocalization experiments were needed. Two different co-localization experiments are presented here: the first shows the colocalization of full length AtRMR1-RFP and of the ΔSRAtRMR1-YFP mutant (figure 29), while, the second shows the colocalization of AtRMR1-RFP and of the deletion mutant YFP-ΔPSAtRMR1 (figure 30). In both cases the two mutants mostly colocalized with full length AtRMR1, i.e. they both localized in the TGN. Therefore neither the PA domain, the Ring-H2 domain, nor the Serine-Rich domains of AtRMR1 are involved in protein localization.

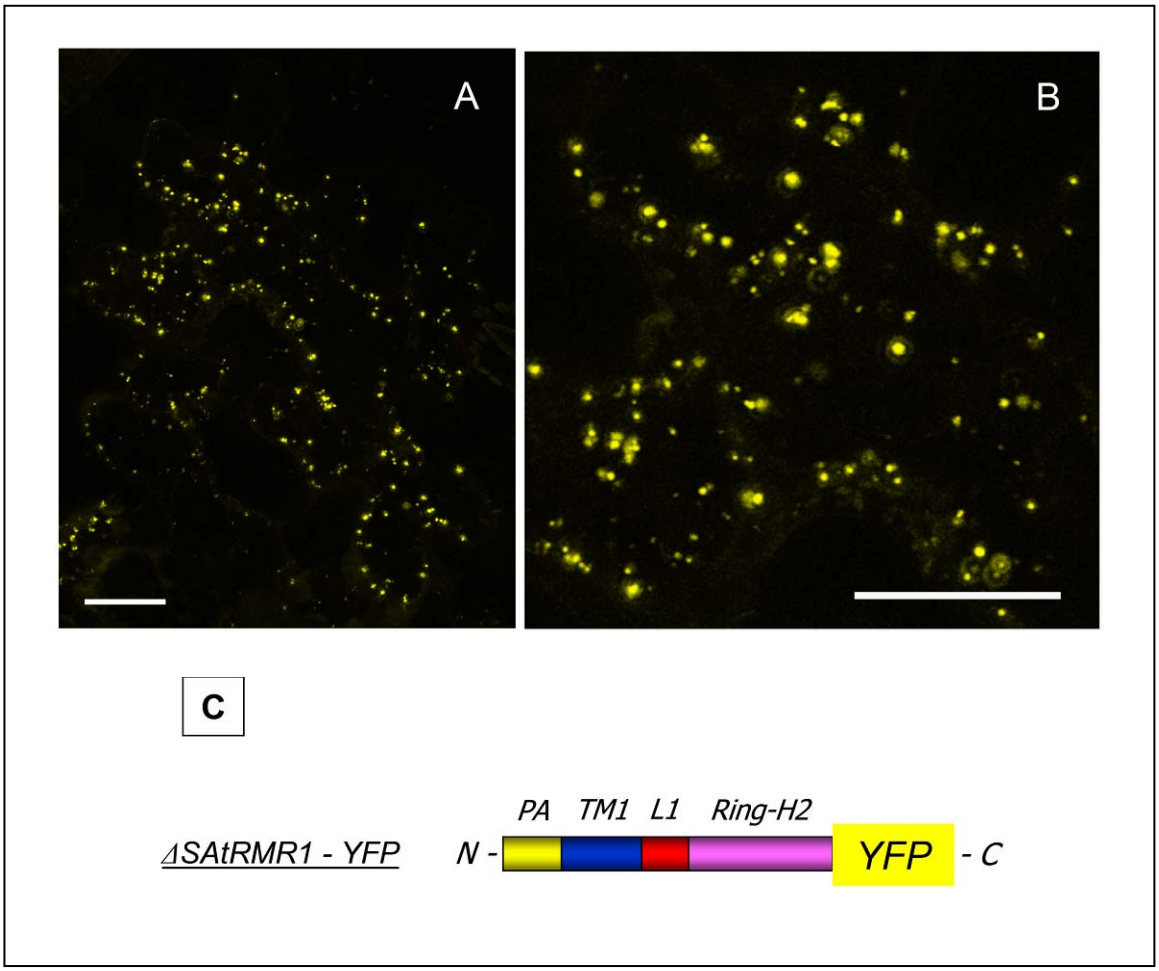

Figure 24: ΔSAtRMR1 localization in *Nicotiana benthamiana* leaves. Stack of confocal images (A whole cell, B higher magnification) of epidermal cells expressing the fusion protein ΔSAtRMR1-YFP. (C) Schematic representation of the fusion protein ΔSAtRMR1-YFP: ΔSAtRMR1 mutant [PA (PA domain, yellow); TM1 (transmembrane, blue); L1 (sequence linker, red); Ring-H2 domain (lilac)] fused at its C-terminal with YFP. (A) Bar = 30 μm; (B) bar = 35

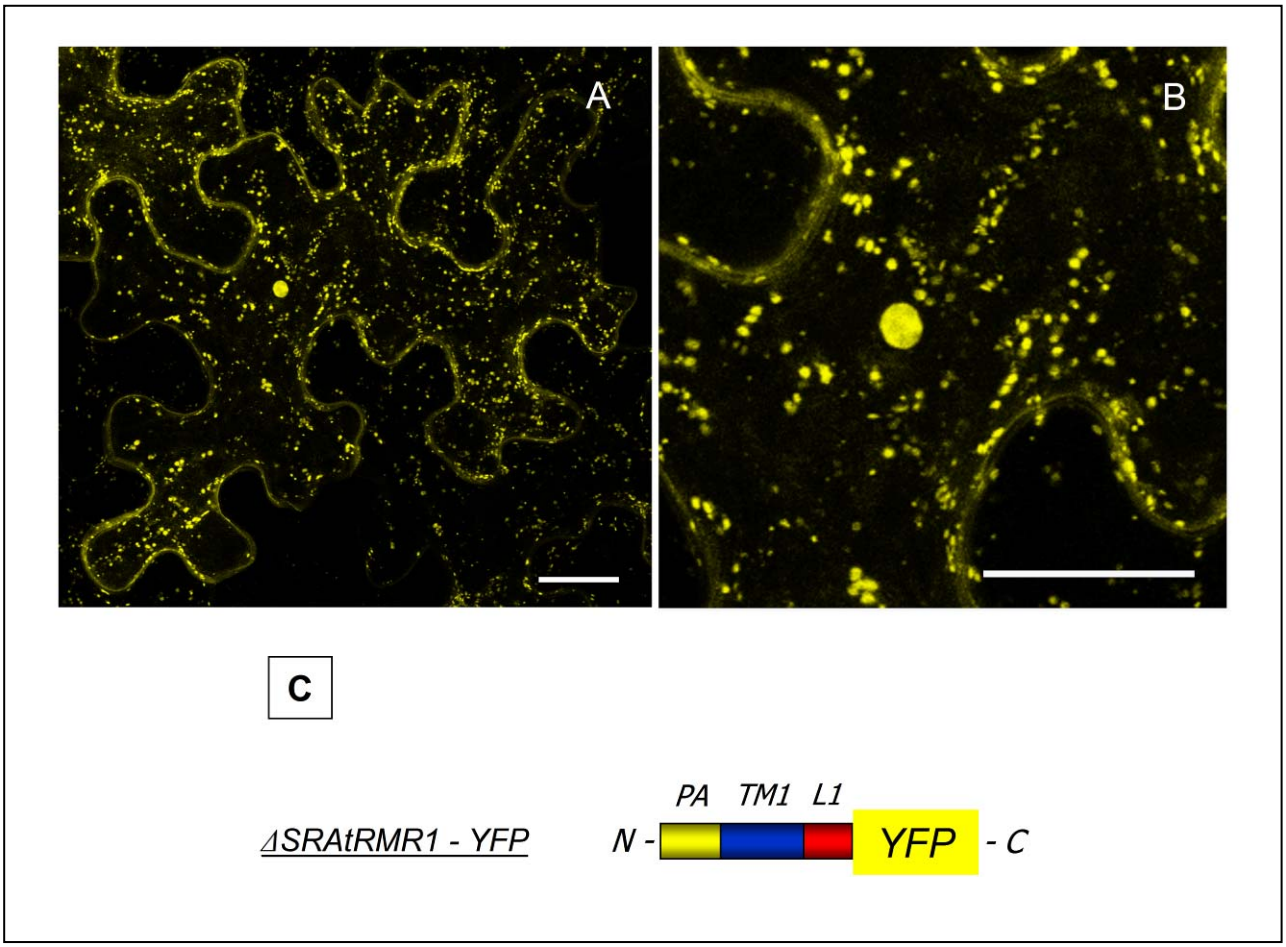

Figure 25: ΔSRAtRMR1 localization in *Nicotiana benthamiana* leaves. Stack of confocal images (A whole cell, B higher magnification) of epidermal cells expressing the fusion protein ΔSRAtRMR1-YFP. (C) Schematic representation of the fusion protein ΔSRAtRMR1-YFP: ΔSRAtRMR1 mutant [PA (PA domain, yellow); TM1 (transmembrane, blue); L1 (sequence linker, red)] fused at its C-terminus with YFP. (A) Bar = 30 μm; (B) bar = 35.

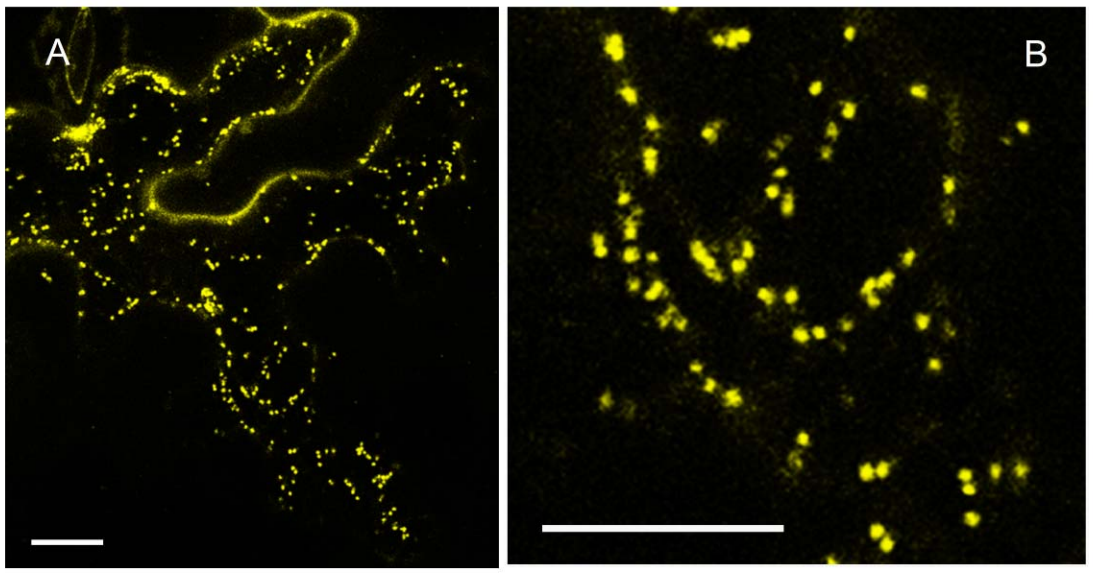

C

Figure 26: ΔPAtRMR1 localization in *Nicotiana benthamiana* leaves. Stack of confocal images (A whole cell, B higher magnification) of epidermal cells expressing the fusion protein YFP-ΔPAtRMR1. (C) Schematic representation of the fusion protein YFP-ΔPAtRMR1: ΔPAtRMR1 mutant [TM1 (transmembrane, blue); L1 (sequence linker, red); Ring-H2 domain (lilac); SER (Serine-Rich domain, cyan)]. (A) Bar = 20 μm; (B) bar = 20.

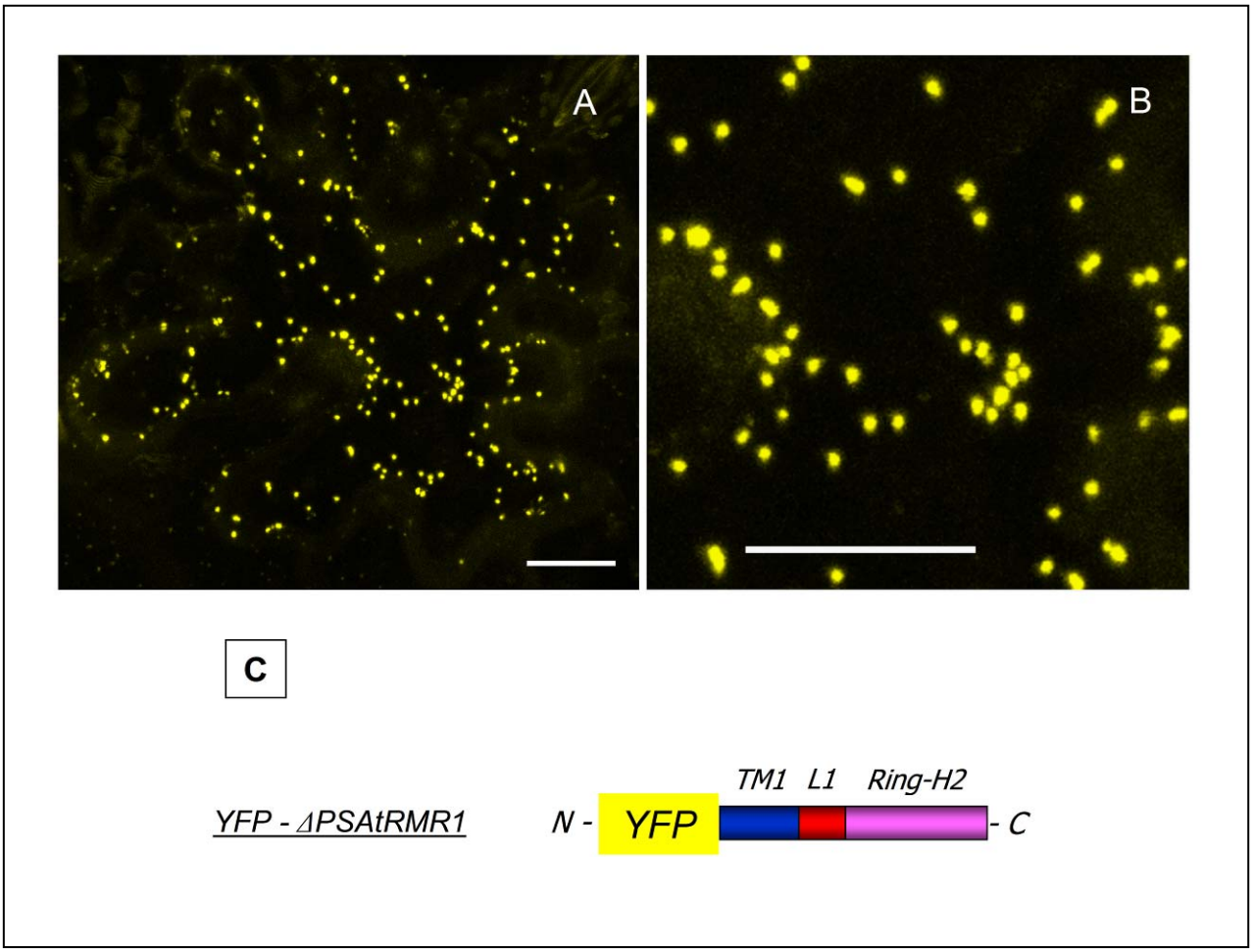

Figure 27: ΔPSAtRMR1 localization in *Nicotiana benthamiana* leaves. Stack of confocal images (A whole cell, B higher magnification) of epidermal cells expressing the fusion protein YFP-ΔPSAtRMR1. (C) Schematic representation of the fusion protein YFP-ΔPSAtRMR1: ΔPSAtRMR1 mutant [TM1 (transmembrane, blue); L1 (sequence linker, red); Ring-H2 domain (lilac)]. (A) Bar = 25 μm; (B) bar = 25.

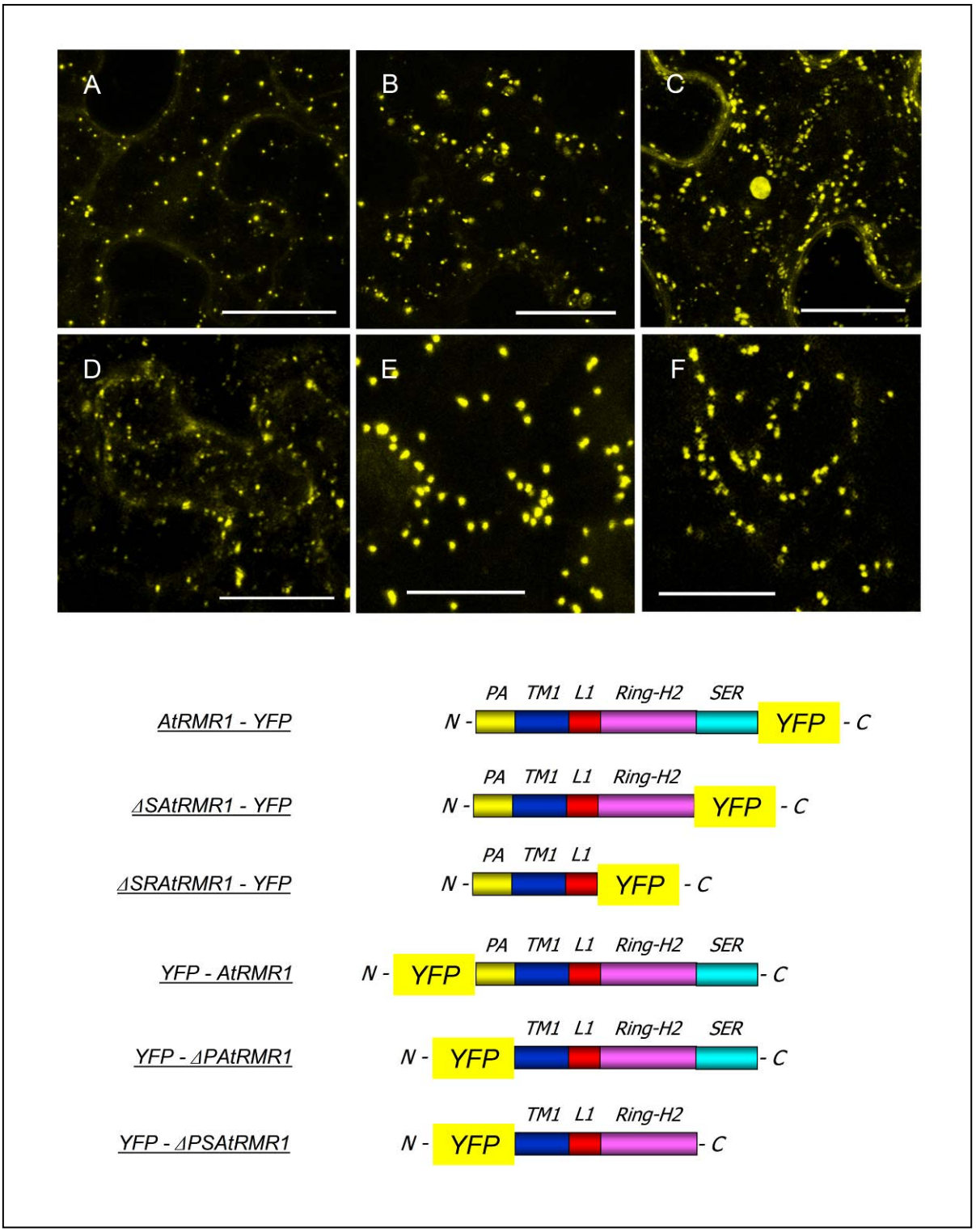

Fig 28: Comparison of different AtRMR1 fusion proteins. Stack of confocal images of epidermal cells expressing the indicated fusion proteins. (A) AtRMR1-YFP; (B) ΔSAtRMR1-YFP; (C) ΔSRAtRMR1-YFP; (D) YFP-AtRMR1; (E) YFP-ΔPAtRMR1; (F) YFP-ΔPSAtRMR1. Below the pictures it is shown a schematic representation of all these fusion proteins: PA (PA domain yellow); TM1 (transmembrane, blue); L1 (sequence linker, red); Ring-H2 domain (lilac); SER (Serine-Rich domain, cyan).
(A) Bar = 35 µm; (B) bar = 35 µm; (C) bar = 35 µm; (D) bar = 25 µm; (E) bar = 25 µm; (F) bar = 20 µm.

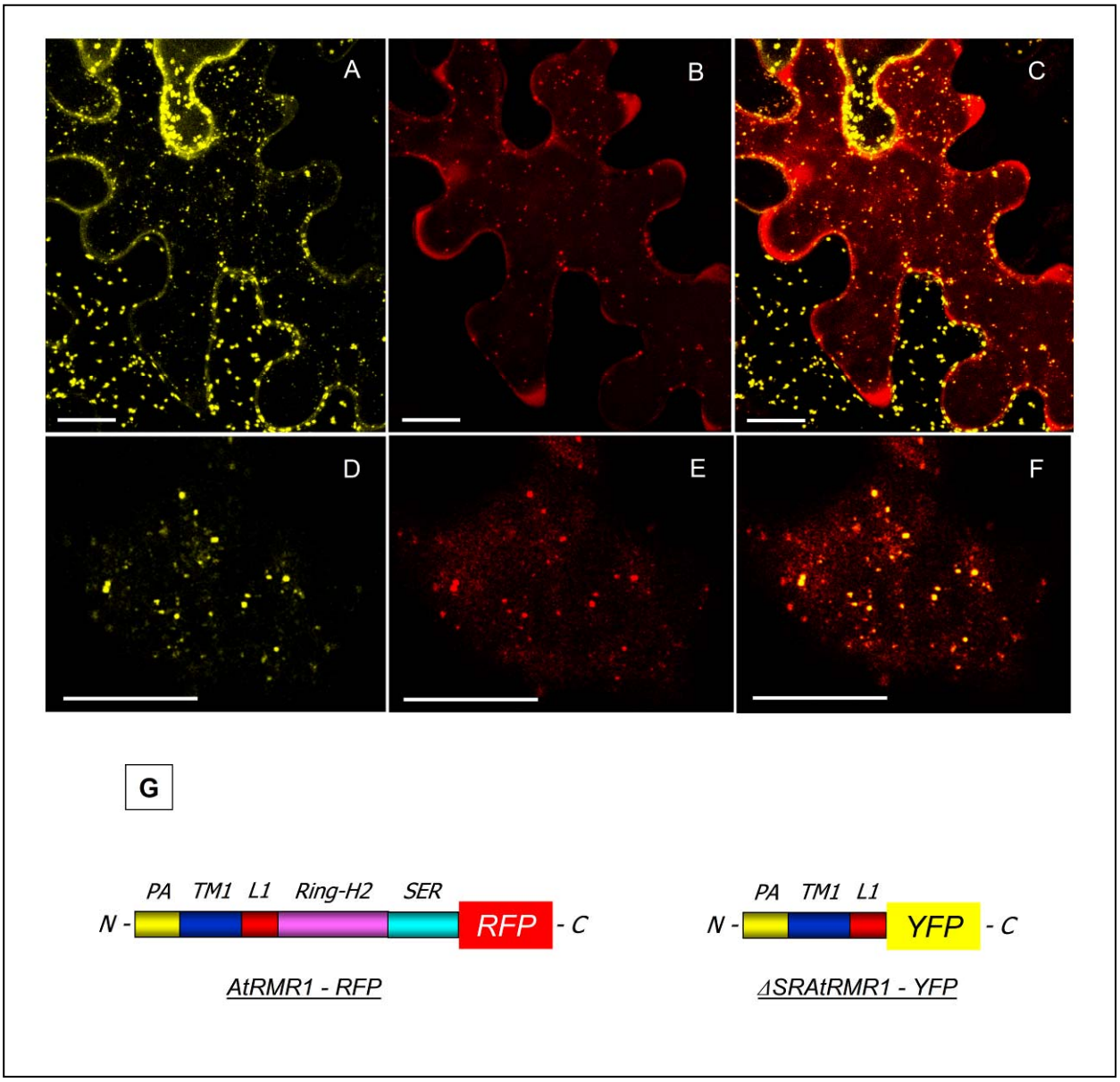

Figure 29: co-expression of AtRMR1-RFP and the mutant ΔSRAtRMR1-YFP in *N. benthamiana* leaves. Confocal images of (A) YFP fluorescence signal; (B) RFP fluorescence signal; (C) merged image of the two fluorescence signals. D-F enlarged portion of the images A-C. A-F bar = 20 µm.
(G) Schematic representation of the two fusion proteins. AtRMR1-RFP: full length AtRMR1 (PA domain, yellow; transmembrane, blue; linker, red; Ring-H2 domain, lilac; Serine-Rich domain, cyan) fused at its C-terminus with RFP. ΔSRAtRMR1-YFP: ΔSRAtRMR1 mutant (PA domain, yellow; transmembrane, blue; linker, red) fused at its C-terminus with YFP.

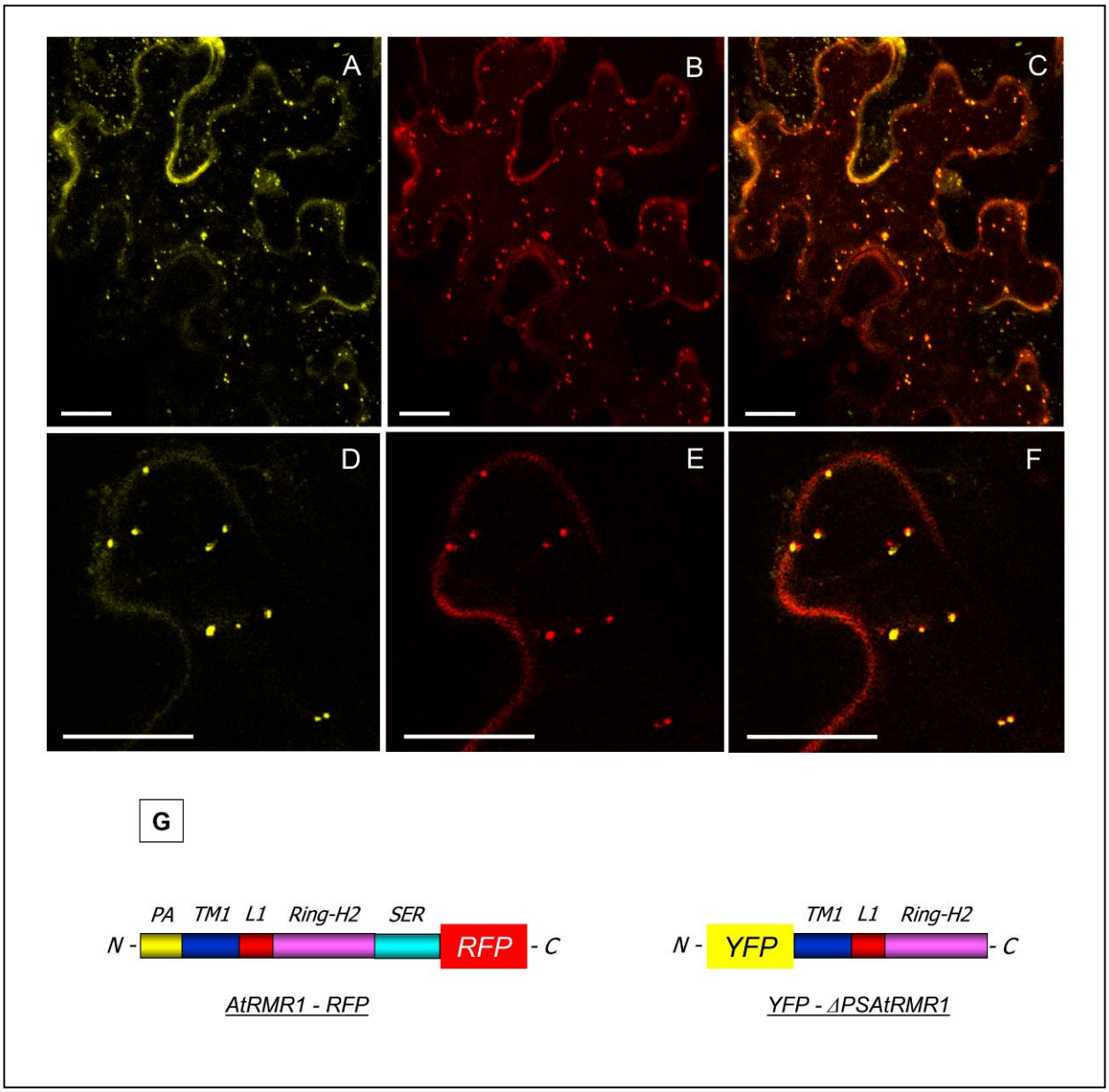

Figure 30: co-expression of AtRMR1-RFP and the mutant YFP-ΔPSAtRMR1 in *N. benthamiana* leaves. Confocal images of (A) YFP fluorescence signal; (B) RFP fluorescence signal; (C) merged image of the two fluorescence signals. D-F enlarged portion of the images A-C. A-F bar = 20 µm.
(G) Schematic representation of the two fusion proteins. AtRMR1-RFP: full length AtRMR1 (PA domain, yellow; transmembrane, blue; linker, red; Ring-H2 domain, lilac; Serine-Rich domain, cyan) fused at its C-terminus with RFP. ΔPSAtRMR1-YFP: ΔPSAtRMR1 mutant (transmembrane, blue; linker, red; Ring-H2 domain, lilac) fused at its N-terminus with YFP.

2.3. Transmembrane domain characterization of AtRMRs

The previous results demonstrated that different luminal and cytosolic domains of AtRMR1 and 2 are not involved in protein localization. Therefore the sequences involved in protein localization could reside at the level of the transmembrane domain and/or in the following short cytosolic linker preceding the Ring-H2 domain.

The transmembrane domain of certain proteins has been demonstrated to be involved in localization, i.e. the length and the composition of the transmembrane domain could determine protein localization (Brandizzi *et al.,* 2002; Sharpe *et al.,* 2010). AtRMR1 and 2 have a transmembrane domain of the same predicted length (23 residues) but they show a completely different localization. Therefore the length alone of these domains cannot be involved in protein localization but the specific sequence of the two domains could play a role. The two transmembrane domains have a high similarity and are about 40% identical.

The role of the transmembrane domains was determined by observing the effects on localization of exchanging them between the two AtRMRs. I have generated two expression vectors coding for the following fusion proteins: AtRMR1 with the transmembrane domain of AtRMR2 fused at its C-terminus with GFP (AtRMR1TM2-GFP; figure 31) and the complementary fusion protein AtRMR2 with the transmembrane domain of AtRMR1 fused to GFP at its C-terminus (AtRMR2TM1-GFP; figure 32). All these fusion proteins were expressed under the control of the 35S promoter and the localization was assessed in *N.benthamiana* leaves transformed by agro-infiltration.

The two mutants did not change their localization compared to wild type proteins. Indeed AtRMR2TM1-GFP localized in the nuclear envelope and in network structures typical of ER localization (figure 32). Moreover the mutant perfectly colocalized with wild type AtRMR2 supporting this localization (figure 33). In contrast, AtRMR2TM1-GFP did not colocalize with wild type AtRMR1 demonstrating that the transmembrane domain exchange had no effect on protein localization (figure 34). No effect in protein localization was also observed for AtRMR1 with the transmembrane domain of AtRMR2 (figure 31). Indeed the mutant AtRMR1TM2-GFP colocalized in punctate structures with wild type AtRMR1 (figure 35), while it did not colocalize with wild type AtRMR2 demonstrating again that the transmembrane domain exchange had no effect on protein localization (figure 36).

These exchange experiments demonstrated that neither transmembrane domain contains critical sequences involved in protein localization. Therefore a putative localization signal has to be searched for in the small cytosolic linker between the transmembrane and Ring-H2 domains of AtRMR1 and 2.

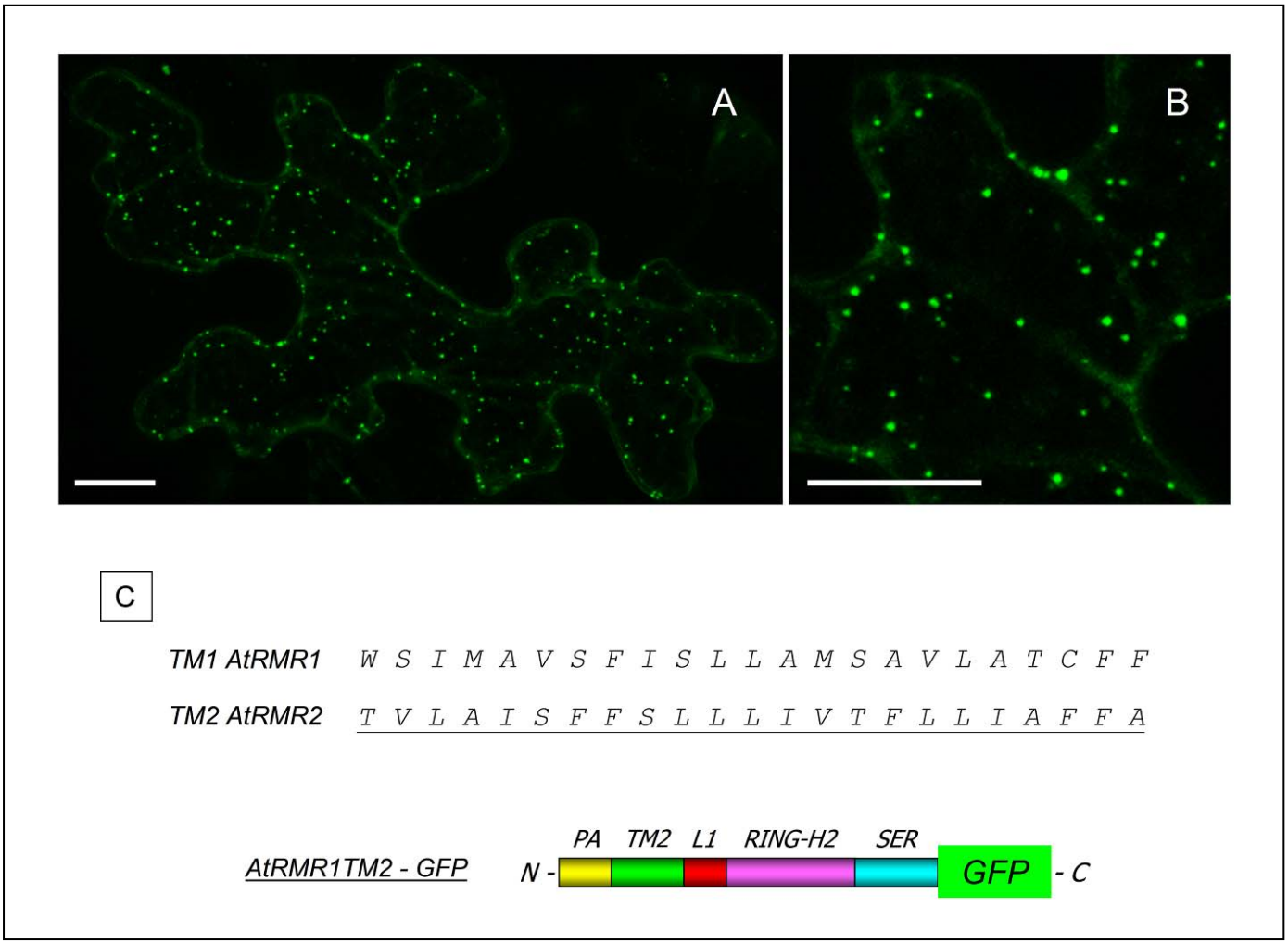

Figure 31: AtRMR1TM2 localization in *N. benthamiana* leaves. Stack of confocal images (A whole cell, B higher magnification) of epidermal cells expressing the fusion protein AtRMR1TM2-GFP. (C) Alignment of the transmembrane of AtRMR1 and AtRMR2 and schematic representation of the fusion protein AtRMR1TM2-GFP: AtRMR1TM2 mutant [PA (PA domain, yellow); TM2 (transmembrane of AtRMR2, green); L1 (sequence linker, red); Ring-H2 domain (lilac); SER (Serine-Rich domain, cyan)] fused at its C-terminus with GFP. A-B scale bar = 20 μm.

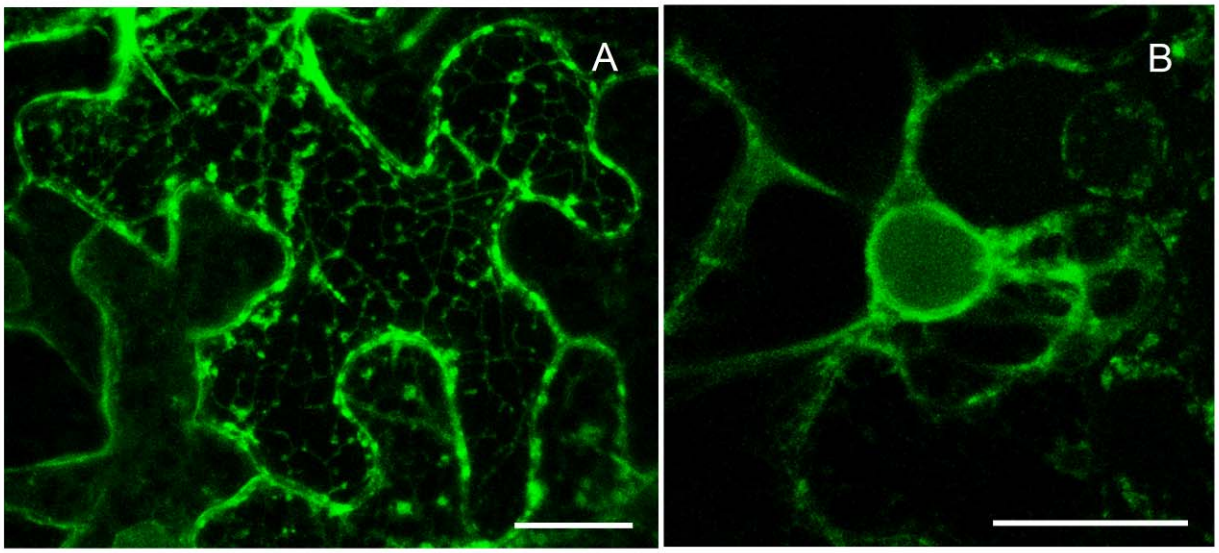

C

TM2 AtRMR2 T V L A I S F F S L L L I V T F L L I A F F A

TM1 AtRMR1 W S I M A V S F I S L L A M S A V L A T C F F

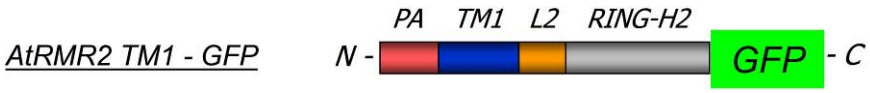

Figure 32: AtRMR2TM1 localization in *N. benthamiana* leaves. Stack of confocal images (A whole cell, B higher magnification) of epidermal cells expressing the fusion protein AtRMR2TM1-GFP. (C) Alignment of the transmembrane of AtRMR2 and AtRMR1 and schematic representation of the fusion protein AtRMR2TM1-GFP: AtRMR2TM1 mutant [PA (PA domain, rose); TM1 (transmembrane of AtRMR1, blue); L2 (sequence linker, orange); Ring-H2 domain (gray); SER (Serine-Rich domain, gray)] fused at its C-terminus with GFP. A-B scale bar = 20 μm.

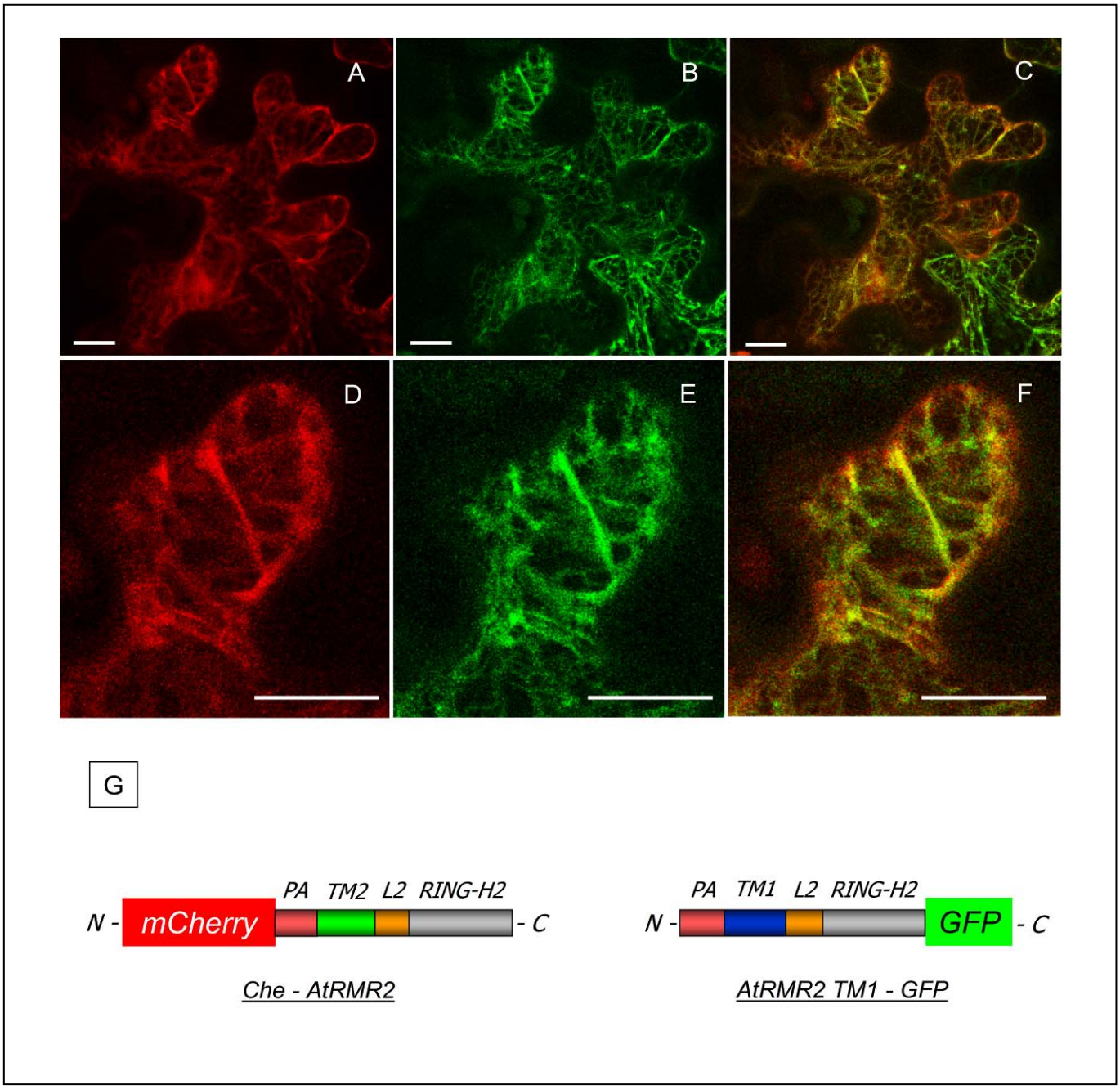

Figure 33: co-expression of Che-AtRMR2 and the mutant AtRMR2TM1-GFP in *N. benthamiana* leaves. Confocal images of (A) RFP fluorescence signal; (B) GFP fluorescence signal; (C) merged image of the two fluorescence signals. D-F enlarged portion of the images A-C. A-F bar = 20 µm.
(G) Schematic representation of the two fusion proteins. Che-AtRMR2: full length AtRMR2 (PA domain, rose; transmembrane, green; linker, orange; Ring-H2 domain, gray) fused at its N-terminus with mCHERRY. AtRMR2TM1 mutant (full length AtRMR2 with the transmembrane of AtRMR1, blue) fused at its C-terminus with GFP.

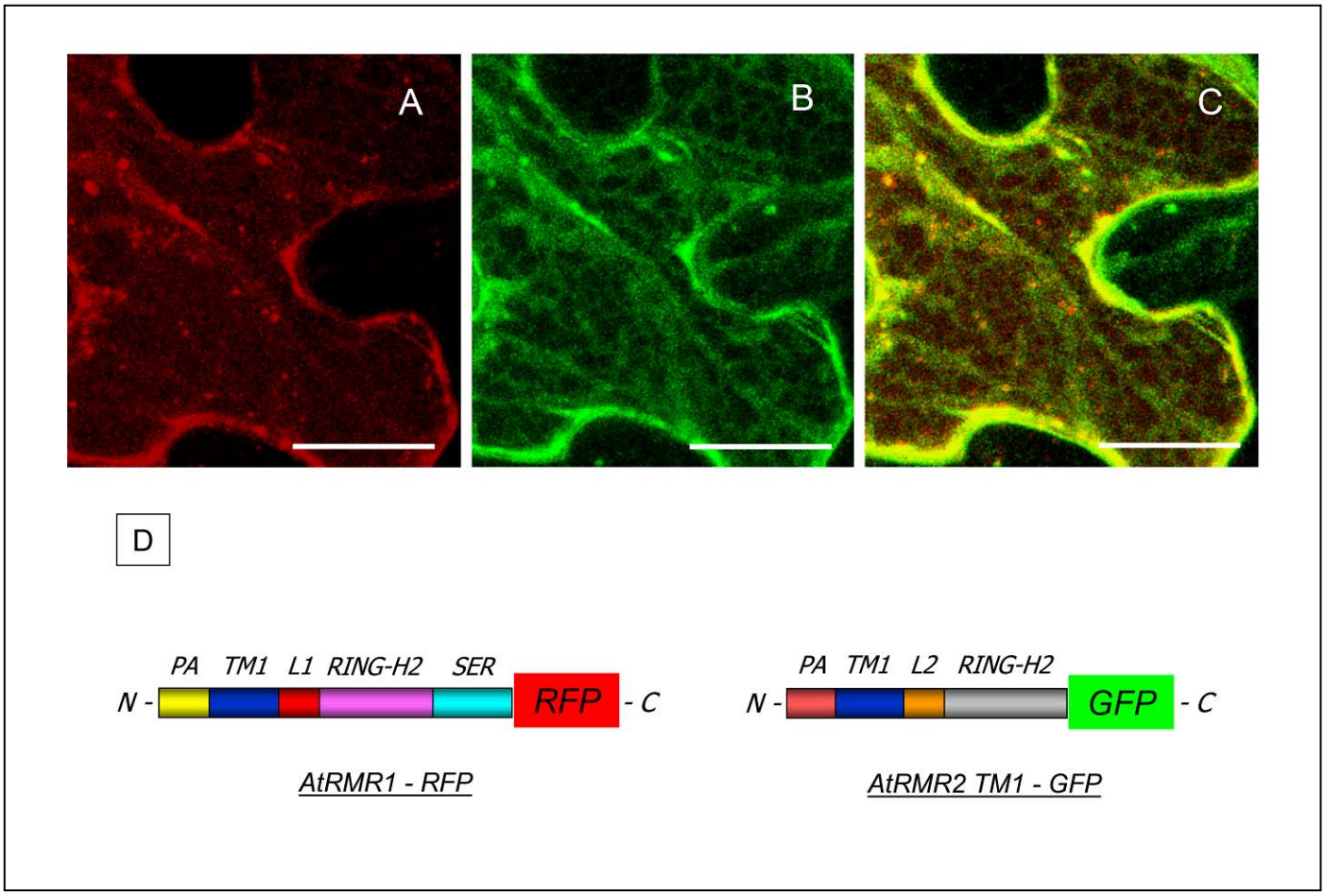

Figure 34: co-expression of AtRMR1-RFP and the mutant AtRMR2TM1-GFP in *N. benthamiana* leaves. Confocal images of (A) RFP fluorescence signal; (B) GFP fluorescence signal; (C) merged image of the two fluorescence signals. A-C bar = 20 µm.
(D) Schematic representation of the two fusion proteins. AtRMR1-RFP: full length AtRMR1 (PA domain, yellow; transmembrane, blue; linker, red; Ring-H2 domain, lilac; Serine-Rich domain, cyan) fused at its C-terminus with RFP. AtRMR2TM1 mutant (full length AtRMR2 with the transmembrane of AtRMR1, blue) fused at its C-terminus with GFP.

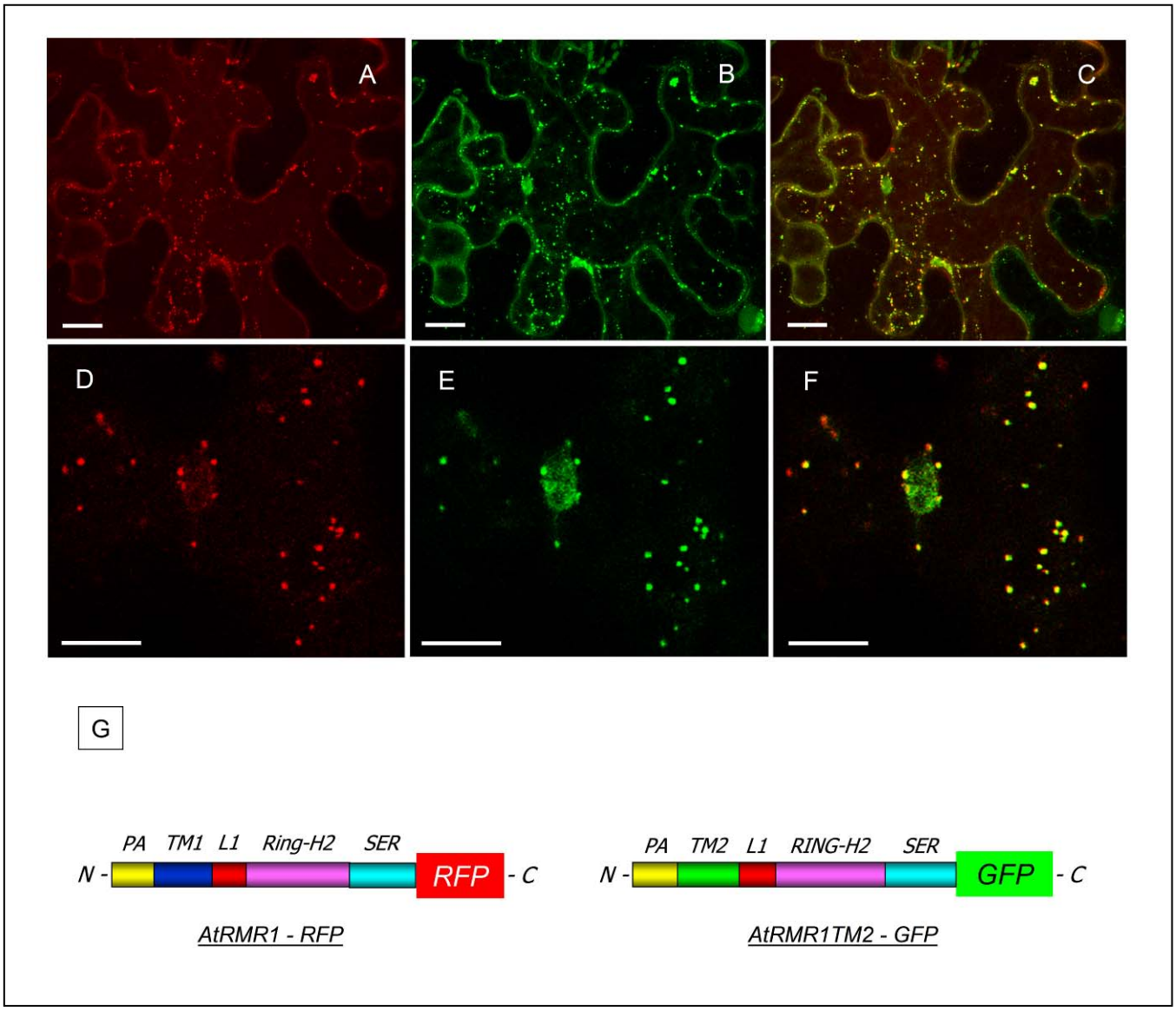

Figure 35: co-expression of AtRMR1-RFP and the mutant AtRMR1TM2-GFP in *N. benthamiana* leaves. Confocal images of (A) RFP fluorescence signal; (B) GFP fluorescence signal; (C) merged image of the two fluorescence signals. D-F enlarged portion of the images A-C. A-F scale bar = 20 µm.
(G) Schematic representation of the two fusion proteins. AtRMR1-RFP: full length AtRMR1 (PA domain, yellow; transmembrane, blue; linker, red; Ring-H2 domain, lilac; Serine-Rich domain, cyan) fused at its C-terminus with RFP; AtRMR1TM2 mutant (full length AtRMR1 with the transmembrane of AtRMR2, green) fused at its C-terminus with GFP.

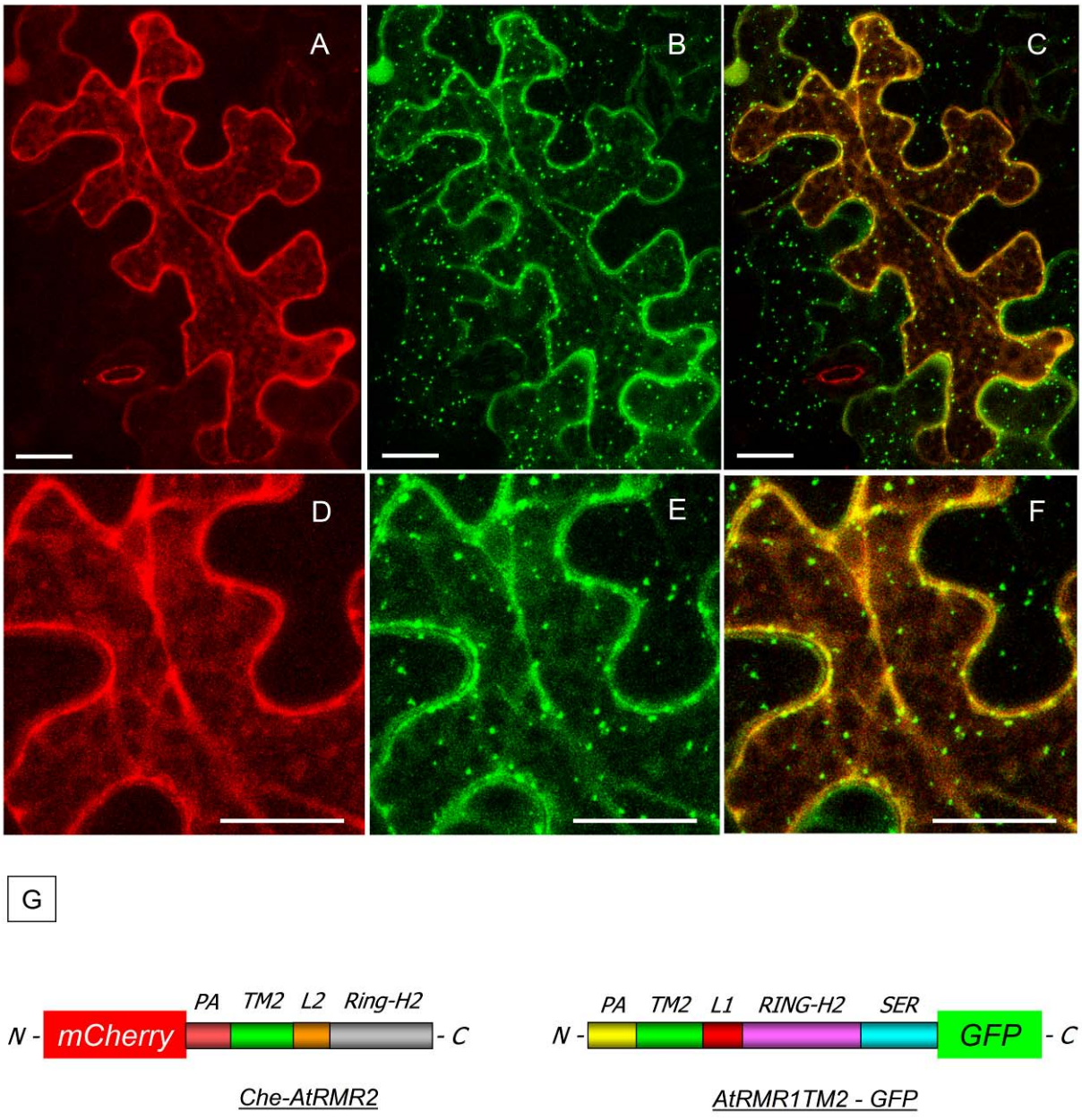

Figure 36: co-expression of Che-AtRMR2 and the mutant AtRMR1TM2-GFP in *N. benthamiana* leaves. Confocal images of (A) RFP fluorescence signal; (B) GFP fluorescence signal; (C) merged image of the two fluorescence signals. D-F enlarged portion of the images A-C. A-F scale bar = 25 µm.
(G) Schematic representation of the two fusion proteins. Che-AtRMR2: full length AtRMR2 (PA domain, rose; transmembrane, green; linker, orange; Ring-H2 domain, gray) fused at its N-terminus with mCHERRY; AtRMR1TM2 mutant (full length AtRMR1 with the transmembrane of AtRMR2, green) fused at its C-terminus with GFP.

2.4. Characterization of the cytosolic linkers of AtRMR1 and 2

As demonstrated in the previous experiments the different luminal, transmembrane and cytosolic domains of AtRMRs analyzed so far are not involved in protein localization. These results leave a last possibility that the localization sequence could be within the short cytosolic linker between the transmembrane and Ring-H2 domains. Indeed, these linkers are the only parts of AtRMRs which were not yet deleted or replaced during our mutant analysis.

These short sequences are in the cytosolic part of the protein immediately following the transmembrane domain. The two sequences are composed of 23 residues and show very low similarity. Therefore their differences could explain the different localization of AtRMR1 and 2. Certain membrane proteins contain indeed short specific aminoacid motifs near their transmembrane domains involved in protein trafficking in the endomembrane system. For instance the vacuolar sorting receptor pea BP80 harbours a tyrosine and an Ile-Met motifs in its short cytosolic tail which is involved in the traffic of the protein through the interaction with CCV coat (Happel *et al.*, 2004; Saint-Jean *et al.*, 2010).

The characterization of the two linkers was made by observing the effect of exchanging them between the two RMRs. I produced two expression vectors encoding the following fusion proteins: AtRMR1TM2L2-GFP (figures 37), where the transmembrane domain (TM1) and linker (L1) of AtRMR1 were replaced by their counterparts sequences from AtRMR2 (TM2 and L2 respectively); and the complementary AtRMR2TM1L1-GFP (figure 38) where TM2 and L2 of AtRMR2 were replaced by TM1 and L1 from AtRMR1. Both mutants were expressed in *N.benthamiana* under the control of 35S promoter and terminator.

As shown in figure 37 the mutant AtRMR1TM2L2 localized in punctate structures as wild type AtRMR1. Moreover the two fusion proteins mainly colocalize in the same compartment demonstrating that the TM sequence and linker of AtRMR2 had not an effect on the localization of the mutant (figure 39). Therefore the linker of AtRMR2 probably does not contain sequences involved in protein localization. Surprisingly however, the mutant AtRMR1TM2L2 seemed to be retained in the ER membrane when co-expressed with AtRMR2 wild type (figure 40). In this figure two epidermal cells are visible, one expressing only AtRMR1TM2L2-GFP while the other expressed both fusion proteins AtRMR1TM2L2-GFP and Che-AtRMR2. In the first cell, the mutant localized in punctate structures (figure 40, yellow arrow) but in the other cell, expressing both fusion proteins, AtRMR1TM2L2 seems to be retained in the ER (figure 40, white arrow). Indeed in this second cell, the number of punctate structures decreased and AtRMR1TM2L2 mainly co-localized with wild type AtRMR2 in the ER membrane. Therefore wild type AtRMR2 seems to

affect AtRMR1TM2L2 localization, probably by direct interaction or maybe by an indirect interaction with other factors.

For the complementary exchange mutant AtRMR2TM1L1, in contrast, it was possible to see an effect of replacing the TM sequence and linker of AtRMR2 with the corresponding sequence of AtRMR1. Indeed AtRMR2TM1L1 was able to exit the ER localizing in punctate structures (figure 38). As shown in the figure 41 this mutant localized in ER network in association with punctate structures which mainly colocalized with AtRMR1 wild type. Moreover the colocalization of AtRMR2TM1L1 with AtRMR2 supports the partial localization of this mutant in the membrane of ER (figure 42).

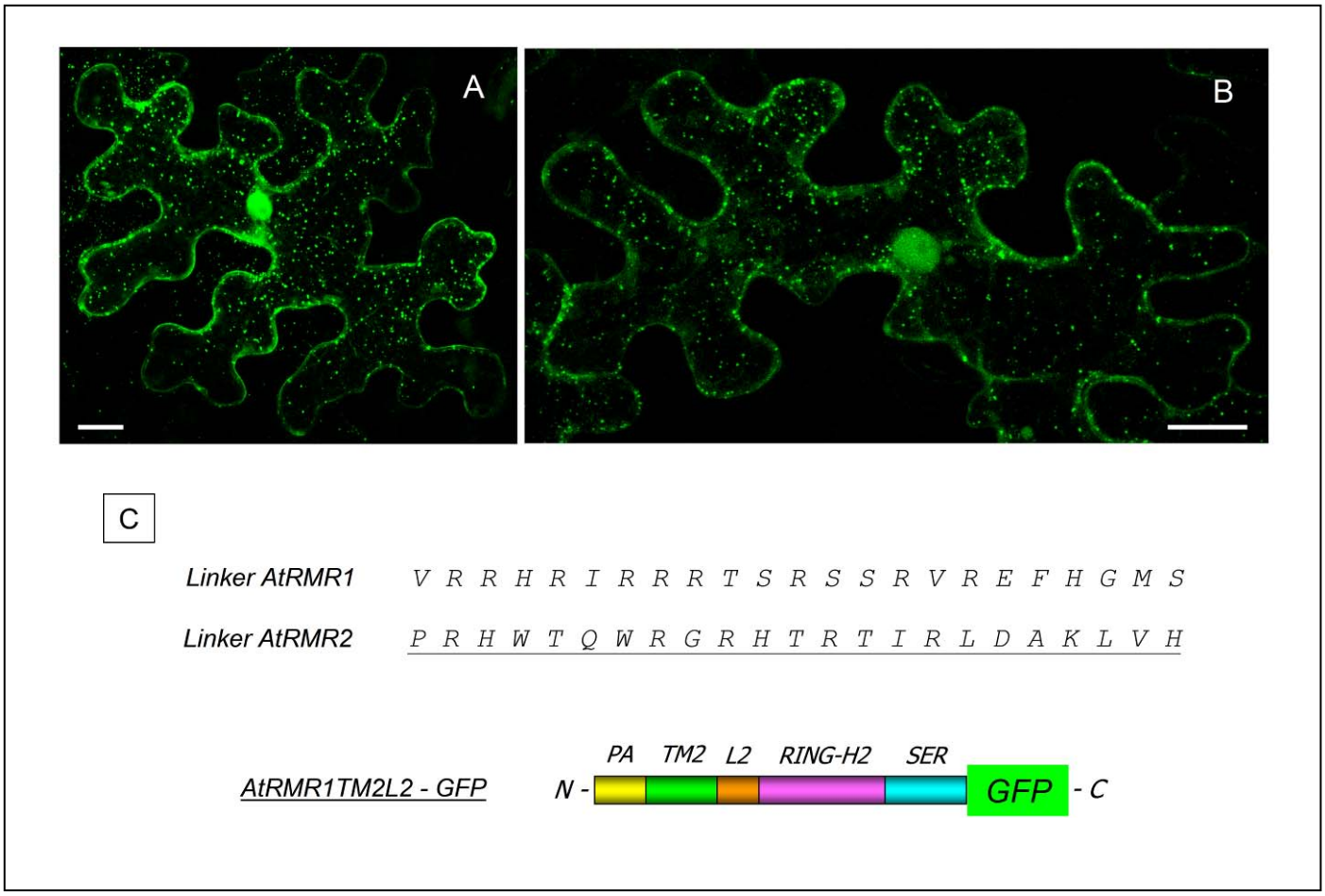

Figure 37: localization of AtRMR1TM2L2-GFP in *N. benthamiana* leaves. Confocal stack images (A and B) of epidermal cells. Bar is 20 µm. C alignment of the linkers of AtRMR1 and AtRMR2 and schematic representation of the fusion protein AtRMR1TM2L2-GFP: AtRMR1 where the transmembrane domain and sequence linker were replaced with the transmembrane domain and sequence linker of AtRMR2 (PA domain of AtRMR1, yellow; transmembrane domain from AtRMR2, green; sequence linker L2 from AtRMR2, orange; Ring-H2 domain of AtRMR1, lilac; Serine-Rich domain of AtRMR1, cyan) fused at the C-terminus with GFP.

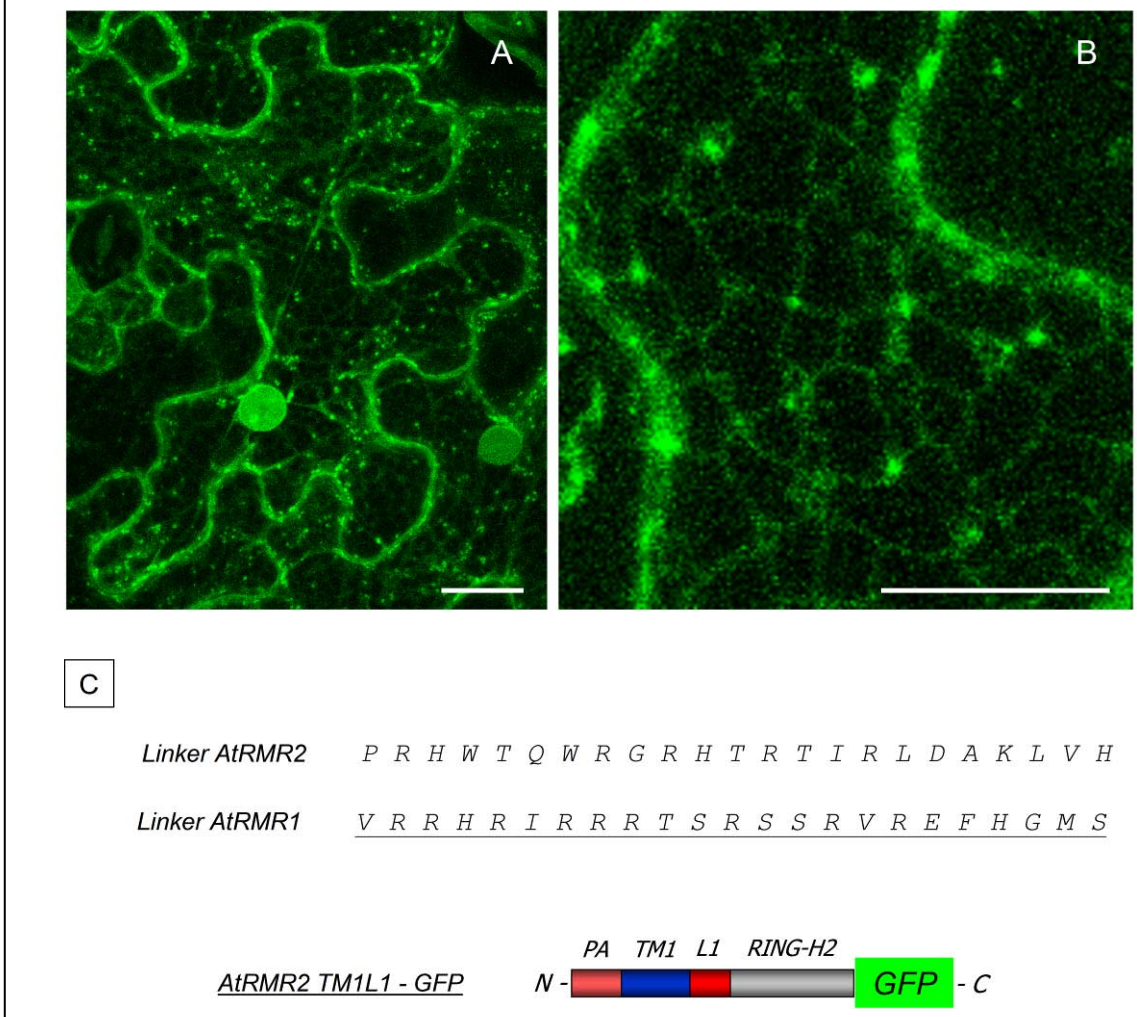

Figure 38: localization of AtRMR2TM1L1-GFP in *N. benthamiana* leaves. Confocal stack images (A and B) of epidermal cells. A bar is 20 µm, B bar is 15 µm. (C) alignment of the linkers of AtRMR2 and AtRMR1 and schematic representation of the fusion protein AtRMR2TM1L1-GFP: AtRMR2 where the transmembrane domain and sequence linker were replaced with the transmembrane domain and sequence linker of AtRMR1 (PA domain of AtRMR2, rose; trans-membrane domain from AtRMR1, blue; sequence linker L1 from AtRMR1, red; Ring-H2 domain of AtRMR2, grey) fused at the C-terminus with GFP.

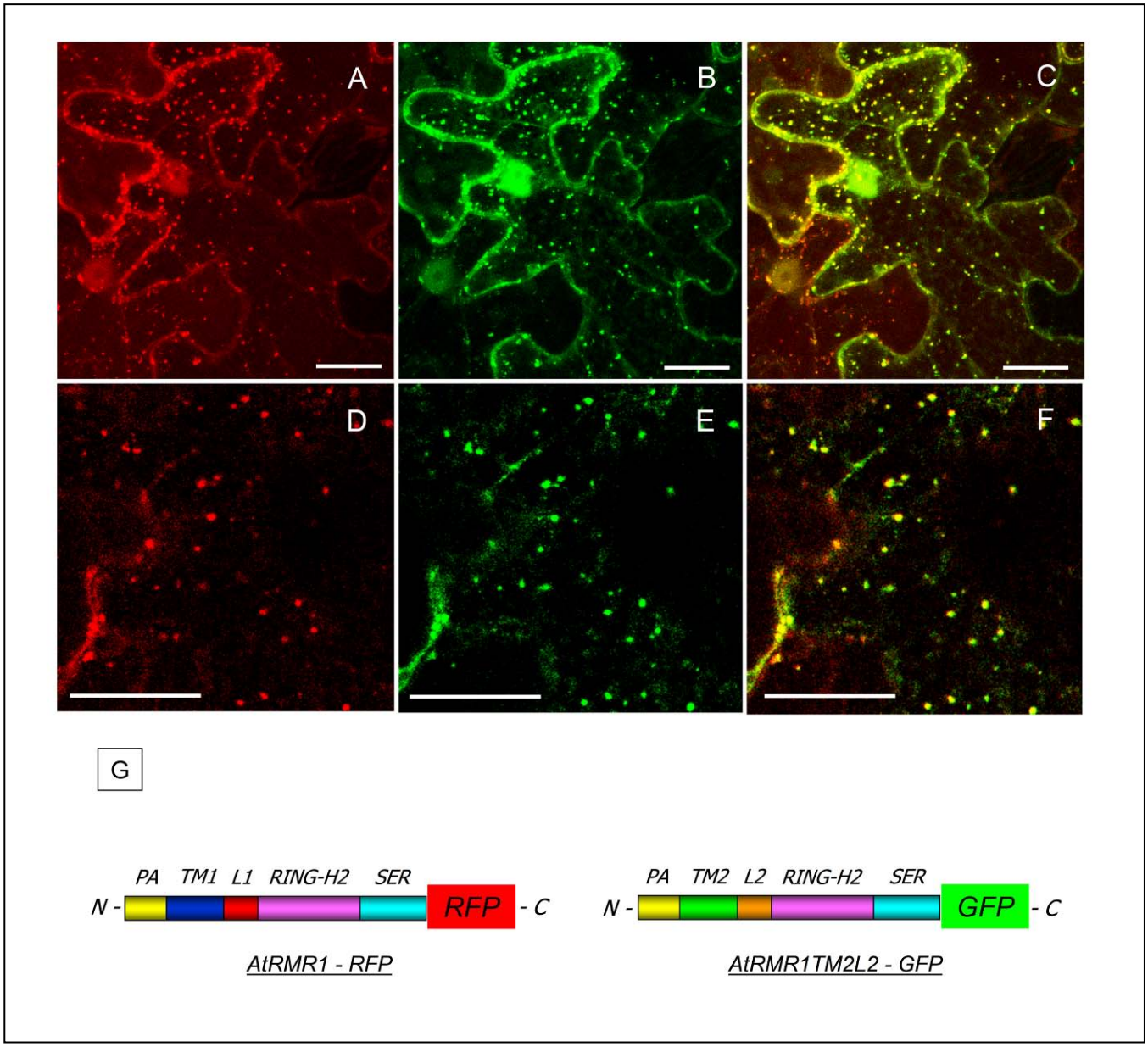

Figure 39: co-expression of AtRMR1-RFP and the mutant AtRMR1TM2L2-GFP in *N. benthamiana* leaves. Confocal images of (A) RFP fluorescence signal; (B) GFP fluorescence signal; (C) merged image of the two fluorescence signals. D-F enlarged portion of the images A-C. A-F bar = 20 µm.

(G) Schematic representation of the two fusion proteins. AtRMR1-RFP: full length AtRMR1 (PA domain, yellow; transmembrane, blue; linker, red; Ring-H2 domain, lilac; Serine-Rich domain, cyan) fused at its C-terminus with RFP. AtRMR1TM2L2 mutant (full length AtRMR1 with the transmembrane, green and linker, orange of AtRMR2) fused at its C-terminus with GFP.

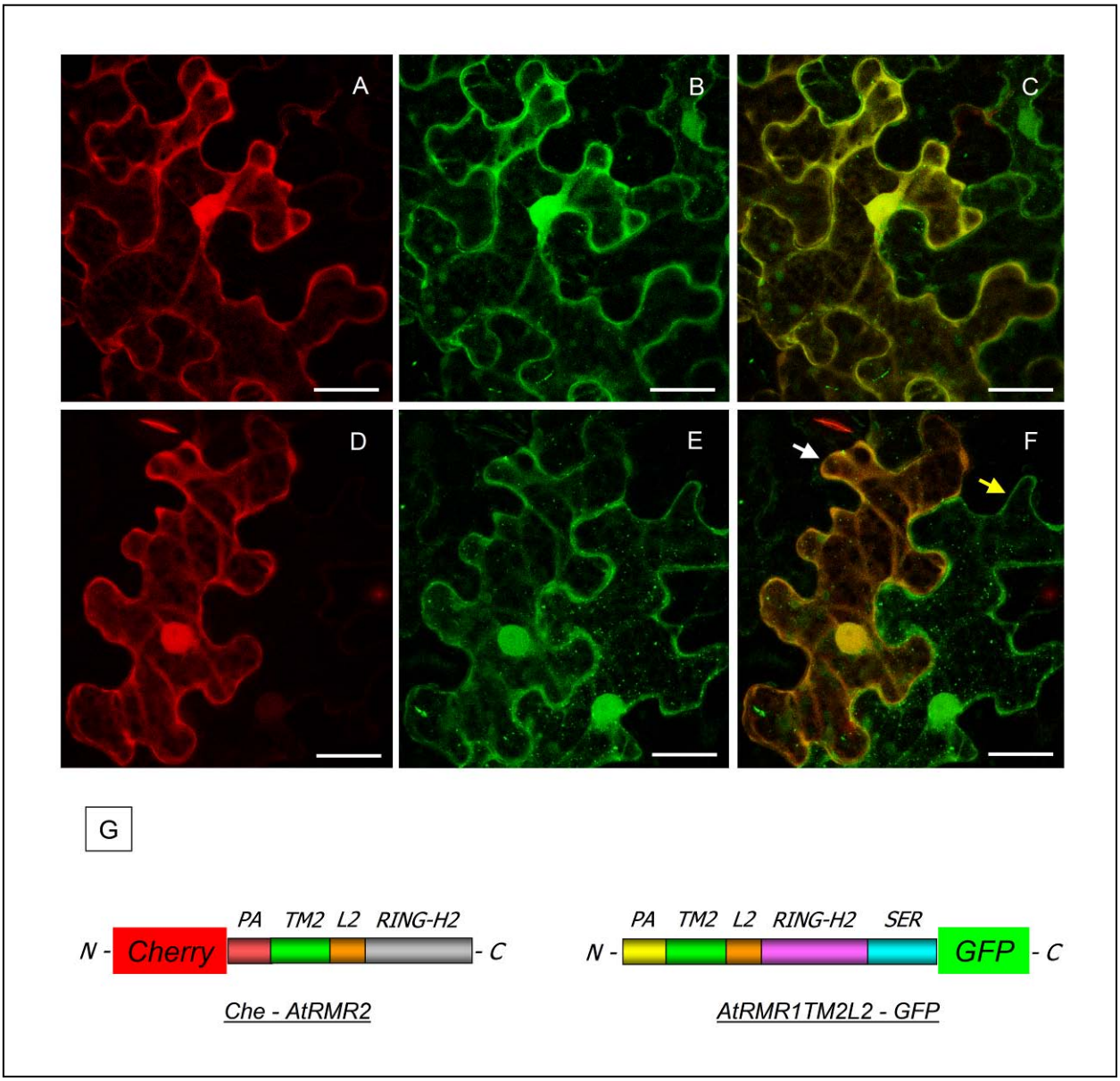

Fig 40: co-expression of Che-AtRMR2 and the mutant AtRMR1TM2L2-GFP in *Nicotiana benthamiana* leaves. Confocal images of two epidermal cells (The first one: Images A, B, C; and the second: Images D, E, F) expressing the two fusion proteins AtRMR1TM2L2-GFP and Che-AtRMR2. (A and D) RFP fluorescent signal; (B and E) GFP fluorescent signal; (C and F) merge images of the two fluorescent signals. The image F shows two cells: The first one (white arrow) expressing the two fusion proteins, Che-RMR2 and AtRMR1TM2L2; the second (yellow arrow) expressing only the mutant AtRMR1TM2L2. A-F scale bar = 20 µm.

(G) Schematic representation of the two fusion proteins, AtRMR1TM2L2-GFP and Che-AtRMR2. AtRMR1TM2L2-GFP: The AtRMR1 mutant where the transmembrane domain and the sequence linker were replaced with the transmembrane domain and the sequence linker of AtRMR2 (PA domain of AtRMR1, in yellow; transmembrane domain of AtRMR2, in green; The sequence linker of AtRMR2 L2, in orange; Ring-H2 domain of AtRMR1, in violet; Serine-Rich domain of AtRMR1, in cyan) fused at the C-terminal with GFP. Che-AtRMR2: The AtRMR2 wild type (PA domain of AtRMR2, in rose; transmembrane domain of AtRMR2, in green; the sequence linker of AtRMR2 L2, in orange; Ring-H2 domain of AtRMR2, in grey) fused at the N-terminal with mCHERRY.

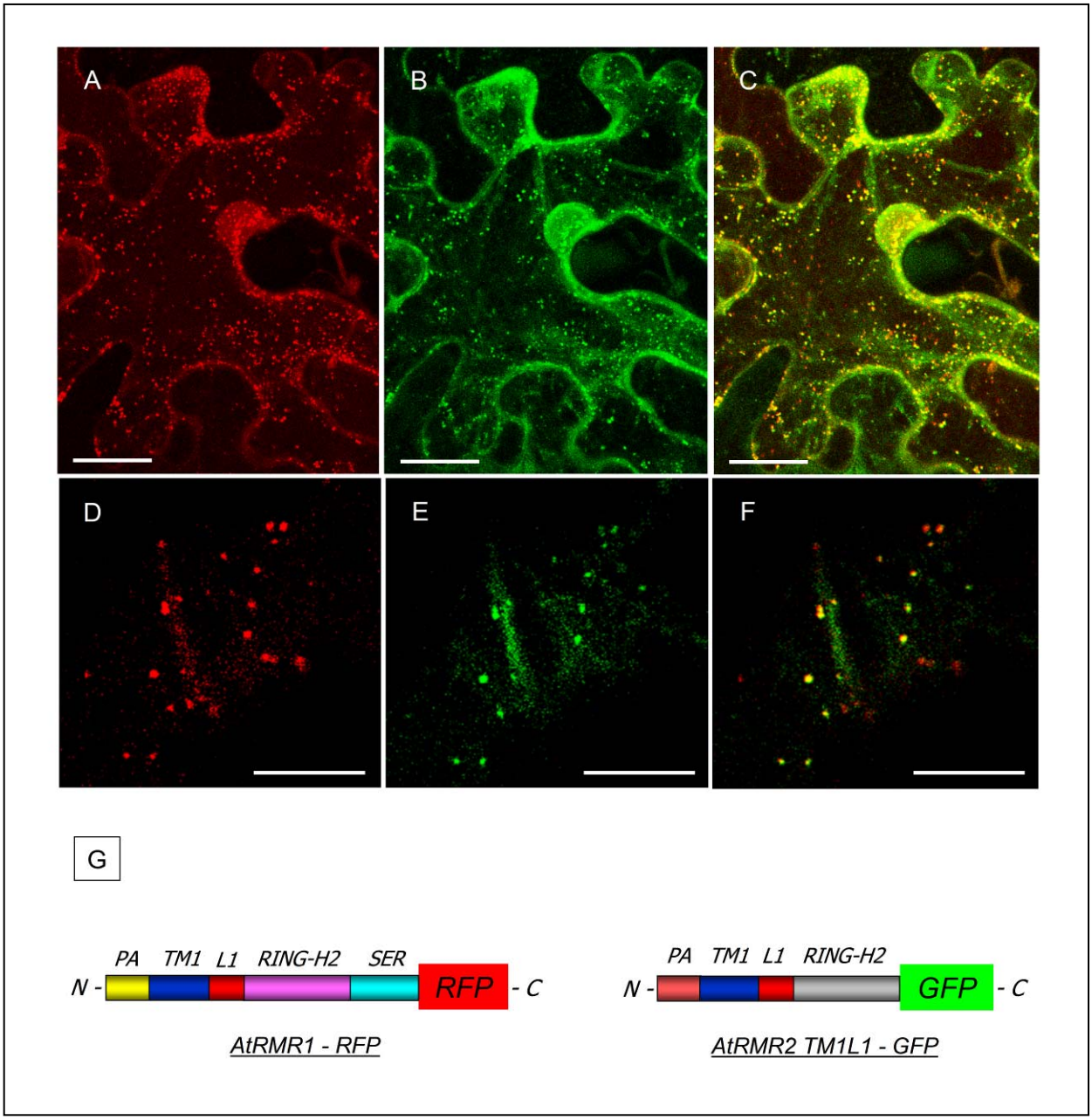

Figure 41: co-expression of AtRMR1-RFP and the mutant AtRMR2TM1L1-GFP in *N. benthamiana* leaves. Confocal images of (A) RFP fluorescence signal; (B) GFP fluorescence signal; (C) merged image of the two fluorescence signals. D-F enlarged portion of the images A-C. A-C bar = 20 µm; D-F bar = 10 µm.
(G) Schematic representation of the two fusion proteins. AtRMR1-RFP: full length AtRMR1 (PA domain, yellow; transmembrane, blue; linker, red; Ring-H2 domain, lilac; Serine-Rich domain, cyan) fused at its C-terminus with RFP. AtRMR2TM1L1-GFP: AtRMR2TM1L1 mutant (full length AtRMR2 with the transmembrane, blue and linker, red of AtRMR1) fused at its C-terminus with GFP.

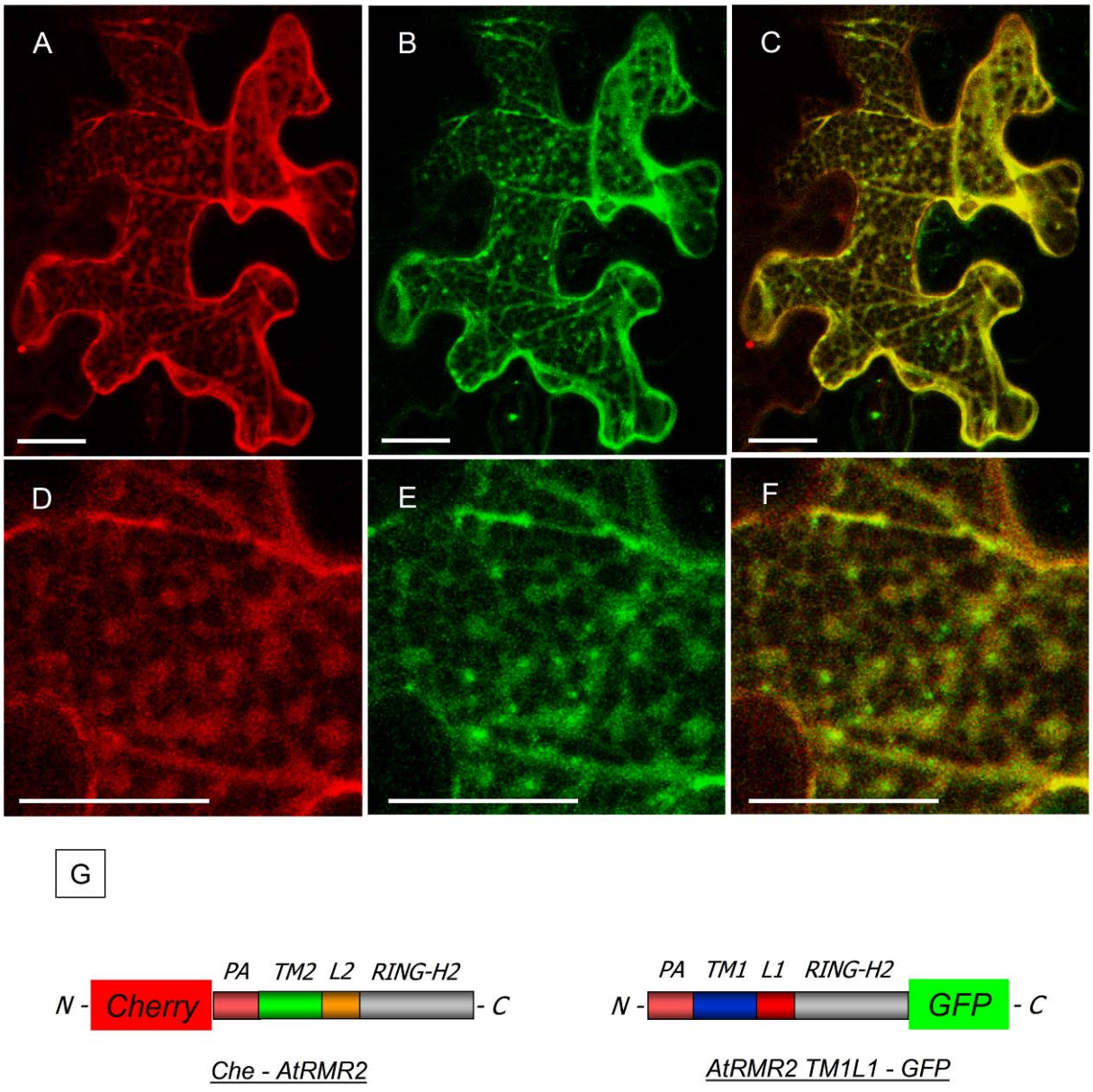

Figure 42: co-expression of Che-AtRMR2 and the mutant AtRMR2TM1L1-GFP in *N. benthamiana* leaves. Confocal images of (A) RFP fluorescence signal; (B) GFP fluorescence signal; (C) merged image of the two fluorescence signals. D-F enlarged portion of the images A-C. A-F bar = 20 µm.
(G) Schematic representation of the two fusion proteins. Che-AtRMR2: full length AtRMR2 (PA domain, rose; transmembrane, green; linker, orange; Ring-H2 domain, gray) fused at its N-terminus with mCHERRY. AtRMR2TM1L1-GFP: AtRMR2TM1L1 mutant (full length AtRMR2 with the transmembrane, blue and linker, red of AtRMR1) fused at its C-terminus with GFP.

2.4.1. Characterization of AtRMR1 linker

Our experiments with the AtRMR2TM1L1 mutant suggest that the linker L1 contains a motif involved in the trafficking of AtRMR1. However prediction programs have not found any common ER export signal involved in protein localization. The first 15 amino acids of linker L1 contain a high percentage (9/15 or 10/17) of arginines which are well known to be important in ER export (Dominguez *et al.*, 1998; Schoberer *et al.*, 2009). In these 15 residues the online software NLStradamus predicts a nuclear localization signal. Indeed arginines are frequently involved in protein sorting to the nucleus. Moreover this sequence also contains three serine residues which were predicted to be phosphorylated (NetPhos 2.0 Server). Post-translational modifications such as protein phosphorylation are an essential step in protein traffic to PSV (Matsuoka *et al.*, 1995). We thus hypothesize that the AtRMR1 linker contains a motif involved in protein localization.

Within the first 15 aminoacids of the linker the arginine residues are probably distributed in two blocks, either of which could constitute a di-basic motif involved in ER export and TGN localization. The first block is within the first five amino acids immediately after the transmembrane domain and the second within the next five residues, while the three potentially phosphorylated serines are within the last five of these 15 amino acids. Therefore the linker was dissected by introducing these blocks in the AtRMR2 linker in substitution for its corresponding sequence blocks and characterizing their effects on localization. I generated four expression vectors coding for the following fusion proteins: AtRMR2 with the transmembrane domain (TM1) and the first 15 residues of the linker (L1_15) of AtRMR1 (AtRMR2TM1L1_15-GFP, figure 43), with TM1 and the first ten residues of L1 (AtRMR2TM1L1_10-GFP, figure 44), with TM1 and the first five residues of L1 (AtRMR2TM1L1_5 GFP, figure 45), and with TM1 and the last five residues of L1 (AtRMR2TM1L1_5S GFP, figure 46). All these mutants were C-terminally fused with GFP and placed under the control of 35S promoter and terminator. These four fusion proteins were generated to determine the trafficking role of all 15 residues (L1_15), the first ten residues (L1_10), the first five residues immediately after the trans-membrane domain (L1_5), and the last five of these 15 aminoacids (L1_5S).

As shown in the figures 45 and 46 the two mutants AtRMR2TM1L1_5-GFP and AtRMR2TM1L1_5S-GFP localized in the ER as well as the wild type AtRMR2, while the other two mutants, AtRMR2TM1L1_10-GFP and AtRMR2TM1L1_15-GFP (figure 44 and 43), localized in the ER network but also in association with few punctate structures. Taking together all these results, I can say that the first 5 residues (L1_5) and the last 5 (L1_5S) do not contain any sequence involved in ER export, while there is a partial effect when replacing the first 10 (L1_10) or 15 residues (L1_15). This effect is not comparable however with the localization effect observed when

replacing the whole linker in the mutant AtRMR2TM1L1. Therefore it is likely that all the linker of AtRMR1 is necessary for an efficient ER export.

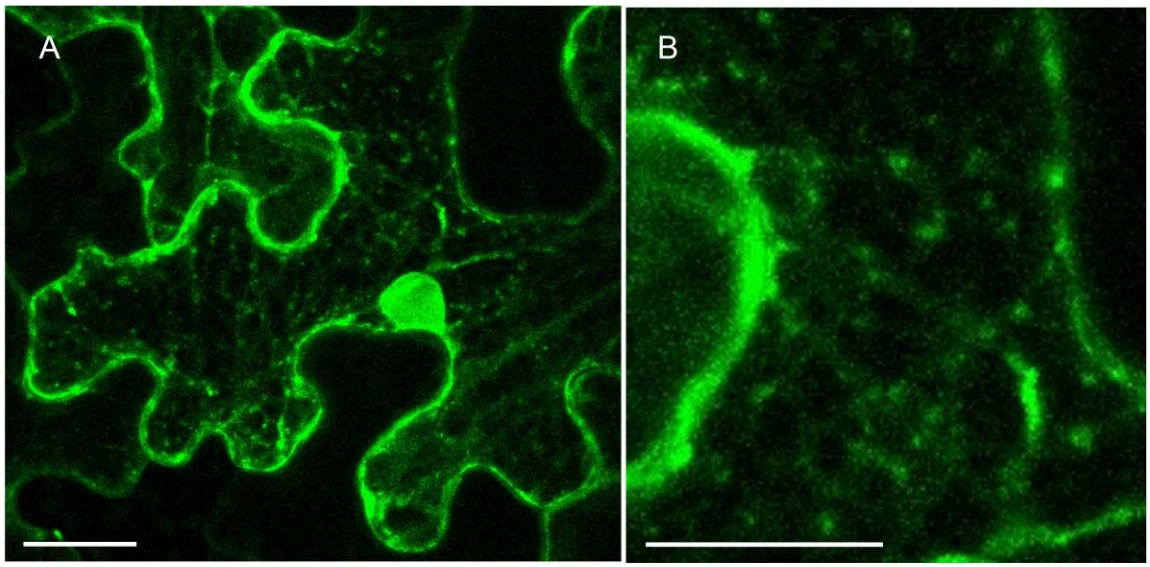

C

Linker AtRMR2 P R H W T Q W R G R H T R T I R L D A K L V H

Linker AtRMR1 V R R H R I R R R T S R S S R V R E F H G M S

V R R H R I R R R T S R S S R R L D A K L V H

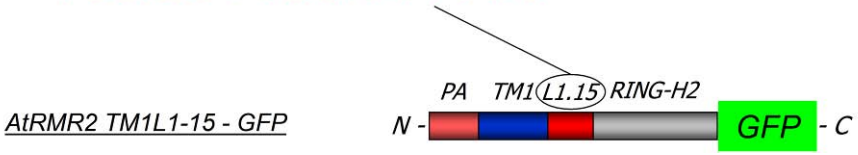

Figure 43: AtRMR2TM1L1_15 localization in *Nicotiana benthamiana* leaves. Confocal stack images (A and B) of epidermal cell from *N.benthamiana* leaf expressing the fusion protein AtRMR2TM1L1_10-GFP. A scale bar = 20 µm. B scale bar = 15 µm.
Below the two pictures it is shown an alignment between the linker of AtRMR2 (in black) and AtRMR1 (in red) (C). Moreover it is shown a schematic representation of the fusion protein AtRMR2TM1L1_15-GFP (C): The AtRMR2TM1 mutant where the first 15 aminoacids of AtRMR2 linker were replaced by the first 15 aminoacids of AtRMR1 linker. (PA domain of AtRMR2, in rose; transmembrane domain of AtRMR1, in blue; the sequence linker L1_15, in red; Ring-H2 domain of AtRMR2, in grey) fused at its C-terminus with GFP. It is also shown the aminoacidic sequence of the resulting L1_15 linker, where the aminoacids of AtRMR1 linker are indicated in red (first 15 aminoacids) and the aminoacids of AtRMR2 linker in black (the following 8 aminoacids) (C).

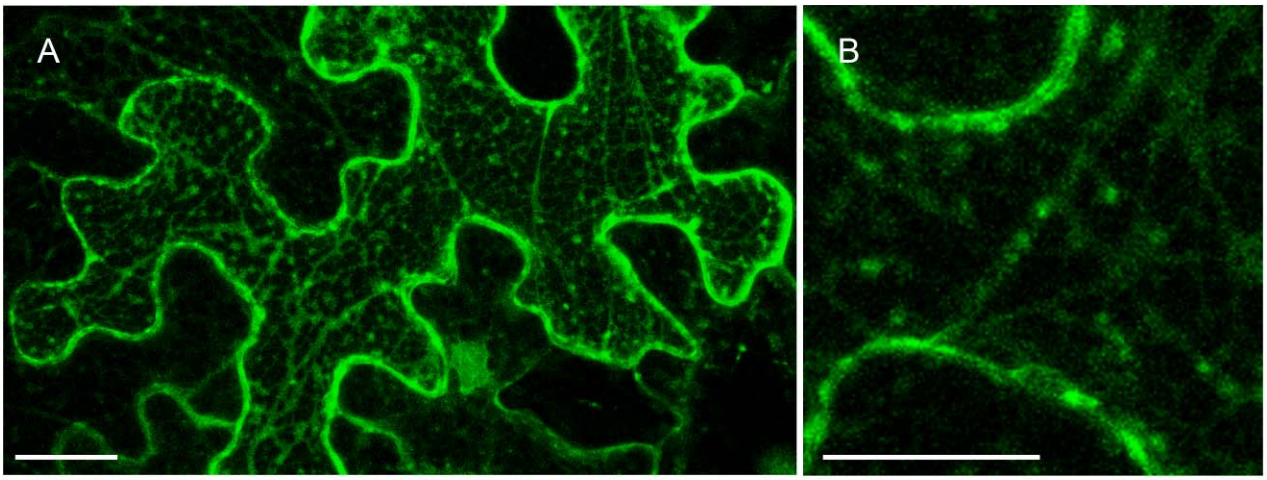

C

Linker AtRMR2 P R H W T Q W R G R H T R T I R L D A K L V H

Linker AtRMR1 V R R H R I R R R T S R S S R V R E F H G M S

V R R H R I R R R T H T R T I R L D A K L V H

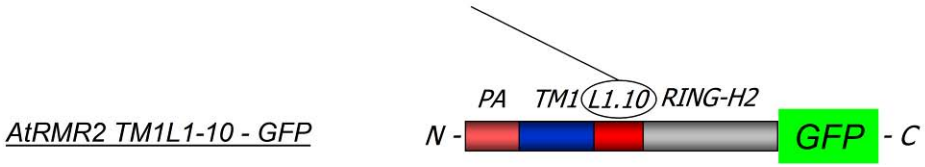

AtRMR2 TM1L1-10 - GFP

Figure 44: AtRMR2TM1L1_10 localization in *Nicotiana benthamiana* leaves. Confocal stack images (A and B) of epidermal cell from *N.benthamiana* leaf expressing the fusion protein AtRMR2TM1L1_10-GFP. A scale bar = 20 μm. B scale bar = 15 μm.
Below the two pictures it is shown an alignment between the linker sequences of AtRMR2 (in black) and AtRMR1 (in red) (C). Moreover it is shown a schematic representation of the fusion protein AtRMR2TM1L1_10-GFP (C): The AtRMR2TM1 mutant where the first 10 aminoacids of AtRMR2 linker were replaced by the first 10 aminoacids of AtRMR1 linker (PA domain of AtRMR2, in rose; transmembrane domain of AtRMR1, in blue; the sequence linker L1_10, in red; Ring-H2 domain of AtRMR2, in grey) fused at its C-terminus with GFP. It is also shown the aminoacidic sequence of the resulting L1_10 linker, where the aminoacids of AtRMR1 linker are indicated in red (first 10 aminoacids) and the aminoacids of AtRMR2 linker in black (the following 13 aminoacids) (C).

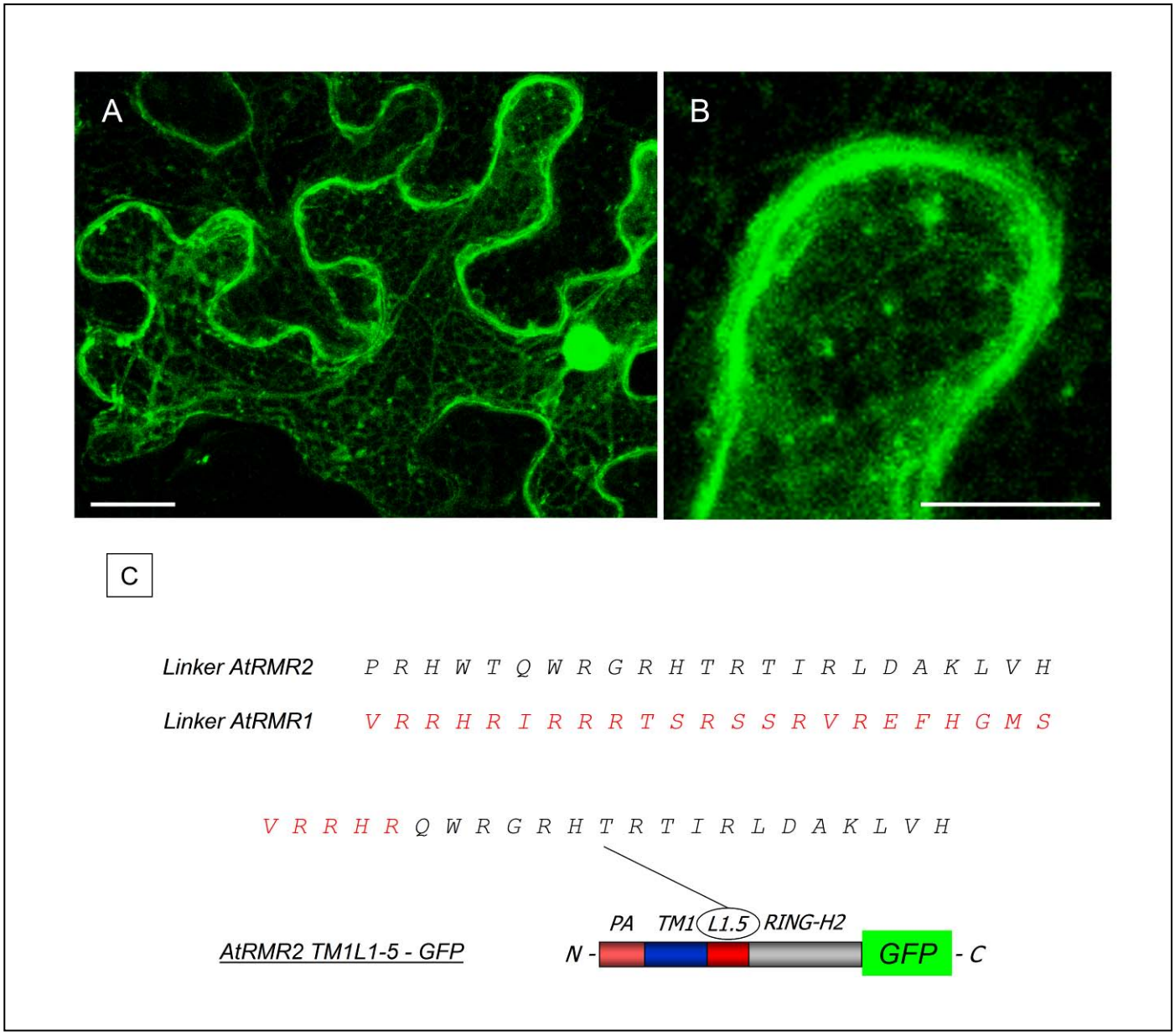

Figure 45: AtRMR2TM1L1_5 localization in *Nicotiana benthamiana* leaves. Confocal stack images (A and B) of epidermal cell from *N.benthamiana* leaf expressing the fusion protein AtRMR2TM1L1_5-GFP. A scale bar = 20 μm. B scale bar = 15 μm.
Below the two pictures it is shown an alignment between the linker sequences of AtRMR2 (in black) and AtRMR1 (in red) (C). Moreover it is shown a schematic representation of the fusion protein AtRMR2TM1L1_5-GFP (C): The AtRMR2TM1 mutant where the first 5 aminoacids of AtRMR2 linker were replaced by the first 5 aminoacids of AtRMR1 linker (PA domain of AtRMR2, in rose; transmembrane domain of AtRMR1, in blue; the sequence linker L1_5, in red; Ring-H2 domain of AtRMR2, in grey) fused at its C-terminus with GFP. It is also shown the aminoacidic sequence of the resulting L1_5 linker, where the aminoacids of AtRMR1 linker are indicated in red (first 5 aminoacids) and the aminoacids of AtRMR2 linker in black (the following 18 aminoacids) (C).

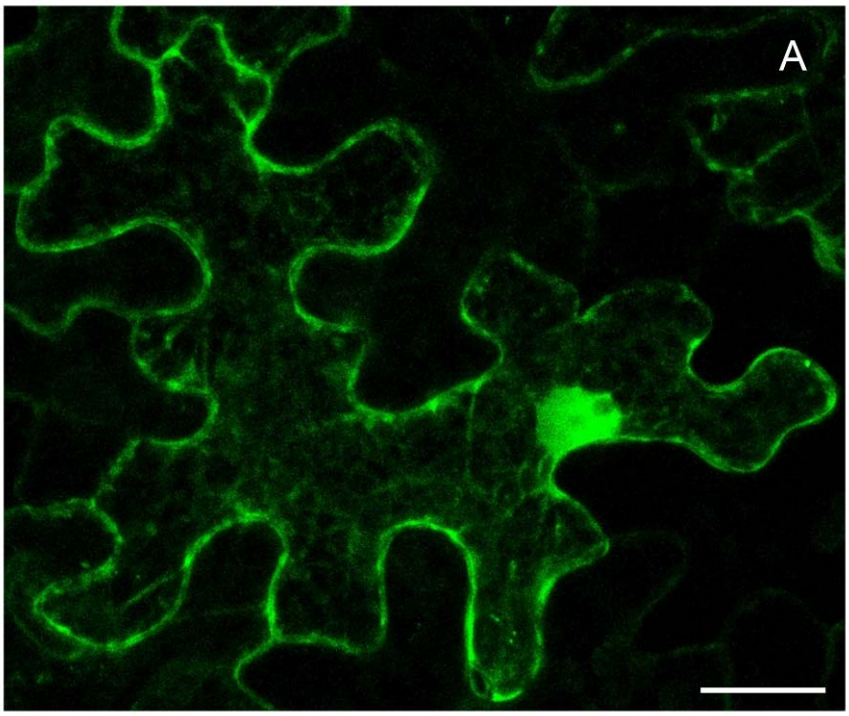

B

Linker AtRMR2 P R H W T Q W R G R H T R T I R L D A K L V H

Linker AtRMR1 V R R H R I R R R T S R S S R V R E F H G M S

P R H W T Q W R G R S R S S R R L D A K L V H

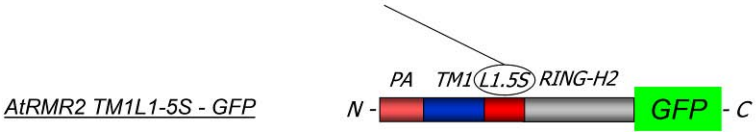

Figure 46: AtRMR2TM1L1_5S localization in *Nicotiana benthamiana* leaves. Confocal stack images (A and B) of epidermal cell from *N.benthamiana* leaf expressing the fusion protein AtRMR2TM1L1_5S-GFP. A-B scale bar = 20 μm.
Below the two pictures it is shown an alignment between the linker sequences of AtRMR2 (in black) and AtRMR1 (in red) (C). Moreover it is shown a schematic representation of the fusion protein AtRMR2TM1L1_5S-GFP (C): The AtRMR2TM1 mutant where the 5 aminoacids from position eleventh to fifteenth of AtRMR2 linker were replaced by corresponding aminoacids of AtRMR1 linker (PA domain of AtRMR2, in rose; transmembrane domain of AtRMR1, in blue; The sequence linker L1_5, in red; Ring-H2 domain of AtRMR2, in grey) fused at its C-terminus with GFP. It is also shown the aminoacidic sequence of the resulting L1_5S linker, where the aminoacids of AtRMR1 linker are indicated in red and the aminoacids of AtRMR2 linker in black (C).

Discussion of localization

1. AtRMR2 localization in *N.benthamiana* leaves and in *A.thaliana* leaf protoplasts

In *N. benthamiana* both fusion proteins AtRMR2-YFP and YFP-AtRMR2 localize in typical ER structures: the fluorescence signal is mainly localized in a cortical network, which extends into the cell and also forms the nuclear envelope. The colocalization with the ER marker protein p6 (Peremyslov *et al.*, 2004) further supports these results. Moreover two AtRMR2 constructs fused to a different fluorescent reporter at either end (AtRMR2-YFP, Che-AtRMR2) also colocalize in the ER membrane. This strongly suggests that the reporters do not interfere with the localization of receptor and consequently that AtRMR2 does not possess N- or C-terminal localization sequences which could be masked by the presence of a reporter. This also suggests the presence of internal sorting sequences in luminal, cytosolic or transmembrane domains.

The localization of AtRMR2 was also confirmed in *A.thaliana* protoplasts transformed with the same constructs, including the colocalization with the ER marker protein p6.

Taking together all these experiments performed in *N.benthamiana* and *A.thaliana* protoplasts suggest that AtRMR2 is an ER-resident protein.

On the other hand AtRMR2 does not colocalize with the Golgi marker GONST1 (Baldwin *et al.*, 2001). As a receptor, AtRMR2 would be most likely involved in the traffic between ER and Golgi. In this hypothesis AtRMR2 should recycle quickly back to the ER preventing its observation in the Golgi. Cotransformation of the two constructs allows visualizing the close association between these two compartments. Indeed we can observe two different groups of Golgi, either associated with the ER, probably at ER export sites, or free in the cytosol.

2. AtRMR2 localization in transgenic plants

In order to confirm the localization of AtRMR2 in transient expression experiments we generated *A.thaliana* stably transformed with AtRMR2-YFP. We could then determine the localization in the plant of origin and visualize possible differences between the two experimental systems. Several independent lines were examined at different development stages observing a faint YFP labelling in all analysed samples. We observed a short increase of the fluorescent signal in old plants probably due to an accumulation of the fusion proteins during the time. This detection problem could be due to RNA silencing. Indeed it is possible that the AtRMR2 mRNA contains specific sequences (e.g.

highly repeated sequences) recognized by the silencing apparatus. In *N.benthamiana* AtRMR2-YFP could indeed only be efficiently expressed by using the silencing inhibitor p19 (Voinnet *et al.,* 2002). p19 is a viral protein, which binds siRNAs and prevents their use by the silencing machinery (Lakatos *et al.,* 2004), stabilizing mRNAs and in consequence increasing the concentration of the encoded proteins.

In all analyzed tissues, i.e. leaf, stem, and root we only detected a signal in the epidermis. No fluorescence was observed in the leaf mesophyll or other internal tissues, despite the fact that AtRMR2-YFP was expressed under the control of the 35S promoter, a constitutive promoter in most cells and tissues. A possible explanation could be silencing involving the 35S promoter (Daxinger *et al.,* 2007). The 35S promoter can be inactivated by methylation probably as part of a defence reaction against viruses. Moreover, the fusion protein could undergo post-translational degradation, which would prevent the observation of YFP in certain tissues. Indeed particular amino acid sequences could accelerate degradation and consequently lead to a rapid protein turnover.

The AtRMR2-YFP labelling in transgenic *A.thaliana* plants supported the ER localization observed in *N.benthamiana*. In stomata and root cells YFP typically labelled the nuclear envelope, while the ER network was not detectable probably because it was expressed below the detection threshold. To confirm the pattern, we performed a series of immuno-gold electro-microscopy experiments using young roots as biological samples. This procedure allowed us to confirm the ER localization of AtRMR2-YFP observed with the confocal microscope. In fact most gold particles were localized around the nuclear envelope. Moreover the signal was also localized in extended compartments surrounded by ribosomes in both cortical and inner parts of the cell. The presence of ribosomes confirmed the identity of this compartment as the rough ER network.

We observed some background signal, which depended on the concentration of antibody. In fact high concentration of antibody could lead to unspecific binding of these molecules to not specific structures inside and outside of the cell. For instance it is possible to observe high unspecific signal in organelles such as plastids. In fact the high protein concentration in plastids increases the unspecific binding of antibodies. However setting the good concentration of antibody we eliminated the background signal conserving only the specific signal in the ER. Consequently the presence of ER labelling even using low concentration of antibody supported the specificity of this signal. Alternatively the expression of fusion proteins is often correlated with protein instability resulting in the possible dissociation of the fluorescent reporter. This led to the presence of some free YFP, which could constitute a problem increasing the cytosolic and the nuclear background signal. The unspecific labelling of the nucleus is due to the presence of a cryptic nuclear localization signal in

GFP based reporter. Finally transgenic AtRMR2 plants grew normally and did not show any evident morphological alteration, suggesting that overexpression of AtRMR2 does not interfere with normal plant development.

This ER localization of AtRMR2 is completely different from the results of Park *et al.,* (2005). They localized the receptor mainly in the PVC but also in the Golgi apparatus, compatible with a role of AtRMR2 in protein sorting to vacuoles. This different result could be due by the different experimental systems, which were used to localize the protein. Park et al. localized both endogenous protein and the HA-tagged protein by immunolabelling in *A.thaliana* leaf protoplasts. In contrast I localized the YFP-tagged AtRMR2 in *N.benthamiana* leaves transiently transformed by agro-infiltration and in transgenic *A.thaliana* plants. We demonstrated that the presence of a fluorescent reporter at either end does not interfere with protein localization. In both cases the fusion proteins showed ER localization in *N.benthamiana*. Therefore it is likely that the fusion protein is not mislocalized compared to the endogenous protein. Moreover we confirmed the ER localization of AtRMR2 in stably transformed *A.thaliana*. These plants allowed us to localize the protein observing different cell types and tissues in the plant of origin. All cell types showed a clear ER labelling, which was confirmed by immuno-gold labelling on root cells. It would be best to check if the fusion proteins have the same localization as the endogenous proteins. For this purpose a specific antibody raised against the native protein should be produced in *Escherichia coli*, which could be use in immuno-electron microscopy experiment (IEM). If the ER localization will be confirmed we could make new hypothesis about the role of AtRMR2.

It is still possible that an ER-localized AtRMR2 plays a role in vacuolar sorting. It could work as a nucleation point for storage protein aggregation directly in the ER, after which a second vacuolar receptor would transport the storage proteins from Golgi to vacuole. This model implies that different receptors work sequentially in the pathway to PSV. Different members of the AtRMR family could function in different subcellular compartments. Consequently this hypothesis supports the possible interaction between the different members of AtRMR family during protein transport to vacuole. It is also possible that AtRMR2 plays a role in vacuolar sorting directly from ER without a second vacuolar receptor in a post-ER compartment. The AtRMR2/vacuolar cargo complex could arrive directly to vacuole, bypassing the Golgi. Such an alternative direct ER-to-PSV transport by PAC vesicles was indeed observed in pumpkin seed storage tissues (Hara-Nishimura *et al.,* 1998).

Alternatively AtRMR2 is not involved in vacuolar sorting but in another cellular process. Indeed, proteins that combine a luminal PA domain and a cytosolic Ring-H2 domain have been found in several non-plant organisms such as *Drosophila, Xenopus*, chicken and mammals (Bocock *et al.,*

2009). These proteins include several Ring-type E3 ubiquitin ligases like GREUL1 from *Xenopus* (Goliath Related E3 Ubiquitin Ligase 1) (Borchers *et al.*, 2002) and GRAIL from *human* CD4+ T cells (Gene Related to T-cell Anergy In Lymphocytes) (Anandasabapathy *et al.*, 2003). These similarities suggest that RMRs have similar E3 ligase activities in plants.

In electron micrographs of root cells from AtRMR2-YFP-transgenic *A.thaliana* plants we observed peculiar circular compartments which have probably never been described in plants. These structures are surrounded by membranes near the plasma membrane and have non electron-dense contents. They seem to be extensions of the plasma membrane, surrounding cytosolic material, but could also derive from a pre-existing internal organelle and have associated with the plasma membrane. They also can have a complex internal structure. In some cases it is possible to observe several internal sub-compartments surrounded by a membrane.
In roots of wild type *A.thaliana*, it is also possible to observe these structures, but their number seems higher in AtRMR2YFP-expressing plants. This increased number could well be due to AtRMR2 over-expression, but AtRMR2 labelling was never observed in these compartments meaning that AtRMR2 is probably not directly involved in their formation, but would rather indirectly stimulate their biogenesis.
Very similar structures have been observed in the plasma membrane of tobacco BY2 cells. They were described as exocyst-positive organelles (Expo), which localized in both inner and cortical parts of the cell. This organelle was defined by the presence of a specific protein maker AtExo70E2, a member of the exocyst complex involved in vesicle docking in exocytosis (Zhang *et al.*, 2010; Chong *et al.*, 2010). In order to confirm the structures we observed in AtRMR2-YFP-expressing *A.thaliana* plants as Expo organelles, it will be necessary to label them using a specific antibody against AtExpo70E2.

3. AtRMR1 localization in *N.benthamiana*

The full length AtRMR1 fused to YFP at either C- or N-terminus localized in dots. To identify this compartment, I coexpressed AtRMR1-YFP with several different markers. It did not colocalize with the ER marker p6-CFP (Peremyslov *et al.*, 2004), nor with the two Golgi markers Sialyltransferase-RFP (Wee *et al.*, 1998) and GONST1-RFP (Baldwin *et al.*, 2001). In these experiments we could observe in some cases AtRMR1-YFP-labeled compartments close to the two Golgi markers. In contrast AtRMR1-YFP perfectly colocalized with the TGN marker SYP61 (Uemura *et al.*, 2004) identifying thus the AtRMR1 compartment. This localization also fits with the occasional association between the two Golgi markers and the AtRMR1-positive organelles, as TGN and Golgi

apparatus have been demonstrated to be spatially separated but also sometimes in close proximity (Uemura *et al.,* 2004; Foresti *et al.,* 2008). Finally AtRMR1-YFP also partially colocalized with the BP80 reporter (Miao *et al.,* 2006), which is predominantly a marker for PVC, but also labels the TGN (Miao *et al.,* 2006) and is assumed to recycle between these two compartments.

4. AtRMR1 localization in transgenic plants

In order to confirm the localization observed in *N.benthamiana*, I generated *A.thaliana* stably transformed with AtRMR1-YFP under the control of the 35S promoter. Unfortunately the fusion protein was not detectable in any generated plant. Even in *N.benthamiana* AtRMR1-YFP was only detectable using the silencing inhibitor p19 (Voinnet *et al.,* 2002). It is possible that AtRMR1 is subject to a rapid degradation of either the mRNA or the protein, preventing over-expression. My results on gene expression indicate that AtRMR1 is more likely regulated at the protein level. Indeed the endogenous promoter is very active in leaves from early stages of development until flowering and the mRNA is detectable in all stages. Consequently it is probable that AtRMR1 is subjected to a fast protein turnover, which prevents its observation unless using p19. AtRMR1 possesses a C-terminal Serine-Rich domain, which contains several serines predicted to be phosphorylated. Posttranslational modification by phosphorylation is implicated is several cellular processes including protein degradation. This domain could thus be involved in AtRMR1 regulation, destabilizing the fusion protein. In contrast, AtRMR2 does not possess a C-terminal Serine-Rich domain and it is visible when overexpressed in transgenic *A.thaliana* plants. Moreover the AtRMR1 deletion mutant without Ser-Rich domain seems to be more expressed then the wild type protein in *N.benthamiana.*

5. Characterization of AtRMR deletion mutants

AtRMR1 and AtRMR2 belong to the same family of protein but have a different subcellular localization. Therefore in order to characterize sequences involved in this different localization I generated different AtRMR deletion mutants of different domains.

The two deletion mutants of AtRMR2 lacking the PA or the Ring-H2 domain show the same ER localization as the wild type protein. Therefore these domains seem not to be involved in protein localization and probably only the transmembrane domain and the few amino acids surrounding it are really important. As for other single membrane spanning proteins such as VSRs, it is likely that the cytosolic sequence linker immediately following the transmembrane domain could contain a motif involved in protein localization (daSilva *et al.,* 2006).

I used the same approach for AtRMR1 generating four different mutants with deletions of different domains (PA, Ring-H2 and Serine-Rich) in different combinations. Again all deletion mutants localized in punctate structures just like the full-length protein. The only mutant that was partly mislocalized was the mutant lacking both RingH2 and Serine-Rich domains (ΔSRAtRMR1-YFP). In this case part of the protein showed the normal localization in punctate structures, but a minor portion of the protein localized in the nucleolus. This mislocalization could due to the presence of a cryptic nucleolar localization signal, which could be exposed in this mutant lacking the two C-terminal domains. This hypothesis is supported by a putative nuclear localization signal, which was predicted in the first cytosolic amino acids immediately after the transmembrane domain: three arginines at the seventh, eighth and ninth position of the cytosolic sequence linker. Alternatively, the nucleolar localization of ΔSRAtRMR1-YFP could be an artefact of overproduction, which could cause a partially mislocalization to unspecific compartments. Indeed the level of expression was much higher than for others constructs.

All deletion mutants localized in dots, but it is difficult to say if they represent the same compartment. These mutants were not expressed at the same level and it is very difficult to say if the number and dimension of dots were comparable. To answer these questions we made several colocalization experiments, which showed that the two deletion mutants ΔSRAtRMR1 and ΔPSAtRMR1 perfectly colocalized with wild type AtRMR1. Therefore the PA, Ring-H2 and Serine-Rich domains are probably not involved in the protein localization. Again only the transmembrane domain and the following short cytosolic linker could contain a localization signal.

6. Characterization of AtRMR transmembrane domains

In the next step I also studied the role of the TM domain of AtRMR1 and AtRMR2 in protein localization. I did not observe any change in protein localization when exchanging the TM domain of AtRMR1 with the TM domain of AtRMR2 in the two wild type proteins. Indeed the two mutants AtRMR1TM2 (AtRMR1 with the TM domain of AtRMR2) and AtRMR2TM1 (AtRMR2 with the TM domain of AtRMR1) localized in TGN and ER, respectively. This was confirmed by co-localizing the two mutants with the respective wild type proteins AtRMR1 and AtRMR2. Consequently it is likely that the transmembrane domains of AtRMR1 and AtRMR2 are not involved in protein localization.

The results obtained with the two TM domain exchange mutants are not so compatible with those of Brandizzi *et al* (2002). They showed that the length of the TM domain alone could determine protein localization in plant cells. Proteins with a short (17 aa) transmembrane domain localized in early secretory compartment such as ER, while proteins with a longer TM domain localized in later

compartments such as Golgi (20 aa) and plasma membrane (23 aa). This change in length reflects the difference in membrane lipid composition and hence thickness of the bilayer between the different compartments. This model cannot explain what we showed for AtRMR1 and 2. In fact these two proteins have a predicted TM domain of the same length (23 residues) but a completely different localization. AtRMR1 localized in TGN according to the length of its transmembrane domain, while AtRMR2 with a TM domain of the same length localized in the ER membrane. Moreover the two TM-exchange mutants AtRMR1TM2 and AtRMR2TM1 did not exchange localization. These results support the notion that the length and sequence of this domain cannot play a fundamental role in AtRMR localization.

It is thus likely that a specific motif present in one of the two sequence linkers plays a dominant role in protein localization.

7. Characterization of the AtRMR linkers

These linkers are small sequences in the cytosolic part of the protein immediately after the TM domain and are composed of 23 amino acids with little sequence similarity. These different sequences could explain the different localization observed for AtRMR1 and 2. Indeed certain membrane proteins harbour there specific motifs involved in protein trafficking through the endomembrane system. For instance membrane proteins trafficking between ER and Golgi possess specific ER-export signals interacting with the COPII machinery (Dominguez *et al.*, 1998). Moreover the vacuolar receptor BP80 presents a tyrosine motif in the small cytosolic tail, which is involved in the protein traffic through the interaction with CCV coat (Happel *et al.*, 2004) and a Ile-Met "dileucine" motif involved in recycling from the prevacuole and for endocytosis (Saint-Jean *et al.*, 2010).

To analyze the two linkers, I used the same approach as for the TM domains. I generated two mutants where I exchanged the wild type TM+linkers with the corresponding sequence from the other RMR: AtRMR1TM2L2 and AtRMR2TM1L1.

Unexpectedly AtRMR1TM2L2 did not change localization despite replacing the linker. Indeed this mutant perfectly colocalized with the wild type protein in characteristic punctate structures. This indicates that the sequence linker of AtRMR2 does not contain an amino acid motif involved in protein localization. In contrast when AtRMR1TM2L2 was co-expressed with wild type AtRMR2, I observed a clear retention of the mutant in the ER membrane. It appears that wild type AtRMR2 is involved in the retention of AtRMR1TM2L2, probably by protein-protein interaction involving the TM domain and/or linker of AtRMR2 present in both proteins. To support this hypothesis I performed BiFC experiments with these two proteins (next chapter).

Interestingly the other exchange mutant AtRMR2TM1L1 was able to exit the ER localizing in AtRMR1-positive punctate structures. This mutant was thus mainly localized in TGN with a residual ER association. This result supports the presence of a localization signal in the linker of AtRMR1, sufficient to redirect an ER-resident protein to the TGN. The same sequence seems dispensable to localize AtRMR1, since when I replaced this sequence with the linker of AtRMR2, the resulting mutant AtRMR1TM2L2 was still localized in punctate structures. The ER-exit motif of the AtRMR1 linker appears to be redundant with another signal of unidentified location within the protein.

7.1. Characterization of the AtRMR1 linker

The linker of AtRMR1 appears to contain a localization motif. In order to identify the relevant amino acids I performed a series of prediction analysis using different softwares, which failed to reveal any common ER export signal. However within the first 15 residues there is a very high percentage (8/15 or 9/17) of basic arginines. The AtRMR2 linker contains fewer arginines (4/15 or 5/16). These arginines could constitute the searched motif. Such a signal is the dibasic motif, which is composed of two pairs of basic amino acids separated by a spacer, [RK] (X) [RK]. For instance some glycosyltransferases possess a dibasic motif, which is required for ER export and Golgi localization (Dominguez *et al.*, 1998; Schoberer *et al.*, 2009).

In addition the AtRMR1 linker also contains three serines, which are predicted to be phosphorylated (NetPhos 2.0 Server). Post-translational phosphorylation is involved in several trafficking processes in plants, e.g. it was found that PIN proteins can be phosphorylated *in vitro* and that this process could be involved in the regulation of protein localization in apical and basal plasma membrane (Jürgens *et al.*, 2007). All these data support the hypothesis that the linker of AtRMR1 may contain a motif involved in protein localization.

It should be noted that the online software NLStradamus also predicts a nuclear localization signal, the arginine triplet at positions seven, eight and nine of the linker. Arginines are indeed also involved in protein sorting to the nucleus. The mouse RING finger protein 13 (RNF13), which has a similar structure as RMRs, namely a luminal PA domain and a cytosolic Ring-H2 domain, is an endosomal protein. RNF13 is very labile, and the Ring-H2 domain is released by proteolysis into the cytoplasm, where it mediates ubiquitination (Bocock *et al.*, 2009). It could thus be that the Ring-H2 domain of the labile AtRMR1 is released from the membrane and subsequently transported into the nucleus.

To dissect the linker of AtRMR1 I generated several mutants, replacing the first, second and third group of 5 amino acids including the arginines and the two serines. The first five residues were not

sufficient for the ER export, while there was some relocalization when the first 10 or 15 amino acids were exchanged: these two mutants were also localized in few punctate structures in association with ER, indicating that the second and third groups of arginines could be involved in ER export but are not sufficient for an efficient localization. Replacing the five amino acids including two serines had no effect, demonstrating that they do not play a role in protein localization.

These results support the notion that the whole linker of AtRMR1 is needed for efficient ER export. The effect does not seem to be due to a specific motif but rather to an additive effect of the whole linker. The signal could also consist of residues close in the three-dimensional structure but not in the primary sequence. Alternatively the linker1 could be involved in the interaction with a second protein partner, which probably possesses a motif involved in protein localization.

Introduction of protein interaction

1. General aspect of protein interaction

In plant and animal cells many proteins present different functions depending on cellular context and interaction with others protein partners. A lot of proteins do not work as a single unit but as a multisubunit complex where several factors interact resulting in a specific cellular structure and function. Protein interaction has a fundamental role in cell life allowing the integration of signals coming from different places and guaranteeing communication between cell compartments. The most of cellular process such as DNA replication, transcription, translation, splicing, cell cycle control and others require specific protein interaction in order to integrate and regulate the different factors involved (Phizicky *et al.,* 1995).

Proteins can interact principally in two different ways, stably or transiently which can be either strong or weak. A lot of membrane complexes are based on stable and strong interactions between different subunits which can be identical or different. For instance the translocator Sec61 form a stable multi-subunit pore involved in exchange of material in and out of the ER. Another example of well characterized multi-subunit complex is the core RNA polymerase which allows gene transcription. The stable and strong nature of all these complexes has allowed studying efficiently the protein interaction by co-immunoprecipitation or pull-down assay. Indeed, the discovery of all these proteins in associated form implies the formation of a stable complex (Phizicky *et al.,* 1995).

Moreover, the presence of many transient complexes which control a large number of processes has also been demonstrated. Transient interaction is involved in the regulation of many cellular pathways which have to be activated temporarily based on different cell development conditions. Therefore, transient interactions require specific processes of regulation in which both cellular and environment factors participate. For instance, proteins interact transiently during a lot of cellular processes such as protein transport, signalling, folding, cell growth, cell cycling and signal transduction. Also, transient interactions are involved in a number of protein modification processes which are catalyzed by enzymes such as kinases, phosphatases, glycosyl-transferases and others (Phizicky *et al.,* 1995).

Based on the transient and weak nature of the interactions, this kind of complexes are very difficult to determine. Therefore, chemical agents which are able to stabilize the protein associations in the specific moment when it occurs can be used. Such chemical agents can be classified as cross-linking molecules which are able to form covalent bonds between two or several subunits (Phizicky

et al., 1995).

There are a lot of different effects which can be determined by protein interactions. First, protein interactions can modify the kinetic of certain enzymes, modifying the affinity with the substrate or the allosteric properties of the complex (Porpaczy *et al.,* 1983). Second, protein interactions can allow the transfer of an intermediate substrate from one protein subunit to the active site of another subunit of the same enzyme. This process is named substrate channelling and is very important for direct substrate transfer without releasing it into the solution (Yanofsky *et al.,* 1958). Third, protein interactions can determine the formation of a new binding site on the complex resulting in the enzyme activation (Weber *et al.,* 1993). Fourth, protein interactions can contribute to protein activation and inactivation, through the binding with inhibitor or activator factors (Susskind *et al.,* 1983). Finally, protein interactions can modify the binding specificity between substrates and enzymes (Hill *et al.,* 1975).

During the evolution, the organisms in general have preferred to select multi-protein complexes rather than single proteins with several active sites. Therefore, a multi-protein complex conserves some advantages compared to a large protein with several active sites. In fact several small subunits are much easier to synthesize, fold and assemble in a multi-protein complex than a single large protein. Moreover, protein subunits can be associated and dissociated in a specific compartment, forming different complexes with different function based on specific cell conditions. Finally, the translation of a big protein is more susceptible to mutations than a small subunit, increasing the probability to lose a specific cell function (Phizicky *et al.,* 1995).

1.1. Protein interactions involve specific protein domain

Complex formation involves the participation of different proteins which interact with each other, determining a specific cell function. The driving force for protein-protein interaction is provided by protein domains able to stably interact with a specific partner.

The first definition of protein domain was elaborated in 1973 by Wetlaufer. A protein domain was described as a part of protein which can autonomously fold, forming a stable unit (Wetlaufer *et al.,* 1973). Therefore a protein domain constitutes a compact structure characterized by a specific cell function and independent evolution origin. Protein domains are characteristic of both prokaryotic and eukaryotic cells. In bacterial a single protein domain often exists as a single protein unit, contrary to eukaryotic cells where more than one domain can be contained in the same protein leading to multidomain and multifunctional proteins. In a multidomain protein, each domain can play its specific function independently or in concert with the others domains. For instance the luminal and the cytosolic part of the same membrane protein can contain different domains which

are spatially separated by the plasma membrane and consequently play two different independent cell functions (Wetlaufer *et al.,* 1973; Richardson *et al.,* 1981; Bork *et al.,* 1991). Moreover, protein domains can differ a lot in term of length, varying between 25 and up to 500 residues. The three-dimensional structure of short domains about 40 aminoacids or less is often stabilized by disulfide bonds or metal ions. On the contrary, the structure of big domains of more than 300 residues is stabilized by hydrophobic interaction of particular aminoacids (Savageau *et al.,* 1986; Garel *et al.,* 1992).

A protein domain is characterized by a specific function such an enzymatic activity or physical role in the interaction with others protein partners. Specifically, a protein interacting domain is a particular three-dimensional portion of interacting protein characterized by the presence of conserved aminoacids forming a motif. The central region of a protein domain is called "hot spot" and contains the main aminoacids involved in the interaction. Therefore, point mutations in this region have a drastic effect on protein functions (Phizicky *et al.,* 1995).

Several domains have been characterized to be involved in protein interaction. They vary in term of structure, size and nature of interaction guaranteeing a wide number of different cell functions. Moreover, the same protein domain can interact with different partner based on different cellular conditions. To study an unknown protein, the protein domain composition could provide research lines about the possible cell function of the investigated protein (Phizicky *et al.,* 1995). For instance the structure of AtRMR receptors is characterized by the presence of a PA domain and a Ring-H2 domain which are both considered potential protein-interaction domains involved in complex formation and/or dimerization (Mahon *et al.,* 2000; d'Azzo *et al.,* 2005). Therefore based on this domain composition, it is probable that AtRMRs interact with other proteins present in plant secretory system.

1.1.1. RING finger domains

The RING finger constitutes a class of protein interaction domains which was originally found in the RING1 gene (Really Interesting New Gene) and therefore called RING finger domain (Lovering *et al.,* 1993). This domain is typical of eukaryotes in which it constitutes the most common motif coordinating zinc (Saurin *et al.,* 1996) (figure XIX).

The role of this domain in protein-protein interaction was originally clarified in c-Cbl, an E3 enzyme involved in ubiquitin-proteasome degradation and able to interact with several kinds of protein substrates (Joazeiro *et al.,* 1999; Waterman *et al.,* 1999). After this first discovery, the RING finger domain was found in a wide number of E3 enzymes involved in ubiquitination process

(Lorick *et al.,* 1999). The absence of this motif in bacteria is in accord with the proposed role in ubiquitination which is absent in prokaryotes.

Therefore, RING finger proteins have an important role in many physiological processes mediated by both poly-ubiquitination and mono-ubiquitination. Poly-ubiquitination mediates protein degradation in eukaryotes, whereas mono-ubiquitination is involved in many physiological processes such as signal transduction, transcription regulation, chromatin remodelling and DNA repair (Deng *et al.,* 2000; Kaiser *et al.,* 2000). For instance the mammalian tumor suppressor BRCA1 is a RING finger protein involved in many cellular processes such as DNA repair, regulation of transcription, cell-cycle control and ubiquitination. It has also been demonstrated that point mutations in the RING domain of BRCA are closely related to high risk of breast cancer (Kerr *et al.,* 2001). Another example is Mdm2 which is involved in p53 ubiquitination and degradation in mammal cells. Also in this case, it was demonstrated that point mutations which prevent Mdm2-mediated p53 degradation are associated with elevated risk of certain kind of cancer (Michael *et al.,* 2002).

The proposed role of RING finger proteins in ubiquitination process is well known in yeast and mammal cells. On the contrary, in plant cells the role of RING finger proteins has to be established. However, almost 5 % of the *A.thaliana* proteome was predicted to be implicated in ubiquitination process and degradation by 26S proteasome. The majority of these proteins was predicted to belong to RING-type E3 ligase supporting this role also in plants (Stone *et al.,* 2005).

The RING finger, also called C3HC4, is a particular domain coordinating zinc which is characterized by the aminoacidic sequence Cys-X_2-Cys-X_{9-39}-Cys- X_{1-3}-His- X_{2-3}-(Cys/His)- X_2-Cys- X_{4-48}-Cys- X_2-Cys, where X is any aminoacid and the number of X residues varies between the different domains. This domain is about 70 aminoacids and is able to fold around two zinc atoms with a characteristic three-dimensional structure. Indeed, specific cysteine and histidine residues of RING fingers are able to coordinate two zinc atoms in a “unique cross-brace” arrangement, forming the specific site involved in protein-protein interactions. Each zinc ion is bound in a tetrahedral coordination structure by four specific residues which work like metal-binding ligands. In C3HC4 motif, four cysteines are involved in the coordination of the first zinc atom, while the second atom is coordinated by three cysteines and one histidine. More precisely, zinc is coordinated by the sulfurs of cysteines and the imidazole rings of histidines (Zheng *et al.,* 2000).

The second group of RING finger proteins is called the Ring-H2 family and is characterized by the presence of a histidine instead of a cysteine in the fourth position (Borden *et al.,* 1996). Therefore, in this case both zinc atoms are coordinated by three cysteines and one histidine.

Moreover a third kind of RING finger called C4C4 has been described. This motif is characterized by the presence of eight cysteines responsible for zinc coordination (Hanzawa *et al.*, 2001).

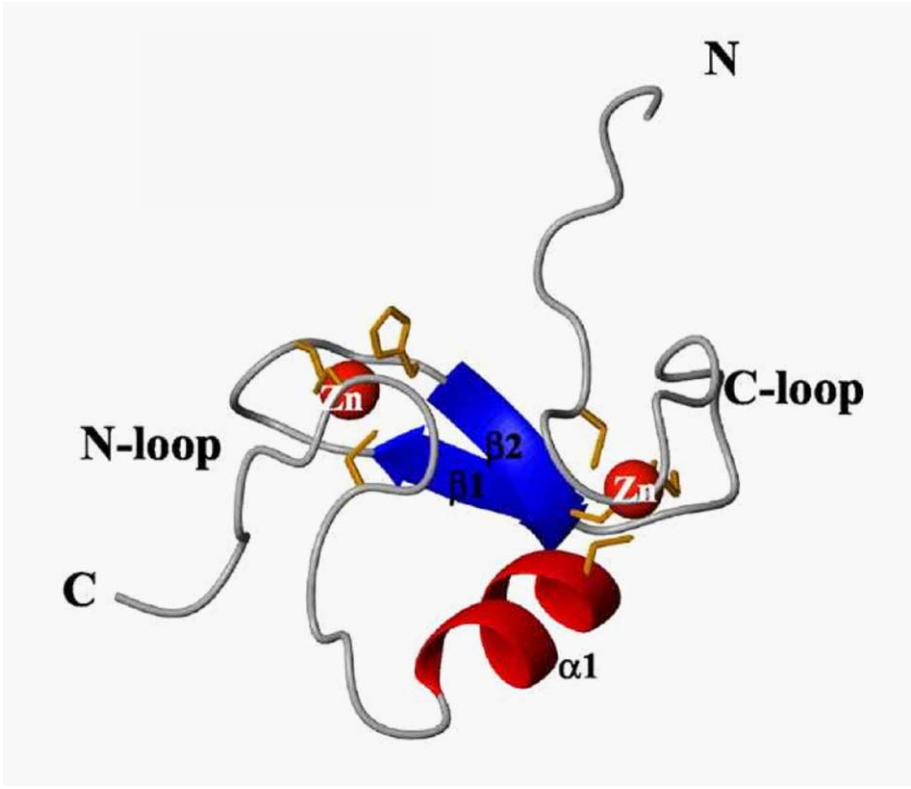

Figure XIX: Three-dimensional structure of the Ring-H2 domain (Katoh *et al.*, 2003). The picture represents the three-dimensional structure ("ribbon" representation) of the Ring-H2 domain of EL5 from rice. Secondary structures are represented in the picture: alpha-helix (α) in red; beta-sheets (β) in blue; N-terminal loop (N-loop); C-terminal loop (C-loop). The arrows indicate the direction of beta-sheets which is from N- to C-terminal end. The N- and C-terminal ends of the Ring-H2 domain are respectively indicated with N and C. The two zinc atoms (Zn) coordinated in the structure are indicated as red circles.

1.1.2. The protease-associated domain

The protease associated domain (PA domain) is a putative protein interaction domain originally found in certain classes of protease. The primary structure of this domain is composed of 170-210 aminoacids which fold forming a β-sandwich with two peripheral helices (Mahon *et al.,* 2000). After this first discovery, the PA domain has been also found in others distinct families of protein characterized by different cell functions (figure XX).

The PA domain is characteristic of the Pyrolysin family of subtilases, enzymes with protease activity which give the name to this particular domain (Siezen *et al.,* 1997). The subtilase family includes the bacterial protease c5a involved in the process of immune response evasion and several plant proteases such as cucumusin which play an important role in many defence responses. Several studies in which the PA domain was deleted from some proteases, suggest that it could be involved in substrate specificity (Mahon *et al.,* 2000).

The PA domain was also found in BP-80 family of receptors involved in the trafficking of vacuolar proteins. So far, it was demonstrated that the PA domain present on these receptors is involved in binding specific vacuolar sorting signals present in proteins destined to lytic vacuole (LV) (Kirsch *et al*., 1994; Paris *et al.,* 1997). Moreover, the PA domain is present in a second family of putative vacuolar receptors called RMR which was proposed to be involved in protein trafficking to protein storage vacuole (PSV). But in this case the role of this domain in the binding of C-terminal vacuolar sorting signal has yet to be demonstrated (Jiang *et al.,* 2000; Park *et al.,* 2005; Park *et al.,* 2007; Hinz *et al.,* 2007).

Finally, the PA domain was also found in the structure of transferrin receptor, involved in transferrin uptake in mammalian cells (Lawrence *et al.,* 1999), and in carboxypeptidase/prostate-specific membrane antigen protein (PSM) (Rawlings *et al.,* 1997) which constitutes the only described example of a cytosolic PA domain.

Several evidences suggest that the PA domain could be involved in protein-protein interactions. Firstly, it was demonstrated that the PA domain present on BP-80 family is involved in binding certain vacuolar sorting signals. Secondly the theoretical model which describes the binding between the transferrin receptor and transferrin predicts that a large part of the PA domain could be involved in binding (Lawrence *et al.,* 1999). Thirdly other experimental evidences are provided by PA deletion mutants of several subtilases. These experiments have shown a drastic decrease in binding affinity resulting in a reduction of substrate specificity, while the catalytic activity was not affected (Bruinenberg *et al.,* 1994). Fourthly, swapping the PA domain between several proteases changed their substrate specificity (Chen *et al.,* 1990). Finally monoclonal antibodies against the PA

domain of proteases are able to decrease the activity of these proteins, supporting the previous results (Bruinenberg *et al.*, 1994).

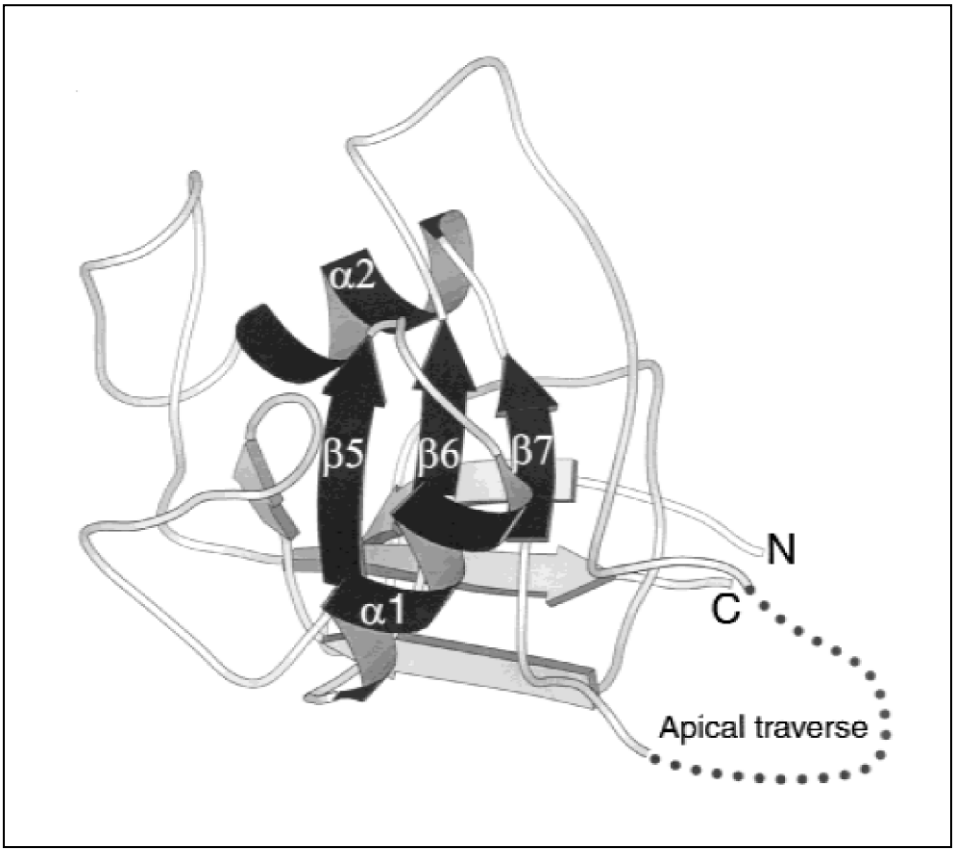

Figure XX: Three-dimensional structure of the PA domain (Mahon *et al.*, 2000). The structure of the PA domain is shown as "ribbon" representation. Secondary structures, alpha-helices (α) and beta-sheets (β) are represented in the picture. The arrows indicate the direction of beta-sheets which is from N- to C-terminal end. The N- (N) and C-terminal (C) ends of the PA domain are respectively indicated in the picture.

1.1.3. The PA/Ring finger proteins

The structure of AtRMR receptors includes both a PA domain and a Ring-H2 domain. Among the homologous proteins which combine a PA domain and Ring-H2 domain, RING-type E3 ubiquitin ligases such as GREUL1 from *Xenopus* (Goliath Related E3 Ubiquitin Ligase 1), GRAIL from *human* CD4+ T cells (Gene Related to T-cell Anergy In Lymphocytes) and the RING finger protein 13 (RNF13) from chicken (Borchers *et al.,* 2002; Anandasabapathy *et al.,* 2003; Bocock *et al.,* 2009) have been described. Proteins with this domain structure were identified in plants, *Xenopus, Drosophila* and mammals, but they have not been found in yeast (Bocock *et al.,* 2009). Moreover some of these proteins were found in the endosomal system, e.g. GRAIL and RNF13 (Anandasabapathy *et al.,* 2003; Bocock *et al.,* 2009) and this localization is consistent with the localization described for the homologue protein AtRMR1 (Occhialini, unpublished results).

Compared to other E3 ligases, the RING-type are the most abundant E3 ligases in nature and their RING-finger domain constitutes the interaction core with E2 enzymes. In fact these proteins work like a scaffold bringing together the active E2 enzyme and the target protein to enable the ubiquitination reaction (Stone *et al.,* 2005).

The E3 enzymes play a central role in the ubiquitination machinery which involves the presence of numerous proteins that interact with each-other making a highly regulated complex. This machinery catalyzes the ubiquitination reaction which is a post-translational protein modification based on ubiquitin's conjugation to lysine residues present in target proteins. This modification is involved in different cell processes depending on the number of conjugated ubiquitin. We can distinguish poly-ubiquitination which is only involved in degradation of target proteins by proteasomes and mono-ubiquitination which is involved in different regulatory processes. For instance, in the case of transmembrane proteins, mono-ubiquitination plays an important role in stability, protein-protein recognition and intracellular localization between plasma membrane and endocytic compartments (Mukhopadhyay *et al.,* 2007).

Based on domain similarity, it is possible that AtRMR receptors are E3 ligases and it is likely that the PA and Ring-H2 domains are involved in protein-protein interaction. Moreover at the C-terminal end of AtRMR1, 3 and 4 there is a domain rich in serines which is one of the most important amino-acids involved in phosphorylation processes in plants. In fact proteins like RNF13 that are similar to RMRs usually have a Ser-Rich domain which is also consistent with a role of this domain in phosphorylation (Bocock *et al.,* 2009). It has also been demonstrated that the phosphorylation of serine residues is involved in the regulation of interactions between E3 and their partners (d'Azzo *et al.,* 2005).

The PA domain of AtRMR receptors is very similar to the PA domain of the transferrin receptor

that it is well known to work as a homo-dimer. The amino-acid structure of the transferrin receptor shows the presence of three different structural domains: In the luminal part, an amino-terminal inactive protease domain with an internal PA domain with binding function and a carboxy-terminal domain that is involved in receptor dimerization (Lawrence *et al.*, 1999). Moreover the transferrin receptor is modified by the addition of a single ubiquitin involved in receptor trafficking and recycling. This receptor is not the only example of a receptor able to form dimers and regulated by mono-ubiquitination; in fact the EGFR (epidermal growth factor receptor) and the alpha factor receptor are regulated in a similar way (Sigismund *et al.*, 2005; Mukhopadhyay *et al.*, 2007). In fact the mono-ubiquitination process is well known to be a specific signal for endocytosis (Rotin *et al.*, 2000), but has also been implicated in the transport from the Golgi to the endosome (Beck *et al.*, 1999) and in the sorting to the internal vesicles of multivesicular bodies (MVBs) (Katzmann *et al.*, 2001).

2. Investigation of protein-protein interactions

Protein-protein interaction has been studied with a wide number of techniques based on different experimental approaches. Most of these procedures imply the direct detection of interactions by biochemical methods such as protein affinity chromatography and immuno-precipitation. All biochemical approaches necessitate extracting the interacting proteins from their cellular compartment. Therefore using these techniques only a direct interaction with proteins partners can be visualized losing all the information about the dynamics and compartment of interaction (Kerppola *et al.*, 2008).

Several bio-informatics methods could be also used for protein-protein interaction prediction. These procedures require information about the three-dimension structure of protein domains which could be involved in complex formation. Indeed, the interaction sites differ from the rest of protein sequence in particular aminoacid motifs. These residues tend to localize forming a cluster in particular regions called “energetic hot spots” which can be predicted (Friedhoff *et al.*, 2005).

In contrast, many genetics approaches were developed to study protein interactions in their normal cellular environment. These methods are based on the observation of a direct effect in protein interactions and complex formation upon specific mutations of interacting proteins. Several procedures were used for research of new interaction partners such as extragenic suppression, multicopy suppression, synthetic lethality and transdominant inhibition (Appling *et al.*, 1999).

Protein-protein interactions can be also studied by the use of cross-linking agents which are chemical compounds able to link associated proteins. Methods involving cross-linking and immuno-purification combined with MS (mass spectrometry) have been described for the

determination of many protein complexes like membrane transporters, multimeric complexes associated with chromatin and others (Akita *et al.,* 1997; Orlando *et al.,* 1997). A variety of cross-linkers with different proprieties and particular uses are commercially available. The use of membrane permeable cross-linking agents in association with the possibility to reverse the cross-linking reaction is very useful to study in *vivo* of protein-protein interaction. These kinds of agents are hydrophobic molecules able to enter directly into living cells through the plasma membrane and to link the protein complex in its subcellular compartment of residence (Vasilescu *et al.,* 2004).

Protein interactions can be investigated using complementation methods which allow to directly visualize protein interaction in their normal environment. These approaches are based on the capacity of certain protein fragments to associate and complement allowing visualizing protein interaction in living cells. However the visualization of the cellular compartment where the complex localizes requires a specific system of revelation. This is possible by using specific fluorescent reporters linked to the investigated proteins, which allows direct observation of the complex under a fluorescence microscope. Alternately two different non-fluorescent fragments able to reconstitute an entire fluorescent reporter can be linked on the investigated proteins (Kerppola *et al.,* 2008).

The visualization of complex formation directly in living cells provides important information about the protein interaction in the normal environment and provides information about subcellular localization. Several fluorescent methods were used to visualize this kind of interaction such as FRET, BRET, BiFC, fluorescent correlation spectroscopy and others (Kerppola *et al.,* 2008).

Alternatively several two-hybrid systems were proposed to study *in vivo* protein-protein interaction using both yeast and bacterial host cells. These techniques are based on the reconstitution of a complete transcription factor upon association between two investigated proteins. Then this interaction is measured by the activation of a reporter gene present in host cells (Fields *et al.,* 1989; Sobhanifar *et al.,* 2003; Causier *et al.,* 2004; Causier *et al.,* 2002).

2.1. Forster resonance energy transfer (FRET)

Forster resonance energy transfer (FRET) (Forster *et al.,* 1948) is a useful method based on fluorescent microscopy which can be use to study molecular dynamics *in vivo*. Indeed this technique has been found an important application in study of protein-protein interaction and protein conformational change. Moreover FRET was used to measure distances or changes in the distance between the interacting proteins during complex formation (figure XXI).

FRET is a technique often used in confocal laser scanning microscopy that is based on non-radiative energy transfer mechanism between two very close chromophores. In this biophysical phenomenon there is a long-range dipole-dipole resonance interaction in which energy is transferred

from a chromophore called “donor” to another molecule chromophore called “acceptor”. This phenomenon is a sort of communication in which an excited donor chromophore gives a virtual photon to an acceptor chromophore increasing its emitted fluorescence. Therefore transfer of energy leads to a reduction of donor fluorescence intensity with a consequent increase in acceptor emission intensity (Yan and Marriott, 2003).

In this technique the two chromophores linked to the two proteins for which a possible interaction has to be investigated. If there is an interaction between the two partners allowing the chromophores to be in a 10 nm range then there will be FRET. For production of a FRET signal, the radius of interacting proteins has to be smaller than the wavelength of emitted energy from donor (Bhat *et al.*, 2006). Therefore FRET is based on measuring the change of either quantum yield or of donor fluorescence lifetime in the presence and absence of acceptor (Yan *et al.,* 2003).

It is very common to use chromophores from the GFP family which have suitable spectral properties for FRET (Tsien *et al.,* 1998). The most common GFP derivates which were used for these techniques are YFP (yellow fluorescent protein) and CFP (cyan fluorescent protein). This technique implies the use of two different chromophores with different spectra of excitation and emission. The most common chromophores used in FRET are CFP and YFP which are respectively the donor and acceptor chromophore.

One of the main problems linked to the use of all these fluorescent proteins is the necessity to use an external illumination for donor excitation. This implies a possible non-specific acceptor excitation resulting in increasing background noise or photobleaching. To solve this problem a new technique named Bioluminescence Resonance Energy Transfer (BRET) was developed. BRET is a technique based on the utilization of a bioluminescent luciferase which is able to emit energy without needing to be excited by an external source. The luciferase is used as a donor instead of CFP in order to produce energy emission compatible with YFP acceptor (Xu *et al.,* 1999).

Another problem for FRET is that the CFP donor and the YFP acceptor have a partial overlap of their emission spectra. Thus if the expression of fusion proteins is too weak, there is the risk to confuse an acceptor signal due to donor contamination in the acceptor channel with a specific FRET signal. A possible solution of this problem is the application of another technique named FRAP, fluorescence recovery after photobleaching (Karpova *et al.,* 2003). This technique is based on the observation of an increasing of donor fluorescence after photobleaching of the acceptor. Indeed upon photochemical destruction of the acceptor, the fluorescence of the donor increases because its energy can not be transferred to the destroyed acceptor. Therefore this experiment is based on the measurement of the fluorescence intensity of the donor before and after photobleaching of the acceptor. The difference of fluorescence intensity allows calculating FRET. One of the main

advantages of this technique is the possibility to use a confocal laser scanning to focus on small cell regions increasing the resolution. Moreover Jovin and Jovin have proposed another technique to study FRET which is based on the photobleaching of donor instead of acceptor (Jovin *et al.*, 1989). In this second case the decreasing fluorescence intensity of the acceptor is measured after photo-chemical destruction of the donor.

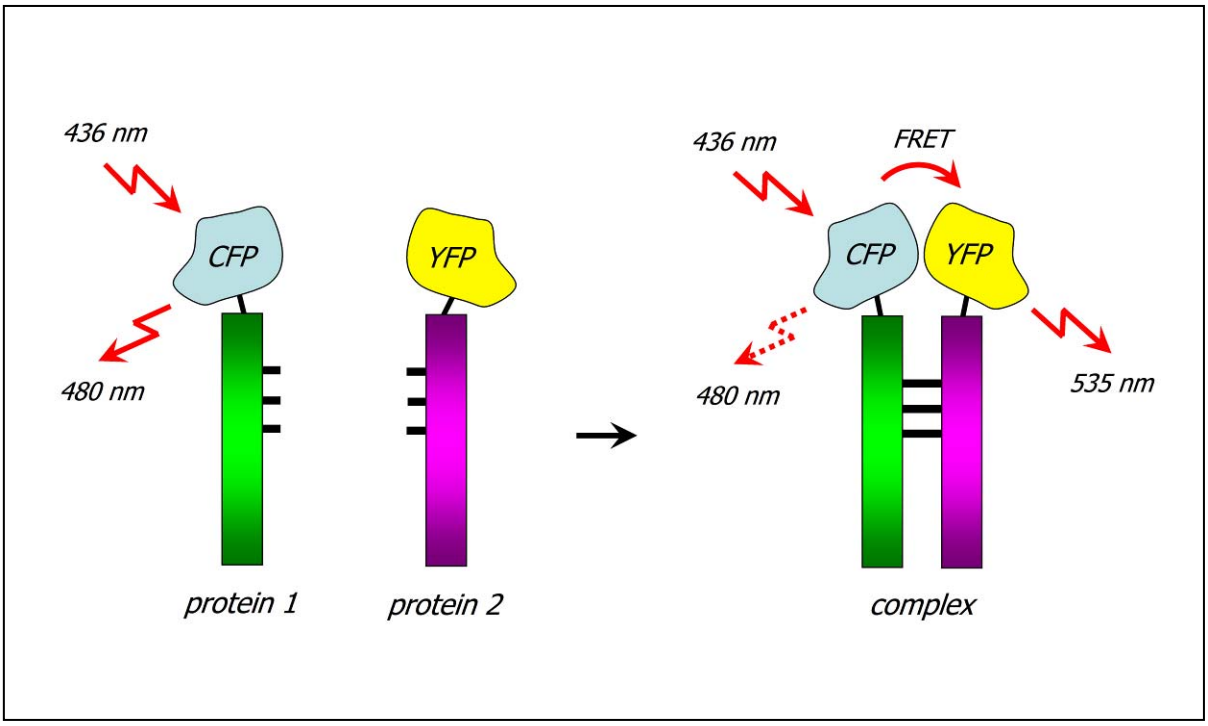

Figure XXI: Foster resonance energy transfer (FRET). Two different fluorescent proteins, CFP (donor) and YFP (acceptor), are fused to the two proteins for which has to be investigated a possible interaction. If the investigated proteins are not able to interact (on the left), there is not energy transfer between CFP and YFP and consequently there is no FRET. On the contrary if there is the complex formation (on the right), CFP and YFP are really close and this allows the transfer of energy between the two proteins resulting in FRET signal.

2.2. Bimolecular Fluorescence Complementation (BiFC)

BiFC is a non-invasive fluorescence method to visualize protein interaction in living cells. This technique can also provide important information about the subcellular compartment of protein complex localization and its change over time (Kerppola *et al.*, 2008) (figure XXII).

The Bimolecular Fluorescence Complementation (BiFC) is based on the reconstitution of a complete fluorescent protein reporter by the interaction between two non-fluorescent fragments. In this technique the two non-fluorescent fragments are fused to two different proteins for which a possible interaction is investigated. The non-fluorescent fragments are not able to spontaneously associate alone. Therefore if the two proteins are able to interact, we should observe the production of a fluorescence signal due to the reconstitution of the complete fluorescent reporter which has the same spectral properties of native reporters (Hu *et al.*, 2002).

BiFC was used to investigate protein interactions for a wide number of proteins in bacteria, yeast, plant and mammal. Originally, this technique was proposed in bacteria using the GFP as a fluorescent reporter and two synthetic peptides able to interact as investigated proteins (Ghosh *et al.*, 2000). Also in plant, the BiFC has been widely used to investigate protein interaction. For instance this technique provided information about the interaction between DICER-LIKE1 (DCL1), HYPONASTIC LEAVES1 (HYL1) and SERRATE (SE), which are three important factors localized in the nucleus and involved in miR processing and storage (Fang *et al.*, 2007). Moreover, BiFC was used to study the interaction between the viral factor VirF and the plant protein VIP1 during *Agrobacterium tumefaciens* infection (Tzfira *et al.*, 2004).

Different fluorescent proteins have been used for BiFC, but the most commonly used reporters belong to the GFP family (Hu *et al.*, 2002; Hu *et al.*, 2003; Shyu *et al.*, 2006). For instance non-fluorescent fragments originated from YFP exhibit high association efficiency and very low base fluorescence when they do not interact. Due to all these advantages, YFP is usually the fluorescent reporter of choice for BiFC. Fragments of YFP generated by truncation in position 155 and 173 were used successfully in both animal and plant cells. In this way it is possible to generate an N-terminal and C-terminal fragments able to stably associate forming a complete fluorescent reporter. Alternately fragments generated from Venus, a synthetic derivate of YFP, can be used with similar truncation positions (Kerppola *et al.*, 2008).

BiFC does not necessitate particular instruments to be detected, but it can be easily visualized using a normal fluorescence microscopy. However the best resolution and sensitivity were obtained using a confocal laser microscopy (Kerppola *et al.*, 2008). These instruments have to be optimized taking into account that a fluorescent reporter originated from the association of two non fluorescent fragments produces less fluorescence signal than a normal fluorescent reporter. It was estimated that

in BiFC the decrease of fluorescent signal is about 10% compared to an intact reporter (Hu *et al.*, 2002).

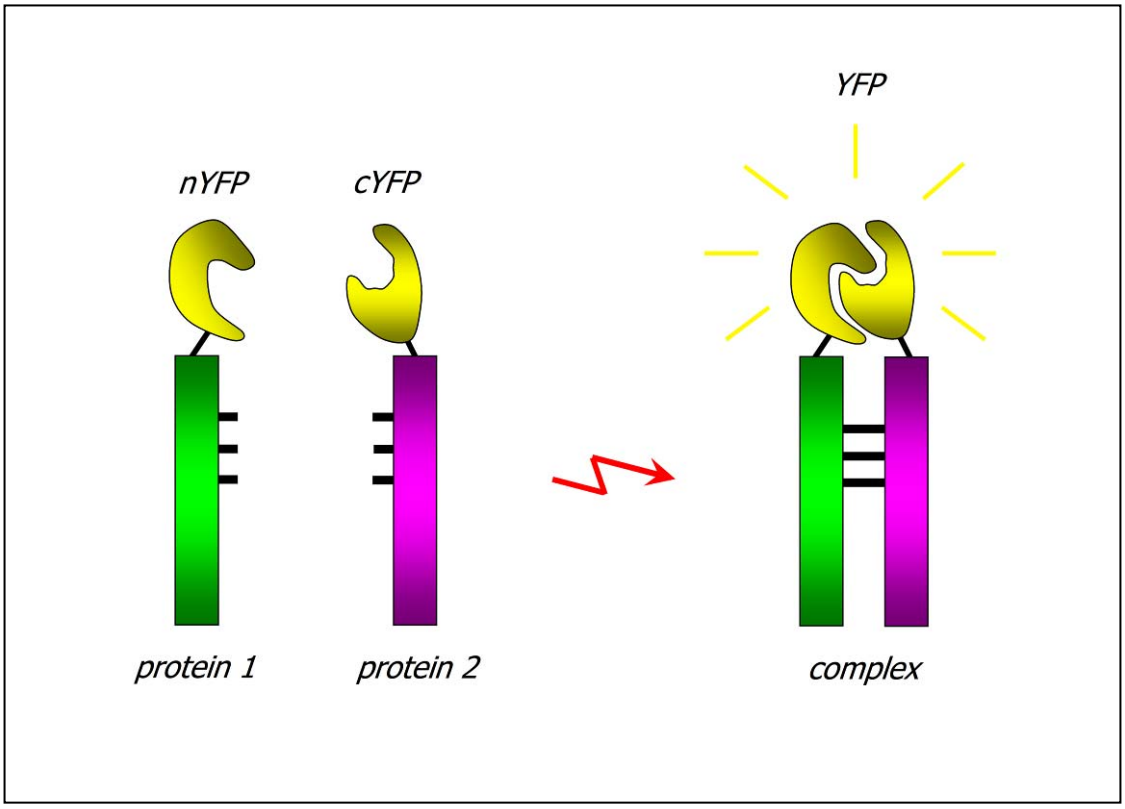

Figure XXII: Bimolecular Fluorescence Complementation Methodology (BiFC). The two YFP non fluorescent fragments, N-terminal YFP (nYFP) and C-terminal YFP (cYFP) are linked on the two proteins for which a possible interaction is tested. If the investigated proteins are able to interact forming a complex, there is the consequent production of fluorescent signal due to the reconstitution of complete fluorescent YFP (to the right).

2.2.1. Advantages and disadvantages of BiFC

The major advantage associated to BiFC is the possibility to study protein interaction and complex localization using relative simple equipment. Moreover this technique does not require particular information regarding the interaction interface of the protein domains involved in the association and their three-dimensional structure. However steric and spatial constrains during the association of the two non fluorescent fragments could prevent their proper association. For instance during the investigation of membrane protein association it necessary that the fluorescent fragments are placed in the same membrane site. Therefore it is really important to try both fusions at N- and C-terminal ends of investigated proteins in different spatial combination (Kerppola *et al.,* 2008; Hu *et al.,* 2003).

In a number of cases, protein-protein interaction occurs in indirect way through the participation of additional factors or upon certain stimuli. The presence of these factors and stimuli only in particular kind of tissues or development stage could prevent protein complex formation (Ohad *et al.,* 2007).

Moreover a correct spatial association between the non-fluorescent fragments could be increased by placing a protein linker between the fragments and the proteins of interest. It was demonstrated that the presence of a liker allows the proteins to get a good native structure aiding the correct association between interaction proteins (Kerppola *et al.,* 2008; Hu *et al.,* 2003).

One other problem correlated with this technique is the necessity to generate fusion proteins which could have different characteristics comparing to native proteins. Indeed the presence of non-fluorescent fragment could modify the subcellular distribution of the protein preventing the correct localization in the cellular compartment where the interaction occurs. Also the presence of the fragment could affect the protein stability and its normal function preventing the normal association between the proteins to be investigated (Kerppola *et al.,* 2008; Hu *et al.,* 2003).

The BiFC can be used in both transient and stable expression systems using a wide number of different promoters in order to have the good level of protein expression. The necessity to overproduce the protein partners by putting them under the control of strong constitutive promoter such as 35S promoter could be represented a problem. Indeed, protein over-expression could result in a mis-localization of proteins partners or could be also involved in non-specific association with other endogenous proteins. Therefore it is really important to choose the best promoter which guarantees a level of expression comparable with the expression level of endogenous partners. This problem can be solved using a weak constitutive promoter or an inducible promoter which is activated only in the presence of certain stimuli. One important advantage of an inducible promoter is the possibility to control protein expression in a short of time. Also, for certain number of

proteins the native promoter could be utilized. In this case the basal expression of the promoter has to be sufficient to guarantee a good amount of protein in order to see the interaction (Kerppola *et al.,* 2008; Hu *et al.,* 2003).

The BiFC require to be validated using both positive and negative controls in order to have adequate references. As it was described the over-expression of protein partners could imply aspecific association with consequent production of aspecific fluorescent signal. This problem could be attenuated using a specific negative control which is based on the co-expression of two non-interacting fusion proteins. Another good negative control could be the introduction of point mutations inside one of the protein domain involved in the interaction in order to prevent protein association. Therefore it really important to use the appropriate negative control in each BiFC experiments in order to eliminate aspecific fluorescent signal. Moreover, it is also important to include a specific positive control which confirms the good functioning of the technique. As a positive control could be use either natural or synthetic protein for which have been demonstrated the interaction (Hu *et al.,* 2002; Hu *et al.,* 2003; Grinberg *et al.,* 2004).

Another pitfall relate to the use of BiFC is the slow maturation time of reconstituted fluorescent reporter which prevent the detection of protein-protein association dynamics in real time (Ghosh *et al.,* 2000; Hu *et al.,* 2002; Kerppola *et al.,* 2006). This problem could be ameliorated by using the Venus reporter which matures faster than normal YFP (Miyawaki *et al.,* 2003; Miyawaki *et al.,* 2005). Moreover the high stability of YFP complex originated by the association of two non-fluorescent fragments prevent the possibility to visualized the dynamics of protein-protein dissociation (Ohad *et al.,* 2007).

2.3. The two-hybrid system

The two hybrid system assay is based on the fact that a functional transcription factor can be reconstituted upon association of a DNA-binding domain (BD) and a transcription activation domain (AD) (figure XXIII). The BD is the domain involved in the binding of the transcription factor to specific DNA elements in proximity of particular genes. While the AD domain is implicated in the activation of the transcription of genes placed upstream these particular DNA sequences. These two domains do not need to be present on the same polypeptide to guarantee efficient gene activation. But BD and AD can be separated in inactive forms not able to activate gene response. Contrary, upon the association of the two domains there is the reconstitution of an active transcription factor able to lead the gene transcriptional activation (Brent *et al.,* 1985; Ma *et al.,* 1988).

In the two hybrid system the AD and BD domain are expressed as fusion proteins physically linked with proteins for which a possible interaction is investigated. The two fusion proteins are functionally distinguished in a “hunter” protein and a “bait” protein. The “hunter” is the AD fused to the putative binding partner and the “bait” is the BD fused to the protein of interest for which the interaction with the binding partner is investigated. If these two fusion proteins are able to physically associate there is the consequent formation of an active transcription factor. This interaction is measured by the activation of a specific reporter gene present in the genome of host cells. Therefore, two different plasmids carrying the coding sequences for the “hunter” and “bait” are transformed into a specific host cell and the level of protein-protein interaction is determined by measuring the activity of the endogenous reporter gene (Sobhanifar *et al.,* 2003; Causier *et al.,* 2002; Causier *et al.,* 2004).

This technique was realized by Fields and Song to investigate the interaction between the two interacting proteins SNF1 and SNAF4 (Field *et al.,* 1989). Originally it was based on the measure of the *lacZ* activity upon reconstitution of a complete GAL4 transcription factor. After this first application several new protocols were proposed using a wide numbers of different transcription factors and reporter genes.

2.3.1. Different methods for two hybrid systems

Several yeast and bacterial two hybrid systems were developed to investigate *in vivo* protein-protein interaction.

The most used yeast two hybrid systems are the GAL4 and LexA method which have found a wide application for plant and animal proteins (Causier *et al.,* 2002; Causier *et al.,* 2004).

GAL4 is a transcriptional activator involved in galactose metabolism in bacteria. As many others transcription factors, GAL4 is constituted by a DNA binding domain (BD) and an activation domain (AD) which allow this protein to be used for two hybrid assays. The host cell used is a yeast strain containing the *E.coli* LacZ gene under the control of the activation sequences from the bacterial GAL1-GAL10 regions. Upon association of the two investigating proteins and the consequent reconstitution of an active GAL4 there is expression of the LacZ gene. Consequently the protein-protein interaction can be visualized by blue staining in medium containing X-gal (Fields *et al.,* 1989).

The second method which can be used for yeast two hybrid assays is called LexA system. This system is based on the DNA-binding domain (BD) of the bacterial repressor LexA which is used in combination with the *E.coli* B42 activation domain. The association between the two investigated

proteins leads to the formation of an active transcription factor able to bind the LexA operator which is placed upstream of a reporter gene such as LacZ (Gyuris *et al.*, 1993).

Moreover a split-ubiquitin membrane yeast two hybrid system (MbYTH) was developed to investigate protein interaction between membrane proteins (Stagljar *et al.*, 1998) (figure XXIV). In this protocol the membrane "hunter" and "bait" are expressed as fusion proteins with two ubiquitin fragments, one protein being fused with the ubiquitin N-terminal fragment (Nub) and the second one with the C-terminal fragment (Cub). The C-terminal ubiquitin fragment is associated with an activator protein such as LexA able to activate the transcription of a reporter gene present in the genome of host cells. If the "hunter" and "bait" specifically associate there is the consequent reconstitution of a complete ubiquitin molecule. This ubiquitin is recognized by ubiquitin specific proteases (UBPs) which are able to cut the covalent bound between the Cub fragment and the reporter protein. Finally the cytosolic reporter protein can localize in the nucleus where it is involved in the activation of a specific reporter gene (Fetchko *et al.*, 2004).

Several genes involved in amino-acids biosynthesis such as TRP1, LEU2, HIS3 and URA3 are used in conjunction with LacZ in yeast two hybrid systems. In fact yeast strains carrying specific mutation in one of these genes are used as alternative host cells. If a specific aminoacid is not present in the medium the correlated yeast strains cannot survived. Consequently the gene involved in this biosynthetic process is used as selective markers to select transformed cells (Causier *et al.*, 2002).

Alternatively a number of bacterial two hybrid systems such as ToxR based system were proposed as alternative methods. This method is based on the signal transduction protein ToxR which is involved in the activation of virulence genes in the human pathogen *Vibrio cholerae*. ToxR is a single spanning membrane protein characterized by the presence of an N-terminal cytoplasmic domain and a C-terminal periplasmic domain. The N-terminal cytoplasmic portion represents the DNA binding/transcription activator which is able to activate gene expression (Martinez-Hackert and Stock, 1997; Krukonis *et al.*, 2000; Hennecke *et al.*, 2005). Indeed ToxR specifically bind a DNA motif named *ctx* which is placed upstream certain genes. Also in this method the *E.coli* LacZ gene can be used as a gene reporter. Interestingly the ToxR factor has the peculiarity to be active upon homo-dimerization which involves the C-terminal periplasmic domain. Therefore a ToxR based system can be use to study protein-protein interaction in bacterial two hybrid assay for both cytosolic and membrane proteins. For this purpose the periplasmic and the trans-membrane domain can be replaced by heterologous proteins for which a possible interaction is investigated (Hennecke *et al.*, 2005). Both bacterial and yeast systems have advantages and disadvantages which influence

the application of the methods to certain experimental conditions (Causier *et al.*, 2002; Causier *et al.*, 2004).

Finally a number of alternative systems have been proposed to study protein-protein interaction under a wide number of interacting proteins. For instance a new three protein system was developed to visualize the formation of a ternary complex upon the association of three different investigating proteins. Moreover a reverse two hybrid system was proposed for dissection studies in order to determine the critic aminoacids involved in complex formation (Causier *et al.*, 2002; Causier *et al.*, 2004).

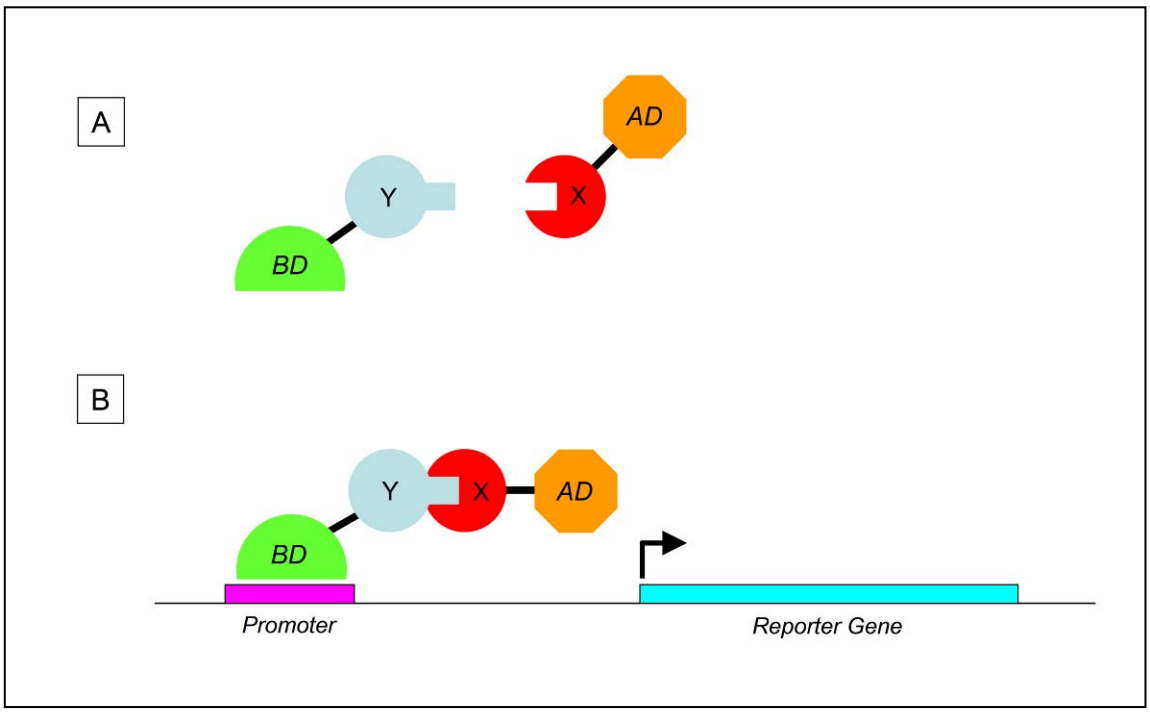

Figure XXIII: Two hybrid system. (A) Two different domains, the activation domain (AD) and the DNA binding domain (BD), are fused to the two proteins for which has to be investigated a possible interaction (respectively protein X and Y). (B) If the investigated protein can interact there is the consequent formation of a complex (BD/Y/X/AD) able to activate a specific reporter gene. The transcriptional activation occurs upon the binding of the BD domain to a specific DNA element present in the promoter of a reporter gene. The AD is the domain involved in the transcriptional activation of the reporter gene.

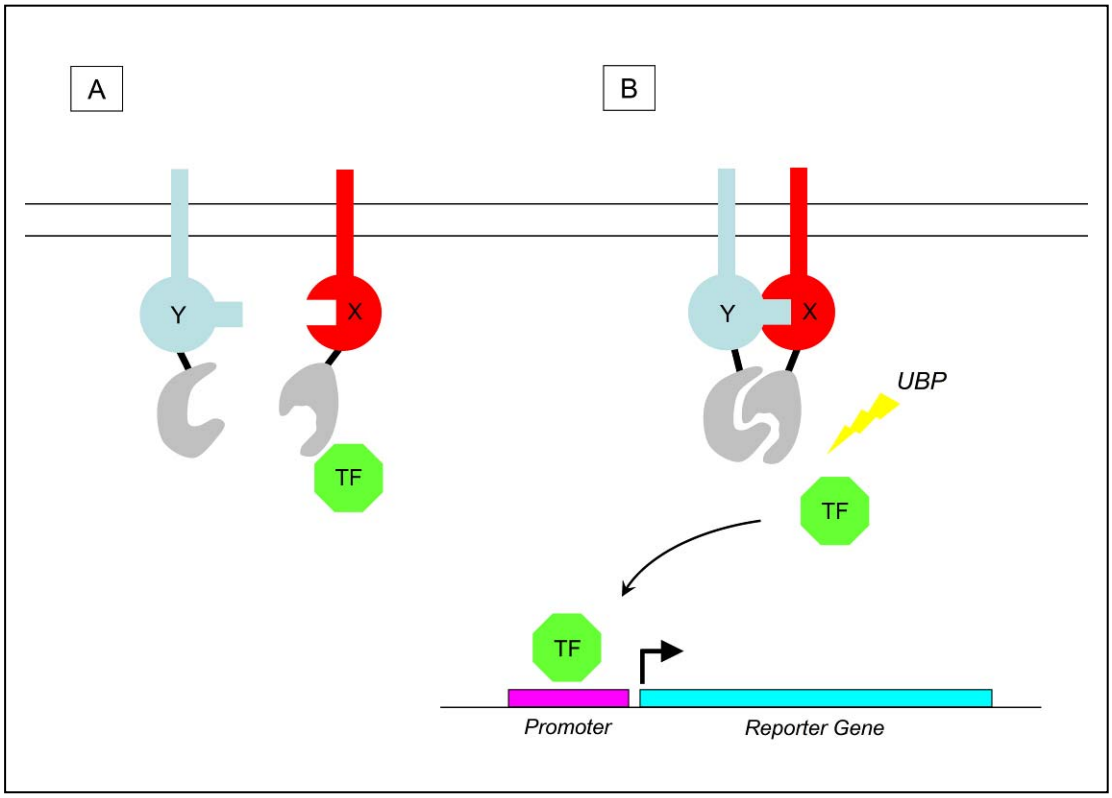

Figure XXIV: Split-ubiquitin membrane yeast two-hybrid system. (A) Two ubiquitin fragments, the N-terminal fragment (Nub) and the C-terminal fragment (Cub) are fused to the two membrane proteins for which has to be investigated a possible interaction (X and Y). The C-terminal fragment is associated with a transcription factor (TF) able to activate an endogenous reporter gene. (B) If the investigated protein can interact there is the consequent reconstitution of a complete ubiquitin molecule. Then the ubiquitin can be recognized by an ubiquitin specific protease (USP) which cuts the binding between Cub and TF. Finally the free TF can reach the nucleus by the presence of a nuclear localization signal. The transcriptional activation occurs upon the binding of the TF to a specific DNA element present in the promoter of a reporter gene.

2.3.2. Advantages and Disadvantages of two hybrid systems

The two hybrid system is one of the most important techniques for protein-protein interaction studies. Indeed, a number of advantages correlated to the method have contributed to increase its success in scientific field.

In fact this method provides information about *in vivo* protein-protein interactions using a number of different host cells. The use of yeast as a host cell constitutes an advantage for several studies which involve plant and animal proteins. Indeed the yeast system has a greater resemblance to higher eukaryotic systems. Alternatively, bacterial host cells can be efficiently used for proteins which do not necessity particular post-translational modifications (Sobhanifar *et al.,* 2003; Causier *et al.,* 2002; Causier *et al.,* 2004).

Moreover, another advantage of the two hybrid system assay is the minimal requirement of the method. In fact it does not necessity the use of a specific antibody or high quantity of purified protein. This method only requires the cDNA of genes coding for the “bait” and “hunter”. The two hybrid system can also be used to investigate weak and transient protein interactions. Indeed a weak interaction between “hunter” and “bait” can be easily visualized upon activation of reporter genes which leads to amplification of the signal (Sobhanifar *et al.,* 2003; Causier *et al.,* 2002; Causier *et al.,* 2004).

This method can be efficiently used either to test a library of putative interaction proteins or to test the interaction between two known proteins. Moreover the two hybrid system is used for mutagenesis studies in order to determine the crucial aminoacids involve in protein-protein interaction. Indeed, by measuring the activation of reporter gene upon point mutation of “hunter” and “bait” proteins it is possible to find out the main aminoacids involved in the association (Sobhanifar *et al.,* 2003; Causier *et al.,* 2002; Causier *et al.,* 2004).

On the contrary, several disadvantages of the two hybrid system have to be taken in to account during the setting of the protocol.

The most important trouble correlate to the use of the method is the presence of false-positive. This could be due to some reporter genes such as LacZ which have a certain rate of basal expression. However several alternative reporter genes can be used to increase the stringency of the methods. In fact a number of genes involved in amino-acids biosynthesis were proposed to be used for an efficient protein interaction studies. The two genes HIS3 and LEU2 are currently used as a valid alternative in two hybrid system assay. For instance the HIS3 reporter can be used in combination with 3-amino-1,2,4-triazole (3-AT) to increase the stringency of the method. The 3-AT is an inhibitor of HIS3 gene product which is used to decrease the background of basal HIS3 expression (Causier *et al.,* 2002; Brent *et al.,* 1997). Moreover, the presence of false-positive could be

correlated to the capacity of some investigated proteins to activate the transcription of reporter gene on their own. This ability of auto-activation should be tested before starting the assays by using appropriate negative controls (Sobhanifar *et al.*, 2003).

Another problem is correlated to the expression of the investigated proteins fused with the two tags, BD and AD. Indeed the presence of physic constraints at N or C-terminal ends could avoid correct protein folding or cover binding sites involve in protein-protein interaction. Therefore the correct folding of investigated proteins should be verified before starting. Sometimes the expression of single domains instead of the entire protein could facilitate protein folding increasing the reliability of the method (Sobhanifar *et al.*, 2003).

Moreover, another trouble could be correlated to the use of a heterologous system as host cells. Indeed both bacterial and yeast systems could not provide an optimal post-transcriptional modification of proteins which could be essential for a correct protein interaction. For instance disulfide bound formation, glycosylation and phosphorylation could not occur properly in bacterial cells. In this case the methods based on the use of eukaryotic cells such as yeast are more suitable to provide correct protein modification and folding (Causier *et al.*, 2002; Causier *et al.*, 2004).

Sometimes the presence of strong localization signals on the investigated proteins could preclude correct nuclear localization of BD and AD with the consequent failure of gene reporter activation. Alternatively some proteins, when expressed in a heterologous system, could have a negative effect on the host cell. For instance the investigated protein may become toxic when is targeted to the nucleus (Sobhanifar *et al.*, 2003).

Finally the two hybrid assay is a protocol which was developed for interaction studies between two investigated proteins the “hunter” and the “bait”. Consequently this method is not suitable for protein interactions which involve the presence of many factors. For instance, the presence of a third factor which bridge the “hunter” and the “bait” can preclude a correct interaction (Sobhanifar *et al.*, 2003).

2.4. *In vivo* cross-linking and mass spectrometry

Protein-protein interactions can be also studied by the use of cross-linking agents which are covalently link closely associated proteins. Methods involving cross-linking and immuno-purification combined with MS (mass spectrometry) have been described for the determination of many protein complexes like membrane transporters, multimeric complexes associated with chromatin and others (Akita *et al.,* 1997; Orlando *et al.,* 1997).

A variety of cross-linkers with different proprieties and particular uses are commercially available. The most used in cellular biology are membrane-permeable cross-linking agents which are able to easily pass the phospholipid bilayer. Widely used are in particular crosslinkers which can be later cleaved to release the partners after e.g. Immunoprecipitation. These properties make them very useful to study in *vivo* protein-protein interaction (Vasilescu *et al.,* 2004).

One of the most common protocols uses paraformaldehyde (PFA) as cross-linking reagent in combination with immuno-affinity purification of the protein complex. Indeed PFA can penetrate into cells and its cross-linking can be easily reversed by heating the sample. This molecule generates short cross-links spanning approximately 2 Å and is thus useful to catch only really close protein partners (Vasilescu *et al.,* 2004).

PFA links lysine residues on interacting proteins, which can be an important limitation depending on the number and availability of lysines on the protein surface. Therefore, the failure to detect protein-protein interactions does not mean that they do not occur. For this reason, it could be useful to try different kinds of cross-linkers with different e.g. amine-reactive or sulfhydryl-reactive groups or their combination in the same reaction (Zeng *et al.,* 2006).

After *in vivo* cross-linking, the next steps are membrane solubilisation using different detergents, total protein extraction and complex purification. There are many techniques for protein purification but immuno-affinity is usually the best approach. This procedure is based on complex capture from a cell lysate by an immobilized antibody raised against the native protein or against a tag fused to the protein (Burgess *et al.,* 2002). After extensive washing of the resin to remove contaminants, the protein complexes are eluted and the cross-linking is reversed. Subsequently the individual complex components are separated by SDS-PAGE and identified using MS (mass spectrometry) after excision and purification from the gel (Vasilescu *et al.,* 2004).

Combining in *vivo* cross-linking and MS, we can obtain a list of possible interacting proteins which were in proximity of the target protein during the cross-linking reaction. This does not imply specific protein-protein interaction and the result must be confirmed using other techniques like BiFC, FRET or two hybrid systems.

Results of Interaction

1. Possible interaction between the different types of AtRMR receptors and other protein partners

The structure of AtRMR receptors is characterized by the presence of a PA and a Ring-H2 domain which are both potential protein interaction domains (Mahon *et al.,* 2000; d'Azzo *et al.,* 2005). Moreover in the C-terminal cytosolic part of AtRMR1, 3 and 4, a Serine-Rich domain is present which could be involved in protein regulation by phosphorylation. In analogy with proteins sharing the same features, it is possible that AtRMRs participate in complex formation. The different members of this family could also be involved in (homo- and/or hetero-) oligomerization during protein sorting to vacuoles or interact with other protein partners in the endomembrane system.

Indeed recent work demonstrated that the vacuolar sorting receptor AtVSR1 forms homodimers during protein transport to the LV (Kim *et al.,* 2010). The small cytosolic tail of the receptor is involved in protein dimerization, and the required sequence included (or was) the Tyr motif involved in adaptin binding. AtRMRs might work in a similar manner in their route conveying vacuolar proteins to PSV.

We therefore colocalized different AtRMR1 and 2 fusion proteins with different fluorescent reporters in order to visualize an overlapping or an alteration of the localization of the receptors. Partial colocalization in a subcellular compartment would support the interaction between different AtRMR receptors. In order to demonstrate a direct interaction during protein sorting to vacuoles we developed a Bimolecular Fluorescence Complementation Strategy (BiFC) (Hu *et al.,* 2002). The same techniques could also help identify the specific subcellular compartment of dimer formation.

1.1. Co-localization of AtRMR1 and AtRMR2

These two AtRMRs showed a different localization in both expression systems, transgenic *A.thaliana* and *N.benthamiana* transiently transformed by agro-infiltration. Indeed, AtRMR2 localized in the ER membrane while AtRMR1 localized in the TGN. This difference does not preclude a temporary interaction between them in a specific compartment. Therefore it is still possible that the two receptors are involved in the same cellular process but work one after the other during protein transport to PSV. According to this hypothesis AtRMR2 would bind protein cargos at an early stage of protein traffic in a pre-Golgi compartment, while AtRMR1 would play a role in a later stage e.g. as the receptor involved in post-Golgi protein traffic. Consequently a temporary

interaction between the two receptors could occur in a common compartment at the interface between pre- and post-Golgi organelles.

In order to test this hypothesis I co-expressed in the same plant cells the two receptors AtRMR1 and 2 fused at their C-terminus with two different fluorescent reporters, RFP and YFP, respectively. In figure 47 *N.benthamiana* leaf cells are shown expressing the two fusion protein. Interestingly in the cells expressing only one of the two constructs each fusion protein shows the same localization as previously shown. In contrast, in cells coexpressing both constructs we observed a changed localization of AtRMR2-YFP to punctate structures in addition to the normal ER labelling. Moreover these punctate structures were also labeled with RMR1-RFP demonstrating a colocalization of the two receptors in the same post-Golgi compartment. This result supports an interaction between AtRMR1 and 2 which leads to ER export of AtRMR2-YFP to the AtRMR1-labeled post-Golgi compartment.

In order to test which domains of AtRMR2 are involved in this interaction, we coexpressed the fusion protein AtRMR1-RFP with two different AtRMR2 deletion mutants, lacking either the N-terminal PA domain or the C-terminal Ring-H2 domain and fused with YFP at the deleted side (figure 48 and 49). As had been demonstrated before these two truncated versions of AtRMR2 showed the same ER localization as the wild type protein. When these deletion mutants were coexpressed with RMR1-RFP, they were relocalized to punctate structures. Again these punctuate structures were RMR1-RFP-labelled. These results support the notion that neither PA nor Ring-H2 domains are involved in the interaction with AtRMR1 and are necessary for the relocalization of AtRMR2. Therefore only the transmembrane domain and/or the adjacent small cytosolic linker are involved in these interactions. Specific sequences in their transmembrane domain have indeed been shown to drive α-helix interactions between two transmembrane proteins. A GXXXG motif (where G is glycine and X any aminoacid) was identified in glycophorin (Brosig *et al.,* 1998) and an Sxx(x)SSxxT motif (where S is serine and T is threonine) was identified in a screen with artificial sequences (Dawson *et al.,* 2002). The transmembrane domains of the two AtRMRs contain serines and threonines which could constitute an Sxx(x)SSxxT motif (figure 50).

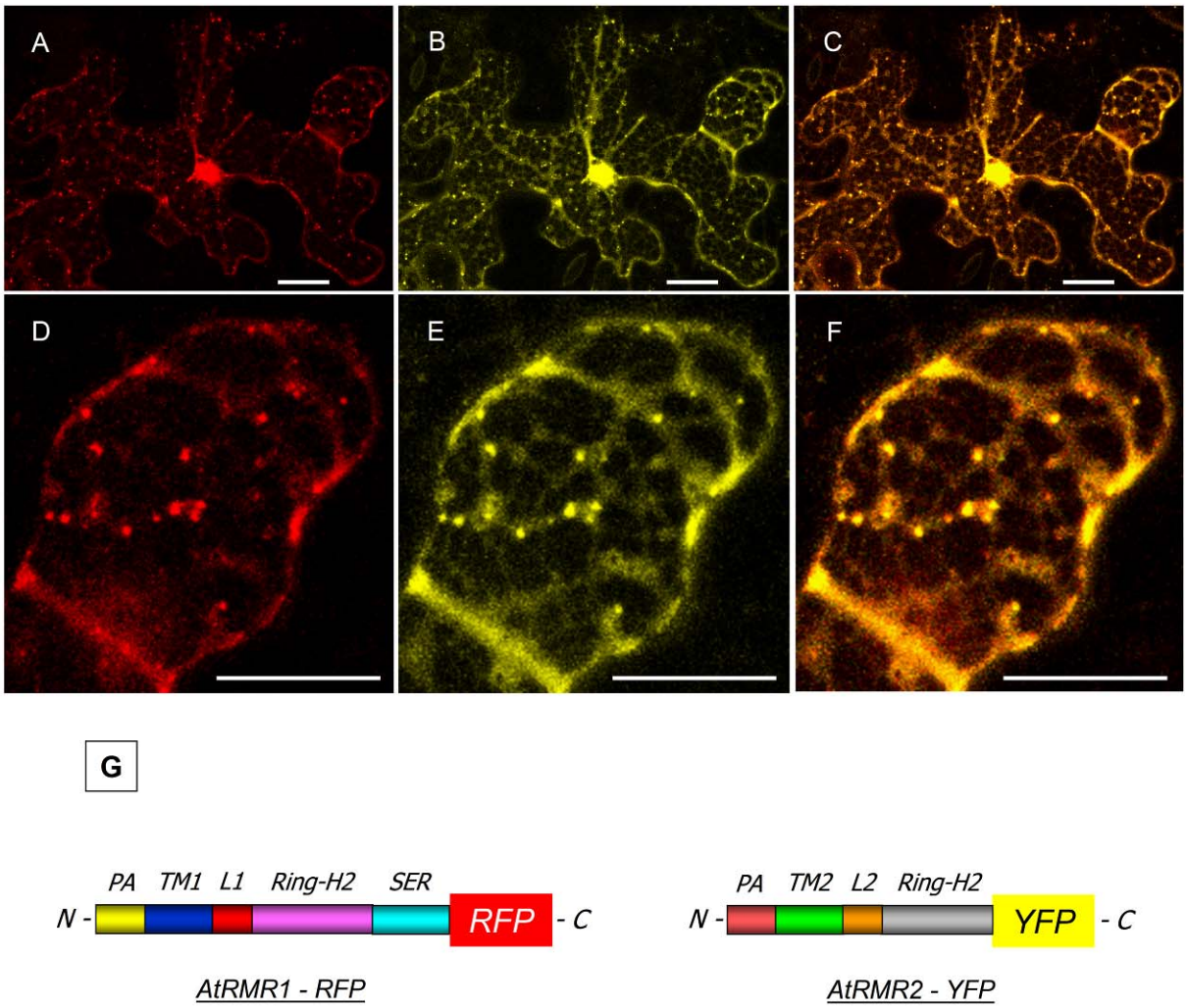

Figure 47: co-expression of AtRMR1-RFP and AtRMR2-YFP in *N. benthamiana* leaves. Confocal images of (A) RFP fluorescence signal; (B) YFP fluorescence signal; (C) merged image of the two fluorescence signals; bar = 20 µm. D-F enlarged portion of the images A-C; scale bar = 15 µm.
(G) Schematic representation of the two fusion proteins. AtRMR1-RFP: full length AtRMR1 (PA domain, yellow; transmembrane, blue; linker, red; Ring-H2 domain, lilac; Serine-Rich domain, cyan) fused at its C-terminus with RFP. AtRMR2-YFP: full length AtRMR2 (PA domain, rose; transmembrane, green; linker, orange; Ring-H2 domain, gray) fused at its C-terminus with YFP.

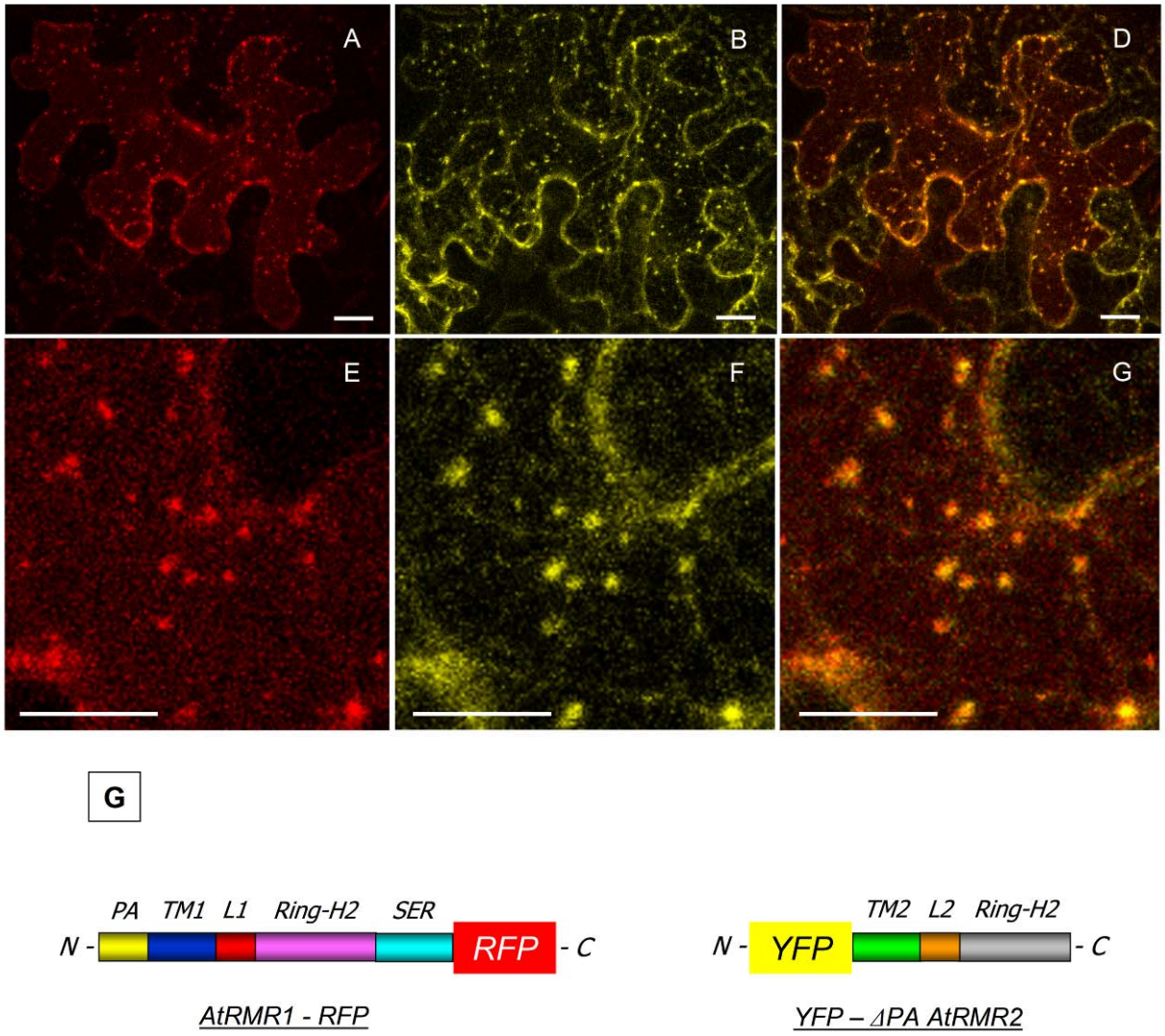

Figure 48: co-expression of AtRMR1-RFP and YFP- ΔPAAtRMR2 in *N. benthamiana* leaves. Confocal images of (A) RFP fluorescence signal; (B) YFP fluorescence signal; (C) merged image of the two fluorescence signals; bar = 20 µm. D-F enlarged portion of the images A-C; scale bar = 15 µm.
(G) Schematic representation of the two fusion proteins. AtRMR1-RFP: as in Fig. 46. YFP-ΔPAAtRMR2: PA domain deleted from AtRMR2, fused at its N-terminus with YFP.

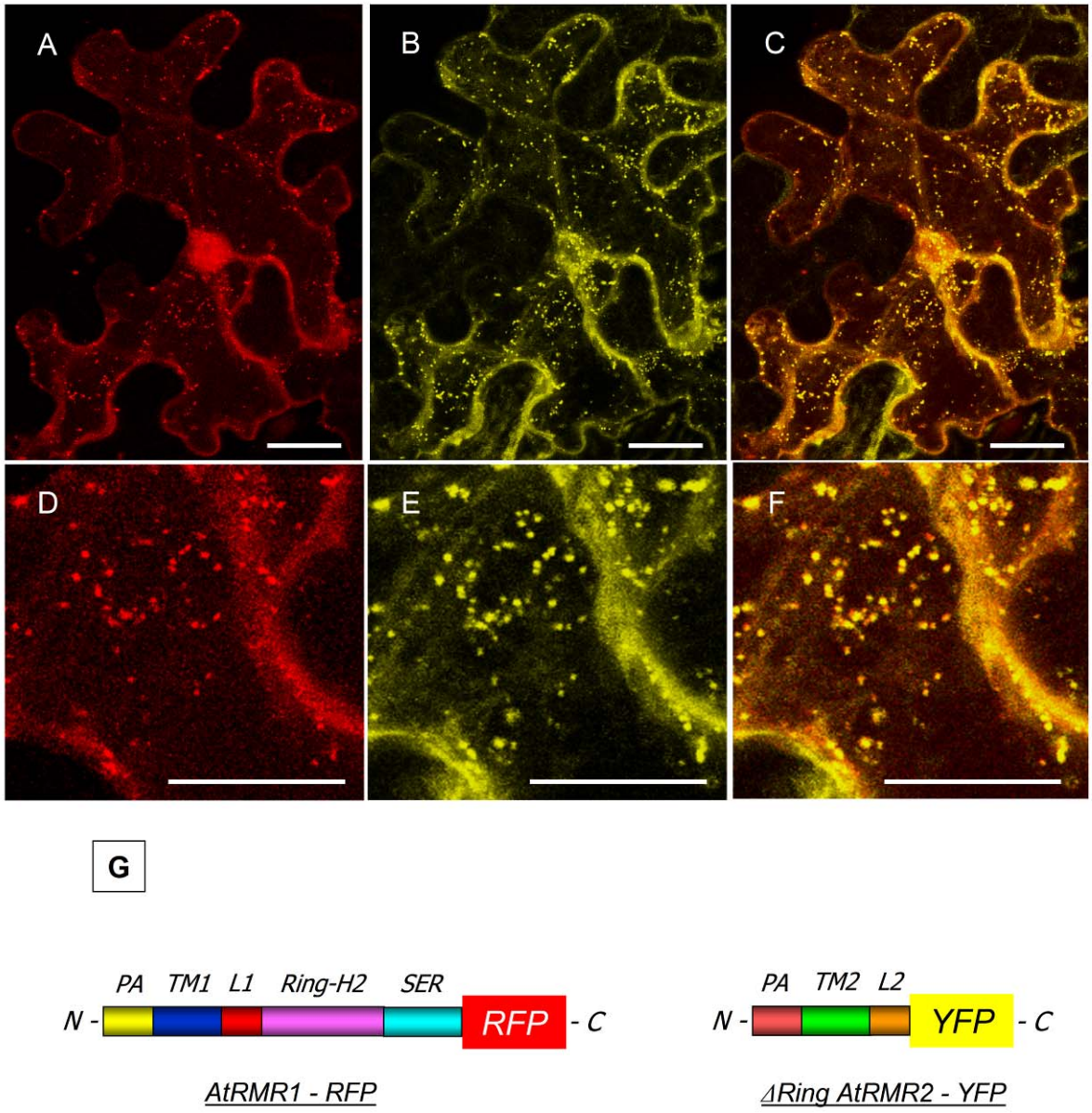

Figure 49: co-expression of AtRMR1-RFP and ΔRingAtRMR2-YFP in *N. benthamiana* leaves. Confocal images of (A) RFP fluorescence signal; (B) YFP fluorescence signal; (C) merged image of the two fluorescence signals; bar = 20 µm. D-F enlarged portion of the images A-C; scale bar = 15 µm.
(G) Schematic representation of the two fusion proteins. AtRMR1-RFP: as in Fig. 46. ΔRingAtRMR2-YFP: Ring-H2 domain deleted from AtRMR2, fused at its C-terminus with YFP.

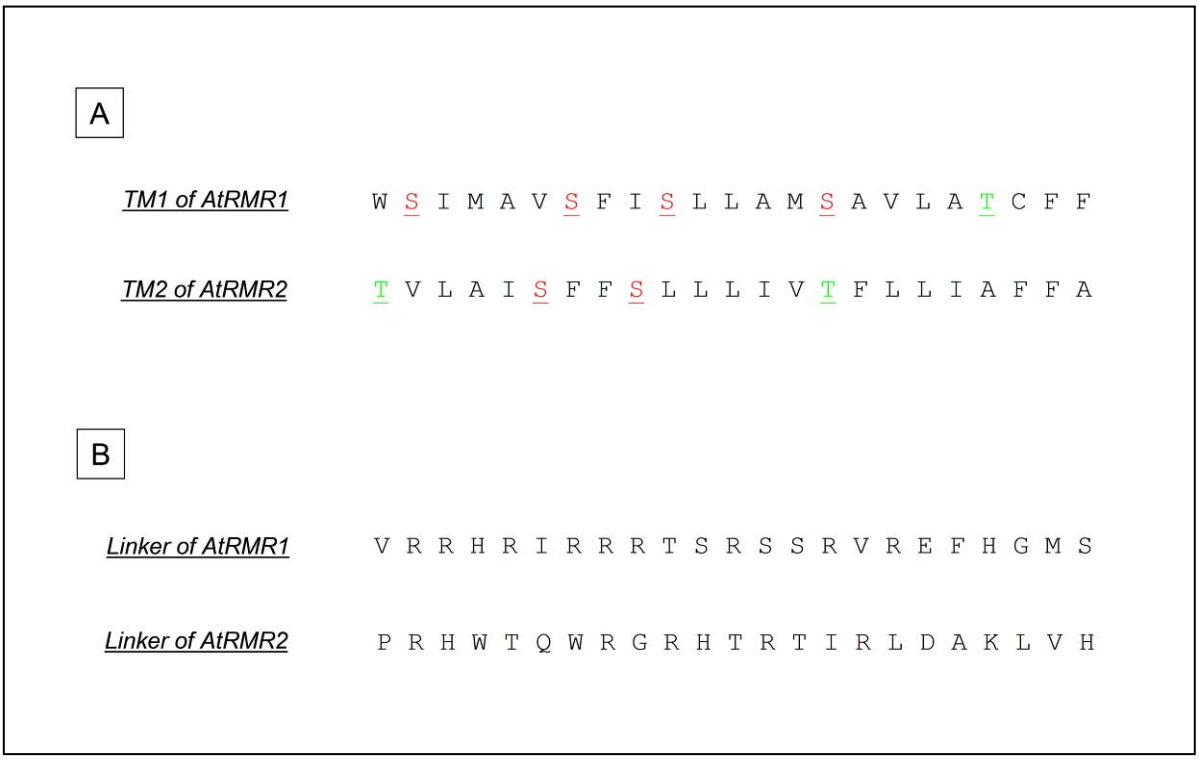

Figure 50: TM1/TM2 and Linker1/Linker2 alignments. (A) Alignment between the aminoacidic sequences of the transmembrane domains of AtRMR1 (TM1) and AtRMR2 (TM2). The putative serine (S, in red) and threonine (T, in green) probably involved in the interactions are indicated in the picture. Probably all these residues constitute specific aminoacidic motifs involved in the interaction between the two transmembrane domains (TM1 and TM2). (B) Alignment between the aminoacidic sequences of the Linker of AtRMR1 and AtRMR2.

1.2. Bimolecular Fluorescence Complementation (BiFC) assay for interaction of different AtRMR receptors

In order to confirm a direct interaction of AtRMR receptors in living cells we chose the BiFC strategy (Hu *et al.,* 2002). For this purpose we generated different fusion proteins of AtRMRs with split YFP fragments: the N-terminal YFP fragment (aminoacids 1 to 154) and the C-terminal YFP fragment (aminoacids 155 to 238) that can associate to form a bimolecular fluorescent complex. We fused these two YFP fragments to different AtRMR, adding a tag (Myc or HA) and a polyglycin linker between the two protein parts.

Finally we used these constructs in different combinations in order to visualize both homo- and heterodimerization between different AtRMR receptors. The technique was validated with appropriate positive and negative controls.

1.2.1. Control of the localization of the viral protein p6

To test the efficiency of BiFC we used the protein p6 from BYV (Beet Yellow Virus) as a positive control. p6 is a 6 kDa membrane protein with a single transmembrane domain that is well known to function as a homodimer. Moreover this interaction is very stable as it involves a disulfide bond in the C-terminal luminal domain of two p6 proteins. The protein has also been localized in the ER membrane (Peremyslov *et al.,* 2004) like AtRMR2. We can take advantage of this similar localization without interaction to use the p6/AtRMR2 combination as a negative control, which is really important to eliminate nonspecific signals.

In order to confirm in *N.benthamiana* the ER localization of p6 we generated a full length p6 –YFP fusion, inserting an HA-tag and a poly-glycine linker between the two proteins. The fluorescence pattern of agro-infiltrated cells indicates that p6-YFP indeed localizes in the ER (figure 51A), confirming the result of Peremyslov *et al* (2004): p6-YFP labelled both nuclear envelope and network structures in the cortical and inner part of the cells.

The presence of the p6-YFP fusion protein in *N.benthamiana* leaves was confirmed by Western blot analysis using antibodies against the HA tag (figure 51B). In total protein extracts we could detect three different bands (figure 51B, lane 2): a higher molecular weight band of approx. 70 kDa and two lower molecular weight bands of 35 and 28 kDa. The 35 kDa band corresponds to the predicted molecular weight for the whole fusion protein p6-YFP. The lower 28 kDa band probably represents free YFP produced by p6-YFP degradation, while the 70 kDa band probably represents a homodimer of two stably associated p6-YFPs. No bands were detected in the total protein extract from untransformed *N.benthamiana* leaves (figure 51B, lane 1).

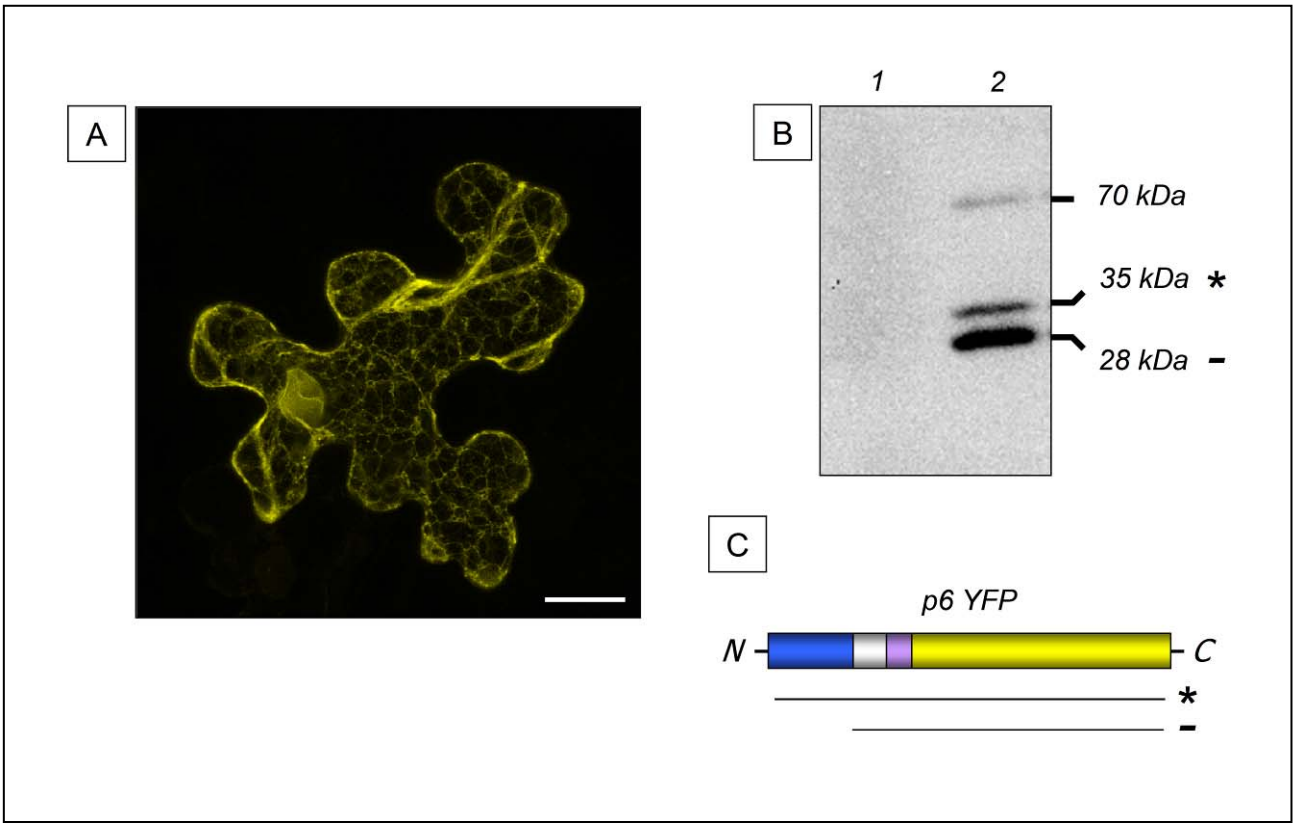

Figure 51: BiFC positive control protein p6. (A) Confocal stack of *N.benthamiana* leaf expressing the fusion protein p6-YFP. (B) Western blot analysis from agro-infiltrated leaves expressing p6-YFP. P6 was detected using an antibody against the HA tag. Lane 1: total protein extract from not-transformed cells; Lane 2: total protein extract from transformed cells expressing the fusion protein p6-YFP. In the lane 2 there are three bands with different molecular weights: a 28 kDa band (YFP alone, indicated with -); a 35 kDa band (fusion protein p6-YFP, indicated with *); a 70 kDa band (homodimer p6-YFP). (C) Schematic representation of the fusion protein p6-YFP: p6 (blue), YFP (yellow), HA-tag (gray) and poly-glycine linker (violet).

1.2.2. Positive BiFC control with split YFP- p6

To test the efficiency of BiFC with p6 as positive control, we fused the p6 protein with the two non-fluorescent YFP fragments (N-terminal YFP and C-terminal YFP) adding a (Myc or HA) tag and a poly-glycine linker between the two proteins. When the two fusion proteins (p6-nYFP and p6-cYFP) were co-expressed in the same cells, we could detect the fluorescence confirming the formation of homodimers (figure 52). Moreover the two BiFC fusion proteins localized in the ER membrane like the wild type protein p6.

The presence of the two fusion protein in transformed leaves was confirmed by Western blotting using an HA antibody to detect p6-nYFP and a Myc antibody to detect p6-cYFP (figure 53). In *N.benthamiana* leaf extracts we could indeed detect one band each at the predicted molecular weights. A 26 kDa band corresponds to p6-nYFP (figure 53A, lane 2) while an 18 kDa band corresponds to p6-cYFP (figure 53B, lane 2). No bands were detected in the negative controls extracts from untransformed *N.benthamiana* leaves (figures 53A and 53B, lane 1).

The sensitivity of the assay was tested by separately expressing the two fusion proteins. We could detect a fluorescence signal only in the cells co-expressing both fusion proteins p6-nYFP and p6-cYFP (figure 54A), while we could not detect any signal in cells expressing only a single of the two constructs (figure 54B and 54C), confirming the inability of each YFP fragment to fluoresce. Moreover, no signal was produced in the cells co-transformed with the two empty vectors and thus expressing the free non-fluorescent halves cYFP and nYFP (figure 54D). This experiment confirmed the inability of the two halves to spontaneously associate in the cytosol.

All these negative controls confirm the specificity of p6 homodimer formation and support the reliability and specificity of BiFC in interaction studies.

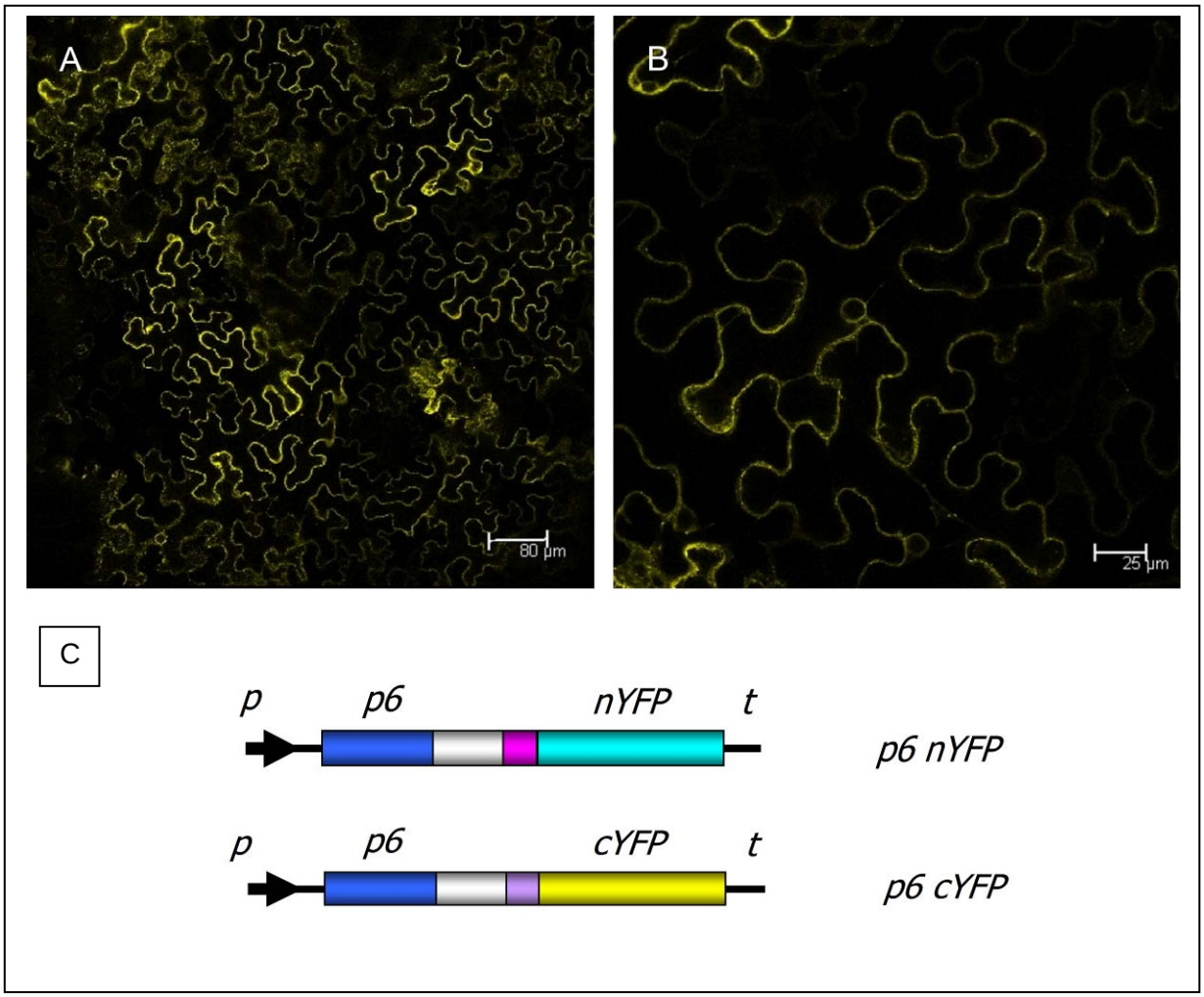

Figure 52: BiFC with split YFP-p6. (A and B) Confocal images of epidermal cells (from *N. benthamiana* leaves) co-transformed by agro-infiltration with the two vectors for BiFC p6-nYFP and p6-cYFP. YFP labelling is concentrated in the nuclear envelope and in a cortical network, the typical ER localization. (C) Expression vectors for Bimolecular Fluorescence Complementation. The full length CDS of p6 protein (blue); nYFP (cyan): amino-terminal half of YFP (aminoacids 1 to 154); cYFP (yellow): carboxy-terminal half of YFP (aminoacids 155 to 238); Myc tag (lilac); HA tag (violet); polyglycine linker (grey).

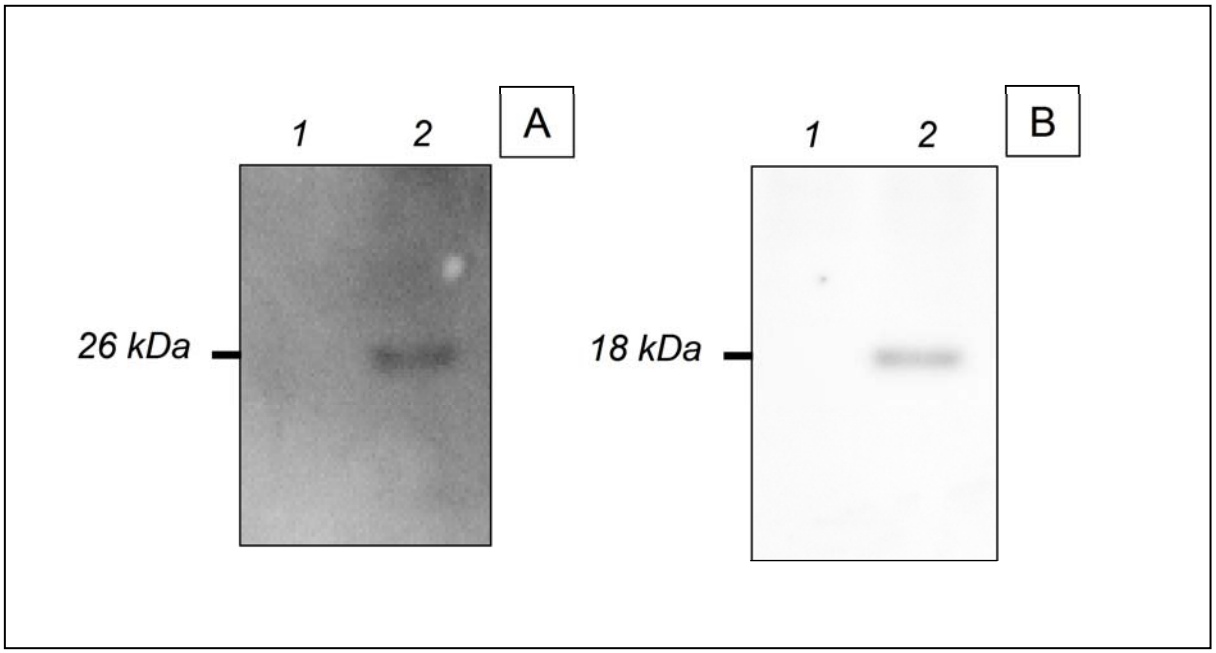

Figure 53: Western blot analysis of leaves expressing split YFP-p6. Extracts from agro-infiltrated *N. benthamiana* leaves expressing the two fusion proteins p6-nYFP and p6-cYFP. Detection with an antibody against HA-tag (A) or Myc-tag (B). Lane 1: control leaves; lane 2A p6-nYFP; lane 2B: p6-cYFP

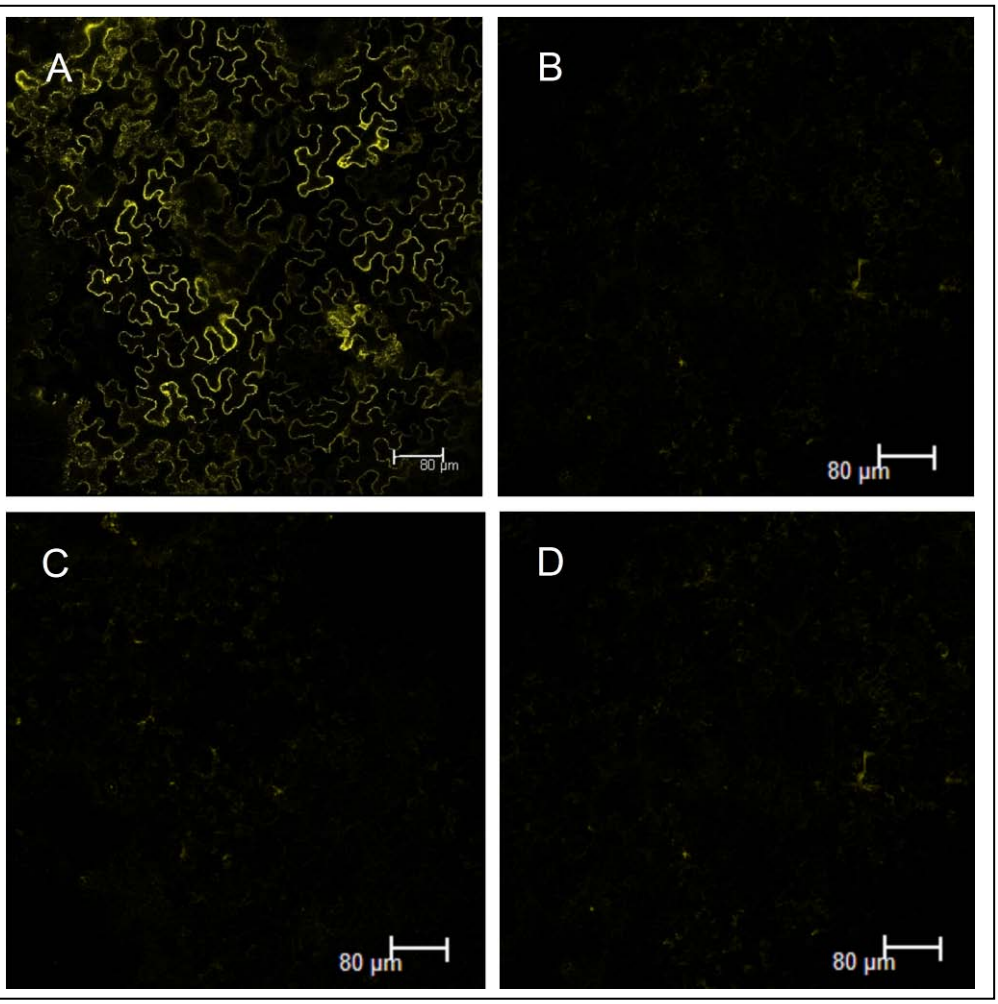

Figure 54: Split YFP-protein p6. Confocal images of epidermal cells (from *Nicotiana benthamiana* leaves) transformed by agro-infiltration with the indicated vectors: p6-nYFP and p6-cYFP (A); p6-cYFP alone (B); p6-nYFP alone (C); two empty vectors nYFP and cYFP (D).

1.2.3. BiFC with split YFP-AtRMRs

We now used the BiFC technique to investigate possible AtRMR-AtRMR interactions during protein sorting to the vacuole. We thus fused AtRMR1 and 2 with the two non-fluorescent YFP fragments and also added a (Myc or HA) tag and a poly-glycine linker between the two proteins (figure 55). These constructs allowed testing the possible homo- and hetero-dimerization between AtRMR1 and 2 proteins.

In figure 56 we present BiFC experiments using different combinations of fusion proteins: AtRMR1-nYFP and AtRMR1-cYFP (homo-dimerization of AtRMR1, figure 56D), AtRMR2-nYFP and AtRMR2-cYFP (homo-dimerization of AtRMR2, figure 56E), AtRMR1-nYFP and AtRMR2-cYFP (hetero-dimerization between AtRMR1 and 2, figure 56F). In all these cases we did not observe a fluorescence signal indicative of the efficient reconstitution of the YFP reporter. In these samples the fluorescence signal was comparable to the background signal in the negative control (figure 56B). As such we used different combinations of protein p6 and AtRMR2 fused to the two different halves of YFP. These two proteins can be used as a negative control because they have the same localization in the endomembrane system but do not interact. As positive control we used protein p6 fused to either halves of YFP (figure 56A).

These results suggest that AtRMR1 and 2 cannot form homo- or heterodimers or that their formation cannot be visualized efficiently enough with this technique.

A possible problem could be the low level of AtRMR expression which could prevent the efficient visualization of dimer formation.

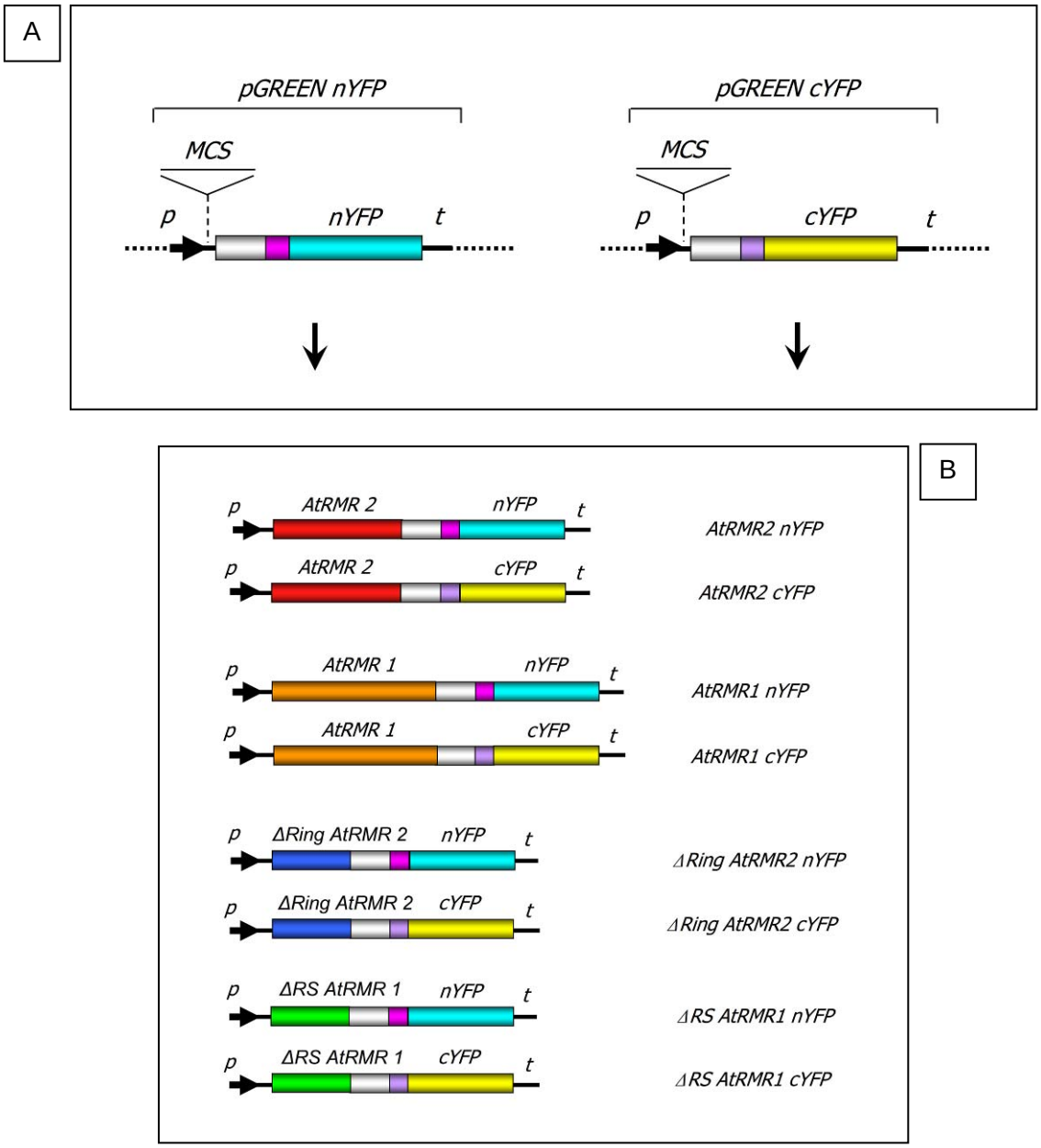

Figure 55: Constructs for AtRMR BiFC. (A) Expression vectors for BiFC (pGREEN nYFP and pGREEN cYFP). The two non-fluorescent halves of YFP were cloned in two different vectors adding a tag, a polyglycin linker and a multi cloning site (MCS). nYFP (in cyan): N-terminal part of YFP (from aminoacid 1 to aminoacid 154); cYFP (in yellow): C-terminal of YFP (from aminoacid 155 to aminoacid 238); tag (Myc, in lilac or HA, in violet) and a polyglycin linker (in grey). The fusion proteins are expressed under the control of 35S promoter (*p*) and terminator (*t*) present in pGREEN plant expression vector [Hellens, 2000]. (B) Different cDNA of AtRMRs were cloned in correspondence of the MCS of the two empty vectors (pGREEN nYFP and pGREEN cYFP) generating the indicated expression vectors for BiFC. AtRMR2: the cDNA full length of AtRMR2 (in red); AtRMR1: the cDNA full length of AtRMR1 (in orange); ΔRingAtRMR2: the cDNA of AtRMR2 lacking the Ring-H2 domain (in blue); ΔSRAtRMR1: the cDNA of AtRMR1 lacking the Ring-H2 and Serine-Rich domain (in green). All the fusion proteins are expressed under the control of 35S promoter (*p*) and terminator (*t*) present in pGREEN plant expression vector (Hellens *et al.*, 2000).

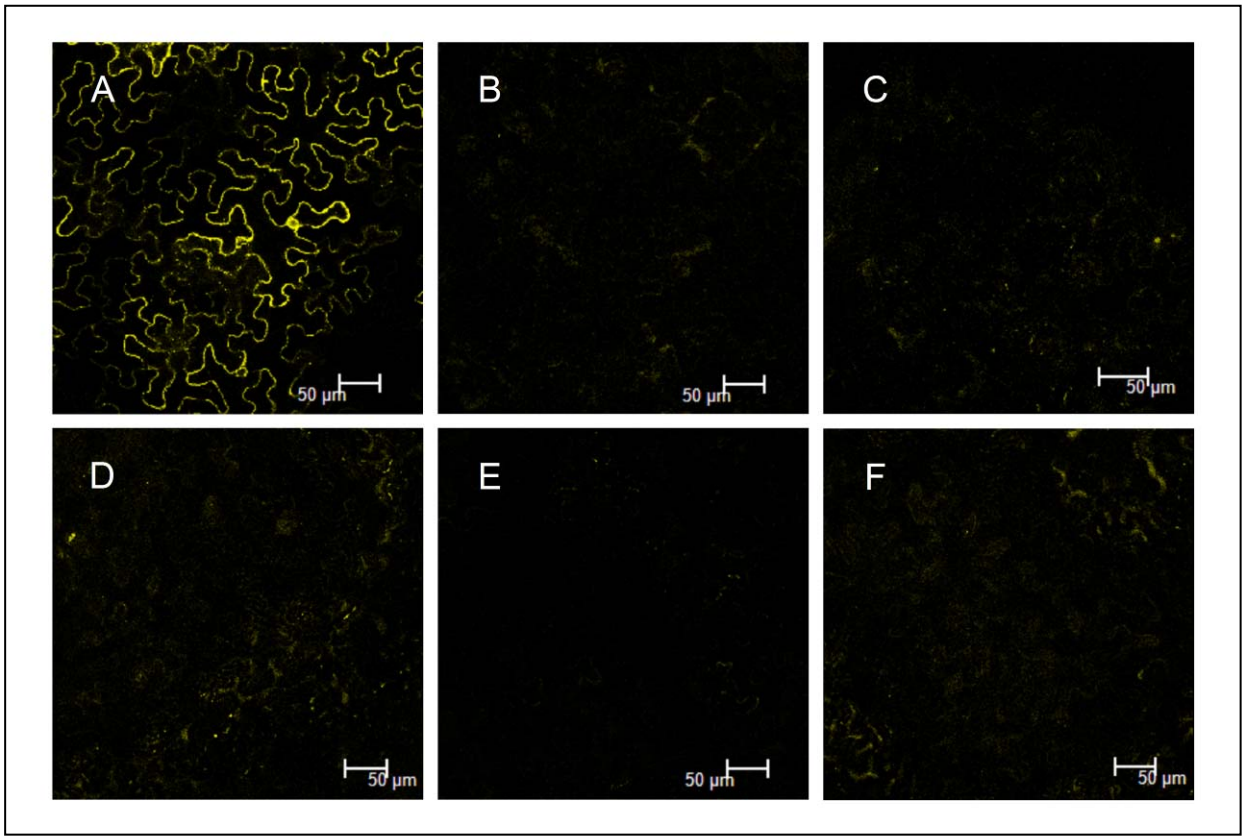

Figure 56: Split-YFP AtRMRs. Confocal images of epidermal cells (from *Nicotiana benthamiana* leaves) transformed by agro-infiltration with the indicated vectors for BiFC: positive control, p6-nYFP and p6-cYFP (A); negative control, p6-nYFP and AtRMR2-cYFP (B); the two empty vectors, nYFP and cYFP (C); AtRMR1-nYFP and AtRMR1-cYFP (D); AtRMR2-nYFP and AtRMR2-cYFP (E); AtRMR1-nYFP and AtRMR2-cYFP (F).

1.2.4. BiFC with split YFP-AtRMR deletion mutants

In order to increase the low level of AtRMR expression I performed several BiFC experiments using AtRMR deletion mutants. As I had shown before, AtRMR deletion mutants of the C-terminal domain are more expressed than the full length protein. Probably the C-terminal Ring-H2 and Serine-Rich domains could be involved in increasing protein turnover.

For this purpose the following constructions were generated, based on the previously presented constructions: ΔRingAtRMR2-nYFP and ΔRingAtRMR2-cYFP, both lacking the Ring-H2 of AtRMR2; ΔRSAtRMR1-nYFP and ΔRSAtRMR1-cYFP, both lacking the Ring-H2 and Serine-Rich domains of AtRMR1 (Figure 55).

The first two constructs were used to test the possible homo-dimerization between two ΔRingAtRMR2 deletion mutants. Indeed in a previous Western blot experiment using a total protein extracts from agro-infiltrated *N.benthamiana* leaves, the fusion protein ΔRingAtRMR2-YFP was detected at higher molecular weight (figure 57). Using an anti-HA antibody, the ΔRingAtRMR2-YFP mutant is present in two different bands (figure 57, lane 2). The higher molecular weight band of nearly 102 kDa is compatible with the homo-dimer produced by the association of two ΔRingAtRMR2-YFP of 53 kDa each. The lower 76 kDa molecular weight band could come from the association between one ΔRingAtRMR2-YFP mutant and an unknown protein of nearly 23 kDa. This association must be very stable to allow its visualization under denaturing and reducing conditions.

The hypothesis of ΔRingAtRMR2 homo-dimerization could not be confirmed in BiFC experiments. I did not visualise any fluorescence signal in plants transformed with two BiFC constructs, ΔRingAtRMR2-nYFP and ΔRingAtRMR2-cYFP (figure 58E). Indeed the signal product in this experiment was similar to the signal product by the negative control (figure 58 B).

More interesting results were obtained with the last two constructs testing the possible homo-dimerization of ΔRSAtRMR1. In this case I observed a clear BiFC signal in *N.benthamiana* leaves (figures 58D and 59A). This supports the notion that AtRMR1 can and does form homodimers and indicates also that the dimerization does not require the presence of the C-terminal luminal part of the protein. Neither the Ring-H2 nor the Serine-Rich domains seem to be important. Consequently this result supports the previous result of AtRMR1 and AtRMR2 coexpression which showed that just the transmembrane domain and a few subsequent aminoacids i.e. the sequence linker, could be involved in protein-protein interactions.

As was demonstrated previously, the localization of AtRMR2 is affected by the coexpression of AtRMR1. In this case AtRMR2 is able to exit from the ER and to colocalize with AtRMR1 in punctate structures. This result suggests the formation of heterodimers between the two proteins. Moreover I showed that the two deletion mutants ΔRingAtRMR2 and ΔPAAtRMR2 showed the same colocalization behaviour with AtRMR1 as the full length AtRMR2, which indicated that the Ring-H2 and PA domains are probably not involved in the interaction.
To confirm this hypothesis I performed BiFC experiments with the two deletion mutants ΔRSAtRMR1 and ΔRingAtRMR2 fused to different YFP fragments. I observed a clear positive BiFC signal (figure 58F and 59B). These results thus supported the ability of AtRMR1 and AtRMR2 to forming heterodimers. Moreover it is also confirmed that the C-terminal Ring-H2 and Serine-Rich domains are not necessary for this interaction. Consequently, the transmembrane domain and the linker could be involved in protein dimerization.

The previous results demonstrated the capacity of AtRMR1 to form homodimers as well as heterodimers with AtRMR2. In the next step I performed a BiFC experiment in order to investigate the possible formation of a complex between two AtRMR1 and at least one AtRMR2 (trimer or tetramer). Therefore I agroinfiltrated *N.benthamiana* leaves with three constructs encoding ΔRSAtRMR1-nYFP, ΔRSAtRMR1-cYFP and ΔRingAtRMR2-RFP (figure 60). Only in case of tri- or tetramerization will it be possible to observe AtRMR1 BiFC in association with AtRMR2 co-localization. To the contrary in cells expressing the three constructs I observed a positive BiFC signal in punctate structures (AtRMR1 pattern) but only ER localization for AtRMR2. Therefore AtRMR1 cannot at the same time homodimerize and associate with AtRMR2. In consequence AtRMR2 cannot exit from the ER.
These results suggest that the formation of a trimer of two AtRMR1 and one AtRMR2 does not take place. Moreover it seems that the AtRMR1 homodimer is more stable than the AtRMR1/AtRMR2 heterodimer, and consequently most AtRMR2 is present in monomeric form in the membrane of ER. However this result does not preclude a certain dynamics of the process and the possible co-existence of both kinds of dimers. In fact it is also possible that in plant cells these two dimers are present in different proportion. It is possible that I was not able to visualize the dynamics of the process because the reconstituted YFP is really stable precluding the later dissociation of AtRMR1 homodimers. Consequently most BiFC-AtRMR1 is present in highly stable dimers leaving monomeric AtRMR2 in the membrane of ER.

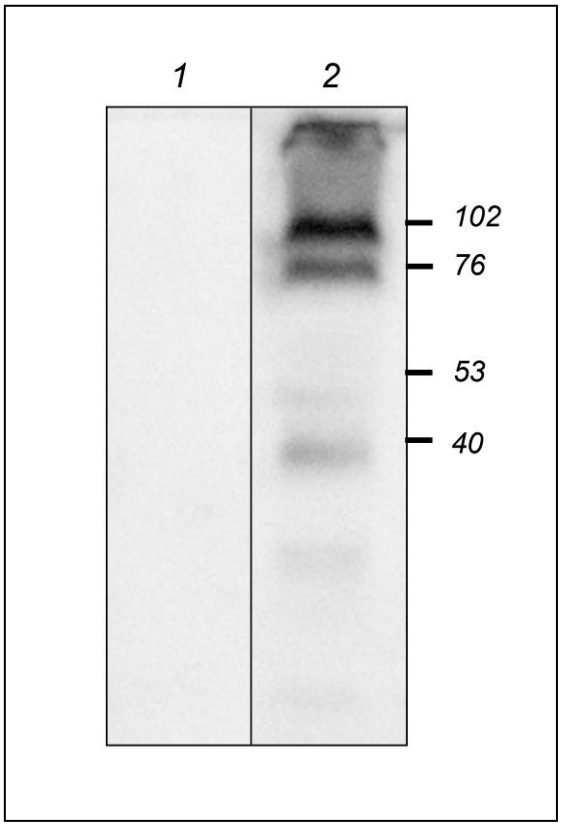

Figure 57: Western blot experiment of ΔRingAtRMR2-YFP. Western blot experiment from agro-infiltrated epidermal cells (from *Nicotiana benthamiana*) expressing the fusion protein ΔRingAtRMR2-YFP. The experiment has been performed using an antibody against HA tag. In total protein extract from transformed leaves the fusion protein ΔRingAtRMR2-YFP is not present at the expected molecular weight (almost 53 kDa). Indeed the fusion protein is present as a higher molecular weight band at 102 kDa and a lower band almost 76 kDa (lane 2). Total protein extract from untransformed *N.benthamiana* leaves has been used as a negative control (lane 1).

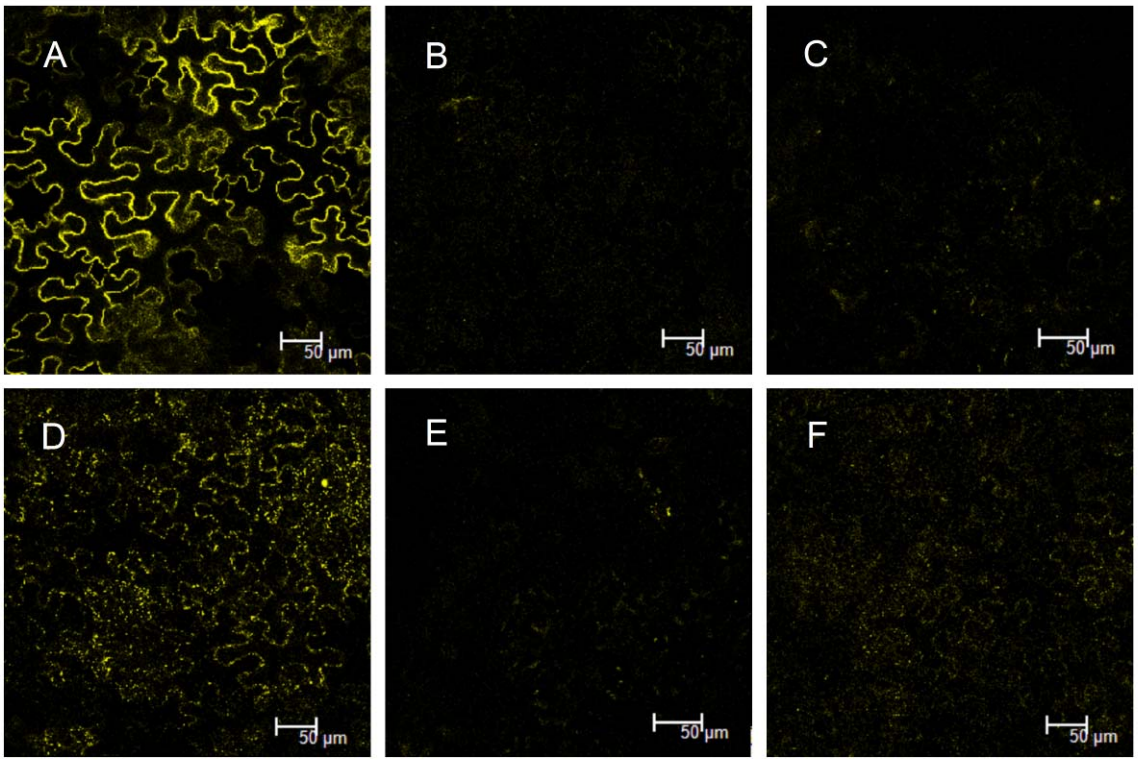

Figure 58: Split-YFP AtRMRs. Confocal images of epidermal cells (from *Nicotiana benthamiana* leaves) transformed by agro-infiltration with the indicated vectors for BiFC: positive control, p6-nYFP and p6-cYFP (A); negative control, p6-nYFP and AtRMR2-cYFP (B); the two empty vectors, nYFP and cYFP (C); ΔRSAtRMR1-nYFP and ΔRSAtRMR1-cYFP (D); ΔRingAtRMR2-nYFP and ΔRingAtRMR2-cYFP (E); ΔRSAtRMR1-nYFP and ΔRingAtRMR2-cYFP (F).

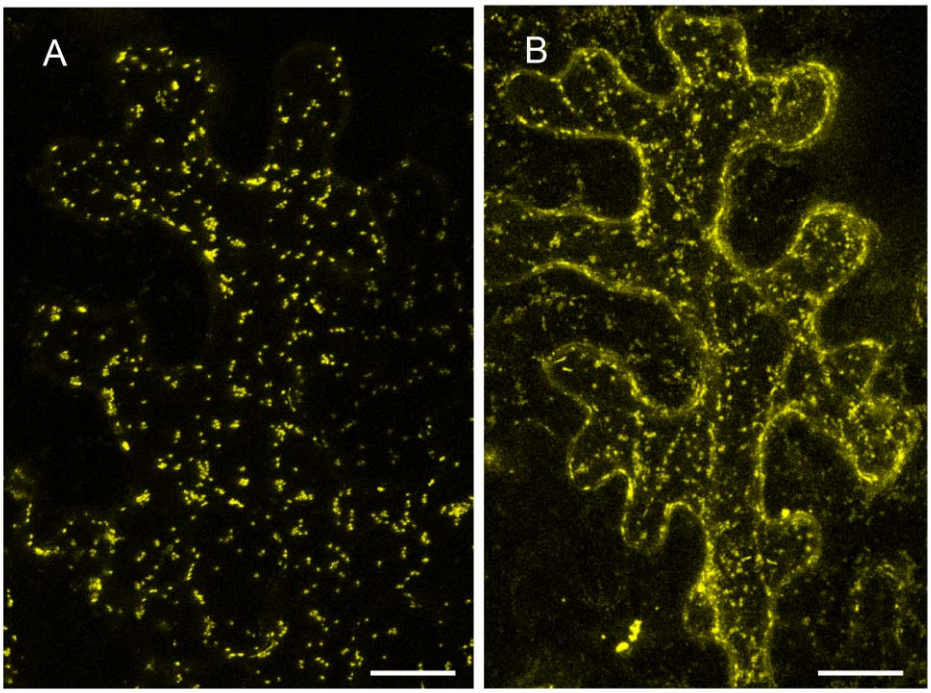

Figure 59: Split-YFP AtRMRs. Confocal stacks of epidermal cells (from *Nicotiana benthamiana* leaves) co-transformed by agro-infiltration with the indicated vectors for BiFC: ΔRSAtRMR1-nYFP and ΔRSAtRMR1-cYFP (A); ΔRSAtRMR1-nYFP and ΔRingAtRMR2-cYFP (B). Scale bar = 20 μm.

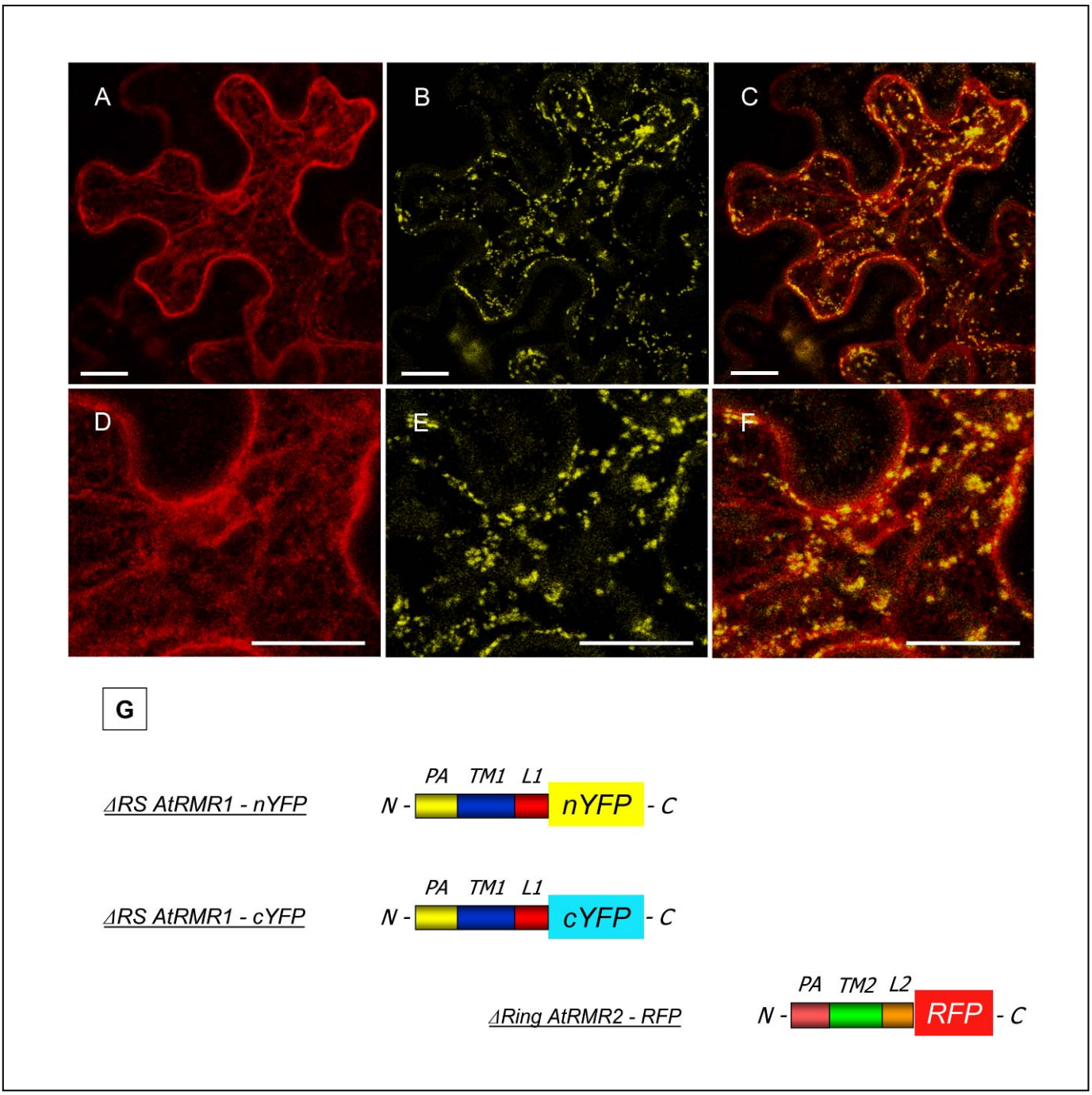

Figure 60: co-expression of ΔRSAtRMR1-nYFP, ΔRSAtRMR1-cYFP and ΔRingAtRMR2-RFP in *N. benthamiana* leaves. Confocal images of (A) RFP fluorescence signal; (B) YFP fluorescence signal; (C) merged image of the two fluorescence signals. D-F enlarged portion of the images A-C. A-F bar = 20 µm.
(G) Schematic representation of the three fusion proteins. ΔRSAtRMR1-nYFP and ΔRSRMR1-cYFP: the ΔRSAtRMR1 mutant (PA domain, yellow; transmembrane, blue; linker) fused respectively at its C-terminus with nYFP (yellow), in the first construct and at its C-terminus with cYFP (cyan), in the second construct. ΔRingAtRMR2-RFP: the ΔRingAtRMR2 (PA domain, rose; transmembrane, green; linker, orange) fused at its C-terminus with RFP.

1.3. *In vivo* cross linking of AtRMR1 in *A .thaliana* leaves (Preliminary results)

The procedure described before could also be used to demonstrate the dimerization and complex formation between AtRMR receptors and others protein partners.

For this purpose three weeks old *A.thaliana* plants were treated for 30 minutes with 1% paraformaldehyde (PFA) which is an optimal concentration for protein cross-linking (Vasilescu *et al.,* 2004). Therefore the use of an optimal concentration of cross-linking agent constitutes a very important experimental variable which can vary under several plant and environment conditions. Indeed a high concentration of PFA could lead to an over-fixation of tissues with the consequent problem in the reversing of cross-linking reaction. Contrary a low concentration of PFA could not be sufficient to catch all the interacting proteins in close proximity.

The other important variable is the incubation temperature for the cross-linking reaction. This experiment was performed at two different temperatures, at 37°C (figure 61: lane 1 and lane 2) and 18°C (figure 61: lane 3 and lane 4). The cross-linking reaction of PFA occurs at an optimal temperature of 37 °C. However this temperature is unfavourable for *A.thaliana*, which is why we decided to perform the experiment also at a lower temperature of 18 °C which is optimal for the plants. The reaction takes longer at low temperature and the time of incubation with PFA needs to be adjusted accordingly. Different incubation times were tested at the two temperatures but finally optimal incubation times were about 30 minutes at both temperatures. Finally in order to validate the experiment, untreated *A.thaliana* plants where used as a negative control (figure 61: lane Nt).

The experiment was performed using 10 μg of total protein extract for each samples. The samples were loaded on SDS acrylamide gel, after reversing (figure 61: lane 1 and lane 3) or not reversing the cross-linking reaction (figure 61: lane 2 and lane 4). Finally the proteins were transferred onto membrane and incubated with an antibody against AtRMR1.

Comparing the two samples, we can see the presence of high molecular weight bands (figure 61: lane 2 and lane 4, indicated with red asterisk) which disappear after reversing the cross-linking reaction (figure 61: lane 1 and lane 3). Endogenous AtRMR1 is predicted to be approx 47.5 kDa (cyan arrow). We recognize three major bands at higher molecular weight: a first band at approx 80 kDa; a second band at approx 140 kDa; and larger band at 175 kDa. These bands are probably cross-linking products between AtRMR1 and other protein partners. Moreover the smear found at molecular weight up to 175 kDa (figure 61: lane 2 and lane 4, third asterisk from the bottom) is probably a big protein aggregate which cannot be resolved properly in this gel system. Around 32.5 kDa we detected a low molecular weight doublet (green arrow). These bands could be considered contaminant proteins or proteolytically processed forms of AtRMR1.

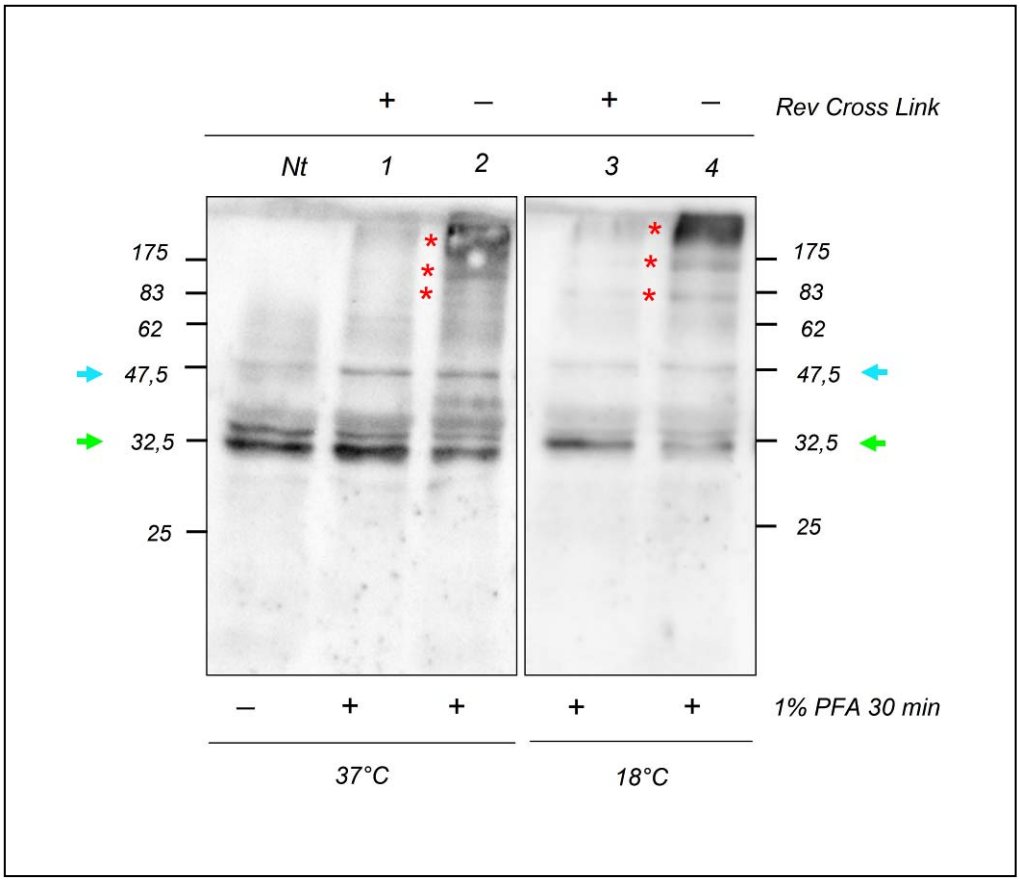

Figure 61: Western blot of cross-linked proteins. *A.thaliana* plants were treated with 1% Paraformaldehyde for 30 min (+ 1% PFA, 30 min) and not treated plants were used as a control (Nt – 1% PFA, 30 min). The cross linking reaction was performed at two different temperature 37°C and 18°C. Subsequently 10 μg of total protein extract for each samples was loaded on SDS acrylamide gel, after reversing of cross-linking (lane 1 and 3, + rev cross link) and not reverse of cross link (lane 2 and 4, - rev cross link). Then the samples were transferred on membrane and treated with antibodies against AtRMR1.
AtRMR1 has a molecular weight of 47.5 kDa (cyan arrow) and red asterisks indicate cross-linking products between AtRMR1 and putative protein partners. In correspondence of 32.5 kDa we can see a low molecular weight doublet (green arrow) which could be a contaminant proteins or a specific form of AtRMR1 proteolytically processed.

Discussion of Interaction

1. ER export of AtRMR2 in the presence of AtRMR1

The two AtRMR family members AtRMR1 and 2 show different localizations in both *N.benthamiana* and *A.thaliana* systems. Indeed AtRMR1 localizes in the TGN as expected for its proposed role in vacuolar sorting. On the contrary AtRMR2 localizes in the ER membrane suggesting an alternative cellular function for this protein. But when the two proteins were co-expressed in *N.benthamiana*, a part of AtRMR2 changed localization to the AtRMR1-labelled punctate structures. AtRMR2 now showed a double localization: in the ER membrane and in the TGN.

The AtRMR1/AtRMR2 co-localization could be due to the formation of heterodimers. When AtRMR2 was expressed alone it was not able to exit from the ER, while in contrary AtRMR1 efficiently localized in the TGN. In the previous chapter I demonstrated that the sequence linker of AtRMR1 contains sequences necessary for this protein localization, which are missing in AtRMR2. Therefore AtRMR2 needs to interact with AtRMR1 to be able to exit from the ER and to localize in the membrane of TGN.

It is likely that AtRMR1 and 2 posses the same profile of tissue expression in *A.thaliana* wild type. Therefore in normal conditions AtRMR2 probably colocalizes with AtRMR1 in the membrane of TGN. This hypothesis is also supported by results of gene expression obtained in our laboratory. In these experiments AtRMR1 and 2 showed a similar expression profile in transgenic *A.thaliana* plants stably transformed with YFP under the control of endogenous promoter and terminator (annex I). In fact for this purpose we generated two *A.thaliana* transgenic lines: the first expressing YFP under the control of endogenous AtRMR1 promoter and terminator and the second expressing YFP under the control of endogenous AtRMR2 promoter and terminator (Sophie Marc-Martin, unpublished data). In these two transgenic plants I observed high YFP fluorescence in the epidermis in different organs, but no significant YFP signal in other tissues.

The different situation observed in *N.benthamiana* could be explained by the absence of an AtRMR1 homologue which could interfere with AtRMR2 localization. Alternatively a homologous protein could be present but in a too low amount to affect AtRMR2 localization. In fact in this experimental system more AtRMR2 is produced because it is over-expressed under the control of the 35S promoter. On the contrary when AtRMR1 and 2 were coexpressed in the same cells, the over-expression of AtRMR1 produced enough interacting proteins for a proper AtRMR2 relocalization to the TGN.

2. AtRMR1 colocalization with different AtRMR2 deletion mutants

The AtRMR family is characterized by the presence of a PA and a Ring-H2 domains which are both potential protein interaction domains (Mahon *et al.,* 2000; d'Azzo *et al.,* 2005). Indeed among homologous proteins with similar domain composition, these two domains are often involved in protein dimerization and interaction with others protein partners in complexes (Lawrence *et al.,* 1999; Mahon *et al.,* 2000; Xinmei *et al.,* 2001; d'Azzo *et al.,* 2005).

In order to know which domains of AtRMR2 were involved in this putative interaction, we performed a series of co-expression experiments between full length AtRMR1 and two truncated versions of AtRMR2 lacking either the N-terminal PA domain or the C-terminal Ring-H2 domain. Both mutants changed localization to AtRMR1-labelled punctate structures when coexpressed with AtRMR1. These results indicate that neither PA nor Ring-H2 domains of AtRMR2 are indispensable for protein dimerization and the localization change. Therefore only the transmembrane domain and the linker are needed. Similarly the transmembrane domain and the short cytosolic tail of AtVSR1 are involved in the homodimerization of this other vacuolar receptor (Kim *et al.,* 2010).

Certain membrane proteins such as glycophorin A and APP (Amyloid Precursor Protein) can dimerize by association between their transmembrane domains (Brosig *et al.,* 1998; Melnyk *et al.,* 2004; Miyashita *et al.,* 2009). Specific aminoacid sequences can drive helix-helix interactions stabilized by hydrogen bonds between specific residues. The most common motif is a GXXXG sequence, where with G as glycine and X as any aminoacid (Brosig *et al.,* 1998). This motif is often associated with a phenylalanine (F) which stabilizes the motif (Unterreitmeier *et al.,* 2007). Alternatively serine (S) and threonine (T) rich motifs (SxxSSxxT) can also drive strong membrane helix interactions (Dawson *et al.,* 2002). The transmembrane domains of AtRMR1 and 2 do not however contain any GXXXG-type motif. The two domains contain several threonines and serine which could constitute a motif (SxxS) involved in dimerization (figure 50).

3. Test for dimerization of AtRMRs by Bimolecular Fluorescence Complementation assays

BiFC is a sensitive method to detect the formation of dimers oligomers of proteins. We chose this technique to investigate the homo- or heterodimerization of members of AtRMR family.

3.1. Positive and negative controls

p6 is a small viral protein which homodimerizes by the formation of a disulfide bond (Peremyslov *et al.*, 2004). p6 dimer formation could be easily visualized by BiFC, confirming the efficiency of this technique and the quality of p6 as a positive control. Expression of the two fusion proteins (p6YFPn and p6YFPc) was confirmed by Western blot. The specificity of BiFC was tested by combining one p6 reporter and an AtRMR2 reporter. Even though both proteins are single membrane-spanning ER proteins they do not associate and there is not BiFC signal. Another negative control was to coexpress in the cytosol the two non-fluorescent YFP fragments (YFPn and YFPc). We confirmed the low affinity of these two halves to spontaneously associate and form a fluorescent protein.

3.2. No detection of dimerization of full length AtRMRs

We performed three different BiFC experiments: split AtRMR1 to visualize homodimerization between two AtRMR1; Split AtRMR2 to visualize homodimerization between two AtRMR2; and split AtRMR1/AtRMR2 to visualize heterodimerization between AtRMR1 and 2. In none of these experiments could we visualize a fluorescence signal significantly above background, in contrast to the high fluorescence visualized in the positive control. It thus seems that AtRMR1 and 2 cannot form homo- or heterodimers or that we could not visualized them. It is possible that a too low expression or accumulation of full length AtRMRs or steric problems could prevent dimer visualization.

3.3. Dimerization of AtRMR deletion mutants

One major problems of BiFC are the steric constraints which could prevent efficient reconstitution of YFP even when the investigated proteins form dimers. The domains to which the two YFP halves are linked must also be brought together. This could be particularly unlikely when the two cytosolic domains of AtRMR1 and 2 differ in length by the presence of a Serine-Rich domain only in the former protein. To solve this problem we generated truncated versions of AtRMR1 and 2 lacking the C-terminal Ring-H2 and Serine-Rich domains. The two fusion proteins ΔRSAtRMR1-

cYFP and ΔRingAtRMR2-nYFP have now the same length increasing the probability of the association between the two YFP fragments.

Another problem could be the low level of protein expression and accumulation. Indeed full length AtRMR1 and 2 could only be visualized in *N.benthamiana* by using the inhibitor of RNA silencing p19 (Voinnet *et al.,* 2003). A too low expression of the two investigated proteins would not allow generating a detectable YFP signal. This problem could also be solved by using the two truncated versions. Expression and stability of these two mutants was higher than for the full length proteins. I have also just demonstrated that the Ring-H2 domain is not necessary for the AtRMR1/AtRMR2 interaction.

I first tested the homodimerization between two ΔRingAtRMR2 deletion mutants. Interestingly the ΔRingAtRMR2-YFP fusion protein was predicted to be 53 kDa but was been found at higher molecular weights in western blot experiments: a higher molecular weight band of nearly 102 kDa which is compatible with homodimerization of the fusion protein and a lower molecular weight band of 76 kDa which is probably one ΔRingAtRMR2-YFP (53 kDa) coupled to a smaller protein of 23 kDa. The nature of this protein could be determined by mass spectrometry after excision and purification from the gel (Vasilescu *et al.,* 2004). This association is so stable to allow visualizing the complex under denaturing and reducing conditions. This suggests covalent binding during complex formation, e.g. by the formation of isopeptide bonds catalyzed by the cross-linking enzyme transglutaminase (TGase). This class of enzymes is widely distributed in animals and plants and catalyzes intra- and intermolecular covalent bond formation between adjacent lysine and glutamine residues in the two associated proteins (Serafini-Fracassini *et al.,* 2008). In mammalian cells for instance, a transglutaminase has been proposed to form covalent bonds between subunits of troponin (Gorza *et al.,* 1996). TGases were studied for their capacity to catalyze the binding of polyamines (Pas) to proteins (Beninati and Folk, 1988).

In a BiFC experiment I could not visualize any fluorescence signal above background for ΔRingAtRMR2, which thus cannot dimerize or its dimer cannot be visualized with BiFC. In contrast, I visualized a positive BiFC signal in *N.benthamiana* leaves expressing ΔRSAtRMR1-nYFP and ΔRSAtRMR1-cYFP, indicating a homodimeric interaction between the two fusion proteins.

Moreover I also observed a positive signal in *N.benthamiana* leaves cotransformed with ΔRSAtRMR1-nYFP and ΔRingAtRMR2-cYFP indicating a heterodimer formation. This result confirmed the AtRMR1/AtRMR2 interaction detected in previous experiments of colocalization which showed a changed localization of AtRMR2 upon coexpression with AtRMR1.

Based on the difference of the BiFC signals it appears that the homodimer formation is more efficient than the formation of heterodimers. If all constructs were expressed at the same level, the association between two ΔRSAtRMR1 was more efficient than the association between a ΔRSAtRMR1 and a ΔRingAtRMR2.

These two experiments also confirm that the C-terminal cytosolic part of the proteins (their Ring-H2 and Serine-Rich domains) is not essential for homo- and heterodimer formation. They support the hypothesis that the transmembrane domain and the linker are involved in protein-protein interactions.

The association between the two transmembrane domains could be tested. E.g. we could perform further BiFC experiments addressing specifically the sequence requirements of the transmembrane domains for these interactions. A series of point mutations directed against the putative serine and threonine could provide important information about their role in AtRMR1/AtRMR2 transmembrane interaction. Alternatively several two hybrid system assays were proposed (Fields *et al.,* 1989), of which the bacterial ToxR-based two-hybrid system was more specifically developed to investigate direct interactions between heterologous transmembrane segments (Hennecke *et al.,* 2005; DiRita *et al.,* 1992; Sobhanifar *et al.,* 2003). A split-ubiquitin yeast two-hybrid system was also proposed to investigate the interaction between membrane proteins (Stagljar *et al.,* 1998).

3.4. No evidence for trimer formation

RMRs could also form trimers. In order to investigate the possible formation of a trimer I coexpressed the three fusion proteins ΔRSAtRMR1-nYFP, ΔRSAtRMR1-cYFP and ΔRingAtRMR2-RFP. In the cells expressing the three fusion proteins I observed a clear BiFC signal indicating an efficient homodimer formation by the two ΔRSAtRMR1. In contrast I did not observe any localization change for ΔRingAtRMR2 indicating that most of this protein remained unpaired and in the ER membrane. Firstly this result indicates that no trimer formation occurred. Secondly it suggests that the homodimer formation by ΔRSAtRMR1 is more efficient than the association between ΔRSAtRMR1 and ΔRingAtRMR2. I had shown before that AtRMR2 could not leave the ER because it lacked an ER exit signal present in the linker of AtRMR1. Therefore ΔRingAtRMR2 can only exit from the ER as part of a heterodimer with ΔRSAtRMR1.

This experiment does not preclude the existence of a dynamic equilibrium between homo- and heterodimers. The BiFC does not allow to visualize this dynamics because the two YFP halves stably bind, preventing the dissociation of the homodimer. Thus most ΔRSAtRMR1-nYFP and -cYFP forms stable homodimers leaving ΔRingAtRMR2 alone. In contrast during of co-expression

of AtRMR1-RFP and AtRMR2-YFP I observed a clear change in AtRMR2 localization to AtRMR1-labelled punctate structures. This result supports the existence of a mixture of homo- and heterodimers.

It is well possible that a dynamic association and dissociation between monomeric and homo/heterodimeric AtRMR1 and AtRMR2 forms play a physiological role in plant cells. These interactions would occur at an early stage of vacuolar trafficking, i.e. directly in the ER membrane. The dimers could bind the vacuolar proteins leading to the formation of the cargo/receptor complex, which would then be exported from the ER to the TGN. Moreover the homo- and heterodimers could have different cargo specificities. In figure 62 is represented a possible model of AtRMR1 and 2 traffic and dimerization.

A similar role for receptor dimerization was reported recently for AtVSR1 in the trafficking of vacuolar proteins. Reportedly both, transmembrane domain and small cytosolic tail were apparently involved in this homodimerization (Kim *et al.,* 2010). Therefore it is possible that AtRMRs work in a similar manner in the route to PSV of certain vacuolar proteins.

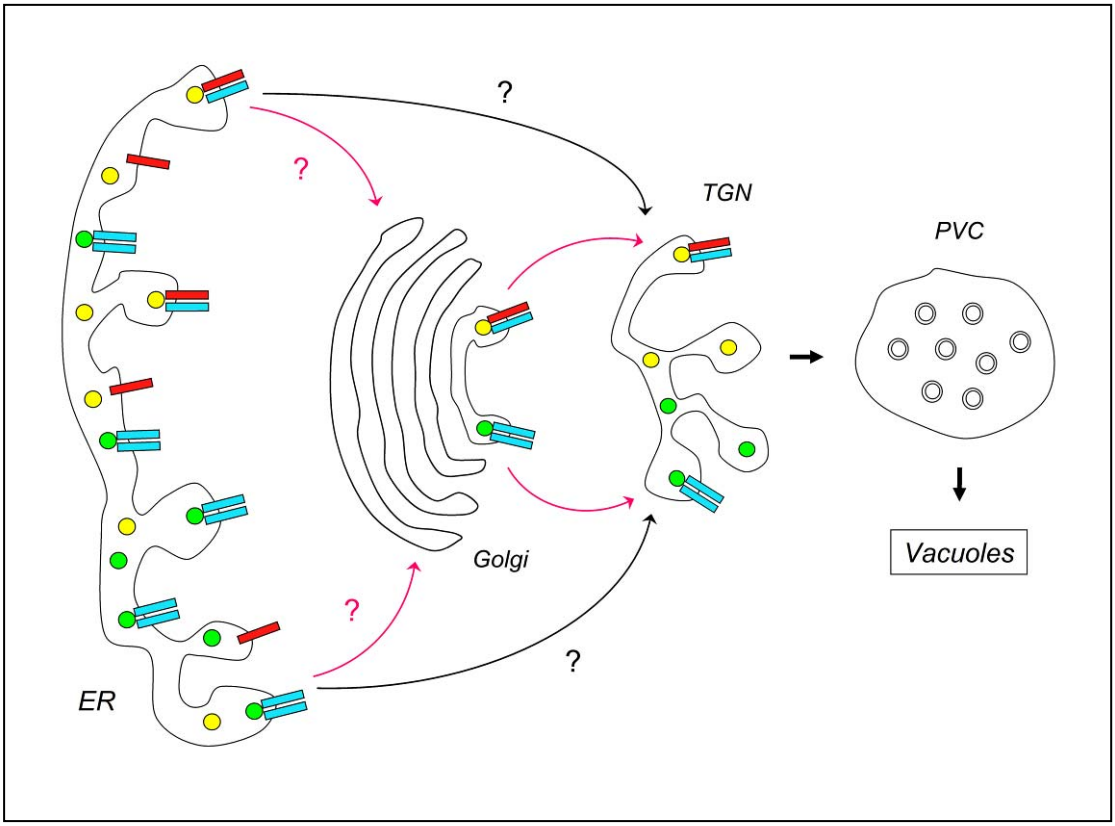

Figure 62: Proposed model of AtRMR1 and 2 traffic and dimerization. AtRMR1 (cyan) and AtRMR2 (red) interact in the membrane of ER. A group of AtRMR1 homodimers and AtRMR1/AtRMR2 heterodimers could coexist in the same cell. In the next step the dimers bind specific vacuolar proteins leading to the formation of complexes cargo/receptor. Green and yellow circles represent two different cargo proteins. Homo- and heterodimers could possess different specificities cargo. AtRMR1 homodimers are more stable and consequently the amount of homodimers is higher than heterodimers. The putative localization signal present in the sequence linker of AtRMR1 is involved in protein localization in the TGN. Two different pathways (indicated with ?) could lead the dimers to TGN: the first one passing by the Golgi (rose arrows); and the second one bypassing the Golgi (black arrows). ER (endoplasmic reticulum); Golgi (Golgi apparatus); TGN (trans-Golgi network); PVC (prevacuolar compartment); vacuoles.

4. *In vivo* cross linking of AtRMR1

The preliminary cross-linking results suggest that AtRMR1 is associated to unknown proteins which are probably protein partners, members of a complex. On the blot we could detect three major bands at higher molecular weight than the endogenous AtRMR1 (47.5 kDa): at 80 kDa, at approx. 140 kDa and around 175 kDa. All these bands could be cross-linking products between AtRMR1 and very closely associated protein partners. Paraformaldehyde has a short cross-linking span and can only really close partners (Vasilescu *et al.,* 2004). The largest band at 175 kDa is probably a big protein aggregate which was not resolved properly in this gel. The experiment should be repeated using a gel with a lower acrylamide concentration, in order to better resolve such high molecular weight complexes. Repeating the experiment with alternative short or long arm cross-linking reagents would also be informative. We also detected a low molecular weight doublet (32.5 kDa). These bands could be considered contaminant proteins specifically recognized by the antibody. In this case in order to test the antibody specificity we should performed a Western blot using a total protein extract from *A.thaliana* ko for AtRMR1. Alternatively the doublet could represent proteolytically processed forms of AtRMR1. Indeed the homologous animal membrane protein RNF13, a Ring finger ubiquitin ligase undergoes a process of proteolytic maturation resulting in the releasing of the Ring finger domain in the cytosol, where it catalyzes the ubiquitination of cytosolic target proteins (Bocock *et al.,* 2009).

The next step of this experiment will be complex purification after membrane solubilisation and total protein extraction. Immuno-affinity purification on a column is usually the best approach. In the last step, after protein elution and cross-linking reversion the individual complex components are separated by SDS-PAGE and identified using MS (mass spectrometry) (Vasilescu *et al.,* 2004).

We will then obtain a list of potential interacting proteins which will have to be confirmed using different techniques such as BiFC, FRET or two hybrid systems.

Outlooks

In the present work I have demonstrated that AtRMR1 and AtRMR2 have a different subcellular localization. AtRMR1, according to its proposed role in vacuolar sorting, localizes in the TGN while AtRMR2 localizes in the ER. I have also demonstrated that the sequence linker of AtRMR1 represents a putative signal involved in TGN localization. Indeed the linker of AtRMR1, when replacing the linker of AtRMR2, is able to relocate this protein to the TGN.
I have also demonstrated by BiFC and coexpression that AtRMR1 can make homodimers and can interact with AtRMR2 making heterodimers. This AtRMR1/AtRMR2 heterodimer localizes in the TGN like the AtRMR1 homodimer, demonstrating that AtRMR2 can exit from the ER with the help of the putative localization determinant in linker 1. Moreover the experiments performed using AtRMR deletion mutants support our hypothesis that the transmembrane and linker domains of AtRMRs are the domains involved in the dimerization process.

A next step will be to confirm the positive BiFC reaction between different AtRMRs by Western blot. For this purpose agroinfiltrated *N.benthamiana* leaves transformed with the two constructs for BiFC will be treated with a short-arm cross-linking reagent. This step is necessary to covalently fix the interacting proteins in order to visualize the dimer under denaturing conditions. After total protein extraction, the dimers can be easily visualized by the different molecular weight on Western blot. Moreover the presence of the two interacting AtRMRs in the band of interest can be proven using two different antibodies: an anti-HA direct to AtRMRx-nYFP fusion proteins and an anti-Myc direct to AtRMRx-cYFP fusion proteins. The possibility to reverse the cross-linking reaction and the consequent dissociation of the dimer will allow us to confirm the AtRMR interaction.

AtRMR receptors are characterized by the presence of a PA and a Ring-H2 domains which are both potential protein interaction domains (Lawrence *et al.*, 1999; Mahon *et al.*, 2000; Xinmei *et al.*, 2001; d'Azzo *et al.*, 2005). In order to describe the function of PA and Ring-H2 domains we performed cross-linking experiments. These preliminary results suggest that AtRMR1 is associated to unknown proteins, probably partners in a complex. In the next step we need to purify these putative complexes after membrane solubilisation and total protein extraction. The immuno-precipitation or the immuno-affinity purification on a column is usually the best approaches. For this purpose a good antibody able to recognize the native protein will be necessary. In the last step, after protein elution and cross-linking reversion the individual complex components are separated

by SDS-PAGE and identified using MS (mass spectrometry) (Vasilescu *et al.*, 2004). All these experiments should be directed to the native protein using wild type *A.thaliana*. Indeed a tagged AtRMR1 is not detectable in stably transformed *A.thaliana* lines generated in the laboratory.

Further experiments have to test for dimerization of AtRMRs by BiFC in the presence of Brefeldine A (BFA) a lactone antibiotic which is able to disorganize Golgi cisternae causing their fusion with the ER to form a hybrid compartment. In fact this compound inhibits the COPI vesicle formation at the Golgi apparatus blocking the traffic ER/Golgi traffic. Using BFA we should obtain important information about the traffic of AtRMR dimers. Indeed a normal TGN localization of dimers in the presence of BFA would demonstrate a direct ER/TGN trafficking. On the contrary dimer accumulation in the membrane of the ER/Golgi hybrid compartment would support a normal ER/Golgi/TGN traffic. In this second case a positive BiFC at the ER/Golgi hybrid compartment will support the ability of AtRMRs to make dimers at an early stage of secretory pathway.

Another important point is that the association and dissociation of AtRMRs to form homo- and heterodimeric forms could play a specific physiological role in plant cells. It is likely that the main function of dimers is to bind the vacuolar proteins leading to the formation of the cargo/receptor complexes. Then this complex could be exported from the ER to the TGN. Consequently one possible role of homo- and heterodimers could be to bind different kinds of vacuolar cargoes. In order to support this hypothesis different combination of AtRMRx BiFC constructs could be coexpressed with different putative cargoes. These experiments would allow visualizing at the same time the dimer formation and the interaction with the putative cargo upon colocalization.

The experiments of BiFC and the colocalization using AtRMR deletion mutants suggest that the transmembrane domains and linker sequences are the domains involved in AtRMR dimerization. Indeed the transmembrane domains of AtRMR1 and 2 contain several threonines and serines which could constitute a motif (SxxS) involved in dimerization. In order to support this hypothesis a direct association between the transmembrane domains and linker sequences should be proven by BiFC. For this purpose new constructs coding only for AtRMR transmembrane domains and linker sequences fused to the two YFP halves should be produced. Alternatively several bacterial and yeast two-hybrid systems can be used to prove direct association between single protein domains. For instance a bacterial ToxR-based two-hybrid system or a split-ubiquitin yeast two-hybrid system can be used (Hennecke *et al.*, 2005; DiRita *et al.*, 1992; Sobhanifar *et al.*, 2003; Stagljar *et al.*, 1998). If a direct association between these domains will be proven, a series of point mutation could

be directed on single residues in order to determine their role in the interaction. In fact a series of point mutation could be directed on serine and threonine residues present in the two transmembrane domains.

Materials and Methods

1. MICROBIOLOGY TECHNIQUES

1.1. Bacterial strains

Escherichia coli XL-1 Blue: *rec*A1, *end*A1, *gyr*A96, *thi*-1 *hsd*R17 (rk-, mk+), *sup*E44, *rel*A1, λ-, *lac*-.

Agrobacterium tumefaciens strain GV3101.

1.2. Medium and bacteria growth conditions

E.coli and *A.tumefaciens* were grown in LB medium [0.5% NaCl; 0.5% (w/v) yeast extract; 1% (w/v) bacto-tryptone in H_2O] for liquid culture. *E.coli* was grown at 37°C shaking at 200 rpm whereas *A.tumefaciens* was grown at 28°C shaking at 150 rpm. For *in vitro* culture, LB agar [LB medium plus 1.6% Agar] was used. Specific antibiotics were added in the medium in order to select bacteria carrying specific plasmids.

1.3. Preparation of heat-shock competent *E.coli* cells

5 ml of selective LB medium (25 μg/ml tetracycline) was inoculated with a single *E.coli* colony and then incubated at 37 °C overnight under shaking. The day after this pre-culture was diluted in 500 ml of fresh liquid LB medium and incubated at 37 °C under shaking. The culture was grown until the OD_{600} reached 0.5 which represent the exponential phase of bacterial growing. The cells were then put on ice and recuperated by centrifugation at 5000 g for 15 minutes at 4 °C. From this step the cells were kept cold throughout the preparation. The bacterial pellet was resuspended in 32 ml of RF1 buffer (100 mM KCl; 30 mM $MnCl_2$; 30 mM K-acetate pH 7.5; 10 mM $CaCl_2$; 15% glycerol; pH 5.8 adjusted with acetic acid) and then left for 20 minutes on ice. The cells were recuperated by centrifugation at 5000 g for 15 minutes at 4 °C and the resulting pellet was resuspended in 8 ml of RF2 buffer (10 mM MOPS pH 6.8; 10 mM KCl; 50 mM $CaCl_2$; 15% glycerol; pH 6.8 adjusted with NaOH). The competent bacteria suspension was incubated for 20 minutes on ice. Finally, 100 μl aliquots were made and then frozen in liquid nitrogen. The tubes were stored at -80 °C.

1.4. Transformation of *E.coli* by heat-shock

Competent *E.coli* cells were thawed on ice and then placed on pre-cooled 1.5 ml Eppendorf tube containing 1 ng of purified plasmid or 10 µl of ligation mixture. The cells were incubated for 5 minutes on ice. Immediately after, they were incubated for 90 seconds at 42 °C and again on ice for 5 minutes. 1 ml of liquid LB-medium without antibiotics was added and then incubated for 1 hour at 37 °C under shaking. Finally, the bacterial culture was plated on a *petri* dish containing selective LB-medium and grown at 37 °C overnight.

1.5. Preparation of electroporation competent *A.tumefaciens* cells

500 ml of selective LB liquid-medium (LB medium; 50 µg/ml rifampicin) were inoculated with 5 ml of fresh overnight culture of *A.tumefaciens*. The cells were grown at 28 °C to an OD_{600} ~ 0.6 which represent the exponential phase of bacterial growing. The bacteria culture was then centrifuged at 4000 g for 15 minutes at 4 °C. From this step the cells were kept cold on ice throughout all steps of the preparation. The cells were washed three times in glycerol solution (10% glycerol in water). At the last wash the cells were resuspended using 1 ml of glycerol solution for each 100 ml of starting culture. Aliquots of 60 µl were made and then they were frozen on dry ice. Finally the aliquots were stored at -80 °C.

1.6. Transformation of *A.tumefaciens* by electroporation

Competent *A.tumefaciens* cells were thawed on ice and then poured on pre-cooled 1.5 ml Eppendorf tube containing 100 ng of plasmid. Bacterial cells were transferred to a chilled electroporation cuvette on ice (1 mm electroporation cuvette Eurogentec) and then transformed using an electroporator (BioRad). The electroporation machine was set at 2 kV of charging voltage. A pulse length about 5 ms indicated a good cell transformation. After transformation, 1 ml of fresh LB liquid-medium (without antibiotics) was added and then the cells were incubated for 1 hour at 28 °C. Finally 1/10 of transformed cells were plated on a *petri* dish containing selective LB agar-medium and incubated at 28 °C for 2 days.

2. PLANT MATERIAL AND PLANT TRASFORMATION TECHNIQUES

2.1. *Arabidopsis thaliana* and *Nicotiana benthamiana* lines

A.thaliana ecotype Columbia-0 was used: to produce transgenic lines expressing AtRMR2-YFP and AtRMR1-YFP; and to isolate protoplasts from leaves.

N.benthamiana was used for leaf transformation by agro-infiltration.

2.2. Growth condition

A.thaliana and *N.benthamiana* plants were grown in the same growth chamber (Mobylux GroBanks) under the same growth conditions. The light intensity was 120 $\mu E/m^2 \cdot s$ using a photoperiod of 16 hours of light and 8 hours of darkness for long day and 8 hours of light and 16 hours of darkness for short day. The humidity (RH) was 65% and the temperature was 22 °C for the day and 18 °C for the night.

2.3. Soils and mediums of growth

In vitro A.thaliana plants were grown in solid Murashige & Skoog (MS) medium [Murashige & Skoog (DUCHEFA) 4.47 g/l; sucrose 20 g/l; Phytagel (SIGMA) 8 g/l; pH 5.6].

A.thaliana and *N.benthamiana* plants grown under no-sterile conditions were grown on normal soil (RICOTER) containing: 45% sand; 10% perlite; 25% compost; 20% peat.

2.4 Seeds sterilization

An appropriate volume of seeds (~ 100 µl) was putted into a 1.5 ml Eppendorf tube. The seeds were incubated with 1 ml of sterilization solution (2% bleach and 0.005 % Triton X-100 in 100% ethanol). The seeds were then agitated for 10 minutes using a bench top shaker. The solution was removed and the seeds were washed several times with ethanol 100% in order to remove the sterilization solution. Finally, the seeds were dried in the hood and than plated on sterile *petri* dishes containing solid MS medium.

2.5 Preparation of *A.thaliana* leaf protoplasts and PEG-mediated transformation

A.thaliana plants (3-4 weeks hold) grown in sterile *petri* dishes under long day condition were used. Plant rosettes were cut and putted in sterile *petri* dishes containing 12 ml of digestion solution [mannitol 400 mM; MES 5 mM; $CaCl_2$ 8 mM; cellulase Onozuka R-10 (SERVA) 1% w/v; macerozyme R-10 (SERVA) 0,25% w/v; pH 5.6] per plate. The plants were then incubated over

night in the darkness at room temperature. The days after protoplasts were released by carefully shaking. The macerate was then filtered on 100 μm mesh filter in order to eliminate leaf debris. The filtrate was poured in 15 ml falcon tubes using a plastic Pasteur and protoplasts were recuperated by centrifugation for 5 minutes at 50 g (brake off) at room temperature. Protoplasts precipitate in the pellet whereas debris stays in the supernatant. After removing of supernatant, the protoplasts were washed three times in W5 solution (NaCl 154 mM; $CaCl_2$ 125 mM; KCl 5 mM; glucose 5 mM; MES 1.5 mM; pH 5.6). 2-3 ml of protoplasts were poured on 6 ml of 21% sucrose and than centrifuged for 10 minutes at 50 g (brake off) at room temperature. At this step, the living protoplasts are in the interface between sucrose and W5, whereas broken protoplasts precipitate in the tube. Living protoplasts were then recuperated by centrifugation for 5 minutes at 50 g (brake off) at room temperature. After that, the protoplasts were washed three times in W5 and then incubated for 30 minutes on ice. Intact round shaped protoplasts were counted using a Burker chamber. Finally, the protoplasts were recuperated by centrifugation and resuspended in an appropriate volume of MaMg (mannitol 0.4 M; $MgCl_2$ 15 mM; MES 0.5 M; pH 5.6) in order to have 1.5 x 10^6 of protoplasts per 300 μl of solution.

For PEG-mediated transformation 25 μg of plasmid and 50 μg of carrier DNA were added to 300 μl of protoplasts and gently mixed. Immediately after, 325 μl of PEG solution [PEG 4000 (Fluka) 40% w/v; mannitol 0.4 M; $Ca(NO_3)_2$ 0.1 M; pH 7-8] were gently added and mixed. The protoplasts were then incubated for 30 minutes a room temperature. 10 ml of W5 solution were gently added mixing the tube from time to time. The protoplasts were then recuperated by centrifugation (as previously) and the supernatant was discarded. Finally, the protoplasts were resuspended in 5 ml of W5 solution and incubated over night in the darkness at room temperature.

2.6 Agro-infiltration of *N.benthamiana* leaves

A.tumefaciens (carrying the construct of interest) was plate on *petri* dishes containing selective LB medium-agar (50 μg/ml kanamycin; 50 μg/ml rifampicin). A single bacterial colony was inoculated in 5 ml of selective LB medium-liquid (LB medium without agar) and incubated at 28 °C over night under shaking. The day after 1 ml of pre-culture was inoculated in 50 ml of fresh selective LB medium-liquid and incubated at 28 °C for 10 hours under shaking. Then 10 ml of each culture were centrifuged at 5000 g for 10 minutes at room temperature and the bacterial pellet was washed three times adding 10 ml of agro-infiltration buffer (50 mM MES; 2 mM Na_3PO_4; 0.5% glucose; pH 5.6). After the last wash the bacterial pellet was resuspended in agro-infiltration buffer containing 100 μM acetosiringone to an optical density (OD_{600}) of 1. The bacterial cells were incubated for 1 hour

at room temperature in the darkness and then infiltrated into 2-4 week-old *N.benthamiana* leaves. Finally the infiltrated plants were put in a grow chamber and left in the darkness over night.

2.7. Floral-dip of *A.thaliana* plants

A single *A.tumefaciens* colony (carrying the construct of interest) grown on selective LB medium was inoculated in 5 ml of fresh liquid medium containing the same antibiotics. The pre-culture was incubated at 28 °C over night under shaking. The day after 3 ml of pre-culture were inoculated in 300 ml of fresh liquid medium and grown to the stationary phase (OD_{600} ~ 2). The cells were then recuperated by centrifuging at 5000 g for 20 minutes at room temperature. The bacterial pellet was resuspended in infiltration medium (5% sucrose; 0,05% Silwett L-77; 100 μM acetosiringone) to an OD_{600} ~ 1 and then incubated for 1 hour in the darkness at room temperature. The culture was used for dipping of *A.thaliana* plants with inflorescences of 5 cm. The floral-dip was performed for 5 second under agitation. The infiltrated plants were then kept in plastic bags and left over night in the darkness at room temperature. The plants were grown in grow chamber until siliques maturation. Then seeds were collected, sterilized and plated on MS medium containing 5 μg/ml BASTA in order to select positive transformants.

2.8. Treatment with cross-linking agents

Several paraformaldehyde (PFA) concentrations, incubation times and temperatures were tested in order to optimize the protocol for plants. The optimization of the protocol was necessary to guarantee an efficient cross-linking reaction but avoiding over-fixation of the tissue.

Plant tissue (seedlings or leaf tissue) was incubated with 1% PFA in PBS 1X. The cross-linking reaction was performed at 18°C and 37°C for 30 minutes. Then the cross-linking reaction was stopped adding 125 mM glycine. All the residues of PFA were eliminated washing several times in 1X PBS. Finally the plant tissue was used for total protein extraction (see below).

The PFA cross-linking reaction is reversible by heating the sample at 100°C for 20 minutes.

3. MOLECULAR BIOLOGY

3.1. PCR

A PCR reaction was performed combining the following components in a nuclease-free micro-centrifuge tube: buffer (final concentration 1X); 0.2 mM for each dNTP; 0.1-1 μM of forward primer; 0.1-1 μM of reverse primer; 1.25 u of DNA polymerase (Promega); 100-500 ng of DNA template; H_2O to a final volume of 50 μl. The reaction was performed in a thermal cycling machine (Biometra).

3.2. DNA digestion

A restriction enzyme digestion was performed assembling the following components in a 1.5 ml sterile Eppendorf tube: 0.2-1.5 μg of substrate DNA; restriction buffer (final concentration 1X); BSA (final concentration 0.1 μg/μl); 5 u of restriction enzyme (Promega); H_2O to a final volume of 20 μl. The reaction was performed for 1-4 hours at 37°C.

3.3. DNA ligase

A DNA ligase reaction was performed mixing the following components in a 1.5 ml sterile Eppendorf tube: 100 ng of vector DNA; 17 ng of insert DNA; 10X ligation buffer (final concentration 1X); 0.1-1 u of T4 DNA ligase (Promega); and H_2O to a final volume of 10 μl. The reaction was performed overnight at 4°C or for few hours at 14°C.

3.4. Total RNA extraction from *A.thaliana* leaves

0.25 g of *A.thaliana* leaves were collected and immediately frozen in liquid nitrogen. The tissue was then grinded in liquid nitrogen using pre-cooled mortal and pestle. The tissue was transferred in a 2 ml Eppendorf tube (RNase free) pre-cooled in liquid nitrogen. Immediately after, 500 μl of plant RNA purification reagent (Invitrogen) were added. The tissue was resuspended by mixing using a vortex and then incubated for 5 minutes at room temperature. The tube was centrifuged for 2 minutes at 15.000 g in order to eliminate cell debris. The supernatant was then transferred in a new Eppendorf tube (RNase free). 100 μl of 5M NaCl were added and then the tube was gently mixed. 300 μl of chloroforme were added and the tube was mixed 3 – 4 times inverting the tube. The tube was then centrifuged at 15.000 g for 10 minutes at 4°C. The aqueous phase was transferred in a new Eppendorf tube (RNase free) and then one volume of isopropanol was added. The tube was incubated for 10 minutes at room temperature and then centrifuged at 15.000 g for 30 minutes at 4°C. The supernatant was discarded and the pellet was washed one time with ethanol 75%. The

pellet was then resuspended in an appropriate volume of H_2O RNase free. Finally the total RNA was treated with DNase (Promega) in order to eliminate contaminant genomic DNA and then quantified using a Nano-Drop spectrophotometer.

3.5. cDNA synthesis

1 µg of total RNA extract was transferred in a 1.5 ml Eppendorf tube (RNase free). Then, 1 µl of primer oligo-dT and 1 µl of 10 mM dNTP were added. The volume was adjusted to 11 µl using and adequate volume of H_2O RNase free. The tube was incubated at 70°C for 5 minutes and then for 1 minute on ice. After, 12 µl of mix [5 µl of 5X transcriptase buffer; 1 µl of 0.1 M DTT; 0.5 µl of SuperScript III RT (Promega); 5.5 µl of H_2O RNase free] was added in the tube. The reaction of reverse transcriptase was performed at 50°C for 1 hour. Finally the tube was incubated for 15 minutes at 70°C in order to inactivate the reverse transcriptase and then immediately transferred on ice. The single strand cDNA was used to amplify AtRMR genes using specific pairs of primers.

3.6. Genomic DNA extraction from *A.thaliana* leaves

The top of an Eppendorf tube was used to collect *A.thaliana* leaf tissue. The tissue was broken using a small pestle and then 400 µl of extraction buffer (200 mM Tris-HCl pH 7.5; 250 mM NaCl; 25 mM EDTA; 0.5% SDS) were added. The tube was mixed for 5 minutes using a vortex and then centrifuged for 5 minutes at 15.000 g in order to eliminate cell debris. 300 µl of supernatant were mixed with an equal volume of isopropanol. The tube was incubated at room temperature for 10 minutes and then centrifuged for 30 minutes at 15.000 g. The DNA pellet was washed one time with 75% ethanol. Finally the DNA was resuspended in an adequate volume of sterile H_2O and then quantified using a Nano-Drop spectrophotometer.

3.7. DNA precipitation

1/10 of the volume of sodium acetate (NaOAc) and 2 volume of ethanol were added to DNA samples. The samples were incubated at – 80°C for few minutes in order to precipitate the DNA. They were centrifuged for 30 minutes at 4°C and then DNA pellets were washed one time with ethanol 70%. Finally, the samples were dried and then resuspended in an adequate volume of sterile H_2O.

3.8. DNA extraction from agarose gel

The DNA extraction from agarose gel was performed using the Wizard SV Gel and PCR Clean-Up system (Promega) as indicated in the protocol.

3.9. DNA purification by phenol/chloroform

1/10 of the volume of 3M sodium acetate (NaOAc) pH 7 was added and then the sample was gently mixed. 1 volume of phenol/chloroform was added and again the sample was gently mixed inverting the tube. The tube was then centrifuged for 5 minutes at 15.000 g. The upper aqueous phase containing DNA was transferred in a new Eppendorf tube. 1 volume of chloroform was added and then the tube was mixed for 30 seconds with a vortex. The sample was centrifuged for 1 minute at 15.000 g. The upper aqueous phase was then transferred in a new Eppendorf tube. 3 volume of ether were added and gently mixed. Then the lower aqueous phase containing DNA was collected in a new Eppendorf tube. Two volumes of 100% ethanol were added and the sample was then incubated on ice for 10 minutes. The sample was centrifuged for 40 minutes at 15.000 g and then the DNA pellet was washed one time with 70% ethanol. Finally the pellet was dried and resuspended in an adequate volume of sterile H_2O.

3.10. Isolation of plasmid DNA from *E.coli* in a small-scale

A single bacterial colony was inoculated into 5 ml of LB medium containing a specific antibiotic. The culture was then incubated overnight at 37°C with shaking (250 rpm). The day after 1.5 ml of culture was centrifuged at 20.000 g in order to pull down bacterial cells. The pellet was resuspended in 150 µl of resuspension buffer P1 (50 mM Tris-HCl pH 8; 10 mM EDTA; 100 mg/ml RNasi). After, 150 µl of lysis buffer P2 (200 mM NaOH; 1% SDS) were added and then the sample was gently mixed for few times. The samples was incubated for 5 minutes at room temperature and then 150 µl of equilibration buffer P3 (3M NaOAc pH 5.5) were added. The samples was gently mixed and incubated for few minutes on ice. The samples were then centrifuged for 15 minutes at 20.000 g in order to precipitate bacterial lysate. The supernatant containing plasmids was transferred in a new Eppendorf tube and then 0.7 volumes of isopropanol were added. The tube was centrifuged at 20.000 g for 30 minutes. The DNA pellet was then washed one time with 70% ethanol. Finally the pellet was dried and resuspended in an adequate volume of sterile H_2O.

Isolation of plasmid DNA for sequencing was performed using the NucleoSpin plasmid kit (MACHEREY-NAGEL) as indicated in the protocol.

3.11. Isolation of plasmid DNA from *E.coli* in a big-scale

Isolation of plasmid DNA in a big-scale was performed using the NucleoBond Xtra Midi Plus kit (MACHEREY-NAGEL) as indicated in the protocol.

3.12. DNA electrophoresis

The DNA electrophoresis was performed using an apparatus Bio-Rad. Agarose gels were prepared adding 0.7-2.5% of agarose (depending on the size of DNA fragment) in 0.5X TBE and using ethidium bromide as a DNA staining. The DNA samples, in a small gel, were separated at 90-95 V whereas the DNA samples, in a big gel, were separated at 120 V. The DNA was visualized under the UV light using a GEL DOC system from Bio-Rad.

4. PROTEIN TECHNIQUES

4.1. Protein extraction from leaves

200 mg of leaf tissue were collected and immediately frozen in liquid nitrogen. Then the tissue was grinded using mortal and pestle and using quartz sand in order to help the grinding. Polyvinylpolypyrrolidone (PVPP) was added to preserve and guarantee a good quality of the leaf extract. After grinding, 400 µl of extraction buffer [500 mM Tris-HCl pH 7.5; 200 mM NaCl; 1X complete (Roche)] was added. The leaf extract was transferred in 2 ml Eppendorf tube and then centrifuged at 15.000 g for 5 minutes at 4 °C. This step of centrifugation was required in order to eliminate leaf debris, chloroplasts and plasma membranes. The supernatant was transferred in a new 2 ml Eppendorf tube. Then the total protein contents were estimated using the method of Bradford.

4.2. Protein precipitation by chloroform/methanol

240 µl of methanol (MeOH) and 80 µl of chloroform ($CHCl_3$) were added to 100 µl of protein sample. The sample was mixed vigorously with a vortex and then 320 µl of H_2O were added. The sample was mixed again inverting the tube and then incubated for 1 minute at room temperature. The interphase containing proteins was collected in a new Eppendorf tube. 240 µl of MeOH were added and then centrifuged for 5 minutes at maximum speed. Finally the protein pellet was dried by air and then resuspended in an adequate volume of SB buffer (see below).

4.3. SDS-PAGE

The SDS-Page was made using a Mini Protean III apparatus (Bio-Rad). A discontinuous gel composed of a stacking and running gels was made. The running and stacking gels were composed respectively of 15% and 4.5% acrylamide/bisacrylamide mix (see below). The gels were then immerged in 1X Tris-glycine electrophoresis buffer [25 mM Tris; 250 mM glycine pH 8.3; 0.1%

(w/v) SDS]. For each lanes 100 μg of total protein extract in 1X SB buffer [50 mM Tris-HCl pH 6.8; 100 mM dithiothreitol (DTT); 2% (w/v) SDS; 0.1% bromophenol blue; 10% (v/v) glycerol] were loaded. Before loading, the samples were boiled for 5 minutes at 100°C in order to denature proteins. Finally the electrophoresis was performed at constant voltage (100 V) until the blue dye reached the bottom of the gel.

Running gel (15%)

H_2O	3.4 ml
30% acrylamide/bisacrylamide mix	4 ml
1.5 M Tris-HCl pH 8.8	2.5 ml
10% ammonium persulfate (APS)	100 μl
TEMED	4 μl

Stacking gel (4.5%)

H_2O	3.15 ml
30% acrylamide/bisacrylamide mix	0.83 ml
0.5 M Tris-HCl pH 6.8	1.26 ml
10% ammonium persulfate (APS)	50 μl
TEMED	5 μl

4.4. Western Blot

After SDS-PAGE the proteins were transferred to a membrane (Immobilon-PSQ 0.2 μm MILLIPORE) using a Mini Protean III system (Bio-Rad). Before blotting, the membrane was activated by soaking in 95% ethanol for 10 minutes. Then the sandwich was assembled (sponge, filter paper, gel, membrane, filter paper, sponge) starting from the black side of cassette (anode) to the white side (cathode). Finally the sandwich was immerged in the cassette containing 1X blotting buffer (25 mM Tris; 192 mM glycine). The transfer was performed at constant voltage (20 V) for 4 – 5 hours at 4°C.

The transfer membrane was then incubated for 1 hour at room temperature in blocking buffer (1X PBS; 5% skimmed milk). This step is necessary to block unspecific antibody-binding sites. The membrane was incubated for 1 hour at room temperature in buffer containing a specific primary antibody (1X PBS; 5% skimmed milk; 0.2% Tween-20; primary antibody diluted 1:5.000). The membrane was then washed 3 times for 15 minutes in washing solution (1X PBS; 0.2% Tween-20).

After the last wash the membrane was incubated for 1 hour at room temperature in buffer containing a secondary antibody (1X PBS; 5% skimmed milk; 0.2% Tween-20; secondary antibody diluted 1:20.000). Then the membrane was washed 3 times in washing solution for 15 minutes. Finally the secondary antibody was revealed using the ECL plus detection kit (GE Healthcare). The chemiluminescent reaction product by HRP-coupled secondary antibody was detected by a Chemidoc XRS System (BioRad).

4.5. Membrane Stripping

In order to dissociate the complex antibodies/investigated protein, a Western blot membrane was incubated with 50 ml of stripping buffer (50 mM Tris-HCl pH 6.8; 2% SDS; 100 mM β-mercaptoethanol). The incubation was performed in a water bath heated at 50°C for 30 minutes. Then the membrane was washed several times with 1X PBS until all β-mercaptoethanol residues were removed. Finally, the membrane was ready for another cycle of immuno-blotting.

5. MICROSCOPY

5.1. Transmission electro microscopy (TEM)

We used a JEM 1400 transmission electron microscope (JEOL) operating at 80 kV.

5.1.1. Preparation of the samples

6-old root tips from *A.thaliana* grown in sterile condition were used as biological samples. Root tips were excised using a scalpel. From 5 to 6 root tips were placed in a planchette (1 mm of thickness) containing Tris-buffer pH 6.6. A second planchette was used to cover the first one containing root tips. Then the planchette was frozen in a high-pressure freezer (HPF010; Bal-Tec). Then the planchette was maintained in liquid nitrogen in order to preserve the quality of the tissue.

The second step of freeze substitution was performed in a freeze substitution unit Leica AFS. The planchette containing root tips was submerged in the pre-cooled substitution solution at -85°C (dry acetone supplemented with 10% methanol and 0.3% uranyl acetate). The substitution was performed at -85°C for 16 hours and then the temperature was gradually increased up to -50°C for almost 5 hours. This procedure allows substituting the cellular liquid phase with the substitution solution. Then, the substitution solution was removed and the sample was infiltrated in resin Lowicryl HM20 (Polysciences). This resin works at an optimal temperature of -50°C. For this step, the root tips were incubated at increasing concentration of HM20 (30%, 50%, 75%, 100%) in 100%

ethanol. Each incubation was performed for 1 hour at -50°C, which is the optimal temperature for this kind of resin. After the last incubation step, the roots tips were placed in small containers containing resin. Finally the polymerization was performed for two days using an UV lamp. The polymerization was proceeding until the temperature arrived above 0°C. An additional polymerization at room temperature is necessary to increase the hardness of the resin.

5.1.2. Immunogold

Included root tip samples were used to prepare thin sections using a microtome. Sections were then placed on a particular grid covered with a plastic film (formavar) and dried for few minutes at room temperature. After, the grid was incubated for 1 hour at room temperature in blocking solution (3% BSA in PBS) in order to block all unspecific antibody-binding sites. The grid was then incubated for 1 hour at room temperature in buffer containing a specific primary antibody (1% BSA in PBS containing primary antibody). Several dilutions of primary antibody anti-GFP were tested, finding an optimal dilution of 1:400. The grid was washed three times with washing solution (1% BSA in PBS) for 10 minutes at room temperature. The grid was then incubated for 1 hour at room temperature in buffer containing a specific secondary antibody (1% BSA in PBS containing secondary antibody). A secondary antibody conjugated with gold particles of 10 nm (BioCell GAR10) was used at a dilution of 1:50. The grid was washed two times with washing solution (1% BSA in PBS) for 5 minutes at room temperature. Then the grid was washed three times with bi-distillate water for 5 minutes at room temperature. Finally the grid was dried using a filter paper.

5.1.3. Post-staining with uranyl acetate/lead citrate

The post staining is necessary to improve the contrast of section for an adequate observation of ultrastructural structures with the TEM. The grid was incubated 1 minute in uranyl acetate solution [2% (w/v) uranyl acetate in bi-distillate water]. The grid was washed 3 times in bi-distillate water in order to eliminate all residues of uranyl acetate solution. Then the grid was incubated for 1 minute in lead citrate solution. The grid was washed 2 times in bi-distillate water. The last wash was vigorously using a pipette. Finally the grid was dried using filter paper and analyzed using a transmission electron microscope.

5.2. Confocal microscopy

Images were collected with a TCS SP5 II confocal laser scanning microscope (Leica). Digital images were acquired using LAS AF (version: 2.0.0 build 1934) and processed using ImageJ 1.41o (National Institute of Health, USA).

6. PLASMIDS AND CONSTRUCTS

For the design of plasmids, see also Annexes II, III, IV, and V.

6.1. Empty vectors and vectors for N- and C-terminal fusion with different fluorescent reporter

The binary vector pGREEN0229/pSOUP was used for plant transformation via *Agrobacterium tumefaciens*.

pGREEN0229 containing:

pSa-ORI: *Agrobacterium* origin of replication

ColEl-ori: *E.coli* origin of replication

NptI: Gene which provides kanamycin-resistance

LB: Left border

RB: Right border

Nos-bar: Gene which provides BASTA-resistance

LacZ: Gene which encodes for the β-galactosidase

MCS: Multi cloning site

pSOUP containing:

RepA: Gene encoding the replicase RepA

trfA: Replication gene

Tet-r: Gene which provides tetracycline-resistance

ColEl-ori: *E.coli* origin of replication

oriV: Origin of replication

pGREEN_35S

pGREEN0229 with the 35S promoter and terminator cloned into XhoI/SacI (MCS) presents in the LacZ gene.

pGREEN_YFP

A multi cloning site (MCS), the sequence encoding for a polyglycin linker (Gly-Gly-Gly-Gly-Gly-Gly) and a HA tag were fused at the 5' sequence of YFP (yellow fluorescent protein) by sequential PCR. The following primers were used: linker_HA_YFP_n fw/c_YFP rev for the first PCR; MCS_linker fw/c_YFP rev for the second PCR. The generated sequence was produced as BamHI/SalI fragment. The fragment was then cloned between the 35S promoter and terminator present in pGREEN_35S using the same restriction enzymes.

pGREEN_CFP

A multi cloning site (MCS), the sequence encoding for a polyglycin linker (Gly-Gly-Gly-Gly-Gly-Gly) and a HA tag were fused at the 5' sequence of CFP (cyan fluorescent protein) by sequential PCR. The following primers were used: linker_HA_YFP_n fw/c_YFP rev for the first PCR; MCS_linker fw/c_YFP rev for the second PCR. The generated sequence was produced as BamHI/SalI fragment. The fragment was then cloned between the 35S promoter and terminator present in pGREEN_35S using the same restriction enzymes.

pGREEN_eGFP

A multi cloning site (MCS), the sequence encoding for a polyglycin linker (Gly-Gly-Gly-Gly-Gly-Gly) and a HA tag were fused at the 5' sequence of eGFP (enhanced green fluorescent protein) by sequential PCR. The following primers were used: linker_HA_YFP_n fw/c_YFP rev for the first PCR; MCS_linker fw/c_YFP rev for the second PCR. The generated sequence was produced as BamHI/SalI fragment. The fragment was then cloned between the 35S promoter and terminator present in pGREEN_35S using the same restriction enzymes.

pGREEN_RFP

A multi cloning site (MCS), the sequence encoding for a polyglycin linker (Gly-Gly-Gly-Gly-Gly-Gly) and a Myc tag were fused at the 5' sequence of RFP (monomeric red fluorescent protein) by sequential PCR. The following primers were used: linker_Myc_RFP fw/RFP rev for the first PCR; linker fw/RFP rev for the second PCR. The generated sequence was produced as BamHI/SalI fragment. The fragment was then cloned between the 35S promoter and terminator present in pGREEN_35S using the same restriction enzymes.

pGREEN_SpYFP

Specific pairs of primers were used in sequential PCR to amplify the YFP gene fused at 5’ end with the sequence encoding for the AtRMR1 signal peptide and at 3’ end with the sequence encoding for a polyglycin linker (Gly-Gly-Gly-Gly-Gly-Gly), a Myc tag and multi cloning site (MCS). The following primers were used: prim1_SpYFP fw/prim1_linker_Myc rev for the first PCR; prim2_SpYFP fw/prim2_linker_Myc rev for the second PCR. The generated sequence was produced as BamHI/SalI fragment. The fragment was then cloned between the 35S promoter and terminator present in pGREEN_35S using the same restriction enzymes.

pGREEN_Sp2YFP

Specific pairs of primers were used in sequential PCR to amplify the YFP gene fused at 5’ end with the sequence encoding for the signal peptide of AtRMR2 and at 3’ end with the sequence encoding for a polyglycin linker (Gly-Gly-Gly-Gly-Gly-Gly), a Myc tag and multi cloning site (MCS). The following primers were used: prim1_Sp2YFP fw/ prim1_linker_Myc rev for the first PCR; prim2_Sp2YFP fw/prim2_linker_Myc rev for the second PCR. The generated sequence was produced as BamHI/SalI fragment. The fragment was then cloned between the 35S promoter and terminator present in pGREEN_35S using the same restriction enzymes.

pGREEN_Sp2mCHERRY

Specific pairs of primers were used in sequential PCR to amplify the mCHERRY gene fused at 5’ end with the sequence encoding for the signal peptide of AtRMR2 and at 3’ end with the sequence encoding for a polyglycin linker (Gly-Gly-Gly-Gly-Gly-Gly), a Myc tag and multi cloning site (MCS). The following primers were used: prim1_Sp2mCHERRY fw/prim1_linker_Myc rev for the first PCR; prim2_Sp2YFP fw/prim2_linker_Myc rev for the second PCR. The generated sequence was produced as BamHI/SalI fragment. The fragment was then cloned between the 35S promoter and terminator present in pGREEN_35S using the same restriction enzymes.

pGREEN_nYFP

A multi cloning site (MCS), the sequence encoding for a polyglycin linker (Gly-Gly-Gly-Gly-Gly-Gly) and a HA tag was fused at the 5’ of the sequence encoding for YFP N-terminal fragment (from the aminoacid 1 to 154) by sequential PCR. The following primers were used: linker_HA_YFP_n fw and n_YFP rev for the first PCR; MCS_linker fw and n_YFP rev for the second PCR. The generated sequence was produced as BamHI/SalI fragment. The fragment was then cloned between the 35S promoter and terminator present in pGREEN_35S using the same restriction enzymes.

pGREEN_cYFP

A multi cloning site (MCS), the sequence encoding for a polyglycin linker (Gly-Gly-Gly-Gly-Gly-Gly) and a Myc tag was fused at the 5' of the sequence encoding for YFP C-terminal fragment (from the aminoacid 155 to 238) by sequential PCR. The following primers were used: linker_Myc_YFP_c fw and c_YFP rev for the first PCR; MCS_linker fw and c_YFP rev. The generated sequence was produced as BamHI/SalI fragment. The fragment was then cloned between the 35S promoter and terminator present in pGREEN_35S using the same restriction enzymes.

6.2. Constructs for AtRMR1 and AtRMR2 localization

pGREEN AtRMR1_YFP

The AtRMR1 full length cDNA was amplified as an EcoRI/SpeI fragment using the following primers: EcoRI_RMR1 fw and RMR1_SpeI rev. The resulting fragment was then cloned in pGREEN_YFP using the same restriction enzymes.

pGREEN AtRMR1_eGFP

The AtRMR1 full length cDNA was amplified as an EcoRI/SpeI fragment using the following primers: EcoRI_RMR1 fw and RMR1_SpeI rev. The resulting fragment was then cloned in pGREEN_eGFP using the same restriction enzymes.

pGREEN AtRMR1_RFP

The AtRMR1 full length cDNA was amplified as an EcoRI/SpeI fragment using the following primers: EcoRI_RMR1 fw and RMR1_SpeI rev. The resulting fragment was then cloned in pGREEN_RFP using the same restriction enzymes.

pGREEN SpYFP_AtRMR1

The cDNA of AtRMR1 without the sequence encoding for the signal peptide was amplified as an EcoRI/SpeI fragment using the following primers: EcoRI_delRMR1 fw and delRMR1_SpeI rev. The resulting fragment was then cloned in pGREEN_SpYFP using the same restriction enzymes.

pGREEN AtRMR2_YFP

The AtRMR2 full length cDNA was amplified as an EcoRI/HindIII fragment using the following primers: EcoRI_RMR2 fw and RMR2_HindIII rev. The resulting fragment was then cloned in pGREEN_YFP using the same restriction enzymes.

pGREEN Sp2YFP_AtRMR2

The cDNA of AtRMR2 without the sequence encoding for the signal peptide was amplified as an EcoRI/HindIII fragment using the following primers: EcoRI_delRMR2 fw and delRMR2_HindIII rev. The resulting fragment was then cloned in pGREEN_Sp2YFP using the same restriction enzymes.

pGREEN Sp2mCHERRY_AtRMR2

The cDNA of AtRMR2 without the sequence encoding for the signal peptide was amplified as an EcoRI/HindIII fragment using the following primers: EcoRI_delRMR2 fw and delRMR2_HindIII rev. The resulting fragment was then cloned in pGREEN_Sp2YFP using the same restriction enzymes.

6.3. Constructs for the characterization of AtRMR1 and 2 domains

pGREEN ΔSAtRMR1_YFP

The cDNA of AtRMR1 without the sequence encoding for the Serine Rich domain (from nucleotide 1 to 810) was amplified as an EcoRI/HindIII fragment using the following primers: EcoRI_RMR1 fw and DS_RMR1_HindIII rev. The resulting fragment was then cloned in pGREEN_YFP using the same restriction enzymes.

pGREEN ΔSRAtRMR1_YFP

The cDNA of AtRMR1 without the sequence encoding for the RingH2 and the Serine Rich domains (from nucleotide 1 to 621) was amplified as an EcoRI/HindIII fragment using the following primers: EcoRI_RMR1 fw and DRS_RMR1_HindIII rev. The resulting fragment was then cloned in pGREEN_YFP using the same restriction enzymes.

pGREEN SpYFP ΔPAtRMR1

The cDNA of AtRMR1 without the sequence encoding for the PA domain (from nucleotide 451 to 1347) was amplified as an EcoRI/HindIII fragment using the following primers: EcoRI_DP_RMR1 fw and delRMR1_HindIII rev. The resulting fragment was then cloned in pGREEN_SpYFP using the same restriction enzymes.

pGREEN SpYFP ΔPSAtRMR1

The cDNA of AtRMR1 without the sequence encoding for the PA and the Serine Rich domains (from nucleotide 451 to 810) was amplified as an EcoRI/HindIII fragment using the following primers: EcoRI_DPS_RMR1 fw and DSP_RMR1_HindIII rev. The resulting fragment was then cloned in pGREEN_SpYFP using the same restriction enzymes.

pGREEN ΔRingAtRMR2_YFP

The cDNA of AtRMR2 without the sequence encoding for the RingH2 domain (from nucleotide 1 to 651) was amplified as an EcoRI/HindIII fragment using the following primers: EcoRI_RMR2 fw and delRing_RMR2_HindIII rev. The resulting fragment was then cloned in pGREEN_YFP using the same restriction enzymes.

pGREEN Sp2YFP_ΔPAAtRMR2

The cDNA of AtRMR2 without the sequence encoding for the PA domain (from nucleotide 448 to 933) was amplified as an EcoRI/HindIII fragment using the following primers: EcoRI_delPA_RMR2 fw and delRMR2_HindIII rev. The resulting fragment was then cloned in pGREEN_Sp2YFP using the same restriction enzymes.

pGREEN ΔRingAtRMR2_RFP

The cDNA of AtRMR2 without the sequence encoding for the RingH2 domain (from nucleotide 1 to 651) was amplified as an EcoRI/HindIII fragment using the following primers: EcoRI_RMR2 fw and delRing_RMR2_HindIII rev. The resulting fragment was then cloned in pGREEN_RFP using the same restriction enzymes.

pGREEN Sp2mCHERRY_ΔPAAtRMR2

The cDNA of AtRMR2 without the sequence encoding for the PA domain (from nucleotide 448 to 933) was amplified as an EcoRI/HindIII fragment using the following primers: EcoRI_delPA_RMR2 fw and delRMR2_HindIII rev. The resulting fragment was then cloned in pGREEN_Sp2mCHERRY using the same restriction enzymes.

6.4. Constructs for the characterization of the trans-membrane and the linker of AtRMR1 and 2

pGREEN AtRMR1TM2_eGFP

Into AtRMR1 cDNA the sequence encoding for the trans-membrane domain (TM1: from nucleotide 484 to 552) was replaced by the corresponding sequence encoding for the trans-membrane domain of AtRMR2 (TM2: from nucleotide 502 to 570). The resulting AtRMR1TM2 sequence was generated as an EcoRI/SpeI fragment by fusing a 5' and a 3' fragments. The two fragments were generated by sequential PCR using the following primers: EcoRI_RMR1 fw/RMR1_TM2a rev for the 5' fragment; RMR1_TM2 fw/RMR1_SpeI rev and RMR1_TM2b fw/RMR1_SpeI rev for the 3' fragment. The AtRMR1TM2 sequence was then cloned in pGREEN_eGFP using the same restriction enzymes.

pGREEN AtRMR1TM2L2_eGFP

Into AtRMR1 cDNA the sequence encoding for the linker (L1: from nucleotide 553 to 621) and TM (from nucleotide 484 to 552) were replaced by the corresponding sequence encoding for the linker (L2: from nucleotide 571 to 651) and TM (from nucleotide 502 to 570) of AtRMR2. The resulting AtRMR1TM2L2 sequence was generated as an EcoRI/SpeI fragment by fusing a 5' and a 3' fragments. The two fragments were generated by sequential PCR the following primers: EcoRI_RMR1 fw/TM2_link2 rev1 and EcoRI_RMR1 fw/TM2_link2 rev2 for the 5' fragment; TM2_link2 fw1/RMR1_SpeI rev and TM2_link2 fw2/RMR1_SpeI rev for the 3' fragment. The AtRMR1TM2L2 sequence was then cloned in pGREEN_eGFP using the same restriction enzymes.

pGREEN AtRMR2TM1_eGFP

Into AtRMR2 cDNA the sequence encoding for the trans-membrane domain (TM2: from nucleotide 502 to 570) was replaced by the corresponding sequence encoding for the trans-membrane domain of AtRMR1 (TM1: nucleotide 484 to 552). The resulting AtRMR2TM1 sequence was generated as an EcoRI/NdeI fragment by fusing a 5' and a 3' fragments. The two fragments were generated by sequential PCR using the following primers: EcoRI_RMR2 fw/RMR2_TM1a_A rv and EcoRI_RMR2 fw/RMR2_TM1a_B rv for the 5' fragment; RMR2TM1b fw2/RMR2_NdeI rv for the 3' fragment. The AtRMR2TM1 sequence was then cloned in pGREEN_eGFP using the same restriction enzymes.

pGREEN AtRMR2TM1L1_eGFP

Into AtRMR2 cDNA the sequence encoding for the linker (L2: from nucleotide 571 to 651) and TM (from nucleotide 502 to 570) were replaced by the corresponding sequence encoding for the linker (L1: from nucleotide 553 to 621) and TM (nucleotide 484 to 552) of AtRMR1. The resulting AtRMR2TM1L1 sequence was generated as an EcoRI/NdeI fragment by fusing a 5' and a 3' fragments. The two fragments were generated by sequential PCR using the following primers: EcoRI_RMR2 fw/TM1_link1 rev for the 5' fragment; TM1_link1 fw/RMR2_NdeI rev for the 3' fragment. The AtRMR2TM1L1 sequence was then cloned in pGREEN_eGFP using the same restriction enzymes.

pGREEN AtRMR2TM1L1_5_eGFP

Into AtRMR2 cDNA the sequence encoding for the first 5 residues of the linker (L2_5: from nucleotide 571 to 585) and TM (from nucleotide 502 to 570) were replaced by the corresponding sequence encoding for the first 5 residues of the linker (L1_5: from nucleotide 553 to 567) and TM (nucleotide 484 to 552) of AtRMR1. The resulting AtRMR2TM1L1_5 sequence was generated as an EcoRI/NdeI fragment by fusing a 5' and a 3' fragments. The two fragments were generated by sequential PCR using the following primers: EcoRI_RMR2 fw/TM1L1_5 rev for the 5' fragment; TM1L1_10 fw1/RMR2_NdeI rev and TM1L1_10 fw2/RMR2_NdeI rev for the 3' fragment. The AtRMR2TM1L1_5 sequence was then cloned in pGREEN_eGFP using the same restriction enzymes.

pGREEN AtRMR2TM1L1_10_eGFP

Into AtRMR2 cDNA the sequence encoding for the first 10 residues of the linker (L2_10: from nucleotide 571 to 600) and TM (from nucleotide 502 to 570) were replaced by the corresponding sequence encoding for the first 10 residues of the linker (L1_10: from nucleotide 553 to 582) and TM (nucleotide 484 to 552) of AtRMR1. The resulting AtRMR2TM1L1_10 sequence was generated as an EcoRI/NdeI fragment by fusing a 5' and a 3' fragments. The two fragments were generated by sequential PCR using the following primers: EcoRI_RMR2 fw/TM1L1_10 rev for the 5' fragment; TM1L1_10 fw1/RMR2_NdeI rev and TM1L1_10 fw2/RMR2_NdeI rev for the 3' fragment. The AtRMR2TM1L1_10 sequence was then cloned in pGREEN_eGFP using the same restriction enzymes.

pGREEN AtRMR2TM1L1_15_eGFP

Into AtRMR2 cDNA the sequence encoding for the first 15 residues of the linker (L2_15: from nucleotide 571 to 615) and TM (from nucleotide 502 to 570) were replaced by the corresponding sequence encoding for the first 15 residues of the linker (L1_15: from nucleotide 553 to 597) and TM (nucleotide 484 to 552) of AtRMR1. The resulting AtRMR2TM1L1_15 sequence was generated as an EcoRI/NdeI fragment by fusing a 5' and a 3' fragments. The two fragments were generated by sequential PCR using the following primers: EcoRI_RMR2 fw/TM1L1_15 rev for the 5' fragment; TM1L1_15 fw/RMR2_NdeI rev and TM1L1_15 fw2/RMR2_NdeI rev for the 3' fragment. The AtRMR2TM1L1_15 sequence was then cloned in pGREEN_eGFP using the same restriction enzymes.

pGREEN AtRMR2TM1L1_5S_eGFP

Into AtRMR2 cDNA the sequence encoding for the residue 11 to 15 of the linker (L2_5S: from nucleotide 601 to 615) and TM (from nucleotide 502 to 570) were replaced by the corresponding sequence encoding for the residue 11 to 15 of the linker (L1_5S: from nucleotide 583 to 597) and TM (nucleotide 484 to 552) of AtRMR1. The resulting AtRMR2TM1L1_5S sequence was generated as an EcoRI/NdeI fragment by fusing a 5' and a 3' fragments the two fragments were generated by sequential PCR using the following primers: EcoRI_RMR2 fw/TM1L1_5S rv for the 5' fragment; TM1L1_15 fw/RMR2_NdeI rv and TM1L1_15 fw2/RMR2_NdeI rv for the 3' fragment. The AtRMR2TM1L1_5S sequence was then cloned in pGREEN_eGFP using the same restriction enzymes.

6.5. Constructs coding for markers of different compartment

pGREEN p6_YFP

The p6 full length cDNA from BYV (Beet Yellow Virus) (Peremyslov *et al.,* 2004) was amplified as an EcoRI/SpeI fragment using the following primers: EcoRI_p6 fw and p6_SpeI rev. The resulting fragment was then cloned in pGREEN_YFP using the same restriction enzymes.

pGREEN p6_CFP

The p6 full length cDNA from BYV (Beet Yellow Virus) (Peremyslov *et al.,* 2004) was amplified as an EcoRI/SpeI fragment using the following primers: EcoRI_p6 fw and p6_SpeI rev. The resulting fragment was then cloned in pGREEN_CFP using the same restriction enzymes.

pGREEN GONST1_RFP

The AtGONST1 full length cDNA (Baldwin *et al.*, 2001) was amplified as an EcoRI/SpeI fragment using the following primers: EcoRI_GONST1 fw and GONST1_SpeI rev. The resulting fragment was then cloned in pGREEN_RFP using the same restriction enzymes.

pGREEN Venus SYP61

It was provided by Uemura *et al*., 2004

pBI121_GFP BP80

It was provided by Miao *et al*., 2006

6.6. Constructs for Bimolecular Fluorescent Complementation (BiFC)

pGREEN AtRMR1_nYFP

The AtRMR1 full length cDNA was amplified as an EcoRI/SpeI fragment using the following primers: EcoRI_RMR1 fw and RMR1_SpeI rev. The resulting fragment was then cloned in pGREEN_nYFP using the same restriction enzymes.

pGREEN AtRMR1_cYFP

The AtRMR1 full length cDNA was amplified as an EcoRI/SpeI fragment using the following primers: EcoRI_RMR1 fw and RMR1_SpeI rev. The resulting fragment was then cloned in pGREEN_cYFP using the same restriction enzymes.

pGREEN ΔSRAtRMR1_nYFP

The cDNA of AtRMR1 without the sequence encoding for the RingH2 and the Serine Rich domains (from nucleotide 1 to 621) was amplified as an EcoRI/HindIII fragment using the following primers: EcoRI_RMR1 fw and DRS_RMR1_HindIII rev. The resulting fragment was then cloned in pGREEN_nYFP using the same restriction enzymes.

pGREEN ΔSRAtRMR1_cYFP

The cDNA of AtRMR1 without the sequence encoding for the RingH2 and the Serine Rich domains (from nucleotide 1 to 621) was amplified as an EcoRI/HindIII fragment using the following

primers: EcoRI_RMR1 fw and DRS_RMR1_HindIII rev. The resulting fragment was then cloned in pGREEN_cYFP using the same restriction enzymes.

pGREEN AtRMR2_nYFP

The AtRMR2 full length cDNA was amplified as an EcoRI/HindIII fragment using the following primers: EcoRI_RMR2 fw and RMR2_HindIII rev. The resulting fragment was then cloned in pGREEN_nYFP using the same restriction enzymes.

pGREEN AtRMR2_cYFP

The AtRMR2 full length cDNA was amplified as an EcoRI/HindIII fragment using the following primers: EcoRI_RMR2 fw and RMR2_HindIII rev. The resulting fragment was then cloned in pGREEN_cYFP using the same restriction enzymes.

pGREEN ΔRingAtRMR2_nYFP

The cDNA of AtRMR2 without the sequence encoding for the RingH2 domain (from nucleotide 1 to 651) was amplified as an EcoRI/HindIII fragment using the following primers: EcoRI_RMR2 fw and delRing_RMR2_HindIII rev. The resulting fragment was then cloned in pGREEN_nYFP using the same restriction enzymes.

pGREEN ΔRingAtRMR2_cYFP

The cDNA of AtRMR2 without the sequence encoding for the RingH2 domain (from nucleotide 1 to 651) was amplified as an EcoRI/HindIII fragment using the following primers: EcoRI_RMR2 fw and delRing_RMR2_HindIII rev. The resulting fragment was then cloned in pGREEN_cYFP using the same restriction enzymes.

pGREEN p6_nYFP

The p6 full length cDNA from BYV (Beet Yellow Virus) (Peremyslov *et al.,* 2004) was amplified as an EcoRI/SpeI fragment using the following primers: EcoRI_p6 fw and p6_SpeI rev. The resulting fragment was then cloned in pGREEN_nYFP using the same restriction enzymes.

pGREEN p6_cYFP

The p6 full length cDNA from BYV (Beet Yellow Virus) (Peremyslov *et al.,* 2004) was amplified as an EcoRI/SpeI fragment using the following primers: EcoRI_p6 fw and p6_SpeI rev. The resulting fragment was then cloned in pGREEN_cYFP using the same restriction enzymes.

Annex I AtRMR1 and AtRMR2 expression in *A.thaliana*

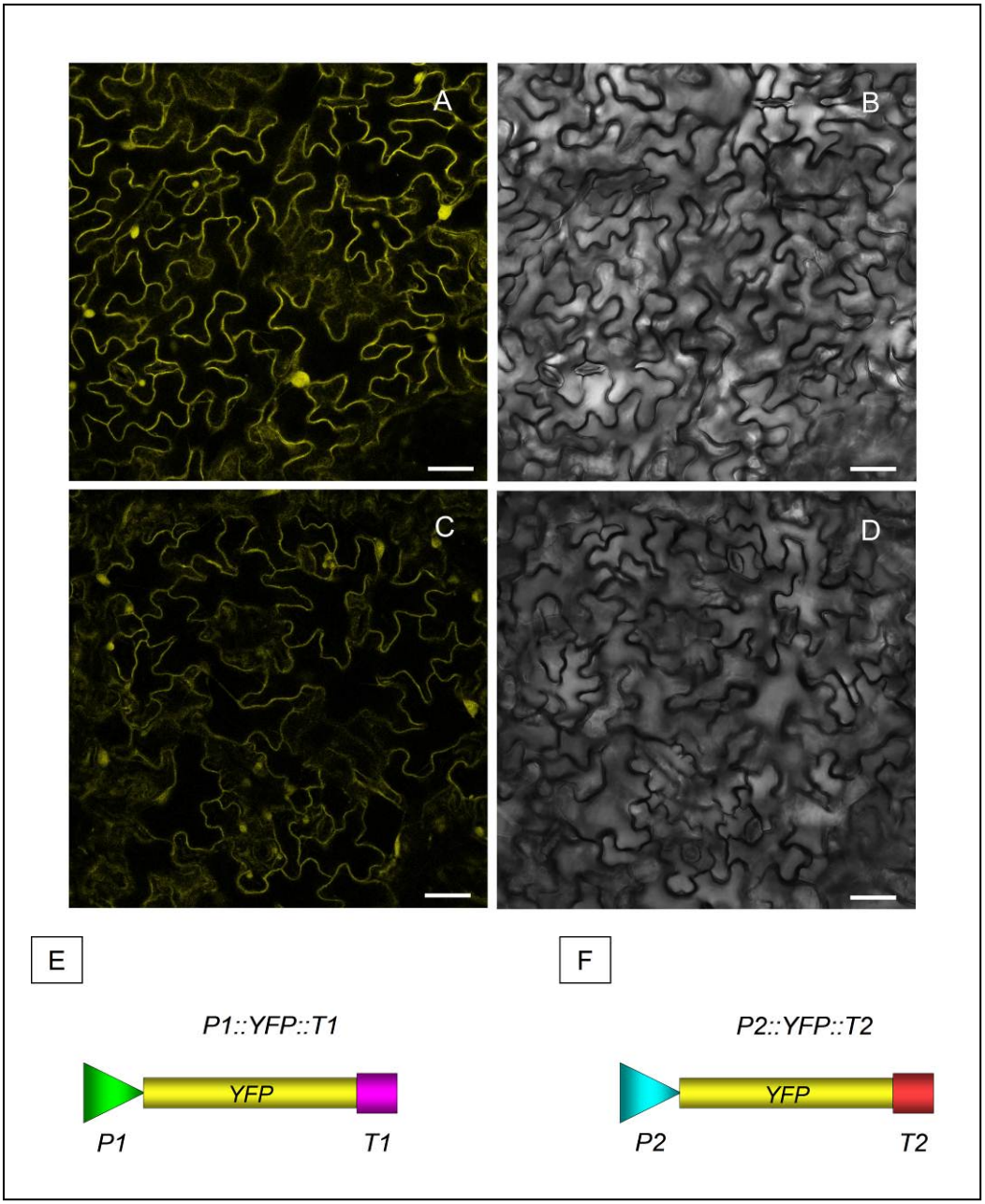

AtRMR1 and AtRMR2 expression in *A.thaliana*.
(A) Leaf epidermal cells of *A.thaliana* stable transformed with YFP under the control of AtRMR1 endogenous promoter and terminator. (B) Bright field of image A. (C) Leaf epidermal cells of *A.thaliana* stable transformed with YFP under the control of AtRMR2 endogenous promoter and terminator. (D) Bright field of image C. Scale bar A-D = 30 µm. (E and F) Schematic representation of the two constructs used to generate transgenic plants. P1::YFP::T1: P1 (AtRMR1 endogenous promoter, green); YFP (yellow); T1 (AtRMR1 endogenous terminator, lilac). P2::YFP::T2: P2 (AtRMR2 endogenous promoter, cyan); YFP (yellow); T2 (AtRMR2 endogenous terminator, red).

Annex II _ Primers

linker_HA_YFP_n fw	GGAGGAGGAGGAGGAGGATACCCATACGACGTCCCAGACTACGCTGTGAGCAAGGGCGAGGAGCTG
Linker_Myc_YFP_c fw	GGAGGAGGAGGAGGAGGAGAACAACAAAAACTTATTTCTGAAGAAGATCTGGACAAGCAGAAGAACGGCATC
linker_Myc_RFP fw	GGAGGAGGAGGAGGAGGAGAACAACAAAAACTTATTTCTGAAGAAGATCTGGCCTCCTCCGAGGACGTCATCA
MCS_linker fw	GCGCGCGGATCCGAATTCTCTAGAAAGCTTACTAGTCATATGGGAGGAGGAGGAGGAGGA
linker fw	GGCCGGGGATCCGAATTCTCTAGAAAGCTTACTAGTCATATGGGAGGAGGAGGAGGAGGAGAACAAC
prim1_SpYFP fw	CTGTTTCTTGTTTAGCTTCAAGCGTGAGCAAGGGCGAGGAGCTGT
prim2_SpYFP fw	GGCCGGGGATCCATGAATCGTGCTTTGGTCCTACTTTTATATGTTTGTACTGTTTCTTGTTTAGCTTCAAG
prim1_Sp2YFP fw	GCTCCTTTTCTCTCCTCTCTGTTACGAGTCTCACTCGCCACTGTTGTGAGCAAGGGCGAGGAGCTGT
prim2_Sp2YFP fw	GGCCGGGGATCCATGAGACTCGTCGTCTCAAGCTGTCTACTAGTTGCAGCTCCTTTTCTCTCCTCTCTGT
prim1_Sp2mCHERRY fw	GCTCCTTTTCTCTCCTCTCTGTTACGAGTCTCACTCGCCACTGTTGTGAGCAAGGGCGAGGAGGATAA
EcoRI_RMR1 fw	GCGCGCGAATTCATGAATCGTGCTTTGGTCC
EcoRI_delRMR1 fw	GGCCGGGAATTCAAAGTTATTTTGATGAGGAATAACATCA
EcoRI_delRMR2 fw	CCGGCCGAATTCACTGTTGTCCTCAATTCCATCT
EcoRI_RMR2 fw	CCGGCCGAATTCATGAGACTCGTCGTCTCAAG
EcoRI_DSP_RMR1 fw	GCGCGCGAATTCGGTTTCCCCGATACGAAAGT
EcoRI_delPA_RMR2 fw	CCGGCCGAATTCAGAGGCCGAGATGGTGAATGC
RMR1_TM2 fw	ATAGTCACTTTCCTGTTGATTGCCTTCTTTGCAGTGCGTAGGCATCGAATAAGAAGGC
RMR1_TM2b fw	GGCCGGTGGCCATCTCCTTCTTCTCTCTCCTTCTTATAGTCACTTTCCTGTTGATTGCC
RMR2_TM1b fw2	GCGCGCAAGCTTGTCGGCTGTTCTCGCTACTTGTTTCTTTCCCAGACACTGGACCCAATGGCGAG
TM2_link2 fw1	CAAAGCTCGTCCACACACTCCCCTGCCGCCGCTTGGTGAAAGCAATGCC
TM2_link2 fw2	GGCCGGCCAGGACCATCAGGTTAGATGCAAAGCTCGTCCACACACTCCCC
TM1_link1 fw	GCGCGCGGTCCTCTCGAGTGCGTGAGTTTCACGGTATGAGCTTCACCTTCACTGATTCTGCTCACC
TM1L1_10 fw1	AAAGCTCGTCCACACACTCCCCTGCTTCACCTTCACTGATTCTGCTCACC
TM1L1_10 fw2	GCGCGCGGACCATCAGGTTAGATGCAAAGCTCGTCCACACACTCCCCTGC
TM1L1_15 fw	CAAAGCTCGTCCACACACTCCCCTGCTTCACCTTCACTGATTCTGCTCAC
TM1L1_15 fw2	GCGCGCGGTCCTCTCGAAGGTTAGATGCAAAGCTCGTCCACACACTCCCCT
EcoRI_p6 fw	GCGCGCGAATTCATGGACTGTGTACTCCGCTC
EcoRI_GONST1 fw	GGCCGGGAATTCATGAAATTGTACGAACACGATG
c_YFP rev	GCGCGCGTCGACTTACTTGTACAGCTCGTC
n_YFP rev	GCGCGCGTCGACTTAGGCCATGATATAGAC
RFP rev	CCGGCCGTCGACTTATGCTCCAGTACTGTGGCGGCCC
prim1_linker_Myc rev	TCTTCAGAAATAAGTTTTTGTTGTTCTCCTCCTCCTCCTCCCTTGTACAGCTCGTCCATGCCG
prim2_linker_Myc rev	CCGGCCGTCGACACTAGTAAGCTTTCTAGAGAATTCCAGATCTTCTTCAGAAATAAGTTTTTGTTG
RMR1_SpeI rev	GCGCGCACTAGTACAGTCTGGAAGCGAGTTTGC
delRMR1_SpeI rev	CCGGCCACTAGTCTAACAGTCTGGAAGCGAG
delRMR2_HindIII rev	CCGGCCAAGCTTCTAACGGCTTTGACTGGATTG
RMR2_HindIII rev	CCGGCCAAGCTTACGGCTTTGACTGGATTGGG
DS_RMR1_HindIII rev	CCGGCCAAGCTTCGTTCTTGCATCTCGTTTGC
DRS_RMR1_HindIII rev	CCGGCCAAGCTTCATTGCTTTCACCAAGCGG
delRMR1_HindIII rev	CCGGCCAAGCTTCTAACAGTCTGGAAGCGAG
DSP_RMR1_HindIII rev	CCGGCCAAGCTTCTACGTTCTTGCATCTCGTT
delRing_RMR2_HindIII rev	CCGGCCAAGCTTGCAGGGGAGTGTGTGGACGA
RMR1_TM2a rev	CCGGCCTGGCCAACACAGTCGCCGAGTTCTCAAAACTTGG
RMR2_TM1a_A rev	TAAACGAAACCGCCATAATAGACCACCAAGCGCTCCCTCTGTCTGGCGG
RMR2_TM1a_B rev	CGCGCGAAGCTTTGCAAGCAGCGAGATAAACGAAACCGCCATAATAGACC
TM2_link2 rev1	GCCATTGGGTCCAGTGTCTGGGTGCAAAGAAGGCAATCAACAGG
TM2_link2 rev2	GGCCGGCCTGGTGTGCCTCCCTCGCCATTGGGTCCAGTGTCTGGGT
TM1_link1 rev	GCGCGCGGACCGAGATGTCCGCCTTCTTATTCGATGCCTACGCACAAAGAAACAAGTAGCGAGAACAGCC
TM1L1_5 rev	GCGCGCGGTCCTGGTGTGCCTCCCTCGCCATTGTCGATGCCTACGCACAAAGAAACAAG
TM1L1_10 rev	GCGCGCGGTCCTGGTGTGTGTCCGCCTTCTTATTCGATGCCTAC
TM1L1_15 rev	GCGCGCGGACCGAGATGTCCGCCTTCTTATTCGATGCCTACGCACAAAGAAACAAGTAGCGAGAACAG
TM1L1_5S rev	GCGCGCGGACCGAGACCTCCCTCGCCATTGAGTCCAGTGTCTGGGAAAGAAACAAGTAGCGAGAACAG
p6_SpeI rev	GCGCGCACTAGTCACGACCGTGGAACGGTTGA
GONST1_SpeI rev	GGCCGGACTAGTGGACTTCTCCCTCATTTTGG

Annex III _ Plasmids and Vectors

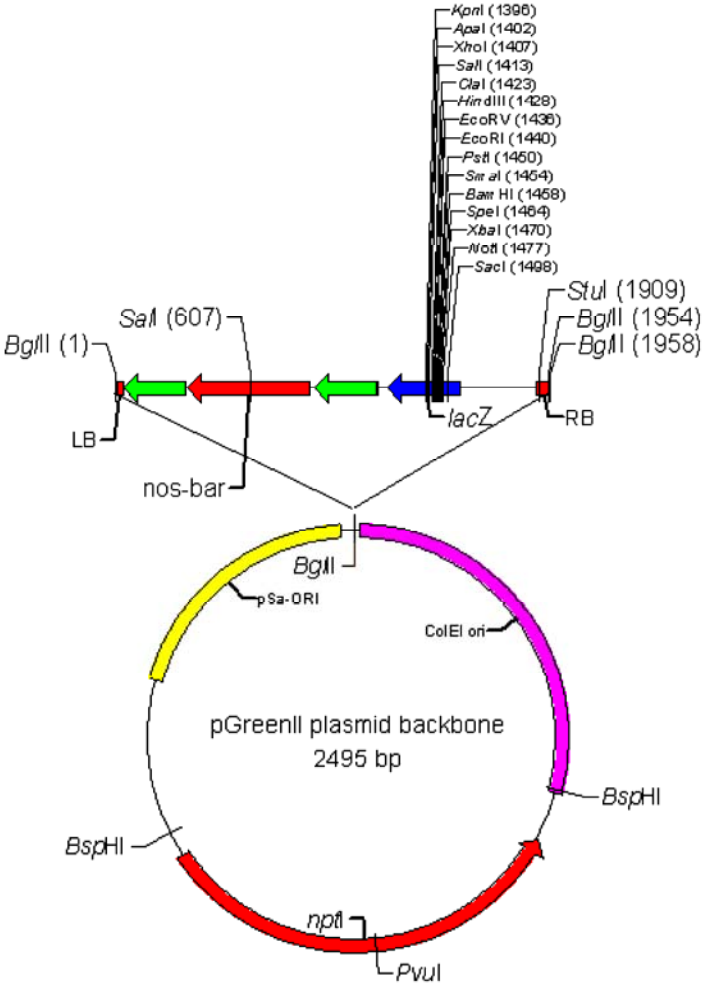

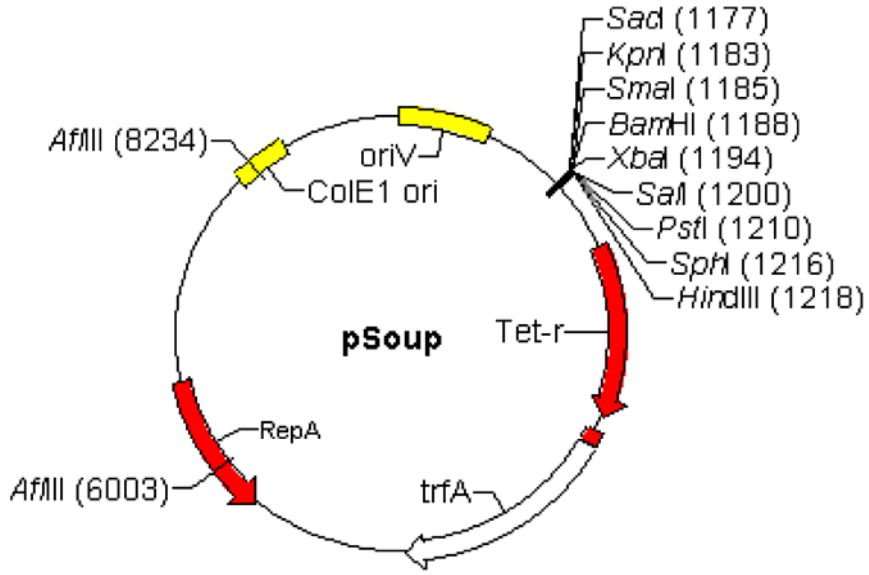

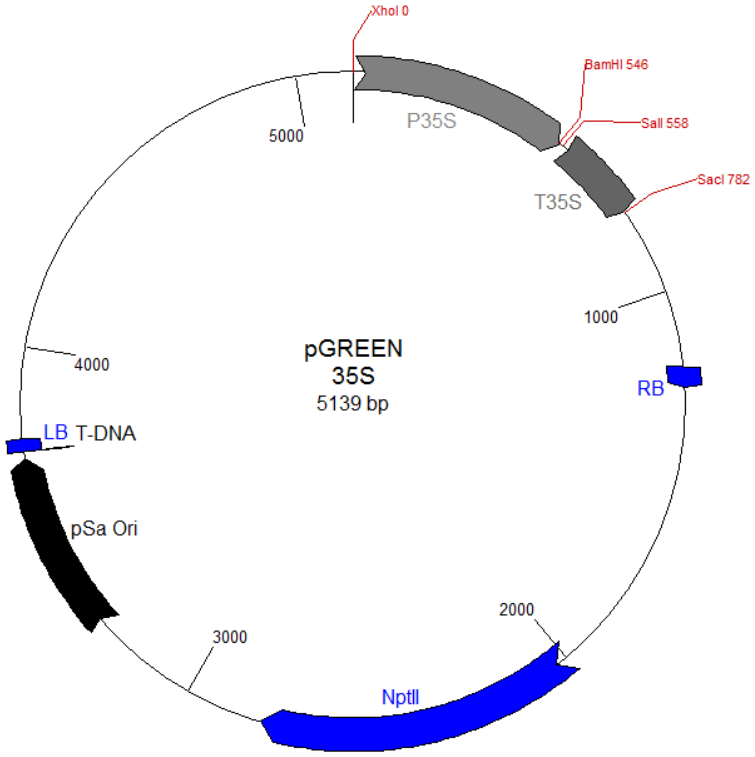
XhoI 0
BamHI 546
SalI 558
SacI 782
P35S
T35S
5000
1000
4000
pGREEN
35S
5139 bp
RB
LB T-DNA
pSa Ori
2000
3000
NptII

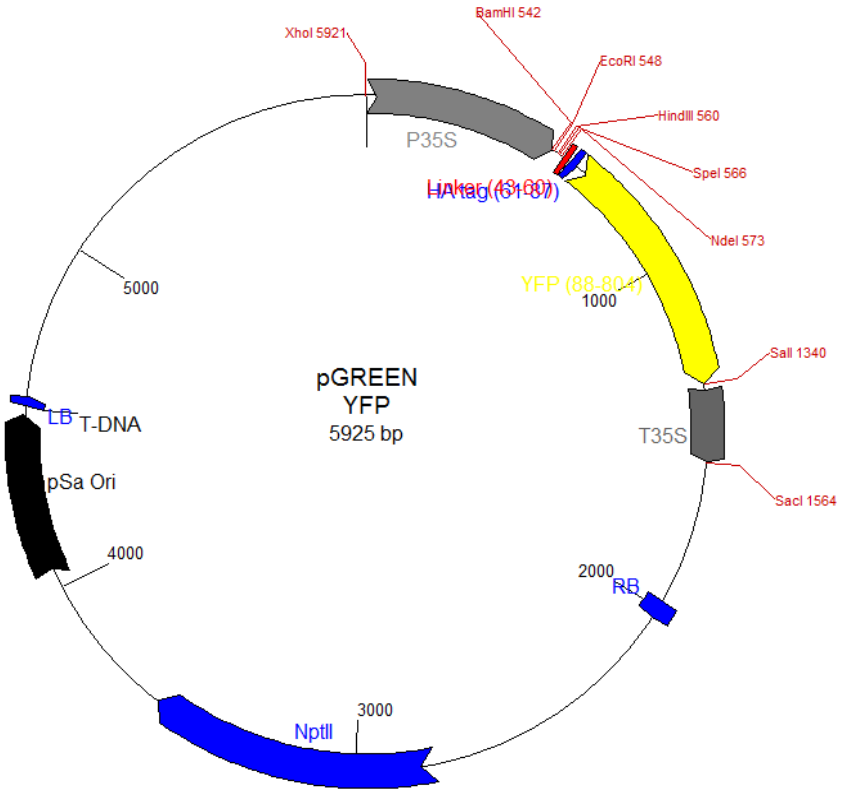
BamHI 542
XhoI 5921
EcoRI 548
HindIII 560
P35S
SpeI 566
NdeI 573
5000
1000
SalI 1340
pGREEN
YFP
5925 bp
T35S
LB T-DNA
SacI 1564
pSa Ori
4000
2000
RB
3000
NptII

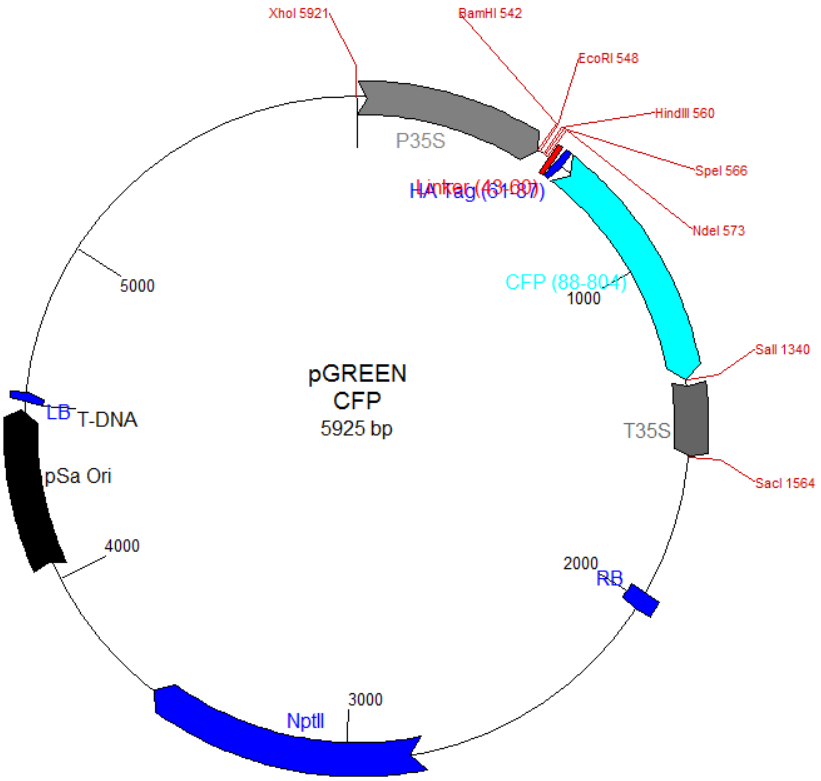
XhoI 5921
BamHI 542
EcoRI 548
HindIII 560
SpeI 566
NdeI 573
P35S
Linker (43-60)
HA Tag (61-87)
CFP (88-804)
1000
5000
SalI 1340
pGREEN
CFP
5925 bp
T35S
LB
T-DNA
pSa Ori
SacI 1564
4000
2000
RB
NptII
3000

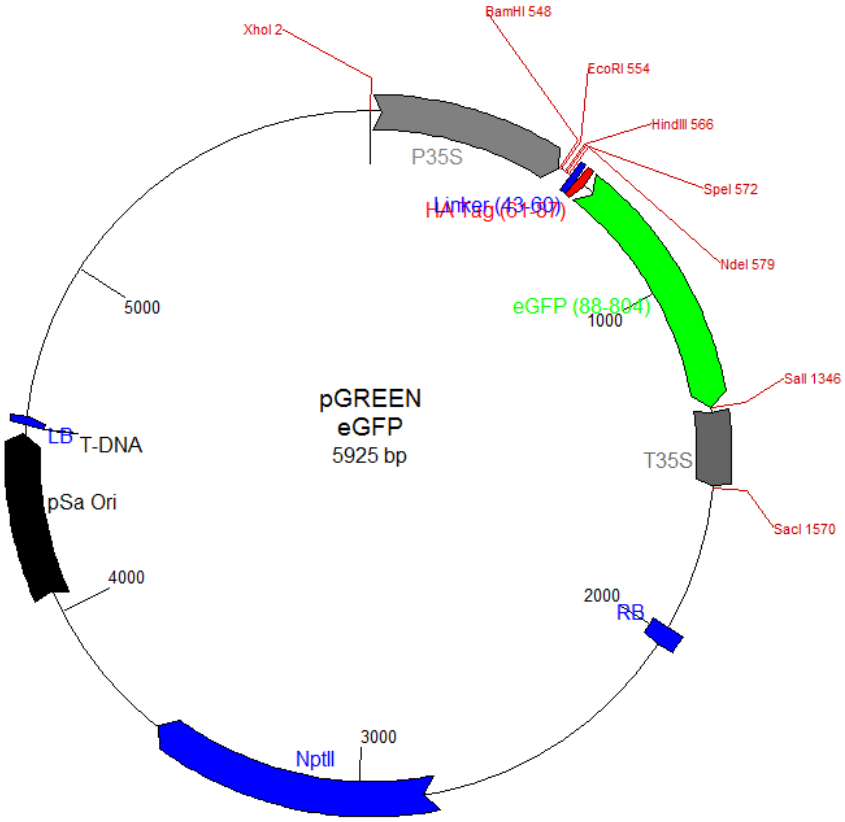
BamHI 548
XhoI 2
EcoRI 554
HindIII 566
P35S
SpeI 572
Linker (43-60)
HA Tag (61-87)
NdeI 579
5000
eGFP (88-804)
1000
SalI 1346
pGREEN
eGFP
5925 bp
T35S
LB
T-DNA
pSa Ori
SacI 1570
4000
2000
RB
NptII
3000

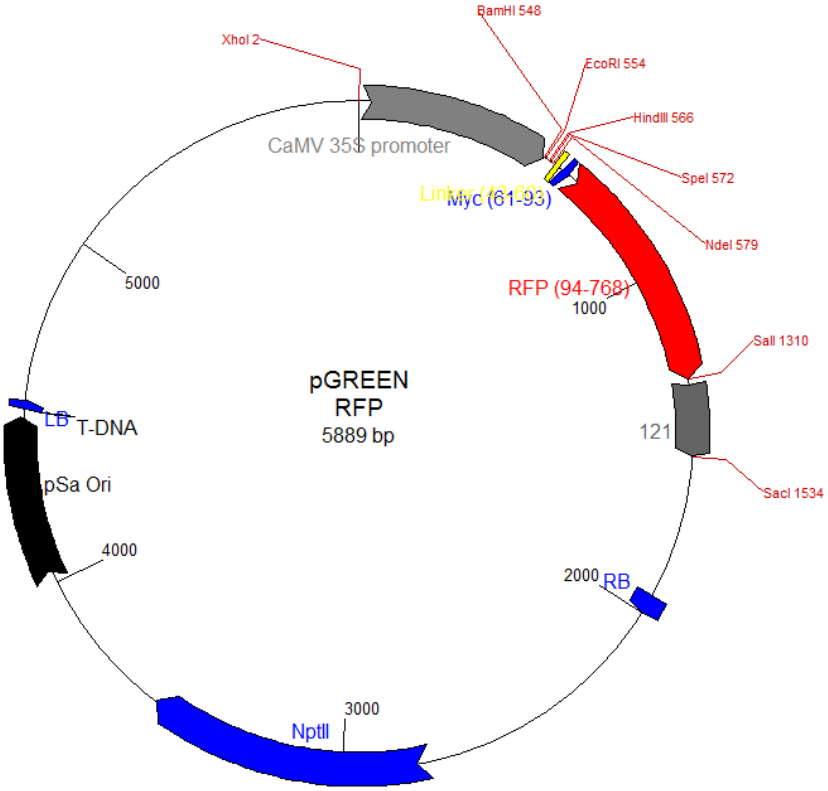
BamHI 548
XhoI 2
EcoRI 554
HindIII 566
SpeI 572
NdeI 579
CaMV 35S promoter
Linker (43-60)
Myc (61-93)
RFP (94-768)
1000
5000
SalI 1310
pGREEN
RFP
5889 bp
LB
T-DNA
121
pSa Ori
SacI 1534
4000
2000
RB
3000
NptII

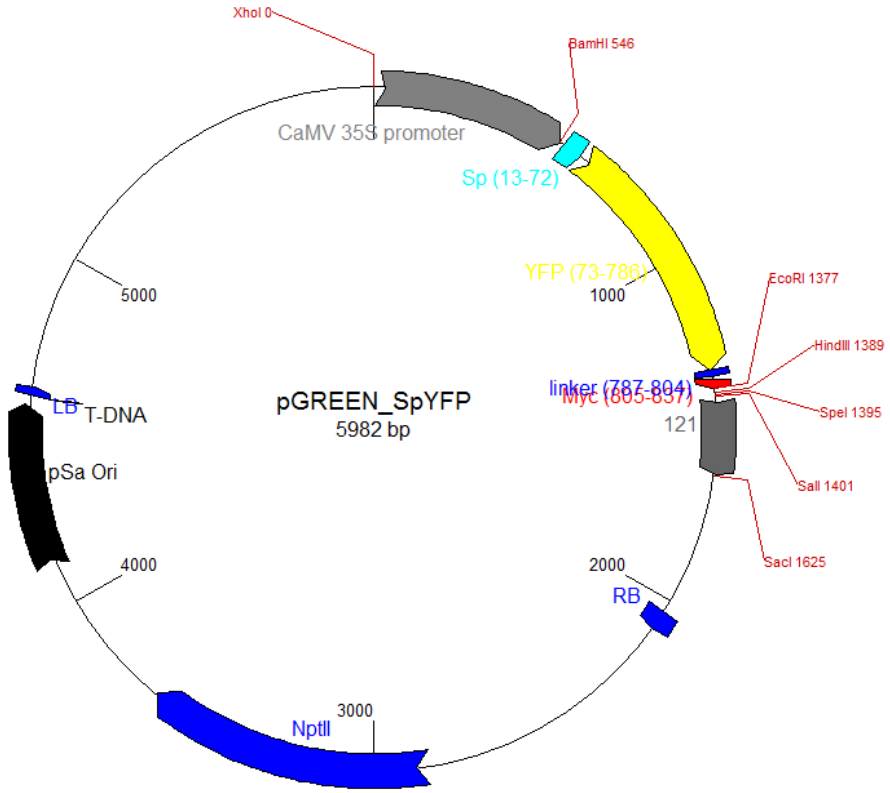
XhoI 0
BamHI 546
CaMV 35S promoter
Sp (13-72)
YFP (73-786)
1000
5000
EcoRI 1377
HindIII 1389
linker (787-804)
Myc (805-837)
SpeI 1395
pGREEN_SpYFP
5982 bp
LB
T-DNA
121
SalI 1401
pSa Ori
SacI 1625
4000
2000
RB
3000
NptII

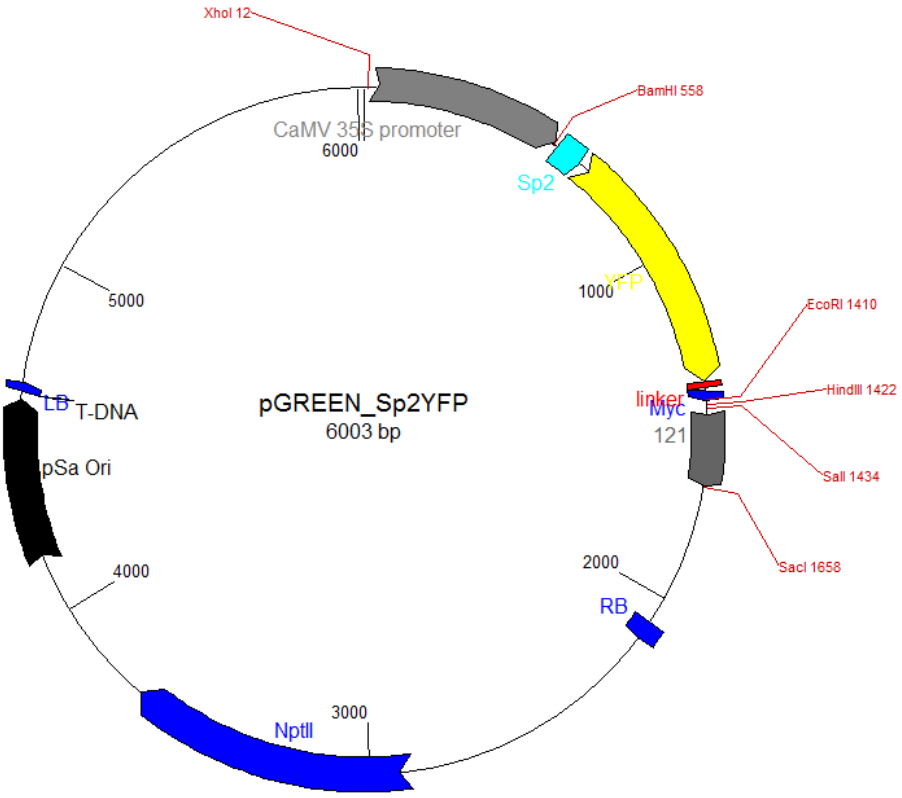
XhoI 12
BamHI 558
CaMV 35S promoter
6000
Sp2
1000
YFP
EcoRI 1410
HindIII 1422
SalI 1434
SacI 1658
5000
LB
T-DNA
pSa Ori
pGREEN_Sp2YFP
6003 bp
linker
Myc
121
2000
RB
4000
3000
NptII

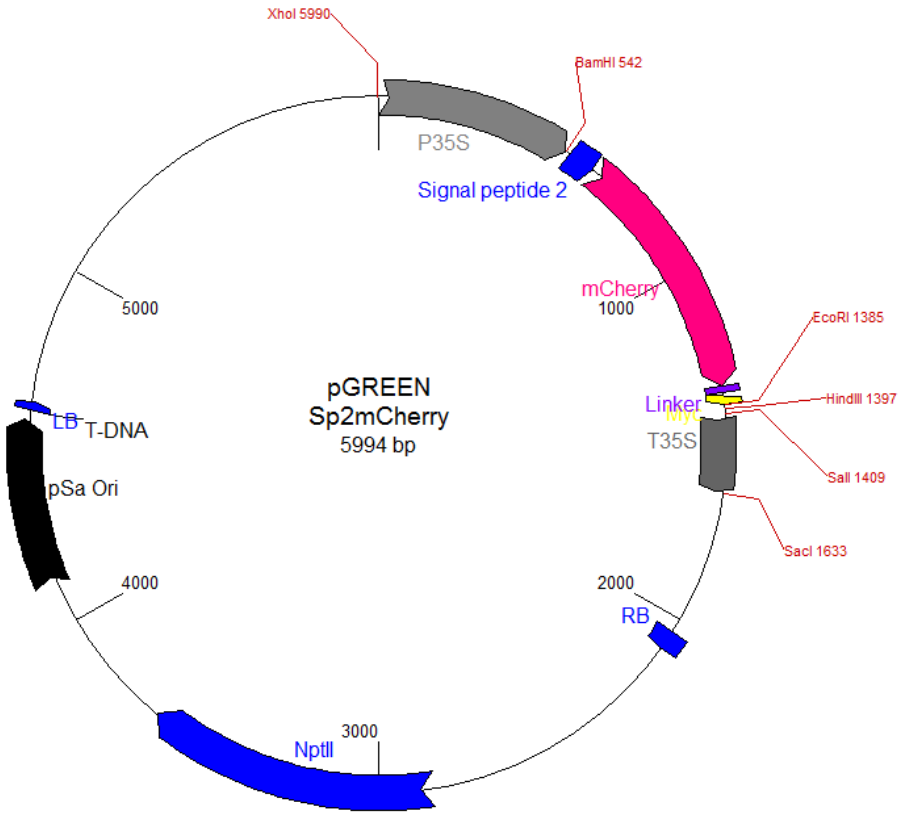
XhoI 5990
BamHI 542
P35S
Signal peptide 2
mCherry
1000
EcoRI 1385
HindIII 1397
SalI 1409
SacI 1633
5000
LB
T-DNA
pSa Ori
pGREEN
Sp2mCherry
5994 bp
Linker
Myc
T35S
2000
RB
4000
3000
NptII

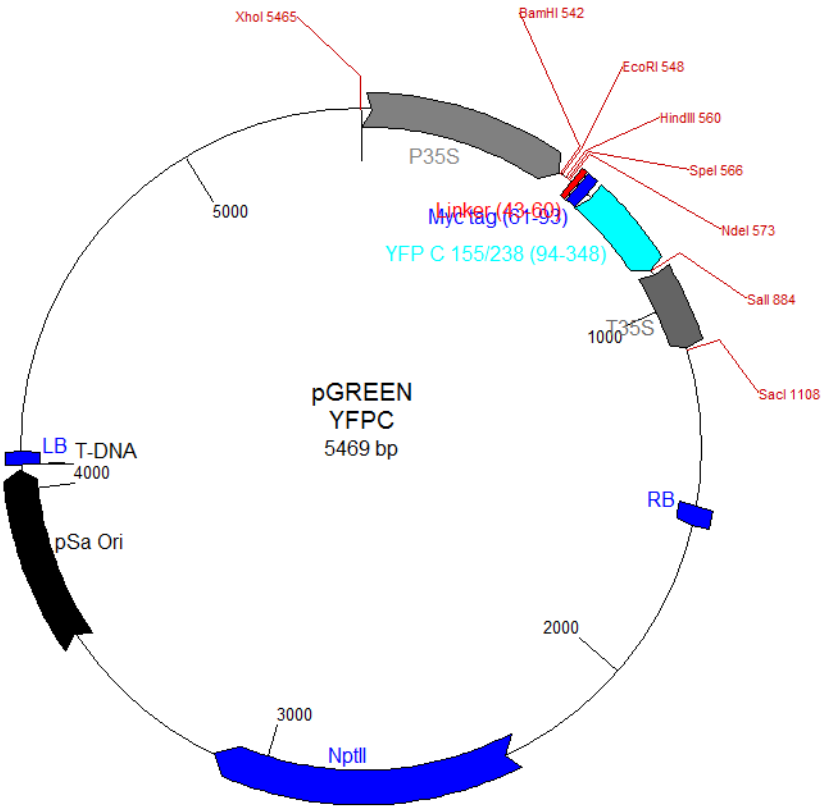
XhoI 5465
BamHI 542
EcoRI 548
HindIII 560
SpeI 566
NdeI 573
SalI 884
SacI 1108
P35S
Linker (43-60)
Myc tag (61-93)
YFP C 155/238 (94-348)
T35S
5000
1000
pGREEN
YFPC
5469 bp
LB
T-DNA
4000
RB
pSa Ori
2000
3000
NptII

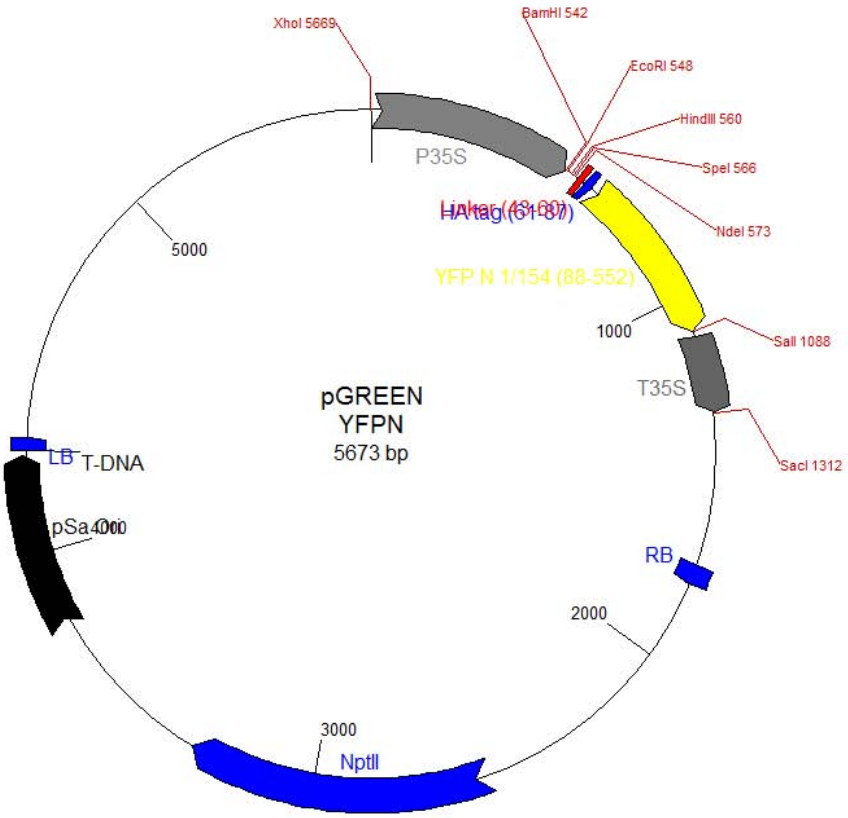
XhoI 5669
BamHI 542
EcoRI 548
HindIII 560
SpeI 566
NdeI 573
SalI 1088
SacI 1312
P35S
Linker (43-60)
HA tag (61-87)
YFP N 1/154 (88-552)
T35S
5000
1000
pGREEN
YFPN
5673 bp
LB
T-DNA
RB
2000
3000
NptII

Annex VI _ AtRMR1 cDNA sequence

Full length cDNA of AtRMR1 including the aminoacid sequence of the whole protein. The picture also includes the exact limits of the domain used for the generation of all deletion/replacement mutants. The different domains forming AtRMR1 are indicated in the picture: signal peptide (cyan); PA domain (blue); transmembrane domain (green); sequence linker (lilac); Ring-H2 domain (black); Serine-Rich domain (orange).

Annex V _ AtRMR2 cDNA sequence

Full length cDNA of AtRMR2 including the aminoacid sequence of the whole protein. The picture also includes the exact limits of the domain used for the generation of all deletion/replacement mutants. The different domains forming AtRMR2 are indicated in the picture: signal peptide (cyan); PA domain (blue); transmembrane domain (green); sequence linker (lilac); Ring-H2 domain (black); Serine-Rich domain (orange).

Bibliography

Ahmed, S. U., E. Rojo, et al. (2000). "The plant vacuolar sorting receptor AtELP is involved in transport of NH_2-terminal propeptide-containing vacuolar proteins in *Arabidopsis thaliana*." J Cell Biol **149**(7): 1335-44.

Akita, M., E. Nielsen, et al. (1997). "Identification of protein transport complexes in the chloroplastic envelope membranes via chemical cross-linking." Journal of Cell Biology **136**(5): 983-994.

Anandasabapathy, N., G. S. Ford, et al. (2003). "GRAIL: An E3 Ubiquitin Ligase that Inhibits Cytokine Gene Transcription Is Expressed in Anergic CD4+ T Cells." Immunity **18**(4): 535-547.

Antonny, B., S. Beraud-Dufour, et al. (1997). "N-terminal hydrophobic residues of the G-protein ADP-ribosylation factor-1 insert into membrane phospholipids upon GDP to GTP exchange." Biochemistry **36**(15): 4675-84.

Aoe, T., E. Cukierman, et al. (1997). "The KDEL receptor, ERD2, regulates intracellular traffic by recruiting a GTPase-activating protein for ARF1." EMBO **16**: 7305-7316.

Appling, D. R. (1999). "Genetic Approaches to the Study of Protein-Protein Interactions." Methods **19**(2): 338-349.

Aridor, M., J. Weissman, et al. (1998). "Cargo Selection by the COPII Budding Machinery during Export from the ER." The Journal of Cell Biology **141**(1): 61-70.

Baldwin, T. C., M. G. Handford, et al. (2001). "Identification and characterization of GONST1, a Golgi-localized GDP-mannose transporter in *Arabidopsis*." Plant Cell **13**(10): 2283-95.

Barlowe, C. (2003). "Signals for COPII-dependent export from the ER: what's the ticket out?" Trends Cell Biol **13**(6): 295-300.

Barth, M. and S. E. Holstein (2004). "Identification and functional characterization of *Arabidopsis* AP180, a binding partner of plant alpha-C-adaptin." J Cell Sci **117**(Pt 10): 2051-2062.

Bassereau, P. "Division of labor in ESCRT complexes." Nat Cell Biol **12**(5): 422-3.

Bassham, D., F. Brandizzi, et al. (2008). The Secretory System of *Arabidopsis*. The *Arabidopsis* Book.

Beck, T., A. Schmidt, et al. (1999). "Starvation Induces Vacuolar Targeting and Degradation of the Tryptophan Permease in Yeast." The Journal of Cell Biology **146**(6): 1227-1238.

Belden, W. J. and C. Barlowe (2001). "Distinct roles for the cytoplasmic tail sequences of Emp24p and Erv25p in transport between the endoplasmic reticulum and Golgi complex." J Biol Chem **276**(46): 43040-8.

Beninati S, F. J. (1988). "Covalent polyamine-protein conjugates: analysis and distribution." Adv Exp Med Biol. **250**: 411-22.

Bethke, P. C., J. E. Lonsdale, et al. (1999). "Hormonally Regulated Programmed Cell Death in Barley Aleurone Cells." Plant Cell **11**(6): 1033-1046.

Bhat, R. A., T. Lahaye, et al. (2006). "The visible touch: in planta visualization of protein-protein interactions by fluorophore-based methods." Plant Methods **2**: 12.

Bocock, J. P., S. Carmicle, et al. (2009). "The PA-TM-RING protein RING finger protein 13 is an endosomal integral membrane E3 ubiquitin ligase whose RING finger domain is released to the cytoplasm by proteolysis." Febs J **276**(7): 1860-77.

Boehm, M. and J. S. Bonifacino (2001). "Adaptins: the final recount." Mol Biol Cell **12**(10): 2907-20.

Boevink, P., B. Martin, et al. (1999). "Transport of virally expressed green fluorescent protein through the secretory pathway in tobacco leaves is inhibited by cold shock and brefeldin A." Planta **208**(3): 392-400.

Boevink, P., K. Oparka, et al. (1998). "Stacks on tracks: the plant Golgi apparatus traffics on an actin/ER network." The Plant Journal **15**(3): 441-447.

Bolwell, G. P. (1988). "Synthesis of cell wall components: Aspects of control." Phytochemistry **27**(5): 1235-1253.

Bonifacino, J. S. and J. H. Hurley (2008). "Retromer." Curr Opin Cell Biol **20**(4): 427-36.

Bonifacino, J. S. and R. Rojas (2006). "Retrograde transport from endosomes to the trans-Golgi network." Nat Rev Mol Cell Biol **7**(8): 568-79.

Borchers, A. G., A. L. Hufton, et al. (2002). "The E3 ubiquitin ligase GREUL1 anteriorizes ectoderm during *Xenopus* development." Dev Biol **251**(2): 395-408.

Borden, K. L. B. and P. S. Freemont (1996). "The RING finger domain: a recent example of a sequence--structure family." Current Opinion in Structural Biology **6**(3): 395-401.

Bork, P. (1991). "Shuffled domains in extracellular proteins." FEBS Lett **286**(1-2): 47-54.

Borner, G. H. H., D. J. Sherrier, et al. (2005). "Analysis of Detergent-Resistant Membranes in *Arabidopsis*. Evidence for Plasma Membrane Lipid Rafts." Plant Physiol. **137**(1): 104-116.

Boston, R. S., P. V. Viitanen, et al. (1996). "Molecular chaperones and protein folding in plants." Plant Mol Biol **32**(1-2): 191-222.

Brandizzi, F., N. Frangne, et al. (2002). "The destination for single-pass membrane proteins is influenced markedly by the length of the hydrophobic domain." Plant Cell **14**(5): 1077-92.

Brandizzi, F., E. L. Snapp, et al. (2002). "Membrane protein transport between the endoplasmic reticulum and the Golgi in tobacco leaves is energy dependent but cytoskeleton independent: evidence from selective photobleaching." Plant Cell **14**(6): 1293-309.

Brent, R. and R. L. Finley, Jr. (1997). "Understanding gene and allele function with two-hybrid methods." Annu Rev Genet **31**: 663-704.

Brent, R. and M. Ptashne (1985). "A eukaryotic transcriptional activator bearing the DNA specificity of a prokaryotic repressor." Cell **43**(3 Pt 2): 729-36.

Brosig, B. and D. Langosch (1998). "The dimerization motif of the glycophorin A transmembrane segment in membranes: Importance of glycine residues." Protein Science **7**(4): 1052-1056.

Brown, D. A. and E. London (1998). "Structure and origin of ordered lipid domains in biological membranes." J Membr Biol **164**(2): 103-14.

Bruinenberg, P. G., P. Doesburg, et al. (1994). "Evidence for a large dispensable segment in the subtilisin-like catalytic domain of the *Lactococcus lactis* cell-envelope proteinas." Protein Engineering **7**(8): 991-996.

Bubeck, J., D. Scheuring, et al. (2008). "The syntaxins SYP31 and SYP81 control ER-Golgi trafficking in the plant secretory pathway." Traffic (Copenhagen, Denmark) **9**(10): 1629-52.

Burgess R., T. N. E., et al (2002). Curr. Opin. Biotechnol. **13:** 304-308.

Cao, X., S. W. Rogers, et al. (2000). "Structural requirements for ligand binding by a probable plant vacuolar sorting receptor." Plant Cell **12**(4): 493-506.

Causier, B. (2004). "Studying the interactome with the yeast two-hybrid system and mass spectrometry." Mass Spectrom Rev **23**(5): 350-67.

Causier, B. and B. Davies (2002). "Analyzing protein-protein interactions with the yeast two-hybrid system." Plant Mol Biol **50**(6): 855-70.

Chen, C. C. and P. P. Cleary (1990). "Complete nucleotide sequence of the streptococcal C5a peptidase gene of Streptococcus pyogenes." J Biol Chem **265**(6): 3161-7.

Chen, Y. A., S. J. Scales, et al. (1999). "SNARE Complex Formation Is Triggered by Ca2+ and Drives Membrane Fusion." Cell **97**(2): 165-174.

Chong, Y. T., S. K. Gidda, et al. (2010). "Characterization of the *Arabidopsis thaliana* exocyst complex gene families by phylogenetic, expression profiling, and subcellular localization studies." New Phytol **185**(2): 401-19.

Craddock, C. P., P. R. Hunter, et al. (2008). "Lack of a vacuolar sorting receptor leads to non-specific missorting of soluble vacuolar proteins in *Arabidopsis* seeds." Traffic **9**(3): 408-16.

Dacks, J. B., P. P. Poon, et al. (2008). "Phylogeny of endocytic components yields insight into the process of nonendosymbiotic organelle evolution." Proceedings of the National Academy of Sciences **105**(2): 588-593.

daSilva, L. L., O. Foresti, et al. (2006). "Targeting of the plant vacuolar sorting receptor BP80 is dependent on multiple sorting signals in the cytosolic tail." Plant Cell **18**(6): 1477-97.

daSilva, L. L. P., E. L. Snapp, et al. (2004). "Endoplasmic Reticulum Export Sites and Golgi Bodies Behave as Single Mobile Secretory Units in Plant Cells." Plant Cell **16**(7): 1753-1771.

Dawson, J. P., J. S. Weinger, et al. (2002). "Motifs of serine and threonine can drive association of transmembrane helices." Journal of Molecular Biology **316**(3): 799-805.

Daxinger, L., B. Hunter, et al. (2008). "Unexpected silencing effects from T-DNA tags in *Arabidopsis*." Trends Plant Sci **13**(1): 4-6.

D'Azzo, A., A. Bongiovanni, et al. (2005). "E3 Ubiquitin Ligases as Regulators of Membrane Protein Trafficking and Degradation." Traffic **6**(6): 429-441.

Dell'Angelica, E. C., C. Mullins, et al. (1999). "AP-4, a novel protein complex related to clathrin adaptors." J Biol Chem **274**(11): 7278-85.

Denecke, J., L. E. Carlsson, et al. (1995). "The Tobacco Homolog of Mammalian Calreticulin Is Present in Protein Complexes *in Vivo*." Plant Cell **7**(4): 391-406.

d'Enfert C, M. G., and C Gaillardin (1992). "Fission yeast and a plant have functional homologues of the Sar1 and Sec12 proteins involved in ER to Golgi traffic in budding yeast
" EMBO J. **11(11)**: 4205–4211.

Deng, L., C. Wang, et al. (2000). "Activation of the I[kappa]B Kinase Complex by TRAF6 Requires a Dimeric Ubiquitin-Conjugating Enzyme Complex and a Unique Polyubiquitin Chain." Cell **103**(2): 351-361.

Dettmer, J., A. Hong-Hermesdorf, et al. (2006). "Vacuolar H+-ATPase activity is required for endocytic and secretory trafficking in *Arabidopsis*." Plant Cell **18**(3): 715-730.

Di Sansebastiano, G. P., N. Paris, et al. (2001). "Regeneration of a lytic central vacuole and of neutral peripheral vacuoles can be visualized by green fluorescent proteins targeted to either type of vacuoles." Plant Physiol **126**(1): 78-86.

Di Sansebastiano, G.-P., N. Paris, et al. (1998). "Specific accumulation of GFP in a non-acidic vacuolar compartment via a C-terminal propeptide-mediated sorting pathway." The Plant Journal **15**(4): 449-457.

DiRita, V. J. (1992). "Co-ordinate expression of virulence genes by ToxR in *Vibrio cholerae*." Mol Microbiol **6**(4): 451-8.

Dominguez, M., K. Dejgaard, et al. (1998). "gp25L/emp24/p24 protein family members of the cis-Golgi network bind both COP I and II coatomer." J Cell Biol **140**(4): 751-65.

Dominguez, R., Y. Freyzon, et al. (1998). "Crystal structure of a vertebrate smooth muscle myosin motor domain and its complex with the essential light chain: visualization of the pre-power stroke state." Cell **94**(5): 559-71.

Donaldson, J. G. and P. S. McPherson (2009). "Membrane trafficking heats up in Pavia." EMBO Rep **10**(2): 132-136.

Donohoe, B. S., B. H. Kang, et al. (2007). "Identification and characterization of COPIa- and COPIb-type vesicle classes associated with plant and algal Golgi." Proc Natl Acad Sci U S A **104**(1): 163-8.

Dulubova, I., S. Sugita, et al. (1999). "A conformational switch in syntaxin during exocytosis: role of munc18." EMBO J **18**(16): 4372-82.

Eakle, K. A., M. Bernstein, et al. (1988). "Characterization of a component of the yeast secretion machinery: identification of the SEC18 gene product." Mol Cell Biol **8**(10): 4098-109.

Ebine, K., Y. Okatani, et al. (2008). "A SNARE Complex Unique to Seed Plants Is Required for Protein Storage Vacuole Biogenesis and Seed Development of *Arabidopsis thaliana*." Plant Cell **20**: 3006-3021.

Ellgaard, L. and A. Helenius (2003). "Quality control in the endoplasmic reticulum." Nature Reviews Molecular Cell Biology **4**(3): 181-191.

Epimashko, S., T. Meckel, et al. (2004). "Two functionally different vacuoles for static and dynamic purposes in one plant mesophyll leaf cell." Plant J **37**(2): 294-300.

Espenshade, P., R. E. Gimeno, et al. (1995). "Yeast SEC16 gene encodes a multidomain vesicle coat protein that interacts with Sec23p." J Cell Biol **131**(2): 311-24.

Fang, Y. and D. L. Spector (2007). "Identification of nuclear dicing bodies containing proteins for microRNA biogenesis in living *Arabidopsis* plants." Curr Biol **17**(9): 818-23.

Fetchko, M. and I. Stagljar (2004). "Application of the split-ubiquitin membrane yeast two-hybrid system to investigate membrane protein interactions." Methods **32**(4): 349-62.

Fields, S. and O. Song (1989). "A novel genetic system to detect protein-protein interactions." Nature **340**(6230): 245-6.

Foresti, O. and J. Denecke (2008). "Intermediate Organelles of the Plant Secretory Pathway: Identity and Function." Traffic **9**(10): 1599-1612.

Förster, T. (1948). "Zwischenmolekulare Energiewanderung und Fluoreszenz." Annalen der Physik **437**(1-2): 55-75.

Fotin, A., Y. Cheng, et al. (2004). "Molecular model for a complete clathrin lattice from electron cryomicroscopy." Nature **432**(7017): 573-9.

Friedhoff, P. (2005). "Mapping protein-protein interactions by bioinformatics and cross-linking." Anal Bioanal Chem **381**(1): 78-80.

Frigerio, L., G. Hinz, et al. (2008). "Multiple vacuoles in plant cells: rule or exception?" Traffic **9**(10): 1564-70.

Garel, J. (1992). "Folding of large proteins: Multidomain and multisubunit proteins." In Creighton, T., editor, Protein Folding, pages 405-454. W.H. Freeman and Company, New York, first edition. .

Geldner, N. and G. Jürgens (2006). "Endocytosis in signaling and development." Curr Opin Plant Biol **9**(6): 589-94.

Geli, M. I., M. Torrent, et al. (1994). "Two Structural Domains Mediate Two Sequential Events in [gamma]-Zein Targeting: Protein Endoplasmic Reticulum Retention and Protein Body Formation." Plant Cell **6**(12): 1911-1922.

Gerst, J. E. (2003). "SNARE regulators: matchmakers and matchbreakers." Biochim Biophys Acta **1641**(2-3): 99-110.

Ghosh, I., A. D. Hamilton, et al. (2000). "Antiparallel Leucine Zipper-Directed Protein Reassembly: Application to the Green Fluorescent Protein." Journal of the American Chemical Society **122**(23): 5658-5659.

Gietl, C. and M. Schmid (2001). "Ricinosomes: an organelle for developmentally regulated programmed cell death in senescing plant tissues." Naturwissenschaften **88**(2): 49-58.

Glick, B. S. (2000). "Organization of the Golgi apparatus." Current Opinion in Cell Biology **12**(4): 450-456.

Glick, B. S. and V. Malhotra (1998). "The Curious Status of the Golgi Apparatus." Cell **95**(7): 883-889.

Gomez, L. and M. J. Chrispeels (1993). "Tonoplast and Soluble Vacuolar Proteins Are Targeted by Different Mechanisms." Plant Cell **5**(9): 1113-1124.

Gommel, D. U., A. R. Memon, et al. (2001). "Recruitment to Golgi membranes of ADP-ribosylation factor 1 is mediated by the cytoplasmic domain of p23." EMBO J **20**(23): 6751-6760.

Gorza, L., R. Menabo, et al. (1996). "Cardiomyocyte troponin T immunoreactivity is modified by cross-linking resulting from intracellular calcium overload." Circulation **93**(10): 1896-904.

Greenwood, J. S., M. Helm, et al. (2005). "Ricinosomes and endosperm transfer cell structure in programmed cell death of the nucellus during Ricinus seed development." Proc Natl Acad Sci U S A **102**(6): 2238-43.

Grinberg, A. V., C. D. Hu, et al. (2004). "Visualization of Myc/Max/Mad family dimers and the competition for dimerization in living cells." Mol Cell Biol **24**(10): 4294-308.

Gyuris, J., E. Golemis, et al. (1993). "Cdi1, a human G1 and S phase protein phosphatase that associates with Cdk2." Cell **75**(4): 791-803.

Hadlington, J. L. and J. Denecke (2000). "Sorting of soluble proteins in the secretory pathway of plants." Curr Opin Plant Biol **3**(6): 461-8.

Hamman, B. D., L. M. Hendershot, et al. (1998). "BiP maintains the permeability barrier of the ER membrane by sealing the luminal end of the translocon pore before and early in translocation." Cell **92**(6): 747-58.

Hanson, P. I. (2000). "Sec1 gets a grip on syntaxin." Nat Struct Mol Biol **7**(5): 347-349.

Hanton, S. L., L. E. Bortolotti, et al. (2005). "Crossing the divide-transport between the endoplasmic reticulum and Golgi apparatus in plants." Traffic **6**(4): 267-77.

Hanton, S. L., L. Chatre, et al. (2007). "*De novo* formation of plant endoplasmic reticulum export sites is membrane cargo induced and signal mediated." Plant Physiol **143**(4): 1640-50.

Hanzawa, H., M. J. de Ruwe, et al. (2001). "The structure of the C4C4 ring finger of human NOT4 reveals features distinct from those of C3HC4 RING fingers." J Biol Chem **276**(13): 10185-90.

Happel, N., S. Honing, et al. (2004). "*Arabidopsis* mu A-adaptin interacts with the tyrosine motif of the vacuolar sorting receptor VSR-PS1." Plant J **37**(5): 678-93.

Hara-Nishimura, I. I., T. Shimada, et al. (1998). "Transport of storage proteins to protein storage vacuoles is mediated by large precursor-accumulating vesicles." Plant Cell **10**(5): 825-36.

Hartl, F. U. (1996). "Molecular chaperones in cellular protein folding." Nature **381**(6583): 571-9.

Hawes, C., A. Osterrieder, et al. (2008). "The plant ER-Golgi interface." Traffic **9**(10): 1571-80.

Hay, J. C. and R. H. Scheller (1997). "SNAREs and NSF in targeted membrane fusion." Current Opinion in Cell Biology **9**(4): 505-512.

Hayashi, M., T. Akazawa, et al. (1988). "Effect of monensin on intracellular transport and posttranslational processing of 11S globulin precursors in developing pumpkin cotyledons." FEBS Letters **238**(1): 197-200.

He, F., F. Huang, et al. (2007). "Protein storage vacuole acidification as a control of storage protein mobilization in soybeans." Journal of Experimental Botany **58**(5): 1059-1070.

Heijne, V. (1990). "the signal peptide." The Journal of Membrane Biology **115**: 195-201.

Helenius A., T. E. S., Herbert D.N. and Simons J.F. (1997). "Calnexin, calreticulin and the folding of glycoproteins." Trends Cell Biol **7**(5): 193-200.

Hellens, R. P., E. A. Edwards, et al. (2000). "pGreen: a versatile and flexible binary Ti vector for *Agrobacterium*-mediated plant transformation." Plant Mol Biol **42**(6): 819-32.

Helms, J. B. and J. E. Rothman (1992). "Inhibition by brefeldin A of a Golgi membrane enzyme that catalyses exchange of guanine nucleotide bound to ARF." Nature **360**(6402): 352-4.

Hennecke, F., A. Muller, et al. (2005). "A ToxR-based two-hybrid system for the detection of periplasmic and cytoplasmic protein-protein interactions in *Escherichia coli*: minimal requirements for specific DNA binding and transcriptional activation." Protein Eng Des Sel **18**(10): 477-86.

Hepler, P. K., B. A. Palevitz, et al. (1990). "Cortical endoplasmic reticulum in plants." J Cell Sci **96**(3): 355-373.

Herman, E. M. and B. A. Larkins (1999). "Protein storage bodies and vacuoles." Plant Cell **11**(4): 601-14.

Hill, R. L. and K. Brew (1975). "Lactose synthetase." Adv Enzymol Relat Areas Mol Biol **43**: 411-90.

Hiller, M. M., A. Finger, et al. (1996). "ER degradation of a misfolded luminal protein by the cytosolic ubiquitin-proteasome pathway." Science **273**(5282): 1725-8.

Hillmer, S., A. Movafeghi, et al. (2001). "Vacuolar storage proteins are sorted in the cis-cisternae of the pea cotyledon Golgi apparatus." J Cell Biol **152**(1): 41-50.

Hinz, G., S. Colanesi, et al. (2007). "Localization of vacuolar transport receptors and cargo proteins in the Golgi apparatus of developing *Arabidopsis* embryos." Traffic **8**(10): 1452-64.

Hinz, G., A. Menze, et al. (1997). "Isolation of prolegumin from developing pea seeds: its binding to endomembranes and assembly into prolegumin hexamers in the protein storage vacuole." Journal of Experimental Botany **48**(1): 139-149.

Hirst, J., N. A. Bright, et al. (1999). "Characterization of a Fourth Adaptor-related Protein Complex." Mol. Biol. Cell **10**(8): 2787-2802.

Hirst, J. and M. S. Robinson (1998). "Clathrin and adaptors." Biochim Biophys Acta **1404**(1-2): 173-93.

Hoh, B., G. Hinz, et al. (1995). "Protein storage vacuoles form de novo during pea cotyledon development." J Cell Sci **108 (Pt 1)**: 299-310.

Holwerda, B. C., H. S. Padgett, et al. (1992). "Proaleurain vacuolar targeting is mediated by short contiguous peptide interactions." Plant Cell **4**(3): 307-18.

Honing, S., I. V. Sandoval, et al. (1998). "A di-leucine-based motif in the cytoplasmic tail of LIMP-II and tyrosinase mediates selective binding of AP-3." EMBO J **17**(5): 1304-14.

Hu, C.-D., Y. Chinenov, et al. (2002). "Visualization of Interactions among bZIP and Rel Family Proteins in Living Cells Using Bimolecular Fluorescence Complementation." Molecular Cell **9**(4): 789-798.

Hu CD, K. T. (2003). "Simultaneous visualization of multiple protein interactions in living cells using multicolor fluorescence complementation analysis." Nat Biotechnol **21**: 539-545.

Huang, M., J. T. Weissman, et al. (2001). "Crystal structure of Sar1-GDP at 1.7 Ã… resolution and the role of the NH2 terminus in ER export." The Journal of Cell Biology **155**(6): 937-948.

Huang, M., J. T. Weissman, et al. (2001). "Crystal structure of Sar1-GDP at 1.7 A resolution and the role of the NH2 terminus in ER export." J Cell Biol **155**(6): 937-948.

Hummel, E., R. Schmickl, et al. (2007). "Brefeldin A action and recovery in *Chlamydomonas* are rapid and involve fusion and fission of Golgi cisternae." Plant Biol (Stuttg) **9**(4): 489-501.

Hunter, P. R., C. P. Craddock, et al. (2007). "Fluorescent reporter proteins for the tonoplast and the vacuolar lumen identify a single vacuolar compartment in *Arabidopsis* cells." Plant Physiol **145**(4): 1371-82.

Hurtley, S. M. and A. Helenius (1989). "Protein oligomerization in the endoplasmic reticulum." Annu Rev Cell Biol **5**: 277-307.

Hwang, I. (2008). "Sorting and Anterograde Trafficking at the Golgi Apparatus." Plant Physiol. **148**(2): 673-683.

Inoue, Y., T. Suzuki, et al. (2006). "AtATG Genes, Homologs of Yeast Autophagy Genes, are Involved in Constitutive Autophagy in *Arabidopsis* Root Tip Cells." Plant and Cell Physiology **47**(12): 1641-1652.

Iwata, Y. and N. Koizumi (2005). "An *Arabidopsis* transcription factor, AtbZIP60, regulates the endoplasmic reticulum stress response in a manner unique to plants." Proc Natl Acad Sci U S A **102**(14): 5280-5.

Jackson, C. L. (2009). "Mechanisms of transport through the Golgi complex." J Cell Sci **122**(4): 443-452.

Jackson, P. K., A. G. Eldridge, et al. (2000). "The lore of the RINGs: substrate recognition and catalysis by ubiquitin ligases." Trends in Cell Biology **10**(10): 429-439.

Jauh, G.-Y., A. M. Fischer, et al. (1998). "Î´-Tonoplast intrinsic protein defines unique plant vacuole functions." Proceedings of the National Academy of Sciences of the United States of America **95**(22): 12995-12999.

Jauh GY, T. P., and JC Rogers (1999). "Tonoplast intrinsic protein isoforms as markers for vacuolar functions." Plant Cell.(11): 1867–1882.

Jiang, L., T. E. Phillips, et al. (2001). "The protein storage vacuole: a unique compound organelle." J Cell Biol **155**(6): 991-1002.

Jiang, L., T. E. Phillips, et al. (2000). "Biogenesis of the protein storage vacuole crystalloid." J Cell Biol **150**(4): 755-70.

Jiang, L. and J. C. Rogers (1998). "Integral membrane protein sorting to vacuoles in plant cells: evidence for two pathways." J Cell Biol **143**(5): 1183-99.

Jiang LW, R. J. (2003). "Sorting of Lytic Enzymes in the Plant Golgi Apparatus Oxford: Blackwell Publishing." Annual Plant Reviews **9**: 144-136.

Joazeiro, C. A. P., S. S. Wing, et al. (1999). "The Tyrosine Kinase Negative Regulator c-Cbl as a RING-Type, E2-Dependent Ubiquitin-Protein Ligase." Science **286**(5438): 309-312.

Johanson, U., M. Karlsson, et al. (2001). "The Complete Set of Genes Encoding Major Intrinsic Proteins in *Arabidopsis* Provides a Framework for a New Nomenclature for Major Intrinsic Proteins in Plants." Plant Physiol. **126**(4): 1358-1369.

Jürgens, G. (2004). "Membrane trafficking in plants." Annu Rev Cell Dev Biol **20**: 481-504.

Jürgens, G. and N. Geldner (2007). "The high road and the low road: trafficking choices in plants." Cell **130**(6): 977-9.

Kaiser, P., K. Flick, et al. (2000). "Regulation of Transcription by Ubiquitination without Proteolysis: Cdc34/SCFMet30-Mediated Inactivation of the Transcription Factor Met4." Cell **102**(3): 303-314.

Kalthoff, C., S. Groos, et al. (2002). "Clint: a novel clathrin-binding ENTH-domain protein at the Golgi." Mol Biol Cell **13**(11): 4060-73.

Kappeler, F., D. R. C. Klopfenstein, et al. (1997). "The Recycling of ERGIC-53 in the Early Secretory Pathway." Journal of Biological Chemistry **272**(50): 31801-31808.

Karpova, T. S., C. T. Baumann, et al. (2003). "Fluorescence resonance energy transfer from cyan to yellow fluorescent protein detected by acceptor photobleaching using confocal microscopy and a single laser." J Microsc **209**(Pt 1): 56-70.

Katoh, S., C. Hong, et al. (2003). "High precision NMR structure and function of the RING-H2 finger domain of EL5, a rice protein whose expression is increased upon exposure to pathogen-derived oligosaccharides." J Biol Chem **278**(17): 15341-8.

Katoh, S., Y. Tsunoda, et al. (2005). "Active Site Residues and Amino Acid Specificity of the Ubiquitin Carrier Protein-binding RING-H2 Finger Domain." Journal of Biological Chemistry **280**(49): 41015-41024.

Katzmann, D. J., M. Babst, et al. (2001). "Ubiquitin-dependent sorting into the multivesicular body pathway requires the function of a conserved endosomal protein sorting complex, ESCRT-I." Cell **106**(2): 145-55.

Kerppola, T. K. (2008). "Bimolecular fluorescence complementation: visualization of molecular interactions in living cells." Methods Cell Biol **85**: 431-70.

Kerr, P. and A. Ashworth (2001). "New complexities for BRCA1 and BRCA2." Curr Biol **11**(16): R668-76.

Kim, C. S., Y. M. Woo Ym, et al. (2002). "Zein protein interactions, rather than the asymmetric distribution of zein mRNAs on endoplasmic reticulum membranes, influence protein body formation in maize endosperm." Plant Cell **14**(3): 655-72.

Kim, H., H. Kang, et al. "Homomeric Interaction of AtVSR1 Is Essential for Its Function as a Vacuolar Sorting Receptor." Plant Physiol. **154**(1): 134-148.

Kirchhausen, T. (2000). "Three ways to make a vesicle." Nat Rev Mol Cell Biol **1**(3): 187-98.

Kirsch, T., N. Paris, et al. (1994). "Purification and initial characterization of a potential plant vacuolar targeting receptor." Proc Natl Acad Sci U S A **91**(8): 3403-7.

Kirsch, T., G. Saalbach, et al. (1996). "Interaction of a potential vacuolar targeting receptor with amino- and carboxyl-terminal targeting determinants." Plant Physiol **111**(2): 469-74.

Klauer, S. F. and V. R. Franceschi (1997). "Mechanism of transport of vegetative storage proteins to the vacuole of the paraveinal mesophyll of soybean leaf." Protoplasma **200**(3): 174-185.

Koide, Y., K. Matsuoka, et al. (1999). "The N-terminal propeptide and the C- terminus of the precursor to 20-kilo-dalton potato tuber protein can function as different types of vacuolar sorting signals." Plant Cell Physiol **40**(11): 1152-9.

Krukonis, E. S., R. R. Yu, et al. (2000). "The *Vibrio cholerae* ToxR/TcpP/ToxT virulence cascade: distinct roles for two membrane-localized transcriptional activators on a single promoter." Mol Microbiol **38**(1): 67-84.

Lakatos, L., G. Szittya, et al. (2004). "Molecular mechanism of RNA silencing suppression mediated by p19 protein of tombusviruses." EMBO J **23**(4): 876-84.

Lam, S. K., C. L. Siu, et al. (2007). "Rice SCAMP1 Defines Clathrin-Coated, trans-Golgi-Located Tubular-Vesicular Structures as an Early Endosome in Tobacco BY-2 Cells." Plant Cell **19**(1): 296-319.

Lam, S. K., Y. C. Tse, et al. (2007). "Molecular Characterization of Plant Prevacuolar and Endosomal Compartments." Journal of Integrative Plant Biology **49**(8): 1119-1128.

Langhans, M., C. Hawes, et al. (2007). "Golgi regeneration after brefeldin A treatment in BY-2 cells entails stack enlargement and cisternal growth followed by division." Plant Physiol **145**(2): 527-38.

Latijnhouwers, M., T. Gillespie, et al. (2007). "Localization and domain characterization of *Arabidopsis* golgin candidates." J Exp Bot **58**(15-16): 4373-86.

Latijnhouwers, M., C. Hawes, et al. (2005). "Holding it all together? Candidate proteins for the plant Golgi matrix." Curr Opin Plant Biol **8**(6): 632-9.

Lawrence, C. M., S. Ray, et al. (1999). "Crystal structure of the ectodomain of human transferrin receptor." Science **286**(5440): 779-82.

Lemmon, M. A. and D. M. Engelman (1994). "Specificity and promiscuity in membrane helix interactions." Q Rev Biophys **27**(2): 157-218.

Letourneur, F., E. C. Gaynor, et al. (1994). "Coatomer is essential for retrieval of dilysine-tagged proteins to the endoplasmic reticulum." Cell **79**(7): 1199-207.

Lewis, B. A. and D. M. Engelman (1983). "Bacteriorhodopsin remains dispersed in fluid phospholipid bilayers over a wide range of bilayer thicknesses." Journal of Molecular Biology **166**(2): 203-210.

Liu, J.-X., R. Srivastava, et al. (2007). "Salt stress responses in *Arabidopsis* utilize a signal transduction pathway related

to endoplasmic reticulum stress signaling." The Plant Journal **51**(5): 897-909.

Liu, Y., M. Schiff, et al. (2005). "Autophagy regulates programmed cell death during the plant innate immune response." Cell **121**(4): 567-77.

Lorick, K. L., J. P. Jensen, et al. (1999). "RING fingers mediate ubiquitin-conjugating enzyme (E2)-dependent ubiquitination." Proc Natl Acad Sci U S A **96**(20): 11364-9.

Losev, E., C. A. Reinke, et al. (2006). "Golgi maturation visualized in living yeast." Nature **441**(7096): 1002-6.

Lovering, R., I. M. Hanson, et al. (1993). "Identification and preliminary characterization of a protein motif related to the zinc finger." Proc Natl Acad Sci U S A **90**(6): 2112-6.

Luan, S. (2002). "Tyrosine phosphorylation in plant cell signaling." Proceedings of the National Academy of Sciences of the United States of America **99**(18): 11567-11569.

Luo, X. and K. Hofmann (2001). "The protease-associated domain: a homology domain associated with multiple classes of proteases." Trends in Biochemical Sciences **26**(3): 147-148.

Ma, J. and M. Ptashne (1988). "Converting a eukaryotic transcriptional inhibitor into an activator." Cell **55**(3): 443-446.

Mahon, P. and A. Bateman (2000). "The PA domain: a protease-associated domain." Protein Sci **9**(10): 1930-4.

Mainieri, D., M. Rossi, et al. (2004). "Zeolin. A new recombinant storage protein constructed using maize gamma-zein and bean phaseolin." Plant Physiol **136**(3): 3447-56.

Malhotra, J. D. and R. J. Kaufman (2007). "The endoplasmic reticulum and the unfolded protein response." Semin Cell Dev Biol **18**(6): 716-31.

Malhotra, V., L. Orci, et al. (1988). "Role of an N-ethylmaleimide-sensitive transport component in promoting fusion of transport vesicles with cisternae of the Golgi stack." Cell **54**(2): 221-7.

Malkus, P., F. Jiang, et al. (2002). "Concentrative sorting of secretory cargo proteins into COPII-coated vesicles." J Cell Biol **159**(6): 915-21.

Martínez-Hackert, E. and A. M. Stock (1997). "Structural relationships in the OmpR family of winged-helix transcription factors." Journal of Molecular Biology **269**(3): 301-312.

Marty, F. (1978). "Cytochemical studies on GERL, provacuoles, and vacuoles in root meristematic cells of Euphorbia." Proc Natl Acad Sci U S A **75**(2): 852-6.

Marty, F. (1999). "Plant vacuoles." Plant Cell **11**(4): 587-600.

Matheson, L. A., S. L. Hanton, et al. (2006). "Traffic between the plant endoplasmic reticulum and Golgi apparatus: to the Golgi and beyond." Current Opinion in Plant Biology **9**(6): 601-609.

Matsuoka, K., D. C. Bassham, et al. (1995). "Different sensitivity to wortmannin of two vacuolar sorting signals indicates the presence of distinct sorting machineries in tobacco cells." J Cell Biol **130**(6): 1307-18.

Matsuoka, K. and J.-M. Neuhaus (1999). "Cis-elements of protein transport to the plant vacuoles." Journal of Experimental Botany **50**(331): 165-174.

Matsuura-Tokita, K., M. Takeuchi, et al. (2006). "Live imaging of yeast Golgi cisternal maturation." Nature **441**(7096): 1007-1010.

Meckel, T., A. C. Hurst, et al. (2004). "Endocytosis against high turgor: intact guard cells of *Vicia faba* constitutively endocytose fluorescently labelled plasma membrane and GFP-tagged K-channel KAT1." Plant J **39**(2): 182-93.

Melia, T. J., T. Weber, et al. (2002). "Regulation of membrane fusion by the membrane-proximal coil of the t-SNARE during zippering of SNAREpins." J Cell Biol **158**(5): 929-40.

Miao, Y., P. K. Yan, et al. (2006). "Localization of Green Fluorescent Protein Fusions with the Seven *Arabidopsis*

Vacuolar Sorting Receptors to Prevacuolar Compartments in Tobacco BY-2 Cells." Plant Physiol. **142**(3): 945-962.

Michael, D. and M. Oren (2002). "The p53 and Mdm2 families in cancer." Current Opinion in Genetics & Development **12**(1): 53-59.

Miller, E. A. a. A., M. A. (1999). "Uncoating the mechanisms of vacuolar protein transport." Trends in Plant Science **4**: 46-48.

Miyashita, N., J. E. Straub, et al. (2009). "Transmembrane structures of amyloid precursor protein dimer predicted by replica-exchange molecular dynamics simulations." J Am Chem Soc **131**(10): 3438-9.

Movafeghi, A., N. Happel, et al. (1999). "*Arabidopsis* Sec21p and Sec23p homologs. Probable coat proteins of plant COP-coated vesicles." Plant Physiol **119**(4): 1437-46.

Mukhopadhyay, D. and H. Riezman (2007). "Proteasome-independent functions of ubiquitin in endocytosis and signaling." Science **315**(5809): 201-5.

Munro (1995). "A comparison of the transmembrane domains of Golgi and plasma membrane proteins." Biochem. Soc. Trans. **23**: 527-530.

Murphy AS, A. B., Susanne E. Holstein, Wendy A. Peer (2005). "ENDOCYTOTIC CYCLING OF PM PROTEINS." Annual Review of Plant Biology **56**: 221 -251

Nebenfuhr, A., L. A. Gallagher, et al. (1999). "Stop-and-go movements of plant Golgi stacks are mediated by the acto-myosin system." Plant Physiol **121**(4): 1127-42.

Neuhaus, J. M., M. Pietrzak, et al. (1994). "Mutation analysis of the C-terminal vacuolar targeting peptide of tobacco chitinase: low specificity of the sorting system, and gradual transition between intracellular retention and secretion into the extracellular space." Plant J **5**(1): 45-54.

Nielsen, K. J., J. M. Hill, et al. (1996). "Synthesis and Structure Determination by NMR of a Putative Vacuolar Targeting Peptide and Model of a Proteinase Inhibitor from *Nicotiana*." Biochemistry **35**(2): 369-378.

Niemes, S., M. Labs, et al. "Sorting of plant vacuolar proteins is initiated in the ER." Plant J **62**(4): 601-14.

Nishimura, N. and W. E. Balch (1997). "A Di-Acidic Signal Required for Selective Export from the Endoplasmic Reticulum." Science **277**(5325): 556-558.

Nufer, O., S. Guldbrandsen, et al. (2002). "Role of cytoplasmic C-terminal amino acids of membrane proteins in ER export." J Cell Sci **115**(Pt 3): 619-28.

Nufer, O., F. Kappeler, et al. (2003). "ER export of ERGIC-53 is controlled by cooperation of targeting determinants in all three of its domains." J Cell Sci **116**(Pt 21): 4429-40.

Ohad, N., K. Shichrur, et al. (2007). "The analysis of protein-protein interactions in plants by bimolecular fluorescence complementation." Plant Physiol **145**(4): 1090-9.

Olbrich, A., S. Hillmer, et al. (2007). "Newly formed vacuoles in root meristems of barley and pea seedlings have characteristics of both protein storage and lytic vacuoles." Plant Physiol **145**(4): 1383-94.

Oliviusson, P., O. Heinzerling, et al. (2006). "Plant retromer, localized to the prevacuolar compartment and microvesicles in *Arabidopsis*, may interact with vacuolar sorting receptors." Plant Cell **18**(5): 1239-52.

Orlando, V., H. Strutt, et al. (1997). "Analysis of chromatin structure by *in vivo* formaldehyde cross-linking." Methods **11**(2): 205-14.

Otegui, M. S., R. Herder, et al. (2006). "The proteolytic processing of seed storage proteins in *Arabidopsis* embryo cells starts in the multivesicular bodies." Plant Cell **18**(10): 2567-81.

Otegui, M. S., Y. S. Noh, et al. (2005). "Senescence-associated vacuoles with intense proteolytic activity develop in leaves of *Arabidopsis* and soybean." Plant J **41**(6): 831-44.

Paris, N. and J. M. Neuhaus (2002). "BP-80 as a vacuolar sorting receptor." Plant Mol Biol **50**(6): 903-14.

Paris, N., S. W. Rogers, et al. (1997). "Molecular cloning and further characterization of a probable plant vacuolar sorting receptor." Plant Physiol **115**(1): 29-39.

Paris, N., C. M. Stanley, et al. (1996). "Plant cells contain two functionally distinct vacuolar compartments." Cell **85**(4): 563-72.

Park, J. H., M. Oufattole, et al. (2007). "Golgi-mediated vacuolar sorting in plant cells: RMR proteins are sorting receptors for the protein aggregation/membrane internalization pathway." Plant Science **172**(4): 728-745.

Park, M., D. Lee, et al. (2005). "AtRMR1 functions as a cargo receptor for protein trafficking to the protein storage vacuole." The Journal of Cell Biology **170**(5): 757-767.

Patterson, G. H., K. Hirschberg, et al. (2008). "Transport through the Golgi Apparatus by Rapid Partitioning within a Two-Phase Membrane System." Cell **133**(6): 1055-1067.

Pelham, H. R. (1988). "Evidence that luminal ER proteins are sorted from secreted proteins in a post-ER compartment." EMBO J **7**(4): 913-8.

Peremyslov, V. V., Y. W. Pan, et al. (2004). "Movement protein of a closterovirus is a type III integral transmembrane protein localized to the endoplasmic reticulum." J Virol **78**(7): 3704-9.

Phizicky, E. M. and S. Fields (1995). "Protein-protein interactions: methods for detection and analysis." Microbiol Rev **59**(1): 94-123.

Pimpl, P., S. L. Hanton, et al. (2003). "The GTPase ARF1p controls the sequence-specific vacuolar sorting route to the lytic vacuole." Plant Cell **15**(5): 1242-56.

Pimpl, P., A. Movafeghi, et al. (2000). "*In situ* localization and *in vitro* induction of plant COPI-coated vesicles." Plant Cell **12**(11): 2219-36.

Porpaczy, Z., B. Sumegi, et al. (1983). "Association between the alpha-ketoglutarate dehydrogenase complex and succinate thiokinase." Biochim Biophys Acta **749**(2): 172-9.

Puertollano, R. (2004). "Clathrin-mediated transport: assembly required. Workshop on Molecular Mechanisms of Vesicle Selectivity." EMBO Rep **5**(10): 942-6.

Puri, S., H. Telfer, et al. (2004). "Dispersal of Golgi matrix proteins during mitotic Golgi disassembly." J Cell Sci **117**(Pt 3): 451-6.

Rapoport, I., Y. C. Chen, et al. (1998). "Dileucine-based sorting signals bind to the beta chain of AP-1 at a site distinct and regulated differently from the tyrosine-based motif-binding site." EMBO J **17**(8): 2148-55.

Raposo, G. and M. S. Marks (2007). "Melanosomes--dark organelles enlighten endosomal membrane transport." Nat Rev Mol Cell Biol **8**(10): 786-97.

Rawlings, N. D. and A. J. Barrett (1997). "Structure of membrane glutamate carboxypeptidase." Biochim Biophys Acta **1339**(2): 247-52.

Richardson, J. S. (1981). "The anatomy and taxonomy of protein structure." Adv Protein Chem **34**: 167-339.

Robinson D.G., H. M.-C., Bubeck J., Pepperkok R. and Ritzenthaler C. (2007). "Membrane Dynamics in the Early Secretory Pathway " Crit Rev Plant Sci **26**: 199-225.

Robinson, D. G., Hoh, B., Hinz, G., and Jeong, B.K. (1995). "One vacuole or two vacuoles: Do protein storage vacuoles arise *de novo* during pea cotyledon development? ." J. Plant Physiol **145**: 654-664.

Robinson, D. G., L. Jiang, et al. (2008). "The Endosomal System of Plants: Charting New and Familiar Territories." Plant Physiol. **147**(4): 1482-1492.

Robinson, D. G., P. Oliviusson, et al. (2005). "Protein sorting to the storage vacuoles of plants: a critical appraisal."

Traffic (Copenhagen, Denmark) **6**(8): 615-25.

Rodionov, D. G. and O. Bakke (1998). "Medium Chains of Adaptor Complexes AP-1 and AP-2 Recognize Leucine-based Sorting Signals from the Invariant Chain." Journal of Biological Chemistry **273**(11): 6005-6008.

Rojo, E., J. Zouhar, et al. (2003). "The AtC-VPS Protein Complex Is Localized to the Tonoplast and the Prevacuolar Compartment in *Arabidopsis*." Mol. Biol. Cell **14**(2): 361-369.

Rojo E., G. C. S., Kovaleva V., Somerville C.R. and Raikhel N.V. (2001). "VACUOLELESS1 is an essential gene required for vacuole formation and morphogenesis in *Arabidopsis*." Developmental Cell **1**: 303-310.

Rothman, J. E. (1994). "Mechanism of intracellular protein transport." Nature **372**(6501): 55-63.

Rothman, J. E. and T. H. Söllner (1997). "Throttles and Dampers: Controlling the Engine of Membrane Fusion." Science **276**: 1212-1213.

Rothman, J. E. and F. T. Wieland (1996). "Protein sorting by transport vesicles." Science **272**: 227-234.

Rotin, D., O. Staub, et al. (2000). "Ubiquitination and endocytosis of plasma membrane proteins: Role of Nedd4/Rsp5p family of ubiquitin-protein ligases." Journal of Membrane Biology **176**(1): 1-17.

Russinova, E., J. W. Borst, et al. (2004). "Heterodimerization and endocytosis of *Arabidopsis* brassinosteroid receptors BRI1 and AtSERK3 (BAK1)." Plant Cell **16**(12): 3216-29.

Rutkowski, D. T. and R. J. Kaufman (2004). "A trip to the ER: coping with stress." Trends in Cell Biology **14**(1): 20-28.

Saalbach, G., R. Jung, et al. (1991). "Different Legumin Protein Domains Act as Vacuolar Targeting Signals." Plant Cell **3**(7): 695-708.

Samaj, J., F. Baluska, et al. (2004). "Endocytosis, actin cytoskeleton, and signaling." Plant Physiol **135**(3): 1150-61.

Samaj, J., N. D. Read, et al. (2005). "The endocytic network in plants." Trends in Cell Biology **15**(8): 425-433.

Samalova, M., M. Fricker, et al. (2006). "Ratiometric fluorescence-imaging assays of plant membrane traffic using polyproteins." Traffic **7**(12): 1701-23.

Sanderfoot, A. (2007). "Increases in the Number of SNARE Genes Parallels the Rise of Multicellularity among the Green Plants." Plant Physiol: pp.106.092973.

Sanderfoot, A. A., S. U. Ahmed, et al. (1998). "A putative vacuolar cargo receptor partially colocalizes with atPEP12p on a prevacuolar compartment in *Arabidopsis* roots." Proceedings of the National Academy of Sciences of the United States of America **95**(17): 9920-9925.

Sanderfoot, A. A. and N. V. Raikhel (1999). "The specificity of vesicle trafficking: Coat proteins and SNAREs." Plant Cell **11**(4): 629-641.

Sanmartin, M., A. Ordonez, et al. (2007). "Divergent functions of VTI12 and VTI11 in trafficking to storage and lytic vacuoles in *Arabidopsis*." PNAS **104**(9): 3645-3650.

Sato, M. H., N. Nakamura, et al. (1997). "The atVAM3 encodes a syntaxin-related molecule implicated in the vacuolar assembly in *Arabidopsis thaliana*." Journal of Biological Chemistry **272**(39): 24530-24535.

Saurin, A. J., K. L. B. Borden, et al. (1996). "Does this have a familiar RING?" Trends in Biochemical Sciences **21**(6): 208-214.

Savageau, M. A. (1986). "Proteins of Escherichia coli come in sizes that are multiples of 14 kDa: domain concepts and evolutionary implications." Proceedings of the National Academy of Sciences of the United States of America **83**(5): 1198-1202.

Schoberer, J., U. Vavra, et al. (2009). "Arginine/lysine residues in the cytoplasmic tail promote ER export of plant glycosylation enzymes." Traffic **10**(1): 101-15.

Seaman, M. N. J., E. G. Marcusson, et al. (1997). "Endosome to Golgi Retrieval of the Vacuolar Protein Sorting Receptor, Vps10p, Requires the Function of the VPS29, VPS30, and VPS35 Gene Products." The Journal of Cell Biology **137**(1): 79-92.

Serafini-Fracassini, D. and S. Del Duca (2008). "Transglutaminases: Widespread Cross-linking Enzymes in Plants." Annals of Botany **102**(2): 145-152.

Sharpe, H. J., T. J. Stevens, et al. "A Comprehensive Comparison of Transmembrane Domains Reveals Organelle-Specific Properties." Cell **142**(1): 158-169.

Shimada, T., K. Fuji, et al. (2003). "Vacuolar sorting receptor for seed storage proteins in *Arabidopsis thaliana*." PNAS **100**(26): 16095-16100.

Shimada, T., N. Hiraiwa, et al. (1994). "Vacuolar processing enzyme of soybean that converts proproteins to the corresponding mature forms." Plant Cell Physiol **35**(4): 713-718.

Shimada, T., Y. Koumoto, et al. (2006). "AtVPS29, a Putative Component of a Retromer Complex, is Required for the Efficient Sorting of Seed Storage Proteins." Plant Cell Physiol **47**(9): 1187-1194.

Shimoi, W., I. Ezawa, et al. (2005). "p125 is localized in endoplasmic reticulum exit sites and involved in their organization." J Biol Chem **280**(11): 10141-8.

Shorter, J. and G. Warren (2002). "Golgi architecture and inheritance." Annual Review of Cell and Developmental Biology **18**: 379-420.

Shyu, Y. J., H. Liu, et al. (2006). "Identification of new fluorescent protein fragments for bimolecular fluorescence complementation analysis under physiological conditions." Biotechniques **40**(1): 61-6.

Siezen, R. J. and J. A. Leunissen (1997). "Subtilases: the superfamily of subtilisin-like serine proteases." Protein Sci **6**(3): 501-23.

Sobhanifar (2003). "Yeast Two Hybrid Assay: A Fishing Tale." Bio Teach journal **1** 81-88.

Song, J., M. H. Lee, et al. (2006). "*Arabidopsis* EPSIN1 Plays an Important Role in Vacuolar Trafficking of Soluble Cargo Proteins in Plant Cells via Interactions with Clathrin, AP-1, VTI11, and VSR1." Plant Cell **18**(9): 2258-2274.

Stagljar, I., C. Korostensky, et al. (1998). "A genetic system based on split-ubiquitin for the analysis of interactions between membrane proteins in vivo." Proc Natl Acad Sci U S A **95**(9): 5187-92.

Stepp, J. D., K. Huang, et al. (1997). "The yeast adaptor protein complex, AP-3, is essential for the efficient delivery of alkaline phosphatase by the alternate pathway to the vacuole." J Cell Biol **139**(7): 1761-74.

Stone, S. L., H. Hauksdottir, et al. (2005). "Functional Analysis of the RING-Type Ubiquitin Ligase Family of *Arabidopsis*." Plant Physiol. **137**(1): 13-30.

Swanson SJ, P. B., and RL Jones (1998). "Barley aleurone cells contain two types of vacuoles. Characterization Of lytic organelles by use of fluorescent probes " Plant Cell **10**: 685-698.

Takeuchi, M., M. Tada, et al. (1998). "Isolation of a tobacco cDNA encoding Sar1 GTPase and analysis of its dominant mutations in vesicular traffic using a yeast complementation system." Plant Cell Physiol **39**(6): 590-9.

Tamura, K., T. Shimada, et al. (2003). "Why green fluorescent fusion proteins have not been observed in the vacuoles of higher plants." Plant J **35**(4): 545-55.

Tse, Y. C., B. Mo, et al. (2004). "Identification of multivesicular bodies as prevacuolar compartments in *Nicotiana tabacum* BY-2 cells." Plant Cell **16**(3): 672-93.

Tsien, R. Y. (1998). "The green fluorescent protein." Annual Review of Biochemistry **67**: 509-544.

Tzfira, T., M. Vaidya, et al. (2004). "Involvement of targeted proteolysis in plant genetic transformation by *Agrobacterium*." Nature **431**(7004): 87-92.

Uemura, T., T. Ueda, et al. (2004). "Systematic analysis of SNARE molecules in *Arabidopsis*: dissection of the post-Golgi network in plant cells." Cell Struct Funct **29**(2): 49-65.

Uemura, T., T. Ueda, et al. (2004). "Systematic analysis of SNARE molecules in *Arabidopsis*: dissection of the post-Golgi network in plant cells." Cell Struct Funct **29**(2): 49-65.

Van der Wilden, W., E. M. Herman, et al. (1980). "Protein bodies of mung bean cotyledons as autophagic organelles." Proceedings of the National Academy of Sciences of the United States of America **77**(1): 428-432.

van Ijzendoorn, S. C. D. (2006). "Recycling endosomes." J Cell Sci **119**(9): 1679-1681.

Vasilescu, J., X. Guo, et al. (2004). "Identification of protein-protein interactions using *in vivo* cross-linking and mass spectrometry." Proteomics **4**(12): 3845-54.

Vitale, A. and R. S. Boston (2008). "Endoplasmic reticulum quality control and the unfolded protein response: insights from plants." Traffic.

Vitale, A. and A. Ceriotti (2004). "Protein Quality Control Mechanisms and Protein Storage in the Endoplasmic Reticulum. A Conflict of Interests?" Plant Physiol. **136**(3): 3420-3426.

Vitale, A., A. Ceriotti, et al. (1993). "The role of the endoplasmic reticulum in protein synthesis, modification and intracellular transport - review article." J Exp Bot **44**(266): 1417-1444.

Vitale, A. and M. J. Chrispeels (1992). "Sorting of Proteins to the Vacuoles of Plant Cells." Bioessays **14**(3): 151-160.

Vitale, A. and J. Denecke (1999). "The endoplasmic reticulum - Gateway of the secretory pathway." Plant Cell **11**(4): 615-628.

Vitale, A. and N. V. Raikhel (1999). "What do proteins need to reach different vacuoles?" Trends in Plant Science **4**(4): 149-155.

Voinnet, O., S. Rivas, et al. (2003). "An enhanced transient expression system in plants based on suppression of gene silencing by the p19 protein of tomato bushy stunt virus." Plant J **33**(5): 949-56.

Wang, J., Y. Li, et al. (2007). "Protein Mobilization in Germinating Mung Bean Seeds Involves Vacuolar Sorting Receptors and Multivesicular Bodies." Plant Physiol.: pp.107.096263.

Waterman, H., G. Levkowitz, et al. (1999). "The RING finger of c-Cbl mediates desensitization of the epidermal growth factor receptor." J Biol Chem **274**(32): 22151-4.

Waters, M. G., T. Serafini, et al. (1991). "'Coatomer': a cytosolic protein complex containing subunits of non-clathrin-coated Golgi transport vesicles." Nature **349**(6306): 248-51.

Weber, J., S. Wilke-Mounts, et al. (1993). "Specific placement of tryptophan in the catalytic sites of *Escherichia coli* F1-ATPase provides a direct probe of nucleotide binding: maximal ATP hydrolysis occurs with three sites occupied." J Biol Chem **268**(27): 20126-33.

Weber, T., B. V. Zemelman, et al. (1998). "SNAREpins: minimal machinery for membrane fusion." Cell **92**(6): 759-72.

Wee, E. G. T., D. J. Sherrier, et al. (1998). "Targeting of Active Sialyltransferase to the Plant Golgi Apparatus." Plant Cell **10**(10): 1759-1768.

Wetlaufer, D. B. (1973). "Nucleation, rapid folding, and globular intrachain regions in proteins." Proc Natl Acad Sci U S A **70**(3): 697-701.

Whittle, J. R. and T. U. Schwartz "Structure of the Sec13-Sec16 edge element, a template for assembly of the COPII vesicle coat." J Cell Biol **190**(3): 347-61.

Xu, Y., D. W. Piston, et al. (1999). "A bioluminescence resonance energy transfer (BRET) system: application to interacting circadian clock proteins." Proc Natl Acad Sci U S A **96**(1): 151-6.

Yamazaki, M., T. Shimada, et al. (2008). "*Arabidopsis* VPS35, a Retromer Component, Is Required for Vacuolar Protein Sorting and Involved in Plant Growth and Leaf Senescence." Plant Cell Physiol.

Yan, Y. and G. Marriott (2003). "Analysis of protein interactions using fluorescence technologies." Curr Opin Chem Biol **7**(5): 635-40.

Yano, K., M. Hattori, et al. (2007). "A Novel type of Autophagy Occurs together with Vacuole Genesis in Miniprotoplasts Prepared from Tobacco Culture Cells." Autophagy **3**(3).

Yanofsky, C. and M. Rachmeler (1958). "The exclusion of free indole as an intermediate in the biosynthesis of tryptophan in *Neurospora crassa*." Biochim Biophys Acta **28**(3): 640-1.

Yoshihisa, T., C. Barlowe, et al. (1993). "Requirement for a GTPase-activating protein in vesicle budding from the endoplasmic reticulum." Science **259**(5100): 1466-8.

Youderian, S. M. M. a. (1983). "Bacteriophage P22 antirepressor and its control. In Lambda II." Cold Spring Harbor Laboratory Press, Cold Spring Harbor N.Y. 347-363.

Zeng, P. Y., C. R. Vakoc, et al. (2006). "*In vivo* dual cross-linking for identification of indirect DNA-associated proteins by chromatin immunoprecipitation." Biotechniques **41**(6): 694, 696, 698.

Zhang, G. F. and L. A. Staehelin (1992). "Functional Compartmentation of the Golgi Apparatus of Plant Cells - Immunocytochemical Analysis of High-Pressure Frozen-Substituted and Freeze-Substituted *Sycamore* Maple Suspension Culture Cells." Plant Physiol **99**(3): 1070-1083.

Zhang, K. and R. J. Kaufman (2004). "Signaling the unfolded protein response from the endoplasmic reticulum." J Biol Chem **279**(25): 25935-8.

Zhang, Y., C. M. Liu, et al. "The plant exocyst." J Integr Plant Biol **52**(2): 138-46.

Zheng, N., P. Wang, et al. (2000). "Structure of a c-Cbl-UbcH7 complex: RING domain function in ubiquitin-protein ligases." Cell **102**(4): 533-9.

Zouhar, J. and E. Rojo (2009). "Plant vacuoles: where did they come from and where are they heading?" Curr Opin Plant Biol.

Books

Molecular Biology of the Cell, 4th edition. Bruce Alberts, Alexander Johnson, Julian Lewis, Martin Raff, Keith Roberts and Peter Walter (New York, Garland Science, 2002).

The Cell: A Molecular Approch, Fifth Edition. Geoffrey M. Cooper and Robert E. Hausman (Sinauer Associates, Inc. 2009).